Towards producing infectious bronchitis virus-like particles in plants as potential vaccine candidates

By

Kamogelo Mmapitso Sepotokele

Submitted in partial fulfilment of the requirements for the degree of Master of Science in the Department of Production Animal Studies in the Faculty of Veterinary Science, University of Pretoria

Date submitted: 01 November 2019

Acknowledgements

My supervisors Professor Celia Abolnik and Dr Martha. M. O'Kennedy for their continuous guidance, support, and encouragement. I would never have managed this without you both. You completely changed my outlook on research. Thank you.

Council for Scientific and Industrial Research (CSIR) for the use of its laboratory facilities and thank you to all the staff of CSIR for their hard work and support, which made this possible.

National Research Foundation (NRF) for the funding provided to complete this research.

University of Pretoria for having me as a student.

Plant Bioscience LTD, Norwich for the use of their CPMV technology (pEAQ-HT expression vector system).

My parents for their unconditional love, support, and constant encouragement. Thank you for always believing in me, and never allowing me to give up.

Table of Contents

Acknowledgements	**pg. ii**
Table of Contents	**pg. iii**
List of Tables	**pg. v**
List of Figures	**pg. vi**
List of Abbreviations	**pg. x**
Summary	**pg. 1**
CHAPTER 1: Introduction	**pg. 3**
CHAPTER 2: Literature Review	**pg. 6**
2.1. Classification and Structure	**pg. 6**
2.2. Genome Organisation	**pg. 7**
2.3. Spike Protein	**pg. 8**
2.4. Serotypes	**pg. 10**
2.5. Global Distribution	**pg. 11**
2.6. Clinical Signs of Disease	**pg. 12**
2.7. Diagnosis	**pg. 14**
2.8. Available Vaccines and Methods of control	**pg. 16**
2.9. The Use of Plants for Transient Protein Expression	**pg. 24**
2.10. Plant Expression Vector Systems	**pg. 25**
CHAPTER 3: Materials and Methods	**pg. 29**
3.1. Synthetic construct design and cloning genes into plant expression vector pEAQ-HT	**pg. 29**
3.2. Transformation of constructs into *A. tumefaciens*	**pg. 33**
3.3. Infiltration of *N. benthamiana* ΔXT/FT leaves with *A. tumefaciens* and crude protein extraction	**pg. 34**

3.4. Analysis of crude plant proteins and visualisation of VLPs **pg. 35**

3.5. Redesign and cloning of recombinant S genes **pg. 39**

CHAPTER 4: Results **pg. 47**

4.1. Experiment 1 **pg. 47**

4.2. Experiment 2 **pg. 56**

4.3. Experiment 3 **pg. 59**

4.4. Experiment 4 **pg. 68**

4.5. Experiment 5 **pg. 78**

CHAPTER 5: Discussion **pg. 91**

References **pg. 98**

Appendix **pg. 118**

List of Tables

Table 1	Forward and reverse primers used for PCR validation	**pg. 32**
Table 2	Primers for modifying the original S gene to create recombinant S genes	**pg. 41**
Table 3	A comparison between the IBV S protein and the IAV HA protein	**pg. 139-140**

List of Figures

Figure 1	Transmission Electron Microscope image of avian IBV virion (native QX-like live IBV strain (ck/ZA/3556/11) stained with uranyl acetate, illustrating the club-shaped spikes on the surface	**pg. 6**
Figure 2	Genome organisation of Infectious Bronchitis Virus encoding the structural and non-structural proteins	**pg. 7**
Figure 3	Spike glycoprotein subunits	**pg. 10**
Figure 4	Native virus vs virus-like particle	**pg. 21**
Figure 5	pEAQ-HT plant expression vector	**pg. 28**
Figure 6	Diagram illustrating the design of pEAQ-HT-S, pEAQ-HT-N, pEAQ-HT-M, and pEAQ-HT-E	**pg. 30**
Figure 7	Recombinant IBV S proteins modified from the original S gene using primers	**pg. 39**
Figure 8	Diagram illustrating the design of pEAQ-HT-S, pEAQ-HT-rIBV-S-IAV-TM, pEAQ-HT-rIBV-S-IAV-TM/CT, pEAQ-HT-mIBV-S-KKSV, and pEAQ-HT-mIBV-S-IAV-TM-KKSV	**pg. 42**
Figure 9	Combinations of *Agrobacterium* suspensions for infiltration	**pg. 43**
Figure 10	Combinations of *Agrobacterium* suspensions for infiltration (with addition of N protein to all combinations)	**pg. 44**
Figure 11	Colony PCR of DH10B cells transformed with pEAQ-HT-E ligation and pEAQ-HT-M	**pg. 48**
Figure 12	PCR products of plasmid DNA miniprepped DH10B cells harbouring pEAQ-HT-S	**pg. 49**
Figure 13	pEAQ-HT harbouring the genes encoding the Spike protein (S), Membrane protein (M), and Envelope protein (E)	**pg. 50-51**
Figure 14	Bolt 4-12% SDS-PAGE analysis of pEAQ-HT IBV S, M, and E proteins co-expressed in *N. benthamiana* 6 dpi.	**pg. 52**

Figure 15 Immunoblot using IBV-specific antiserum to detect pEAQ-HT IBV S, M, and E proteins co-expressed in *N. benthamiana* 6 dpi. **pg. 53**

Figure 16 Immunoblot using IBV-specific antiserum to detect pEAQ-HT IBV S, M, and E proteins co-expressed in *N. benthamiana* 6 and 8 dpi. **pg. 54**

Figure 17 Protein confirmation using LC-MS/MS-based peptide sequencing of IBV structural proteins (S, M, and E) **pg. 55-56**

Figure 18 Bolt 4-12% SDS PAGE analysis of pEAQ-HT IBV S, M, and E proteins co-expressed in *N. benthamiana* 6 dpi. **pg. 57**

Figure 19 Immunoblot using IBV-specific antiserum to detect pEAQ-HT IBV S, M, and E proteins co-expressed in *N. benthamiana* 6 dpi. **pg. 58**

Figure 20 PCR of miniprepped DH10B cells transformed with pEAQ-HT-rIBV-S-TM and pEAQ-HT-rIBV-S-TM/CT **pg. 60**

Figure 21 pEAQ-HT harbouring the genes encoding the recombinant S proteins, rIBV-S-TM and rIBV-S-TM/CT **pg. 61-62**

Figure 22 Bolt 4-12% SDS PAGE analysis of pEAQ-HT IBV S (or rIBV-S-TM or rIBV-S-TM/CT), M, E, and IAV M2 ion channel proteins co-expressed in *N. benthamiana* 6 dpi. **pg. 64**

Figure 23 Immunoblot using IBV-specific antiserum to detect pEAQ-HT IBV S (or rIBV-S-TM or rIBV-S-TM/CT), M, and E proteins co-expressed in *N. benthamiana* 6 dpi. **pg. 65**

Figure 24 Protein confirmation using LC-MS/MS-based peptide sequencing of IBV structural proteins (S, rIBV-S-TM, rIBV-S-TM/CT, M, and E) **pg. 66-67**

Figure 25 PCR of plasmid DNA from DH10B cells transformed with pEAQ-HT-mIBV-S-KKSV **pg. 69**

Figure 26 PCR of plasmid DNA from DH10B cells transformed with pEAQ-HT-mIBV-S-TM-KKSV **pg. 70**

Figure 27 pEAQ-HT harbouring the genes encoding the recombinant S proteins, mIBV-S-KKSV and mIBV-S-TM-KKSV **pg. 71**

Figure 28	Bolt 4-12% SDS PAGE analysis of pEAQ-HT IBV S (or rIBV-S-TM or rIBV-S-TM/CT or mIBV-S-KKSV or mIBV-S-TM-KKSV), M, E, and IAV M2 ion channel proteins co-expressed in *N. benthamiana* 6 dpi.	**pg. 73**
Figure 29	Bolt 4-12% SDS PAGE analysis of pEAQ-HT IBV S (or rIBV-S-TM or rIBV-S-TM/CT or mIBV-S-KKSV or mIBV-S-TM-KKSV), M, E and IAV M2 ion channel proteins co-expressed in *N. benthamiana* 6 dpi.	**pg. 74**
Figure 30	TEM images of potential plant-produced homogenous IBV VLPs	**pg. 75-77**
Figure 31	Colony PCR of DH10B cells transformed with pEAQ-HT-N	**pg. 79**
Figure 32	pEAQ-HT harbouring the gene encoding the Nucleocapsid protein (N)	**pg. 80**
Figure 33	Bolt 4-12% SDS PAGE analysis of pEAQ-HT IBV S (or rIBV-S-TM or rIBV-S-TM/CT or mIBV-S-KKSV or mIBV-S-TM-KKSV), M, E, N, and IAV M2 ion channel proteins co-expressed in *N. benthamiana* 6 dpi.	**pg. 82**
Figure 34	Immunoblot using IBV-specific antiserum to detect pEAQ-HT IBV S (or rIBV-S-TM or rIBV-S-TM/CT or mIBV-S-KKSV or mIBV-S-TM-KKSV), N, M, and E proteins co-expressed in *N. benthamiana* 6 dpi.	**pg. 83**
Figure 35	Protein confirmation using LC-MS/MS-based peptide sequencing of IBV structural proteins (S, rIBV-S-TM, rIBV-S-TM/CT, mIBV-S-KKSV, mIBV-S-TM-KKSV, N, M, and E	**pg. 84-86**
Figure 36	Unstained and stained TEM images of immunogold labelled leaf sections	**pg. 87-90**
Figure 37	Restriction enzyme digest of pUC57-S plasmid with *Age*I and *Xho*I restriction enzymes	**pg. 131**
Figure 38	Restriction enzyme digest of pUC57-N plasmid with *Age*I and *Xho*I restriction enzymes	**pg. 131**
Figure 39	Restriction enzyme digest of rIBV-S-IAV-TM PCR product with *Age*I and *Xho*I restriction enzymes	**pg. 132**
Figure 40	Restriction enzyme digest of rIBV-S-IAV-TM/CT PCR product with *Age*I and *Xho*I restriction enzymes	**pg. 132**

Figure 41 Restriction enzyme digest of mIBV-S-KKSV PCR product with *Age*I and *Xho*I restriction enzymes **pg. 133**

Figure 42 Restriction enzyme digest of mIBV-S-IAV-TM-KKSV PCR product with *Age*I and *Xho*I restriction enzymes **pg. 133**

Figure 43 KAPA HIFI PCR product of rIBV-S-IAV-TM using Fw TM-CT and Rv TM primers **pg. 134**

Figure 44 KAPA HIFI PCR product of rIBV-S-IAV-TM/CT using Fw TM-CT and Rv TM-CT primers **pg. 134**

Figure 45 KAPA HIFI PCR product of mIBV-S-KKSV using Fw mIBV-S and Rv IBV-S-KKSV primers **pg. 135**

Figure 46 KAPA HIFI PCR product of mIBV-S-IAV-TM-KKSV with Fw mIBV-S and Rv IBV-S-KKSV primers **pg. 135**

Figure 47 Bolt 4-12% SDS PAGE analysis of pEAQ-HT IBV S, M, and E proteins co-expressed in *N. benthamiana* 6 dpi. Bands were cut out for LCMS-MS/MS based peptide sequencing **pg. 136**

Figure 48 Bolt 4-12% SDS PAGE analysis of pEAQ-HT IBV S or rIBV-S-TM or rIBV-S-TM/CT, M, and E proteins co-expressed in *N. benthamiana* 6 dpi. Bands were cut out for LCMS-MS/MS based peptide sequencing **pg. 137**

Figure 49 Bolt 4-12% SDS PAGE analysis of pEAQ-HT IBV S or rIBV-S-TM or rIBV-S-TM/CT or mIBV-S-KKSV or mIBV-S-TM-KKSV, N, M, and E proteins co-expressed in *N. benthamiana* 6 dpi. Bands were cut out for LCMS-MS/MS based peptide sequencing **pg. 138**

List of Abbreviations

%	Percentage
°C	Degrees Celsius
µF	Microfarads
µl	Microlitre
µm	Micrometre
µM	Micromolar
aa	Amino acid
AGP	Agar gel precipitation test
bp	Base pairs
BSA	Bovine serum albumin
cm	Centimetre
CPMV	Cowpea mosaic virus
CT	Cytosolic tail
C-terminal	Carboxyl terminal
CTLs	Cytotoxic T lymphocytes
DIVA	Distinguish between infected and vaccinated animals
DNA	Deoxyribonucleic acid
dNTP	Deoxyribonucleotide triphosphate
dpi	Days post infiltration
E	Envelope protein
ELISA	Enzyme-linked immunosorbent assay
ER	Endoplasmic reticulum
Fr	Fraction
Fw	Forward
g	Grams
Goat α-chicken HRP	Anti-chicken IgG (H+L)-Peroxidase antibody produced in goat
HA	Hemagglutinin
HI	Hemagglutination inhibition

HPAI	High pathogenic IAV
HRP	Horseradish peroxidase
HT	Hypertranslatable
IAV	Influenza A virus
IBV	Infectious Bronchitis Virus
IgG	Antibodies
kb	Kilobase
kDa	Kilo Daltons
kV	Kilovolt
L	Litre
LC-MS/MS	Liquid chromatography-tandem mass spectrometry
LPAI	Low pathogenic IAV
M	Membrane protein
M2	Matrix-2
MES	N-morpholinoethanesulfonic acid
min	Minutes
ml	Millilitre
mM	Millimolar
mRNA	Messenger ribonucleic acid
N	Nucleocapsid protein
N. benthamiana	*Nicotiana benthamiana*
NA	Neuraminidase
NCBI	National Centre for Biotechnology Information
ng	Nanograms
nm	Nanometre
N-terminal	Amino terminal
OD	Optical density
OIE	Office International des Epizooties (World Organisation for Animal Health)
ORF	Open reading frame
PAGE	Polyacrylamide gel electrophoresis

PBS	Phosphate-buffered saline
PC6	Proprotein convertase 6
PLP	Papain-like protease
polyA	Polyadenylated
PVDF	Polyvinylidene difluoride
RNA	Ribonucleic acid
rpm	Revolutions per minute
RT-PCR	Reverse transcription polymerase chain reaction
Rv	Reverse
S	Spike protein
SDS	Sodium dodecyl sulphate
sec	Seconds
SOC	Super Optimal broth with Catabolite repression
SPF	Specific-pathogen-free
T-DNA	Transfer deoxyribonucleic acid
TEM	Transmission electron microscope
TM	Transmembrane
US	United states
UTR	Untranslated region
V	Volts
VLP	Virus-like particle
VN	Virus-neutralisation
w/v	Weight by volume
YMB	Yeast mannitol broth
α	Alpha
β	Beta
Ω	Ohm

Summary

Towards producing infectious bronchitis virus-like particles in plants as potential vaccine candidates

By: Kamogelo Mmapitso Sepotokele (BSc Hons)

Supervisor: Professor C. Abolnik

Co-supervisor: Dr M. M. O'Kennedy

Department: Production Animal Studies

Degree: MSc

Infectious Bronchitis Virus (IBV) causes a highly contagious respiratory disease that affects chickens and other poultry. This OIE-listed disease has global economic implications with losses per flock estimated at 10% to 20% of the market value. The South African poultry industry makes up the largest subsector within the country's agricultural sector, producing an annual turnover of over R40 billion. Therefore, it would be beneficial to the poultry industry to prevent economic losses due to diseases such as IBV. Current autogenous IBV vaccines are effective but require the passage of live viruses in embryonated chicken eggs. Therefore, safe, efficacious, new-generation vaccines are imperative. Biopharming is the production of recombinant pharmaceutical proteins by making use of plants as bioreactors. Plants are capable of producing large quantities of target proteins cost-effectively, offering attractive alternatives for the production of vaccines, antigens for diagnostics, and other pharmaceuticals.

The aim of this project was to produce infectious bronchitis virus-like particles (VLPs) displaying the major surface antigen, the Spike protein, in *Nicotiana benthamiana* plants by transiently co-expressing and assembling the structural proteins of IBV. VLPs are multiprotein structures that mimic the authentic virus, while lacking the genome, resulting in safe, efficacious, DIVA (distinguish between infected and vaccinated animals) compliant vaccine candidates that induce both cellular and humoral immune responses. In addition, the speed of gene synthesis and production of VLPs in plants will facilitate a rapid update of the IBV spike protein that is tailored and antigenically matched, in vaccine formulations.

The native as well as recombinant versions of the spike glycoprotein of QX-like IBV were individually cloned into a plant expression vector, as were the membrane, envelope and nucleocapsid proteins. Various *Agrobacterium* strains were tested to identify the most appropriate strain to mediate the production of IB VLPs in plants. IBV structural proteins were successfully expressed in *N. benthamiana* ΔXT/FT plant leaf material, as confirmed by immunological detection, but low yields were obtained. No VLPs were detected using transmission electron microscopy, indicating that VLPs may not have assembled. In future, alternative designs of the spike protein and the addition of molecular chaperone genes will potentially elevate the numbers of VLPs produced, resulting in a commercially viable vaccine product.

Key words: Infectious bronchitis, plant production, virus-like particle (VLP), vaccine, chickens, spike glycoprotein

CHAPTER 1

Introduction

As an economically important OIE-listed disease, IBV needs to be controlled through strict biosecurity as well as vaccination. The Massachussetts vaccine has been registered for use in South Africa since the 1960s, but since 2013, variant vaccines such as 793B, QX and Variant 02 have been registered and applied, and this has contributed to higher field virus diversity in the country (Dr Fambies van Biljoen, personal communication). Deltamune (Pty) Ltd (South Africa) has also developed live tailored autogenous vaccines to control IBV.

The development of more novel, effective vaccines has been researched, but is hindered by cost and method of application (Jackwood and de Wit, 2013). IBV vaccines that are currently available commercially cause an unacceptable reduction in the hatchability of eggs when applied *in ovo*. Therefore, there is a huge need for novel IBV vaccines that are cost-effective and efficacious for use in the poultry industry.

Variant inactivated IBV vaccines have great potential to offer better protection against IBV infections than current live vaccines do (Ladman *et al*., 2002). Using inactivated autogenous vaccines also removes the risk of the virus spreading and affecting other flocks, which is a risk associated with using live variants (Jackwood and de Wit, 2013).

Plant-based transient expression is the most cost-effective and speedy recombinant platform currently available (D'Aoust *et al*., 2008). It can be used to efficiently assemble virus-like particle (VLP) vaccines. Where traditional pharmaceutical manufacturing methods prove inadequate, plant-based expression systems are easily scalable and can be used in situations where rapid responses are required (Rybicki, 2009; Stoger *et al*., 2014). This makes them appealing in developing countries that lack the infrastructure for the traditional production of pharmaceuticals and are most affected by infectious diseases as a result (Hefferon, 2013; Ma *et al*., 2013; Rybicki *et al*., 2013). Plants are safer to use than other expression systems as the growth of potentially infectious prions or viruses is not supported and endotoxins are not produced (Moustafa *et al*., 2016). Plants are also able to assist with post-translational modifications such as glycosylation and the formation of disulphide bonds (Tschofen *et al*., 2016). The plasticity of the plant proteome also makes the expression of more than one protein

possible, allowing the assembly of heteromultimeric protein complexes such as VLPs (Castilho and Steinkellner, 2012; Castilho *et al.*, 2010).

VLPs have been produced for various animal viruses in plants (Liu *et al*., 2013a). One of the earliest examples of the successful expression and production of VLPs in plants is avian influenza virus (IAV) VLPs (D'Aoust *et al*., 2008, 2010). VLPs for IBV have not yet been successfully produced in plants.

Many influenza hemagglutinin (HA) glycoproteins have been shown to have high expression levels *in planta* and form VLPs (D'Aoust *et al*., 2008; Shoji *et al*., 2011). Both Medicago, Inc (Canada) and Fraunhofer Society (Germany) have proprietary VLP products for pandemic and seasonal influenza in advanced clinical trials. As such, it is the only plant-expressed viral glycoprotein that has been analysed in human trials (Pillet *et al*., 2016). Recently, superior efficacy of an antigen-matched plant-produced influenza VLP subunit vaccine against the H6 subtype in chickens has been demonstrated, showing the potential for poultry health (Smith *et al*., 2019).

With this information in mind, it is important to consider the key differences between IBV and IAV, such as the VLP budding site and the properties of the structural proteins. These differences may give insight into what may be required to successfully produce IB VLPs in tobacco plants. The goal of this study was to assemble IB VLPs expressing the IBV Spike protein as a potential candidate vaccine. Ultimately, the IB VLP vaccine candidates will be tested for safety and efficacy to confer clinical protection in poultry, but this falls outside the scope of the proposed work.

Aims and Objectives of the project

The main aim of this research project was to transiently express infectious bronchitis virus (IBV) structural proteins and to assemble virus-like particles (VLPs) displaying the full-length S protein using the pEAQ-HT plant-based expression system in *N. benthamiana* ΔXT/FT. A South African strain of IBV of the QX-like serotype was used as the basis of the investigation.

The specific objectives were:

- To design and have the IBV target genes codon-optimised and chemically synthesised by BioBasic (Canada)
- To clone the target genes encoding IBV native Spike (and recombinant versions thereof), Membrane, Nucleocapsid and Envelope proteins into the pEAQ-HT plant expression vector
- To transform the sequence-validated constructs into different *Agrobacterium tumefaciens* strains (AGL-1, GV3101::pMP90 and LBA4404) in order to facilitate *Agrobacterium*-mediated transient expression of target proteins
- To agroinfiltrate *A. tumefaciens* harbouring the constructs of interest into *Nicotiana benthamiana* leaves
- To identify the most appropriate *A. tumefaciens* strain with which to express IBV structural proteins and assemble VLPs
- To harvest and successfully purify the IB VLPs
- To confirm IB VLP formation by immunoblotting using IBV-specific antiserum, transmission electron microscopy (TEM) and liquid chromatography-mass spectrometry (LC-MS/MS) based peptide sequencing of the structural proteins.

CHAPTER 2

Literature Review

2.1. Classification and Structure

Avian infectious bronchitis virus (IBV) is an extremely contagious respiratory disease of chickens and other poultry species, which has significant economic implications in the poultry industry globally (Liu *et al*., 2013b). IBV is a *gammacoronavirus* belonging to the *Coronaviridae* family of the order *Nidovirales* (Wickramasinghe *et al*., 2014; de Groot *et al*., 2011; de Groot *et al.*, 2012). It falls under the subfamily *Coronavirinae* (Jackwood and de Wit, 2013), predominantly affecting chickens (*Gallus gallus*) (Eteradossi and Britton, 2013; Wickramasinghe *et al*., 2014). The virus is an enveloped RNA virus with a spherical (or pleomorphic) morphology of between 80 and 120 nm in diameter. It has club-shaped spikes with lengths of approximately 20 nm (16 – 21 nm) projecting from its surface (Figure (Fig. 1)) which make the virus appear crown-like (Liu *et al*., 2013b; Jackwood and de Wit, 2013). This is what gives the virus its name - *Corona*, which is Latin for the word crown (Jackwood and de Wit, 2013). IBV particles fully covered in spikes have a sucrose density of 1.18 g/ml, while particles with fewer spikes may have a density as low as 1.15 g/ml (Jackwood and de Wit, 2013).

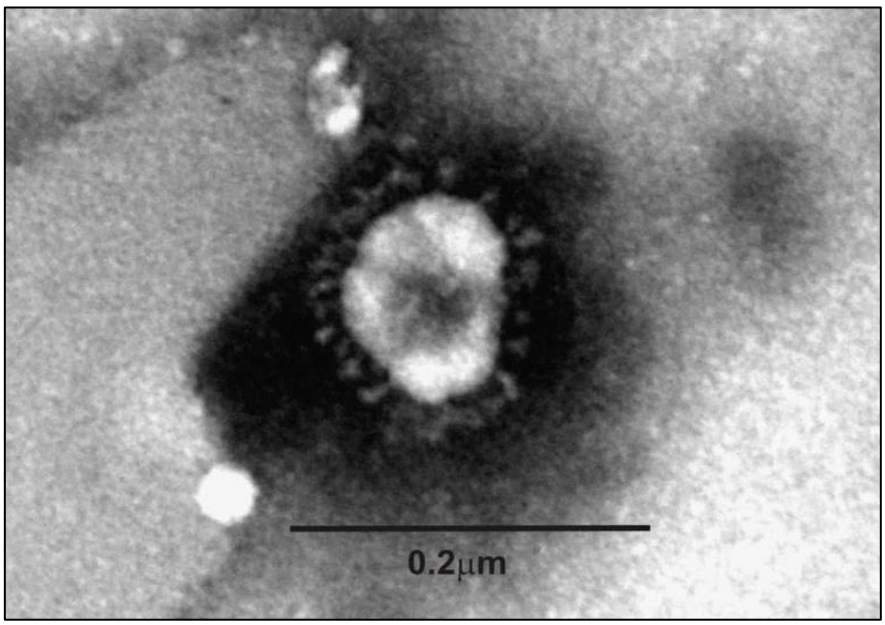

Figure 1: TEM image of avian IBV virion (native QX-like live IBV strain (ck/ZA/3556/11) stained with uranyl acetate, illustrating the club-shaped spikes on the surface.

2.2. Genome Organisation

IBV is a single-stranded positive-sense linear RNA virus (Fig. 2) with a genome length of approximately 27.5 - 28 kb (Masters and Perlman, 2013; Zhang *et al*., 2010; Jackwood and de Wit, 2013). The genome has a 5' cap as well as a polyA tail on its 3' end (Zhang *et al*., 2010). The first two thirds of the genome on the 5' end code for two overlapping polyproteins, 1a and 1b, which are further processed by a papain-like protease (PLP) into 15 non-structural replicase proteins that play a role in RNA replication and transcription (Liu *et al*., 2014; Perlman *et al*., 2008; Ziebuhr *et al*., 2000). It is these non-structural proteins that comprise the RNA-dependent RNA polymerase of the virus (Perlman *et al*., 2008). The last one third of the genome on the 3' end codes for four structural proteins. These are the spike protein (S), the membrane protein (M), the envelope protein (E), and the nucleocapsid protein (N). S, M, and E are involved in formation of the virus particle, while N is involved in packaging the genome (Cavanagh, 2007). The E protein is a small integral membrane protein that plays a role in the assembly of the virus particle (Ruch and Machamer, 2011), while the M glycoprotein spans the envelope of the virus three times with part of the amino end exposed on the viral surface (Jackwood and de Wit, 2013). The N phosphoprotein forms the helical nucleocapsid inside the virus particle by encapsulating the RNA genome of the virus. It also interacts with both the E and M proteins to assist in assembly of the virus particle (Jayaram *et al*., 2006).

The genome organisation is as follows:

5'UTR-leader-Replicase (1a-1b)-S-3a-3b-E-M-5a-5b-N 3'UTR (Jackwood and de Wit, 2013). The functions of 3a, 3b, 5a, and 5b non-structural proteins are unknown (Jackwood and de Wit, 2013; Boursnell *et al*., 1987).

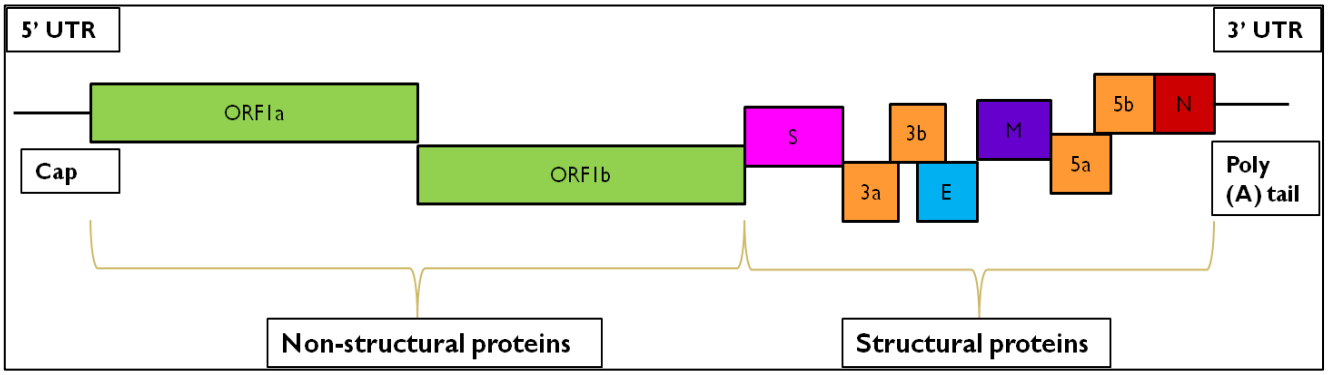

Figure 2: Genome organisation of Infectious Bronchitis Virus (adapted from Jackwood and de Wit, 2013) (not drawn to scale) encoding the structural and non-structural proteins.

IBV replicates within the host cell's cytoplasm producing a 3' co-terminal set of 5 subgenomic messenger RNAs, each of which has a 5' leader sequence that, during transcription, gets joined to the mRNA (Jackwood and de Wit, 2013). Some of these subgenomic messenger RNAs are polycistronic, however, most of them code for the protein at the farthest 5' end. The full-length genome of IBV, mRNA1, codes for the polyproteins of the viral polymerase while the 5 subgenomic messenger RNAs code for the following: mRNA2 - Spike, mRNA3 - 3a/3b/Envelope, mRNA4 - Membrane, mRNA5 - 5a/5b, and mRNA6 - Nucleocapsid (Jackwood and de Wit, 2013). Once the virus enters the cell, the genome behaves similarly to mRNA coding for non-structural proteins 2-16, creating the viral polymerase inside of double membrane vesicles at the Golgi apparatus (Hagemeijer *et al*., 2010). The viral subgenomic messenger RNAs are transcribed in the cytoplasm along with the translation of the viral proteins (Jackwood and de Wit, 2013). The M, E and S proteins are inserted into the membrane of the Golgi, while the N protein binds itself to the viral genome that has been synthesised, thus forming the nucleocapsid (Jackwood and de Wit, 2013). The E, M and N proteins interact with each other in order to allow the virus particles to bud from the endoplasmic reticulum (ER) on the cytoplasmic surfaces. These particles are then transported in vesicles to the plasma membrane, where they fuse and bud from the cell (Jackwood and de Wit, 2013).

2.3. Spike Protein

The S glycoprotein is a trimer that is made up of subunits S1 and S2 (Fig. 3a) of approximately 520 and 625 amino acids in length respectively (Jackwood and de Wit, 2013). These subunits are generated through post-translational cleavage of the S protein by a furin-like host cell protease (Liu *et al*., 2013b; Cavanagh *et al.*, 1986). The S1 subunit associates noncovalently with the S2 subunit which anchors it to the membrane (Lai and Cavanagh, 1997). Not only does the S1 subunit contain the receptor-binding domain that facilitates attachment of the virus to host cell (Promkuntod *et al*., 2014), it is also the part of the S protein that induces neutralizing antibodies (Kant *et al*., 1992; Koch *et al*., 1990). The S1 subunit at the N-terminal forms the bulb of the oligomeric S protein and is part of the large ectodomain, while the S2 subunit at the C-terminal end forms a narrow stalk as well as the short transmembrane (TM) and endodomain, and forms the smaller part of the ectodomain (Fig. 3b) (Wickramasinghe *et al.*, 2014). The S2 subunit not only helps with attaching the virus to the host cell, but it also contains antigenic epitopes (Toro *et al*., 2014). Prior to glycosylation, the S protein monomer has a molecular

mass of approximately 128 kDa (Masters and Perlman, 2013). The S protein is directed to the ER by a cleaved N-terminal signal peptide where it becomes terminal N-linked glycosylated which increases the size of the protein to approximately 200 kDa (Binns *et al*., 1985; Wickramasinghe *et al*., 2014). Thereafter, the monomers form dimers or trimers through oligomerisation (Lewicki and Gallagher, 2002).

Mutations that occur in the S1 region of the S protein lead to new genotypes and serotypes of the virus (Liu *et al*., 2003). Existing vaccine serotypes may offer partial or poor protection against them (Liu *et al*., 2003). Because this gene determines the IBV serotype, sequencing it is useful for characterising different strains of the virus and therefore selecting a suitable vaccine for controlling the virus in different areas (Liu *et al*., 2003). S is a type 1 membrane protein that is made up of a receptor binding domain, precoil domain, heptad repeat regions, a cleavage site, interhelical domain, fusion peptide, TM, as well as a cytoplasmic tail (CT) (Koch *et al*., 1990; Perlman *et al*., 2008). The S protein is a class 1 viral fusion peptide that is involved in attachment of the virus to the host cell (mediated by the variable S1 domain), as well as fusion to the host cell membrane and entry of the virus into the cell (mediated by the conserved S2 domain) (Casais *et al*., 2003; Wickramasinghe *et al*., 2011; Masters and Perlman, 2013). Antibodies for hemagglutination inhibition (HI) as well as virus-neutralisation and serotype-specific antibodies are directed against the first third of the amino part of the S glycoprotein (Koch *et al*., 1990). In chickens that are infected with the virus, both cellular and humoral immune responses are induced by the S protein (Cavanagh, 2007). The production of antibodies in the chickens does not necessarily mean that the chicken will be protected against the virus (Cavanagh *et al*., 1986; Collisson *et al*., 2000). This is because cytotoxic T lymphocytes (CTLs) are important for preventing the disease caused by IBV. Cytotoxic T lymphocyte determinants are found not only in the N protein, but also in the S glycoprotein (Collisson *et al*., 2000). An epitope that is responsible for inducing CTL responses to the N protein is located on the N protein's carboxyl terminus (Collisson *et al*., 2000). Chicks could be protected from acute IBV infection by IBV primed CD8+,αβ T lymphocytes when immune T cells were transferred to them before they were infected (Collisson *et al*., 2000).

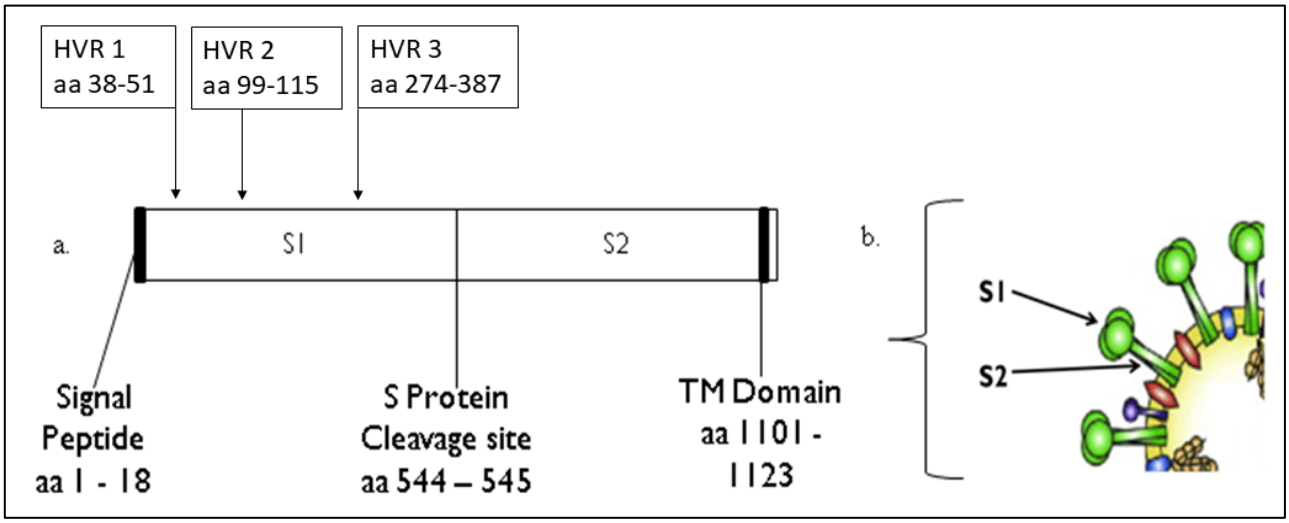

Figure 3: S glycoprotein subunits (adapted from (a.) Umar *et al.*, 2016 and (b.) Cook, 1984).

2.4. Serotypes

Molecular evolution of IBV results in different serotypes of the virus. This can be through genetic shift caused by recombination events (Kusters *et al*., 1990) as well as genetic mutations caused by natural errors made by the RNA-dependent RNA polymerase (Hanada *et al.*, 2004). New serotypes of IBV emerge when selection acts on those molecular changes (Jordan, 2016). Different sources including the use of different vaccines in the commercial poultry industry can result in selection pressures (Jackwood *et al*., 2012). Because new serotypes and variants of those serotypes are constantly emerging, poultry producers and animal health companies are constantly forced to produce new, more effective vaccines, as well as re-evaluate their current plans for vaccination (Jordan, 2016). Jungherr *et al.*, (1956) reported that a Connecticut IBV strain did not cross-protect against challenge with a Massachusetts strain, thus showing that the virus existed as different serotypes that did not necessarily cross-protect or cross-neutralise. Virus neutralisation (VN) tests or HI tests have been used to determine IBV serotypes (Gelb and Jackwood, 2008; Ruano *et al*., 2000).

The specific circulating antibodies that are developed against the epitopes of the S protein following exposure define the IBV serotype (Jackwood and de Wit, 2013). The epitopes that induce neutralizing antibodies are very closely linked to three hypervariable regions (HVRs; Fig. 3) that are located in the S1 part of the S gene (Cavanagh *et al*., 1988). Both serotype and genotype are based on the S protein's sequence. Neutralising antibody treatment is used to classify IBV isolates by serotype, whereas classifying the isolates by genotype is done by

examining the S1 protein sequence (Jackwood and de Wit, 2013). Generally (not always), 90% or more amino acid similarity of the HVRs in the S1 gene (genotype) means that strains are of the same serotype (Jackwood and de Wit, 2013; Cavanagh, 2001).

2.5. Global Distribution

IBV was the first of the coronaviruses described in the 1930s in the United States (Schalk and Hawn, 1931). Several serotypes of IBV have since been described worldwide in regions of America, Europe, Asia, Africa, and Australia (Cavanagh, 2007; Jackwood, 2012). Over 20 different serotypes of the virus have been found globally with new variants of serotypes still increasing (Zhou *et al*., 2004). It is found both in commercial, as well as backyard chickens (Jackwood, 2012; Cook *et al.*, 2012). Most of the IBV serotypes that have been identified over the past twenty years have become endemic to some areas or disappeared completely (Bochkov *et al.*, 2006). Others have become more prevalent, significantly impacting the poultry industry over the years (Terregino *et al.*, 2008). Some serotypes of IBV have been seen to co-circulate in specific regions. Some strains can be found on more than one continent while others can only be found in one region (Jackwood and de Wit, 2013). IBV is classified as an OIE (World organisation for animal health) notifiable disease (https://www.oie.int/en/animal-health-in-the-world/oie-listed-diseases-2019/).

IBV is considered to be endemic in Africa, being one of the most common viral respiratory diseases that affect chickens. The virus is rife in both unvaccinated as well as vaccinated poultry farms (Casais *et al*., 2003; Liu *et al*., 2003). It has been suggested that the most important variants of IBV may originate from North Africa, but these have not been well studied and may therefore also occur in European countries (Jones *et al*., 2004). Such variants include 793B, 4/91, and CR88. In France, the 793B variant was found to have existed since 1985, and originated from North Africa (Cavanagh *et al*., 1992). In Morocco, the 793B IBV variant was isolated in 1983 for the first time (Jones *et al*., 2004; El-Houadfi *et al*., 1986). Infectious bronchitis was initially described in North Africa in the 1950s by Ahmed (1954) who observed respiratory signs in birds. Eissa *et al*., (1963) later confirmed this, followed by El Houadfi & Jones (1985) in 1983.

In Egypt, IBV isolates from various poultry farms were serologically shown to be closely associated with the 4/91, D-08880, Dutch D3128, D274, and the Massachusetts variants of the virus (Ahmed, 1964; Eid, 1998). Similarly, IBV variants D, E, F, H, and M from Morocco were

serologically identified as the Massachussets serotype (El-Houadfi & Jones, 1985). A new genotype (referred to as the Moroccan 'G') was identified by El-Houadfi *et al*., (1986) and it was found to be serologically different from the Massachusetts variant. However, collected S1 sequence data showed that the Moroccan 'G' IBV variant was related to the 4/91 variant, and may have originated from the same region (Jones *et al*., 2004). This led to the suggestion that the parts of Africa where IBV variants have not been well studied, may be a reservoir for the virus, even though several reservoirs may exist in other countries, as indicated by the increasing amount of IBV variants being identified (Khataby *et al*., 2016).

In Southern Africa, IBV was first isolated by Morley and Thompson (1984). The vaccines developed from the Massachusetts strain offered poor protection to the isolated variant (Cook *et al*., 1999). The potential presence of infectious bronchitis in all bird flocks of Chitungwiza, in Zimbabwe was later shown by Kelly *et al*., (1994) using serological techniques such as ELISA and the prevalence of the virus was 86%. The QX-like IBV genotype was reported in commercial chickens in Zimbabwe for the first time in 2011 (Toffan *et al*., 2011). Serological studies in Botswana also identified IBV antibodies in poultry farms that were unvaccinated (Mushi *et al*., 2006). Few studies are published on the prevalence and genetic variation of IBV in South Africa. Thekisoe *et al.*, (2003) reported a serological IBV prevalence of 43% in QwaQwa, South Africa in 2000, and later Knoetze *et al.*, (2014) identified two distinct IBV genotypes that were circulating in South African provinces, namely the Massachusetts variant, as well as variants of the QX-like genotype. In spite of a lack of published data, South African commercial producers routinely use the services of private diagnostic laboratories that identify circulating IBV genotypes using advanced genetic techniques. Massachusetts, 793B and QX-like variants are common locally (Dr Fambies van Biljoen, personal communication).

2.6. Clinical Signs of Disease

IBV is a disease of the upper-respiratory tract which is transmitted by ingestion or inhalation of infectious particles during direct contact with other infected birds within a flock (Jackwood and de Wit, 2013; Matthijs *et al*., 2008). Transmission may also occur indirectly through faeces or aerosol droplets, as well as by being exposed to objects likely to carry and spread the disease (Jackwood and de Wit, 2013). Because IBV has a short incubation period, clinical signs will usually develop within 24 - 48 hours of infection. These include coughing, gasping, sneezing, nasal discharge and tracheal rales (Jackwood and de Wit, 2013; Cavanagh and Gelb, 2008).

Some chickens may develop swollen sinuses and watery eyes. The chickens also seem depressed and tend to huddle themselves around heat sources. These clinical signs are then followed by a reduction in feed consumption and ultimately weight loss (Jackwood and de Wit, 2013). Other signs include urogenital lesions and effects on kidney pathology (Cavanagh and Naqi, 1997). Although all ages are susceptible to the disease, these signs are usually more pronounced in younger chicks. The older the chickens, the more resistant they become to the nephropathogenic effects of the virus, the lesions of the oviducts, as well as the likelihood of mortality caused by the infection (Butcher *et al*., 1990; Chong and Apostolov, 1982). IBV is at its highest concentration in the trachea during the first 3 to 5 days following infection with the virus. Thereafter, the virus titre decreases rapidly, sometimes dropping to below detection levels within the second week post-infection (Jackwood and de Wit, 2013). During infection, all birds within the flock become infected with the virus, however, mortality is dependent on various factors including the strain of the virus, the age and immunity status of the bird, as well as additional stresses. The highest rate of mortality is usually expected in young birds infected with nephropathogenic strains of the virus (Jackwood and de Wit, 2013). A nephropathogenic strain of IBV causes widespread kidney disease that can be reproduced in experimental conditions (Jackwood and de Wit, 2013). Clinical signs include pale, swollen kidneys, as well as ureters and tubules that tend to be distended with urates (Jackwood and de Wit, 2013; Cumming, 1963). Many IBV strains are associated with nephritis to some extent. The significance of kidney complications may be linked to environmental factors (Jackwood and de Wit, 2013). Birds that are younger than 2 weeks old display more severe nephritis, while older birds are more resistant to the nephropathogenic effects of IBV infections (Jackwood and de Wit, 2013).

In infected broiler chickens, the respiratory clinical signs seem to dissipate after the respiratory phase, only to be replaced by signs such as ruffled feathers, wet droppings, depression, increased intake of water, and death (Cumming, 1969). In laying chickens, clinical signs include a noticeable decrease in the production and quality of eggs (such as misshapen, soft-shelled, thin, or rough-shelled; as well as decreased shell pigment) along with the usual respiratory signs, which can be very mild or absent. The decrease in egg production can vary from slightly to a decrease of up to 70% depending on the strain of IBV causing the infection, the chicken's level of immunity, the stage of egg development at the time of infection, as well as co-infection with another virus (Box and Ellis, 1985; van Eck, 1983). The albumin may also be thin and watery and eggs may fail to hatch (Jackwood and de Wit, 2013). Production levels

can drop to as low as 35% of the expected production values of healthy chickens (Broadfoot *et al*., 1954).

2.7. Diagnosis

Diagnosing IBV requires analysis of clinical signs, the use of antibody-based antigen capture assays, lesions, clinical history of the infected bird, sero-conversion, isolation of the virus, as well as detection of the viral RNA (Gelb and Jackwood, 2008). The virus genotype or serotype needs to be identified in order for the correct vaccine to be used (Jackwood and de Wit, 2013). VN or HI tests have often been used to determine the virus serotype. VN tests are time consuming as well as labour intensive, while HI tests have the major disadvantage of nonspecific cross-reactivity, therefore these two tests have been replaced by molecular-based tests (Jackwood and de Wit, 2013).

IBV affects not only cells of the respiratory tract, but also epithelial cells of the gastrointestinal tract, kidney, and oviduct (Jackwood and de Wit, 2013). Detection of IBV is dependent on knowledge of its pathogenesis (Dhinaker and Jones, 1997). In order to diagnose the virus, the bird's immune status, as well as the time that passes between infection and sampling, are two important factors to consider (de Wit, 2000). Within the first week of infection, the preferred sample is fresh tracheal tissue or tracheal swabs. The samples need to be kept cold until they are ready to be tested (Jackwood and de Wit, 2013). A sample swabbed from the trachea or tracheal tissue has to be analysed within the first 3 - 5 days of infection after which IBV titres will decrease rapidly as the virus spreads (Jackwood and de Wit, 2013). After its initial growth in the upper respiratory tract, the virus spreads to nonrespiratory tissues. This means that kidney and cecal tonsil samples collected post mortem can be useful in post mortem examinations where more than one week has passed after the bird was infected (Jackwood and de Wit, 2013). Cloacal swabs and faecal material are difficult samples to isolate IBV from even though the virus is able to replicate in the gastrointestinal tract. Depending on the clinical history of the flock, oviduct, kidney, and lung samples should also be taken (Jackwood and de Wit, 2013).

Samples are taken from healthy and unhealthy birds when sampling a large flock. The samples are then inoculated into specific-pathogen-free (SPF) embryonating chicken eggs or tracheal organ cultures, the fluids are harvested from the chosen culture system, and passaged 3 to 4 times prior to being called negative. This would be based on its failure to cause ciliostasis in tracheal organ cultures, lesions or death in embryos (Gelb and Jackwood, 2008). Thereafter,

the presence of the virus is confirmed by HI, VN, immunofluorescence, electron microscopy, immunochemistry, or viral nucleic acid detection (Jackwood and de Wit, 2013).

Immunoperoxidase assays, immunofluorescence, or immunohistochemistry, using IBV-specific polyclonal sera or monoclonal antibodies can be used to detect the presence of IBV grown in embryonating eggs or by obtaining post-mortem material from tracheal mucosa or other tissue scrapings (Jackwood and de Wit, 2013; de Wit, 2000). Non-specific reactions make the results difficult to interpret (Jackwood and de Wit, 2013). Allantoic fluid and tracheal material can be used in an agar gel precipitation (AGP) test which has a sensitivity that is not lower than that of more contemporary assays when it is used directly on organs (de Wit, 2000). The AGP test can also be used to test for IBV presence in inoculated eggs, resulting in an increased sensitivity due to the virus having been replicated (Gelb *et al*., 1981).

Indirect or antigen-capture ELISA (enzyme-linked immunosorbent assay) using monoclonal antibodies can be used to detect and classify IBV that has grown in tracheal organ cultures or from allantoic fluid (Ignjatovic and Ashton, 1996). ELISA tests are widely used to serologically test for antibodies against IBV. This is because not only can a large number of samples be tested in a short amount of time, the test is also inexpensive (Jackwood and de Wit, 2013). Antibodies (IgG) can be detected from one week after infection with the virus using commercially available tests (Mockett and Darbyshire, 1981; Marquardt *et al*., 1981). However, AGP, ELISA, and immunofluorescence tests cannot be used for the purpose of distinguishing between different serotypes because they all bind antibodies to group-specific antigens (Jackwood and de Wit, 2013).

Real time or quantitative RT-PCR (reverse transcription polymerase chain reaction) is becoming commonly used for the purpose of detecting IBV from clinical samples (Callison *et al*., 2006). Not only are these tests cost-effective, but several samples can be examined within a short space of time. The tests can also quantify the level of viral nucleic acid that is present within the sample (Jackwood and de Wit, 2013). In contrast, conventional RT-PCR may require serial passaging in embryonating eggs in order to detect the IBV nucleic acid in a sample. Nested RT-PCR has been used in cases where little viral RNA is available, however, the test is too sensitive for routine testing, leading to false positives from cross-contamination. Not only that, but even if a positive result is obtained, it is not enough to determine the IBV serotype (Jackwood and de Wit, 2013).

Identifying the strain of IBV in the sample requires the analysis of the S1 gene amplicons using genotyping methods. These include genotype-specific RT-PCR, restriction fragment length polymorphism, and sequence analysis of the hypervariable regions of the S1 gene (Kwon *et al*., 1993; Jackwood and de Wit, 2013).

The diagnosis of an IBV infection requires demonstrating rising antibody titres against the virus between preclinical and convalescent sera. The conserved regions within the S2 gene as well as the high amino acid sequence similarity between the N and M proteins result in common epitopes amongst all serotypes of the virus (Jackwood and de Wit, 2013).

2.8. Available Vaccines and Methods of Control

Managing IBV requires high biosecurity, strict isolation of infected chickens, and repopulation with chicks that are a day old. The poultry house must be cleaned and disinfected, along with any equipment that may have come into contact with the virus via poultry, litter, compost or waste removal. Birds must also be vaccinated to prevent further spread of the virus. Vaccination may protect chickens from challenge by the same virus strain, but not necessarily from other strains (Jackwood and de Wit, 2013).

The first vaccine was reported by van Roeckel *et al*., (1942). The van Roeckel M-41 strain, a Mass serotype of the virus isolated by the University of Massachusetts in 1941, was used to develop the first IBV vaccine in the US, and is the parent of the Mass 41 vaccines that are currently used (Jackwood and de Wit, 2013).

The most commonly used vaccine strains in most countries are live Mass/Mass41/41 and Mass/H120/55 of the Massachusetts serotype (Jackwood and de Wit, 2013). Producers usually vaccinate with more than one vaccine serotype to broaden flock protection, but this requires constant updates regarding the knowledge of existing serotypes due to the evolution of IBV (Jordan, 2017). Sometimes only two IBV vaccine serotypes that provide an extensive level of heterologous cross-protection are applied (Cook *et al*., 1999). This vaccination strategy is known as protectotype vaccination. Unlike other vaccination strategies which are based on sterilizing immunity provided by specific neutralizing antibodies, protectotype vaccination is based on reducing the infection caused by IBV enough to protect the tracheal cilia (Jordan, 2017). Protecting the trachea from ciliostasis reduces the chances of a secondary bacterial infection occurring. It is these secondary infections that contribute to most of the losses caused

by an IBV infection (Jackwood *et al*., 2015). Previous studies have demonstrated that the more differences there are between the S1 sequences of two different IBV strains, the lower the degree of cross-protection there will be between them (Cavanagh *et al*., 1997; Ladman *et al*., 2006). Chickens that have recently been vaccinated or that were recently infected by IBV will be protected from getting infected by the same virus again. This is called homologous protection. There is variation in the degree of protection against other strains of the virus (heterologous protection) (Jackwood and de Wit, 2013). The level of cross-protection observed does correlate with the amino acid identity. That being said, some strains that have a low similarity have shown a higher level of cross-protection while strains with a higher similarity have shown poor cross-protection (de Wit *et al*., 2011).

2.8.1. Live attenuated vaccines

Live vaccines, which are attenuated by serial passaging in embryonating chicken eggs (Bijlenga *et al*., 2004) are used in broiler chickens and for initial vaccination of layer and breeder types (Jackwood and de Wit, 2013). Locally, this method is used to develop tailored autogenous vaccines by Deltamune (Pty) Ltd, South Africa. An autogenous vaccine is a vaccine that has been produced from a pathogen or antigen isolated from an animal, with its intended use being to immunize or treat that specific animal (Saléry, 2017).

The disadvantage of live vaccines is that extensive passaging can lead to reduced immunogenicity. There is also a variation in the degree and stability of live attenuation between vaccines (Jackwood and de Wit, 2013). Hopkins and Yoder (1986) demonstrated evidence that back-passage in chickens led to some vaccines becoming more virulent. This showed that a rolling infection (constant circulation) of the vaccine virus could increase the virulence of live vaccines leading to only a fraction of the chickens in a flock being properly vaccinated. Fractional doses of live attenuated IBV vaccines can enhance cyclic infections in poultry flocks and increase the virulence of the vaccines (Jackwood and de Wit, 2013).

Recombinant IBV generated by reverse genetics are promising as vaccine candidates. This is because an attenuated live vaccine against a new strain of IBV can be developed faster using recombinant techniques than through attenuation by passage in embryonated eggs (Jordan, 2017). The development of this vaccine involves cloning the genome of a live IBV vaccine virus and manipulating the clone via PCR, homologous recombination, or by cloning other genes of interest into the genome (Jordan, 2017; Casais *et al*., 2001). These manipulated

genomes get transfected into cell culture lines which replicate the genome, producing the viral proteins required to assemble a fully functional infectious bronchitis virus particle (Jordan, 2017).

It has been shown that replacing the spike gene of a recombinant IBV with the spike gene of an IBV of another serotype changes the recombinant IBV into that serotype. This can then be used to induce protective immunity against that serotype (Hodgson *et al*., 2004; Jordan, 2017).

This method has many advantages, the main ones being that the method of application is practical for large scale poultry vaccination. The initial one-time cost for developing the recombinant virus may be high, but once produced, it can be maintained in embryonated eggs like any other vaccine could (Jordan, 2017). These recombinant IBVs also have potential as vectors for antigen delivery (Bentley *et al*., 2013).

The biggest disadvantage is licensing. Each new recombinant IBV vaccine that is created would need to be licensed; a process which can take approximately two years (Jordan, 2017). This takes away from the advantage of being able to speedily develop attenuated live vaccines. There is also the risk of reversion to virulence through recombination or point mutation (McGinnes and Morrison, 2014). When used as live vaccines, novel strains may emerge as a result of mutation and recombination, which is a major safety concern (Wu *et al*., 2019).

2.8.2. Inactivated variant vaccines

Inactivated virus vaccines are also used, which offer protection to the kidney and reproductive tracts, as well as the internal tissues (Box *et al*., 1980; de Wit *et al*., 2011; Ladman *et al*., 2002). They are also able to induce high levels of serum antibody titres (Jackwood and de Wit, 2013). These are administered to breeders and layers before they begin to produce eggs. Unlike live vaccines, these do not need to be attenuated because the seed virus is inactivated using a suitable inactivant such as beta-propiolactone or formalin (Jackwood and de Wit, 2013). This vaccine is usually formulated by making use of mineral oil adjuvants (Jansen *et al*., 2006). The main disadvantage of inactivated vaccines is that they must be administered individually by injection (intramuscular or subcutaneous), which is impractical for larger flocks. They are also less effective at preventing respiratory tract infections than live vaccines when challenged with the homologous virulent virus (Cook *et al*., 1986). Killed vaccines are able to induce humoral immunity, but do not induce a cell-mediated immune response (Bande *et al*., 2016).

It is possible to formulate inactivated autogenous vaccines using variant strains that can be used to control the virus in layers. This reduces the risk of live variants spreading to neighbouring flocks and infecting them. These variant inactivated vaccines could possibly offer better protection against variant live IBV than inactivated vaccines could (Ladman *et al*., 2002).

2.8.3. Recombinant vaccines

Recombinant IBV vaccines expressing only IBV antigens, or IBV antigens along with antigens from other pathogens have also been developed but, along with being more difficult to administer, they do not offer the same protection from IBV challenge as live or inactivated vaccines (Li *et al*., 2016; Yang *et al*., 2016; Jordan, 2017). They are most commonly produced from the vector backbones of fowlpox virus or turkey herpesvirus (Jordan, 2017). An acceptable immune response in chickens has been effectively induced by inserting genes coding for infectious laryngotracheitis virus, infectious bursal disease virus and Newcastle disease virus, into these viral backbones (Morgan *et al*., 1992; Darteil *et al*., 1995; Vagnozzi *et al*., 2012). These viral backbones have been used to attempt to develop a recombinant IBV vaccine which expresses the S1 region of the IBV spike gene. These resulted in different levels of protection from homologous virus challenge (Johnson *et al*., 2003; Toro *et al*., 2014a). Other recombinant vaccines have been evaluated, which involved the S1 or S2 region of the IBV spike protein being incorporated into different viral backbones. These backbones included duck enteritis virus, Newcastle disease virus, and avian metapneumovirus (Li *et al*., 2016; Toro *et al*., 2014b). As these backbone viruses have a tropism for respiratory cells, they may induce a stronger immune response in the lymphoid tissues of the head (Jordan, 2017). A study that made use of a recombinant adenovirus vaccine which contained the IBV S1 glycoprotein showed an induced antibody response conferring 90-100% protection against tracheal lesions. This was after heterologous and homologous challenge with N1/62 and Vic S strains of IBV (Johnson *et al*., 2003).

These viral vector vaccines reduce the issues found with live attenuated IBV vaccines that come with RNA mutation (Song *et al*., 1998), however, they are limited by maternally-derived and pre-existing immunity which interferes with the live vector, decreasing the ability of the antigen-presenting cells to take up the antigen, therefore the expression of the transgene, and consequently, negatively affecting the specific immune response (Faulkner *et al*., 2013). The epitope arrangement and conformation that affect the vaccine's efficacy and immunogenicity

may also be affected by a lack of glycosylation, proper protein folding, and post-translational modifications within the host system (Dertzbaugh, 1998).

There are currently no licensed recombinant IBV vaccines used commercially (Jordan, 2017).

2.8.4. Subunit, peptide, and DNA vaccines

Subunit, peptide, and DNA vaccines have also been considered and have demonstrated partial protection against IBV challenge (Yang *et al*., 2009), but are again hindered by cost and method of application for use in a large-scale poultry industry. These vaccines are centred on stimulating the host immune system to develop antibodies against a disease agent, by presenting it with an antigen (Jordan, 2017). Subunit vaccines are usually an antigenic protein that comes from a pathogen while peptide vaccines are small fragments of amino acids from an antigenic protein that comes from a pathogen. Plasmid-based DNA and non-plasmid-based nucleic acid vaccines code for an antigenic protein which is expressed within the cells of the host (Jordan, 2017). The development of multi-epitope peptide vaccines that can be used against many different serotypes of IBV have become a focus for many researchers (Bande *et al*., 2015). Yang *et al*., (2009) used multiple epitopes from the N-protein and S1 protein genes to develop a peptide vaccine against IBV. These synthetic peptides were subjected to immunisation studies and expression analyses, which resulted in significant cellular and humoral immune responses that offered over 80% protection against challenge with a live IBV (Yang *et al*., 2009). Subunit vaccines are safe to use as no infectious virus particles are used in their production. They are highly stable and easy to mass produce as they are genetically engineered (Bande *et al*., 2015; Yang *et al*., 2009).

IBV DNA vaccines have been shown to induce protective immunity in many cases (Song *et al*., 1998; Yu *et al*., 2001; Guo *et al*., 2010). Avian DNA vaccines are able to minimise interference from maternal antibodies and overcome the limitations of immune systems that are not yet fully developed (Oshop *et al*., 2002; Siegrist, 2001). Vaccination using DNA vaccines require naked DNA to be injected, which is impractical in the large-scale poultry industry. Multiple studies have overcome this limitation by using an attenuated strain (*Salmonella enterica* serovar Typhimurium) as a delivery system for the DNA vaccine. In these studies, strong cellular and humoral immune responses are induced by delivering recombinant antigens from pathogens either nasally or orally (Ning *et al*., 2009; Pan *et al*., 2009).

2.8.5. VLP vaccines

Virus-like particles are multiprotein nanostructures that mimic authentic virus particles (McGinnes and Morrison, 2014; Ong *et al*., 2017). The structural proteins of either an enveloped or non-enveloped virus are expressed and self-assemble in order to form VLPs (Jennings and Bachmann, 2008; Chroboczek *et al*., 2014; Ong *et al*., 2017). VLPs do not contain any viral genetic material (Fig. 4) making them non-infectious (McGinnes and Morrison, 2014). This makes them safe as they are unable to replicate (Noad and Roy, 2003).

VLPs that contain a monovalent or multivalent antigen can be produced, which comply with serological surveillance requirements. VLP-based animal vaccines are a promising approach in the development of DIVA vaccines (Liu *et al*., 2013a). VLPs have been produced for various animal viruses and should be considered as new-generation DIVA compliant vaccine candidates in endemic areas (Liu *et al*., 2013a).

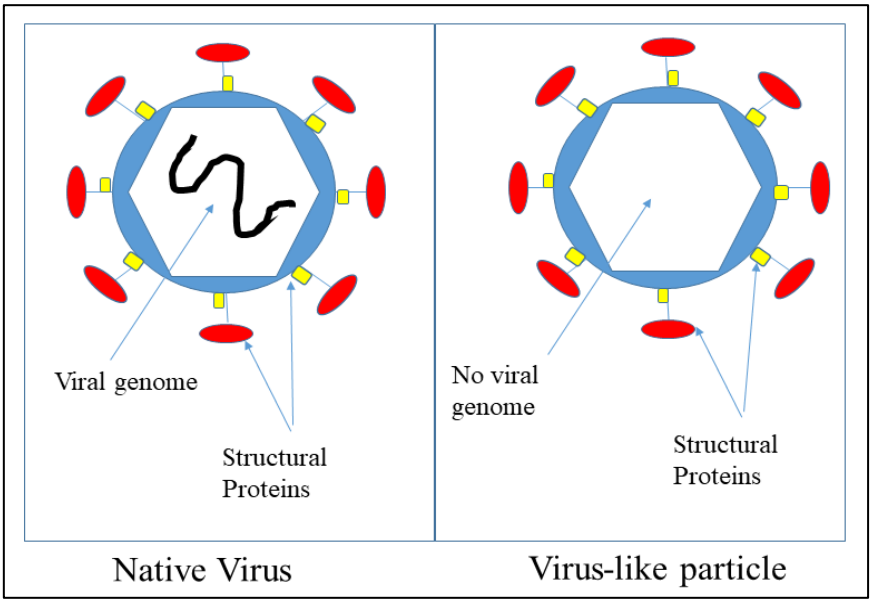

Figure 4: Native virus vs virus-like particle. Adapted from Bellier and Klatzmann (2013).

Virus-like particles are able to induce both cellular and humoral immunity without causing disease like the authentic virus would (Bright *et al*., 2007; Grgacic and Anderson, 2006; Urakami *et al*., 2017). They are highly stable, safe, modifiable particles that have great potential as vaccine candidates (Blokhina *et al*., 2013; Şereflioğlu *et al*., 2017). Purified plant-produced VLPs are free from cell and pathogen contamination (McGinnes and Morrison, 2014). VLP vaccines can be speedily produced in plant-based expression systems (Zdanowicz and Chroboczek, 2016).

2.8.5.1. VLPs produced in SF9 insect cells with Baculovirus expression systems

A study by Liu *et al*., (2013b) demonstrated the assembly of IB VLPs consisting of only the M and full S proteins by making use of a baculovirus expression system in Sf9 cells. These VLPs were evaluated and shown to be as effective at inducing a humoral immune response in chickens and mice as the inactivated H120 vaccine. The IBV-specific neutralising antibodies elicited by the IB VLPs were also comparable to those of the inactivated H120 vaccine. The IB VLPs induced a much higher cellular immune response in mice than the inactivated H120 vaccine did (Liu *et al*., 2013b). This suggested that a simpler approach (compared to one utilising all of the IBV structural proteins) could be used for developing IB VLPs and developing a vaccine against IBV (Liu *et al*., 2013b).

Xu *et al*., (2016) generated IB VLPs by co-infecting Sf9 cells with three recombinant baculoviruses which each coded for either the E, M, or S genes. The S gene was modified by fusing the S1 subunit to the TM and CT domains of the S2 subunit with a flexible peptide linker in between (-GlyGlySerSer-), creating a recombinant S protein. The recombinant S protein retained its ability to self-assemble into VLPs (Xu *et al*., 2016). Not only were the generated VLPs similar in size and morphology to native IBV particles, but they were also shown to be as efficient at eliciting IBV antibodies as an inactivated M41 vaccine. They elicited a strong humoral immune response in chickens when inoculated subcutaneously (Xu *et al*., 2016). Slightly higher neutralizing antibody titres were induced by these VLPs after booster vaccination than with the inactivated M41 vaccine (Xu *et al*., 2016).

2.8.5.2. Chimeric VLP vaccines

Substituting a part, or the entirety, of the extracellular domain of a VLPs surface antigen with that of another virus generates chimeric VLPs. These chimeric VLPs are able to induce an immune response against the surface antigen of the second virus (Weber *et al*., 1995).

Lv *et al*., (2014) investigated the possibility of using influenza VLPs as a platform to express the S1 protein of IBV in order to produce a candidate vaccine. The S1 protein of IBV was fused to the TM and CT domains of the neuraminidase protein of the IAV H5N1 virus producing a fusion protein. This fusion protein assembled with the IAV matrix 1 protein and formed chimeric VLPs that resembled reported IAV VLPs. This was done using a baculovirus expression system. The chimeric VLPs were able to elicit both cellular and humoral immunity

as well as a neutralisation antibody response in both chickens and mice at a considerably higher level than those elicited by the H120 vaccine (Lv *et al*., 2014). This makes them an attractive IBV vaccine candidate.

In a study by Wu *et al*., (2019), the TM and CT domain of the S protein of IBV was separately fused to the IBV S1 protein (producing a recombinant S - rS) and the ectodomain of the Newcastle disease (NDV) F protein (producing a recombinant F - rF). A chimeric IBV-NDV VLP vaccine was constructed which contained both rS and rF, as well as the IBV M protein. This was done using a baculovirus expression system. These VLPs resembled the native IBV particle in both size and morphology (Wu *et al*., 2019). SPF chickens were immunised with the chimeric vaccine in three doses and efficient cellular and immune responses were observed. When challenged with live NDV or IBV, the chimeric IBV-NDV VLPs were able to fully protect against death while reducing the levels of viral RNA in tissues and swabs (Wu *et al*., 2019). The chimeric VLPs were highly immunogenic and were able to completely protect against challenge from both NDV and IBV, making them a promising vaccine candidate and platform for multivalent antigens (Wu *et al*., 2019).

2.8.5.3. Known Requirements for VLP formation

The S protein is the main antigenic determinant of IBV, making it the major target protein for the design and development of new vaccines against the virus (Liu *et al*., 2013b). Interactions between the M and S protein mediate the incorporation of the S protein into the virus particle (or VLP) (Godeke *et al*., 2000). The E and M proteins interact with each other via their CT domains, which may be essential for the assembly of virus (or virus-like) particles (Lim and Liu, 2001; Corse and Machamer, 2003). Many studies suggest that the N protein of coronaviruses is able to form high-order oligomers (He *et al*., 2004). This *N*-oligomerisation is thought to generate a scaffold or improve stability in order to promote M oligomerisation thus aiding in the assembly of virus (or virus-like) particles (Ujike and Taguchi, 2015).

In a study by Ho *et al*., (2004), the formation of human SARS coronavirus VLPs in Sf21 cells required both the M and E proteins. In 293T cells and Vero E6 cells however, the E, M as well as N proteins were essential for the same VLPs (Siu *et al*., 2008; Nakauchi *et al*., 2008). These studies suggest that the assembly of coronavirus VLPs requires at least both the M and E proteins.

In contrast, a study by Liu *et al*., (2013b) demonstrated the assembly of IBV VLPs consisting of only the M and S proteins by making use of a baculovirus expression system in Sf9 cells.

Because VLPs for IBV have not yet been produced in plants, the minimum requirements are not yet established, therefore, different combinations of all four proteins were investigated.

2.9. The Use of Plants for Transient Protein Expression

Recombinant proteins have been produced in plants by stable transformation. This method modifies the genome of the plant species used and allows the foreign gene sequence to be passed down genetically by the production plant (Floss *et al*., 2007; Pogue *et al*., 2010). The advantage of this method is that it shows robust protein expression. The disadvantage is that it can take months to years to derive enough seed to use for recombinant protein production due to slow genetic transformation (Pogue *et al*., 2010). There is also the risk of horizontal transmission of the recombinant gene (Pogue *et al*., 2010).

In transient expression systems, however, the foreign gene is not passed down genetically by the production plant, nor is it transmitted by insects or pollen (Pogue *et al*., 2010). Transient expression systems allow for the speedy expression of proteins, as well as the development and analysis of constructs within a few days (Rybicki, 2010).

Plants are considered a useful alternative host for heterologous protein expression. The advantages being that they are cost-effective and void of contaminating animal pathogens (Thuenemann *et al*., 2013). They are also robust and highly scalable (Chen *et al*., 2006). Plant-based expression systems are safer to use than traditional expression systems because they do not support the growth of infectious viruses or produce contaminating endotoxins (Moustafa *et al*., 2016). Plants are also able to mediate necessary post-translational modifications such as glycosylation or the formation of disulphide bonds (Faye *et al*., 2005). The plasticity of the plant proteome also supports the co-expression of more than one protein which enables the secretory pathway to be manipulated for producing proteins that have homogenous mammalian-like glycosylation (Castilho *et al*., 2010; Castilho and Steinkellner, 2012). Plant-derived vaccines may also allow for oral immunisation (Rybicki, 2009). Transient expression is used to evaluate plant cell ability to produce certain proteins (Sainsbury *et al*., 2009).

Plant-based transient expression is the most cost-effective and speedy recombinant platform currently available. It makes use of the ability that *Agrobacterium tumefaciens* has to transfer

T-DNA into the nucleus of a plant host cell (Gelvin, 2003). It involves transferring genetic information from *A. tumefaciens* to appropriate plant cells via agroinfiltration using a plant expression vector system (D'Aoust *et al*., 2008). This limits expression to the leaf tissue that was infiltrated with the *Agrobacterium* suspensions (Sainsbury *et al*., 2009).

Nicotiana benthamiana leaf tissue supports high levels of heterologous protein expression and is amenable to infiltration. This makes it a desirable host for transient gene expression (Sheludko *et al*., 2007). Up to 1.5 g/kg recombinant protein yields have been obtained using transient protein expression in *N. benthamiana* (Sainsbury and Lomonossoff, 2008).

Using transient expression systems is useful for rapid expression, development, as well as testing of constructs within a few days (Rybicki, 2010). Plant expression systems have been used to assemble VLPs with the immunological properties of live viruses, and this has been achieved within days of infiltration (Theuenemann *et al*., 2013). Plant expression only takes a few days. This means that milligram quantities of recombinant target proteins can be speedily produced. This production speed is an important advantage of plant expression systems because quick responses to the outbreaks of infectious diseases are becoming increasingly important (Margolin *et al*., 2018).

On the other hand, it can take as long as a year to attenuate a live field virus for the purpose of producing a live attenuated vaccine (Jordan, 2017). This disadvantage, amongst others previously discussed, point to an inadequacy with regards to the effectiveness of live-attenuated vaccines.

2.10. Plant Expression Vector Systems

2.10.1. Cowpea Mosaic Virus

Cowpea Mosaic Virus (CPMV) is a *Comovirus* and forms part of the *Comoviridae* family (Sainsbury *et al*., 2010). It infects many legume species including its natural host, cowpea (*Vigna unguiculata*) in which it multiplies to high titres, as well as *N. benthamiana* which is the most commonly used experimental host for the virus (Sainsbury *et al*., 2010, 2012). The CPMV genome is made up of two separately encapsidated positive-stranded RNA molecules that are both required for infection (Sainsbury *et al*., 2010). RNA-1 (5889 nucleotides) encodes

the viral replication and polyprotein processing proteins, while RNA-2 (3481 nucleotides), which depends on RNA-1 for its replication, encodes the proteins that are responsible for cell-to-cell movement and systemic spread of the virus (Sainsbury *et al*., 2010, 2012). CPMV is naturally bipartite, meaning that two RNA molecules have to be replicated in the same cell; therefore, virus exclusion does not occur. Virus exclusion occurs when two constructs that are based the same virus are introduced into a cell, but the first replicating construct prevents the second construct from replicating (Sainsbury *et al*., 2013). This means that monopartite systems can only be used for producing a single protein in a cell, unless a different virus that does not compete with the first, is used for expressing a second protein (Giritch *et al*., 2006). This make CPMV attractive as a virus-based vector (Sainsbury *et al*., 2012) for expression and for assembling a number of heteromultimeric protein complexes, such as VLPs, in the same plant cell.

2.10.2. CPMV-based expression systems

CPMV-based expression systems focus on the modification of the RNA-2 sequence, with co-inoculated RNA-1 constructs providing any required replication functions (Sainsbury *et al*., 2010, 2012). One of the initial vectors (replication-competent deleted vector - pM81B-S2NT-1) allowed the entire RNA-2 open reading frame downstream of the second in-frame AUG at position 512 to be removed by restriction enzyme digestion and replaced with any sequence with compatible ends (Sainsbury *et al*., 2012). These constructs were then transformed into *A. tumefaciens* and co-infiltrated into *N. benthamiana* leaves with plasmids that contained RNA-1 and a suppressor of gene silencing P19 (Sainsbury *et al*., 2012). These vectors had the advantage of biocontainment compared to CPMV vectors that were based on the full-length RNA-2 molecules (Sainsbury *et al*., 2010).

2.10.3. CPMV-HT expression system

Sainsbury and Lomonossoff (2008) discovered that replication of the deleted version of RNA-2 was not necessary to obtain high levels of protein expression in plants. The replication-competent RNA-2 system required the sequence to be fused to AUG 512, making cloning a more complicated two-step strategy, with a separate construct containing a silencing suppressor also required (Sainsbury *et al*., 2012). Eliminating the first in-frame AUG at position 161 and

an out-of-frame AUG at 115, thus stopping replication, amplified the levels of expression of many proteins (Sainsbury *et al*., 2010). This was caused by the mRNAs being rendered "hypertranslatable" (HT) by the modified 5' - UTR. The resulting expression system was called CPMV-HT (Sainsbury *et al*., 2010, 2012). The advantages of eliminating replication while still achieving high levels of expression removed any problems that involved virus exclusion and genetic drift, while having no limits on the size or complexity of foreign sequences expressed (Sainsbury *et al*., 2012). The host range of HT leaders is also extended past host species that require the replication of CPMV to occur (Sainsbury *et al*., 2010). Therefore, the CPMV-HT system allowed for simultaneous expression of multiple proteins in the same cell (Sainsbury, *et al*., 2012). However, this system still required a two-step cloning procedure as well as the co-infiltration of a silencing suppressor (Sainsbury *et al*., 2012).

2.10.4. pEAQ vector expression system

The pEAQ series of binary vectors was developed based on the abovementioned CPMV-HT system. The pEAQ series has been derived from a deleted version of RNA-2 of CPMV (Sainsbury *et al*., 2009, 2012). This expression system is used to transiently express high levels of a foreign protein rapidly in plants. This is performed without viral replication (Sainsbury *et al*., 2012, Sainsbury and Lomonossoff, 2008). The pEAQ plasmids are small binary vectors that are modular and allow multiple coding sequences to be inserted on the same T-DNA segment (Sainsbury *et al*., 2012).

To do this, the CPMV-HT expression cassette as well as the P19 silencing suppressor was placed in the T-DNA region of a binary vector (Fig. 5) (Sainsbury *et al*., 2010).

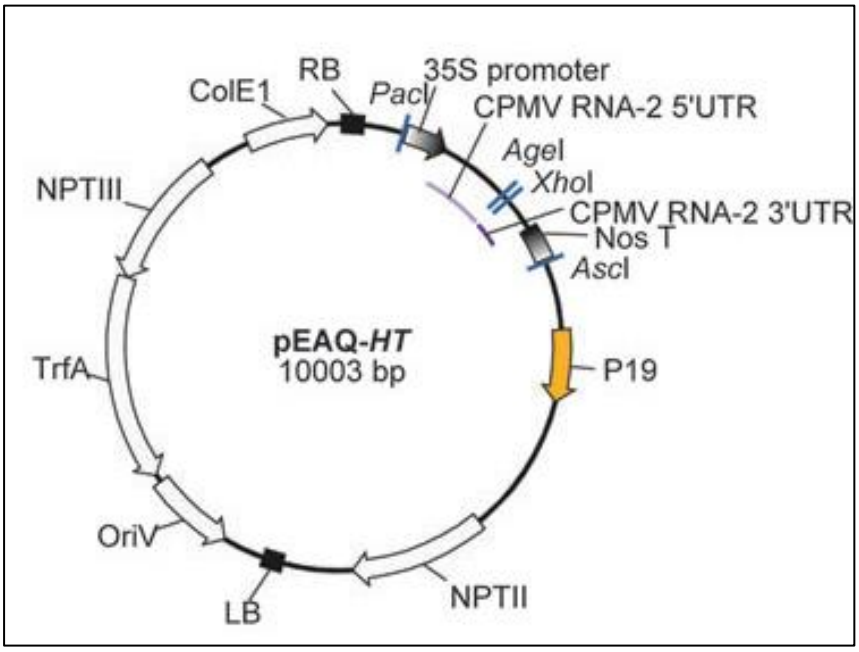

Figure 5: pEAQ-HT plant expression vector (Theunemann *et al*., 2013).

Each pEAQ vector contains a polylinker of restriction sites which can be used to insert any expression cassette or sequence. Removing reading frame dependence meant that a one-step cloning procedure could be utilised through restriction enzyme-based cloning or using the GATEWAY® system of recombination-based cloning (Sainsbury *et al*., 2010, 2012). These expression vectors are also equipped with the sequences required for His-tagging proteins of interest at either the N- or C- terminus, which is useful for purification of proteins from plant tissue (Sainsbury *et al*., 2012). The pEAQ vector series is useful for situations where large amounts of protein need to be synthesised (Saunders *et al*., 2009; Vardakou *et al*., 2012), as well as situations whereby the co-expression of more than one protein is required, such as the manipulation of metabolism, the expression of antibodies (Sainsbury *et al*., 2012), or the assembly of more than two structural proteins to form VLPs in plants. The pEAQ-HT vector was used in this research project. CSIR Biosciences and UP each have licence agreements (Plant Bioscience Ltd., PBL, Norwich) to use the CPMV technology for research purposes until 2023 with the option to extend the licence agreement thereafter.

CHAPTER 3

Materials and Methods

3.1. Synthetic construct design and cloning of genes into plant expression vector pEAQ-HT

3.1.1. Design of Constructs

Gene sequences encoding the Spike (S) (Protein ID AKC34133.1), Envelope (E) (Protein ID AKC34135.1), Membrane (M) (Protein ID AKC34136.1) and Nucleoprotein (N) (Protein ID AKC34140.1) structural proteins of IBV (QX-like strain ck/ZA/3665/11, Abolnik, 2015) were obtained from the National Centre for Biotechnology Information (NCBI). The gene sequences were chicken codon-optimised by BioBasic using their proprietary algorithm. These genes were then chemically synthesised by BioBasic Inc. Canada with unique *Age*I and *Xho*I sites on the 5' and 3' ends, respectively, as well as a stop codon downstream of each gene. All other *Age*I and *Xho*I sites within the genes were eliminated. Chemically synthesised genes were shipped to South Africa in lyophilised form. Four µg of each pUC57 vector-based construct were provided and resuspended to a final concentration of 200 ng/µl in sterile milliQ H_2O. All reagents were molecular biology grade and obtained from Sigma Life Science unless otherwise indicated.

3.1.2. Restriction enzyme digests

Each sequence was then cloned independently into a pEAQ-HT expression vector via sticky-end directional *Age*I/ *Xho*I restriction enzyme-based cloning (Fig. 6). Each insert (S, E, M and N) as well as the pEAQ-HT plasmid was digested with *Age*I and *Xho*I restriction enzymes (Thermo Fisher Scientific) in order to generate compatible sticky-ends for ligating (37°C for 45 minutes). The digests were then resolved on a 1.2% agarose gel. The inserts, as well as the pEAQ-HT vector were cut out using a sterile scalpel blade (for each individual gene and

backbone) and purified using the Zymoclean™ Gel DNA Recovery Kit and eluted in 10 µl of sterile milliQ H_2O.

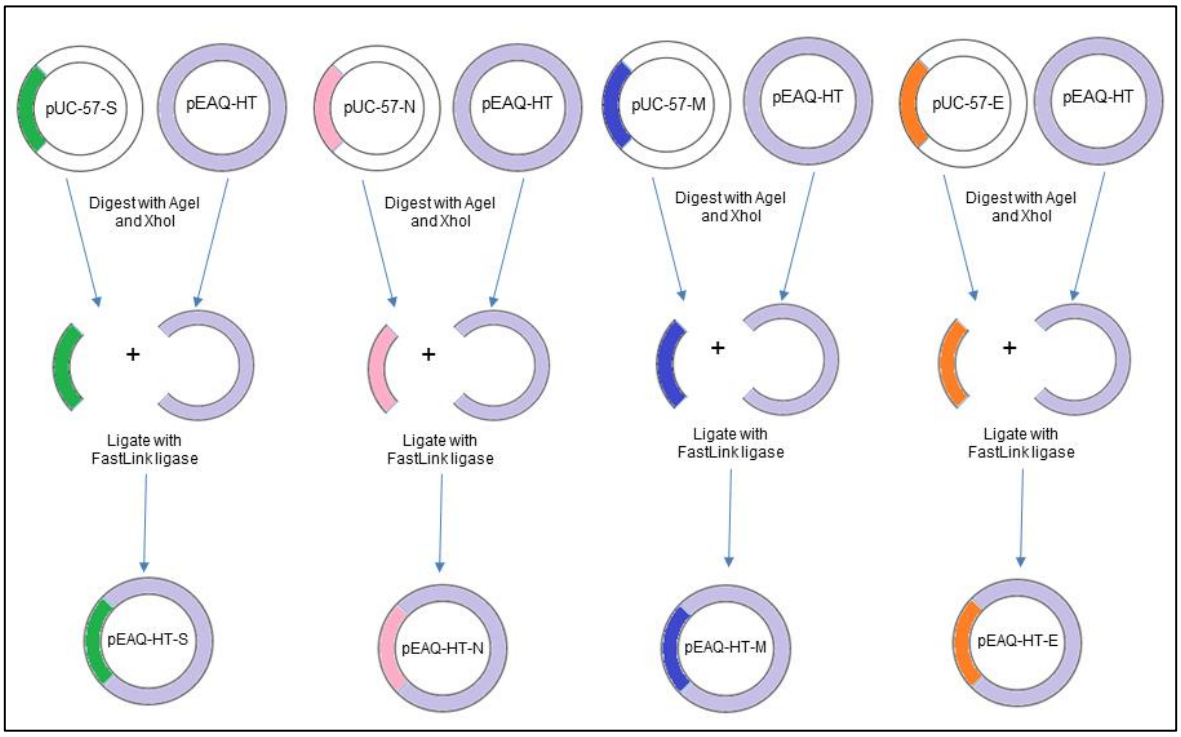

Figure 6: Diagram illustrating the design of pEAQ-HT-S, pEAQ-HT-N, pEAQ-HT-M, and pEAQ-HT-E.

3.1.3. Ligation reactions

Four separate ligation reactions were set up containing linearised vector DNA (pEAQ-HT) and each insert DNA (S, E, M or N) at a molar ratio of 1:3 along with Fast-link DNA ligase and ligase buffer found in the Fast-link™ DNA Ligation Kit (Epicentre). The ligation reactions were then incubated for an hour producing four pEAQ-HT constructs each containing one of the genes encoding the IBV structural proteins (S, E, M and N) (Fig. 6). They were then heat inactivated at 70°C for 15 minutes.

3.1.4. Transformation

Each pEAQ-HT construct was independently transformed into electrocompetent DH10B cells (ThermoFisher Scientific) using a Gene Pulser™ (Bio-Rad) at 1.8 kV, 200 Ω, and 25 µF. The transformed cells were recovered in SOC (0.5% (w/v) yeast extract, 2% (w/v) Tryptone, 10

mM NaCl, 2.5 mM KCl, 2.5 mM $MgCl_2$, 20 mM MgSO4, 20 mM Glucose) media on a rotary shaker (175 rpm) at 37°C for an hour. Thereafter, they were plated onto Luria Bertani (LB) agar (10 g/L NaCl, 5 g/L yeast extract, 10 g/L Tryptone, 15 g/L agar) plates containing Kanamycin (50 µg/ml) for selection of pEAQ-HT constructs and incubated at 37°C overnight. The next day, colonies were picked and verified via colony PCR using pEAQ-HT specific primers (Table 1) for pEAQ-HT-E, pEAQ-HT-N, and pEAQ-HT-M to confirm the presence of the inserts. pEAQ-HT specific forward and reverse primers were used unless otherwise specified.

For pEAQ-HT-E, pEAQ-HT-N, and pEAQ-HT-M, PCR mixes were prepared using sterile filter tips (as for all PCR reactions). The PCR mixes contained a final concentration of 0.2 µM forward/reverse primer (Table 1) (pEAQ-HT primers for E and M, and FSC5 primers for N) and the Ampliqon DNA polymerase master mix red. The latter contained Taq DNA polymerase enzyme including dNTPs and 1.5 mM $MgCl_2$ (Cat. No.: A180306, Ampliqon). Colonies picked from the Luria agar plate using sterile tips were resuspended in the PCR mix. The reactions were then set up according to the manufacturer's instructions and performed in the GeneAmp 2720 Thermocycler (Applied Biosystems). The cycling conditions were as follows: 1 cycle of 94˚C for 2 min, followed by 35 cycles of 94˚C for 15 sec, 55°C for 30 sec and 72°C for 30 sec followed by 1 cycle of 72°C for 3 min. The PCR products were separated on a 1.2% agarose gel. Molecular weight marker (GeneRuler DNA ladder mix, SM0331, Thermo Fisher Scientific) was used and pEAQ-HT containing a known insert served as a positive control. Insert-containing colonies (for E, N, and M) were propagated, and the plasmids were extracted. The structural protein encoding sequences were verified via dideoxy Sanger DNA sequencing (Inqaba Biotechnical Industries (Pty) Ltd). Glycerol stocks of each confirmed colony were prepared and stored at -80°C.

Due to the large size of the S protein (3.4 kb) the construct was miniprepped (Zyppy Plasmid Miniprep kit) before PCR confirmation of pEAQ-HT-S using pEAQ-HT specific primers (Table 1). In all PCR experiments, Ampliqon was used for inserts of 1-1.5 kb and Phusion flash for inserts beyond 3 kb.

For pEAQ-HT-S, a PCR mix was prepared containing a final concentration of 0.5 µM forward/reverse primer (Table 1) and the Phusion Flash High-Fidelity PCR Master Mix containing Phusion Flash II DNA Polymerase enzyme (Catalog number: F548S, Thermo Fisher Scientific) and were set up according to the manufacturer's instructions and performed

in the GeneAmp 2720 Thermocycler (Applied Biosystems). The cycling conditions were as follows: 1 cycle of 98˚C for 10 sec, followed by 30 cycles of 98˚C for 1 sec, 65°C for 5 sec and 72°C for 55 sec, followed by 1 cycle of 72°C for 1 min. The PCR products were separated on a 1% agarose gel. Molecular weight marker (GeneRuler DNA ladder mix, SM0331) was used and pEAQ-HT containing a known insert served as a positive control. Insert-containing colonies (for S) were propagated, and the plasmid DNA was extracted. The structural protein encoding sequence was verified via dideoxy Sanger DNA sequencing (Inqaba Biotechnical Industries (Pty) Ltd). Glycerol stocks of each confirmed colony were prepared and stored at -80°C.

Table 1: Forward and reverse primers used for PCR validation

Code	Sequence (5'-3')	Concentration (µM)	Tm value (°C)
pEAQ-HT - F	ACTTGTTACGATTCTGCTGACTTTCGGCGG	10	74.7
pEAQ-HT - R	CGACCTGCTAAACAGGAGCTCACAAAGA	10	63.6
FSC5 - F	GGTTTTCGAACTTGGAGAAA	10	48.7
FSC5 - R	AGAAAACCGCTCACCAAACATAGA	10	56

The pUC57 vectors (containing the original inserts) were also transformed into electrocompetent DH10B cells (Thermo Fisher Scientific) using the Gene Pulser™ (Bio-Rad) at 1.8 kV, 200 Ω, and 25 µF. The transformed cells were recovered in SOC media on a rotary shaker (175 rpm) at 37°C for an hour. Thereafter, they were plated into LB agar plates containing Carbenicillin (for Ampicillin resistance) (50 µg/ml) for selection of the pUC57 vector and incubated at 37°C overnight. The next day, colonies were picked and propagated in Luria broth (10 g/L NaCl, 5 g/L yeast extract, 10 g/L Tryptone). Glycerol stocks of each construct were made and stored at -80°C.

3.2. Transformation of constructs into *A. tumefaciens*

3.2.1. Transformation into *A. tumefaciens*

The sequence-validated recombinant pEAQ-HT plasmids were transformed into electrocompetent *A. tumefaciens* (AGL-1, GV3101::pMP90, or LBA4404 strains) using a Gene Pulser™ (Bio-Rad) (1.44 kV, 200 Ω, and 25 μF) in order to determine the most appropriate *Agrobacterium* strain for expression and assembly of VLPs in *N. benthamiana* ΔXT/FT plants (ΔXT/FT is a mutant strain of *N. benthamiana* that facilitates mammalian-like glycosylation (Strasser *et al*., 2008)) which offer improved protein expression. The transformed cells were recovered in SOC medium on a rotary shaker (175 rpm) at 30°C for 3 hours. The cells were then plated onto LB agar plates containing Kanamycin (50 μg/mL) (to select for pEAQ-HT) plus Rifampicin to select for *Agrobacterium* and the appropriate antibiotic for the chosen *A. tumefaciens* strain (i.e. Carbenicillin (100 μg/mL) for AGL-1, Gentamycin (10 μg/mL) for GV3101::pMP90, or Streptomycin (100 μg/mL) for LBA4404) and incubated at 28°C for 2-3 days. Colonies were then picked and propagated in LB broth (for AGL-1 and GV3101::pMP90) or YMB (0.1% yeast extract, 1% Mannitol, 1.7 mM NaCl, 0.8 mM $MgSO_4.7H_20$, 2.2 mM $K_2HPO_4.3H_2O$) media (for LBA4404) containing the appropriate antibiotics for selection and incubated on a rotary shaker (175 rpm) at 28°C overnight until the OD_{600} was ≥ 2. These cultures would be used for *N. benthamiana* ΔXT/FT agroinfiltration. Glycerol stocks of each confirmed colony were made using 65% glycerol (50:50 ratio) and stored at -80°C.

3.2.2. Culturing of *A. tumefaciens*

The target cultures were streaked onto LB agar plates with the appropriate antibiotics for each strain and cultured at 28°C overnight for 48 hours. The streaked cultures were then scraped off the agar plates and each inoculated separately into 200 ml LB medium (for AGL-1 and GV3101::pMP90) or YMB (for LBA4404) medium (containing 200 μM 3,5- Dimethoxy-4-hydroxy-acetophenone, Sigma Life Science) with the appropriate antibiotics, and incubated overnight at 28°C on a shaker incubator (200 rpm).

3.2.3. Preparing Inoculum

Cells were harvested from the prepared overnight cultures by centrifuging them at 7000 rpm for 7 minutes at 10°C. The cell pellets were resuspended in 2-(N-morpholino)ethanesulfonic acid (MES) infiltration buffer (10 mM MES pH 5.6, 10 mM $MgCl_2$, 200 µM 3,5- Dimethoxy-4-hydroxy-acetophenone). Various combinations of the *Agrobacterium* suspensions were prepared: S alone; S and E; S and M; S, E, and M in 1:1 or 1:1:1 ratios. These were then diluted to a final OD_{600} of 1-2. The solutions were then left at room temperature for 0.5 - 3 hours prior to infiltration.

3.3. Infiltration of *N. benthamiana* ΔXT/FT leaves with *A. tumefaciens* and crude protein extraction

3.3.1. Infiltration of plant leaves

The leaves of 3-4 week old *N. benthamiana* ΔXT/FT plants (~20 cm in height) were syringe-infiltrated with the abovementioned *Agrobacterium* combinations. A pEAQ-HT (without insert) *Agrobacterium* suspension was used as a negative control. The plants were then incubated at 27°C for 6-8 days post-infiltration (dpi) and watered daily.

3.3.2. Harvesting of leaf material

The *Agrobacterium*-infiltrated leaves were harvested at two different time points (6 and 8 dpi) in order to determine the optimal time for protein expression and VLP formation. The leaves were harvested, weighed, and the crude plant proteins were prepared for extraction.

3.3.3. Extraction of crude plant proteins

The leaf tissue that was harvested at each interval was extracted in two volumes of VLP extraction buffer using a multipurpose juice extractor. Two different buffers were tested, PBS and Bicine buffer: 1X PBS (10X PBS pH 7.4 – 18 mM KH_2PO_4, 100 mM Na_2HPO_4, 27 mM KCl, 140 mM NaCl) buffer (1X PBS with the addition of 0.04% sodium metabisulfite) or

Bicine (50 mM bicine, pH 8.4; 20 mM NaCl). Both dithiothreitol (1 mM DTT, ThermoFisher Scientific) and protease inhibitor cocktail (Sigma, P2714) were added shortly before extraction. The large cell debris was removed by filtering the juice through two layers of cheesecloth and centrifuging the plant lysate at 7000 rpm for 4 minutes at 4°C. The supernatant was kept for analysis.

3.4. Analysis of crude plant proteins and visualisation of VLPs

3.4.1. Protein purification

The IBV virus-like particles (VLP) were purified using Iodixanol (Optiprep™, Sigma) density gradient centrifugation. The Iodixanol solutions were prepared by dissolving ultra-high quality Iodixanol into VLP dilution buffer (1 X PBS buffer) and layered into gradients of 10% incrementing steps from 60% to 20%. The following volumes of Optiprep™ concentrations were used: 1 ml 60%, 1 ml 50%, 1.5 ml 40%, 1.5 ml 30%, 1 ml 20%. The step gradients were prepared in 13.2 ml ultra-clear™ Beckman tubes (Beckman Coulter, Cat no. 344059). The clarified cell lysates were layered on top of the step gradients, and centrifuged at 32 000 x g for 2 hours at 10°C using the ultracentrifuge (SW Ti 41 Rotor – Beckman Coulter). Thereafter, the gradients were harvested in 500 µl fractions using a Minipuls2 peristaltic pump (Gilson). Selected fractions were analysed by denaturing SDS-PAGE and Immunoblotting for the presence of structural proteins of IBV VLPs.

3.4.2. Protein confirmation

3.4.2.1. Sodium dodecyl sulphate-polyacrylamide gel electrophoresis (SDS PAGE)

Fractions 7-12 (20-40% iodixanol fractions) from 6 dpi were chosen for analysis in order to identify the fraction containing the IB VLPs. A 4-12% Bis-Tris Bolt™ (Life Technologies) mini gel was prepared for analysing the protein content in each of the chosen fractions. A master mix containing sample buffer and reducing agent was prepared and 14 µl was added to 26 µl of each density gradient fraction according to the manufacturer's recommendations. The

samples were then heated at 70°C for 10 minutes and loaded onto a 4-12% Bis-Tris Bolt™ mini gel along with a SeeBlue® Plus2 prestained protein marker (Invitrogen), pEAQ-HT empty (negative control), and an IBV QX-like strain (positive control). The gel was run in Bolt® MES SDS running buffer using the Mini-PROTEAN® Tetra system (Bio-Rad) at a constant voltage of 200 V for approximately 20 minutes.

The gel was stained in Coomassie Brilliant Blue G250 Staining Solution (50% methanol (Minema), 10% acetic acid (Minema), 0.1% Coomassie Brilliant Blue G250 (Merck)) for 30-60 minutes before destaining overnight in destaining solution (10% ethanol, 10% acetic acid, 10% isopropanol) on a Belly Dancer Orbital shaker (Sigma). The gel was then visualised for protein content using the ChemiDoc™ MP Imaging System (Bio-Rad). Fractions 10 and 11 were thereafter used in all future experiments as the highest content of IBV VLP structural proteins were established to be present those fractions.

After establishing the fractions with the highest protein content, fractions 10 and 11 from both 6 and 8 dpi were mixed with the Bolt™ sample buffer and reducing agent (as described above). The SDS PAGE protocol was repeated as explained above and the gel was then visualised for protein content.

3.4.2.2. SDS-PAGE for immunoblotting

Eighteen microlitres of density gradient fractions 10 and 11 from both 6 and 8 dpi were mixed with Laemmli protein sample buffer (4% SDS, 20% glycerol, 10% 2-mercaptoethanol, 0.004% bromophenol blue and 0.125 M Tris HCl, pH 6.8) and heated at 95°C for 5 minutes to denature the proteins. The samples were then loaded onto a 10% SDS polyacrylamide gel which was prepared according to the manufacturer's instructions (BioRad TGX™ and TGX stain-free™ FastCast™ Acrylamide Kit) along with the Precision Plus Protein™ Western C™ standard protein marker (BioRad), pEAQ-HT empty (negative control), and an IBV QX-like strain (positive control). The gel was run in 1 X TGS buffer (25 mM Tris-HCl; pH 8.3, 200 mM glycine, 0.1% SDS) using the Mini-PROTEAN® Tetra system (Bio-Rad) at an applied current of 50V for 20 minutes and thereafter an applied current of 130V for approximately 1.5 hours.

3.4.3. Immunoblotting

SDS-PAGE gels were subjected to an Immunoblotting protocol using QX-like IBV-specific antiserum from a vaccinated flock (provided by the Poultry Section, Department of Production Animal Studies, University of Pretoria) in order to confirm the identity as well as the position of the IBV structural proteins on the gels. The QX-like IBV-specific antiserum was optimally matched with the QX-like antigen being used in this study. The internal proteins are more conserved between IBV serotypes and would be detected by immunoblotting even if the S protein was not identical. The protocol was done by immunoblotting the protein samples onto a PVDF membrane within the Trans-blot® Turbo™ Transfer Pack (Bio-Rad) using the Trans-blot® Turbo™ Transfer system (Bio-Rad) mixed molecular weight application (1.3 A; 25 V; 20 minutes). The membrane was then incubated in 3% blocking solution (BSA in 1 X PBS) overnight at room temperature with gentle agitation. The next day, the blocking solution was poured off, and replaced with more blocking solution and 1:1000 per 10 ml of the QX-like IBV-antiserum (primary antibody). This was then incubated for 2 hours at room temperature with gentle agitation. The solution was then decanted, and the membrane was washed three times for 10 minutes each with wash buffer (1 X PBS and 0.1% TWEEN® 20 (Merck)), shaking at room temperature. The membrane was then incubated in 1 X PBS TWEEN with 1:2000 per 10 ml of Goat α-chicken HRP (secondary antibody, Sigma Aldrich: (SAB370199-2MG)) and Precision Protein™ StrepTactin-HRP conjugate (BioRad) for 2 hours at room temperature with gentle agitation. The solution was then decanted, and the membrane was washed three times for 10 minutes each with wash buffer (1 X PBS and 0.1% TWEEN® 20 (Merck)), shaking at room temperature. The proteins were then detected by adding the Clarity™ Western ECL chemilluminescence substrate (BioRad) to the membrane and visualising using the ChemiDoc™ MP Imager (Bio-Rad). The Chemi Hi Resolution application was used to take photographs of the chemilluminescence signals approximately every second for 15 seconds.

3.4.4. LC-MS/MS based peptide sequencing

Candidate viral protein bands of the correct size were cut out from the SDS-PAGE gel and sent for LC-MS/MS based peptide sequencing (a commercial service offered at CSIR Biosciences). The gel bands were trypsin digested following the protocol described in Shevchenko *et al*., (2007). To summarise, the gel bands were destained in 50 mM NH_4HCO_3/50% MeOH. This was followed by in-gel protein reduction (50 mM DTT in 25 mM NH_4HCO_3) and alkylation

(55 mM iodoacetamide in 25 mM NH_4HCO_3). The proteins were digested at 37°C overnight using 5-50 µl (depending on the size of the gel piece) of 10 ng/µl trypsin. The digests were then resuspended in 20 µl of 2% acetonitrile/0.2% formic acid and analysed using a Dionex Ultimate 3000 RSLC system coupled to an AB Sciex 6600 TripleTOF mass spectrometer. The peptides were de-salted on an Acclaim Pep/map C18 trap column (100 µM x 2 cm) for 2 minutes at 15 µl/min using 2% acetonitrile/0.2% formic acid. They were then separated on an Acclaim PepMap C18 RSLC column (300 µM x 15 cm, 2 µm particle size). Peptide elution was then performed by making use of a flow-rate of 8 µl min-1 with a gradient 4-60% B in 15 minutes (A: 0.1% formic acid; B: 80% acetonitrile per 0.1% formic acid). An electrospray voltage was applied to the emitter (5.5 kV). The 6600 TripleTOF mass spectrometer was operated in Data Dependent Acquisition mode. The precursor scans were acquired from m/z 400-1500 by using an accumulation time of 250 ms followed by 30 product scans, acquired from m/z 100-1800 at 100 mn each. This was done for a total scan time of 3.3 seconds. Multiply charge ions (2+ -5+, 400 – 1500 m/z) were automatically fragmented in Q2 collision cells with nitrogen as the collision gas. The collision energies were chosen automatically as a function of m/z as well as charge. Protein pilot v5 making use of paragon search engine (AB Sciex) was used in order to compare the obtained MS/MS spectra with the Uniprot Swissprot protein database. Only the proteins with a threshold above ≥ 99.9% confidence were reported.

3.4.5. Negative staining TEM visualisation of VLPs

The IBV VLPs were visualised by adsorbing the samples onto carbon-coated holey copper grids and stained. The protein adsorption was done by floating the grids on the undiluted protein sample for 5 minutes. The excess sample was blotted off onto filter paper and the grids were washed 5 times in 5µl of milliQ water, blotting the excess water off into filter paper each time. The grids were then stained in 2% uranyl acetate, pH 4.2 for 30 seconds and the excess stain was blotted off onto filter paper. Alternatively, Iodixanol gradient fractions were adsorbed onto holey carbon-coated copper grids and stained with sodium phosphotungstate, pH 7.0. The grids were air dried and imaged using a CM10 Transmission electron microscope (Philips) at Onderstepoort, Laboratory for Microscopy and Microanalysis under the supervision of Ms Antoinette Lensink at UP (University of Pretoria). The measuring tool on the Gatan Digital Micrograph software was used to measure the diameters of the visualised particles.

3.5. Redesign and cloning of recombinant S genes

3.5.1. Design of Recombinant Constructs

A gene sequence encoding the Spike (S) structural protein of IBV (QX-like strain ck/ZA/3665/11, Abolnik, 2015) was obtained from the National Centre for Biotechnology Information (NCBI). Four genetically modified versions of the S protein were designed with the aim of improving protein expression in plants and assembly of virus-like particles by making use of the C-terminal sequences of the IAV HA gene (H6 Sublineage 1) (Fig. 7). The recombinant constructs were as follows: 1 – original S gene (Protein ID AKC34133.1); 2 – recombinant S gene with the TM domain substituted with that of the IAV HA gene; 3 - recombinant S gene with the TM and CT domains substituted with those of the IAV HA gene; 4 – recombinant S gene with a murine signal peptide replacing the native signal peptide, KOZAK sequence added, and the ER retention signal removed; 5 - recombinant S gene with a murine signal peptide replacing the native signal peptide, KOZAK sequence added, TM domain substituted with that of the IAV HA gene, and the ER retention signal (KKSV) removed. Primers that would appropriately modify the S gene, and add the required *Age*I/*Xho*I sites were also ordered from Integrated DNA Technologies Inc (IDT) (Table 2).

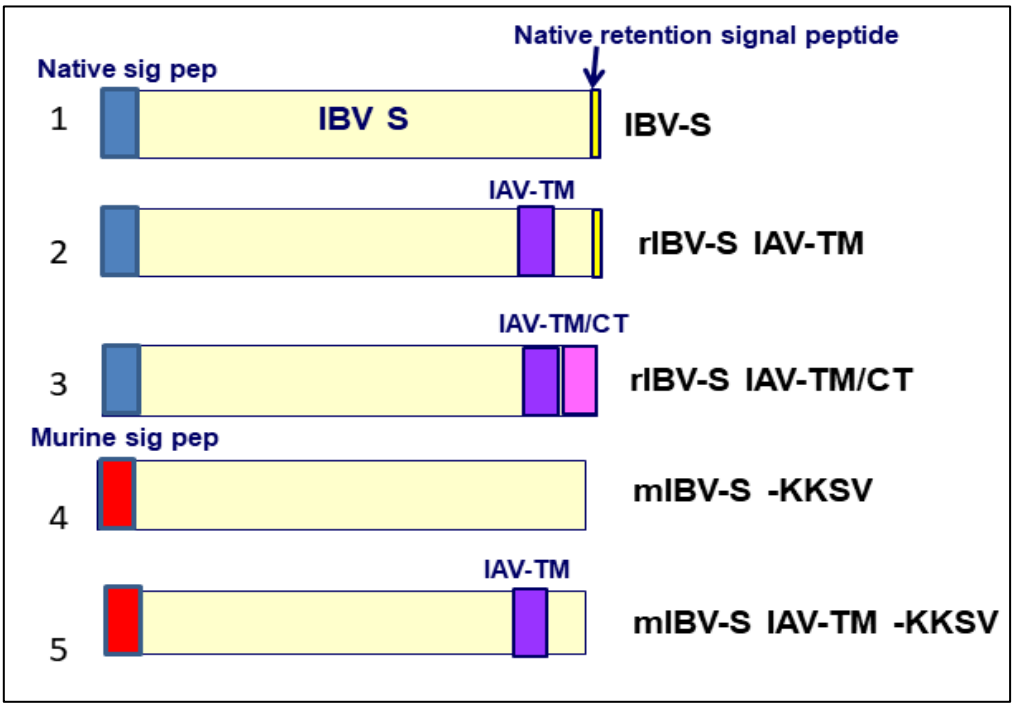

Figure 7: Recombinant IBV S proteins modified from the original S gene using primers.

The gene sequences were chicken codon-optimised as per the algorithm of BioBasic. IBV-S-IAV-TM and IBV-S-IAV-TM/CT were then synthesised by BioBasic Inc. Canada with a stop codon downstream of each gene. All *Age*I and *Xho*I sites in the genes were silenced. Four µg of each pUC57 vector-based construct were obtained in lyophilised form. Each sample was resuspended to a final concentration of 200 ng/µl in sterile milliQ H_2O. The primers were also obtained in lyophilised form, resuspended in sterile milliQ H_2O to a stock concentration of 100 µM and further diluted to a working concentration of 10 µM. rIBV-S-IAV-TM and rIBV-S-IAV-TM/CT (Fig. 7) were then synthesised by using primers to insert *Age*I *and Xho*I sites, N-terminal and C-terminal, respectively for each of the genes. mIBV-S-KKSV (Fig. 7) was synthesised by modifying the original S gene (gene 1, Fig. 7) using primers (Table 2) and mIBV-S-IAV-TM-KKSV was synthesised by modifying gene 2 (Fig. 7) using the same primers. All reagents were molecular biology grade and obtained from Sigma Life Science unless otherwise indicated.

3.5.2. PCR Amplification

PCR mixes were prepared which contained a final concentration of 0.3 µM forward/reverse primer (Table 2), the 5X KAPA HIFI buffer, KAPA dNTP mix, and KAPA HIFI DNA polymerase enzyme (KAPA Biosystems) and were set up according to the manufacturer's instructions and performed in the GeneAmp 2720 Thermocycler (Applied Biosystems). The cycling conditions were as follows: 1 cycle of 95°C for 3 min, followed by 10 cycles of 98°C for 20 sec, 60°C for 15 sec and 72°C for 150 sec, followed by 25 cycles of 98°C for 20 sec, an annealing temperature gradient from 60°C to 64°C for 15 sec and 72°C for 200 sec, followed by 1 cycle of 72°C for 5 min. The PCR products were separated on a 1% agarose gel. Molecular weight marker (Gene Ruler ladder mix, SM0331) was used. Target bands were cut out and purified using the Zymoclean™ Gel DNA Recovery Kit and eluted in milliQ water.

Table 2: Primers for modifying the original S gene to create recombinant S genes

Gene	Code	Sequence (5'-3')	Concentration (µM)	Tm value (°C)
rIBV-S-IAV-TM	Fw TM-CT	GACACCGGTATGCTGGTGAAGAGCCTGTT	10	65.1
	Rv TM	TTGCTCGAGTCACACGCTTTTCTTAGGTCTGTA	10	63.2
rIBV-S-IAV-TM/CT	Fw TM-CT	GACACCGGTATGCTGGTGAAGAGCCTGTT	10	65.1
	Rv TM-CT	TAGCTCGAGTCAGATGCACACTCTACACTGCAT	10	64.2
mIBV-S-KKSV Ultramer primer	Fw mIBV-S	TTAACCGGTGCCACCATGGGATGGAGCTGGATC TTTCTTTTCCTCCTGTCAGGAGCTGCAGGTGTCC ATTGCAACCTGTTTGATAGCGAT	10	73.3
	Rv IBV-S-KKSV	CCGCTCGAGTCATGGTCTATACTGCTC	10	61.7
mIBV-S-IAV-TM-KKSV Ultramer primer	Fw mIBV-S	TTAACCGGTGCCACCATGGGATGGAGCTGGATC TTTCTTTTCCTCCTGTCAGGAGCTGCAGGTGTCC ATTGCAACCTGTTTGATAGCGAT	10	73.3
	Rv IBV-S-KKSV	CCGCTCGAGTCATGGTCTATACTGCTC	10	61.7

3.5.3. Restriction enzyme digests

Each fragment was cloned independently into a pEAQ-HT expression vector via sticky-end directional *Age*I/ *Xho*I restriction enzyme-based cloning. Each PCR product (rIBV-S-IAV-TM, rIBV-S-IAV-TM/CT, mIBV-S-KKSV and mIBV-S-IAV-TM-KKSV) as well as the pEAQ-HT plasmid was digested with *Age*I and *Xho*I restriction enzymes (ThermoFisher Scientific) in order to generate compatible sticky-ends for ligation (37°C for 45 minutes). The digests were then resolved on a 1% agarose gel. The inserts, as well as the pEAQ-HT vector were cut out using a sterile scalpel blade (for each individual gene and backbone) and purified using the Zymoclean™ Gel DNA Recovery Kit and eluted in 10 µl of sterile milliQ H_2O.

3.5.4. Ligation reactions

Four separate ligation reactions were set up containing linearised vector DNA (pEAQ-HT) and each insert DNA at a molar ratio of 1:3 along with Fast-link DNA ligase and ligase buffer found in the Fast-link™ DNA Ligation Kit (Epicentre). The ligation reactions were then incubated for an hour producing four new pEAQ-HT constructs each containing one of the

genes encoding the recombinant S protein (Fig. 8). They were then heat inactivated at 70°C for 15 minutes.

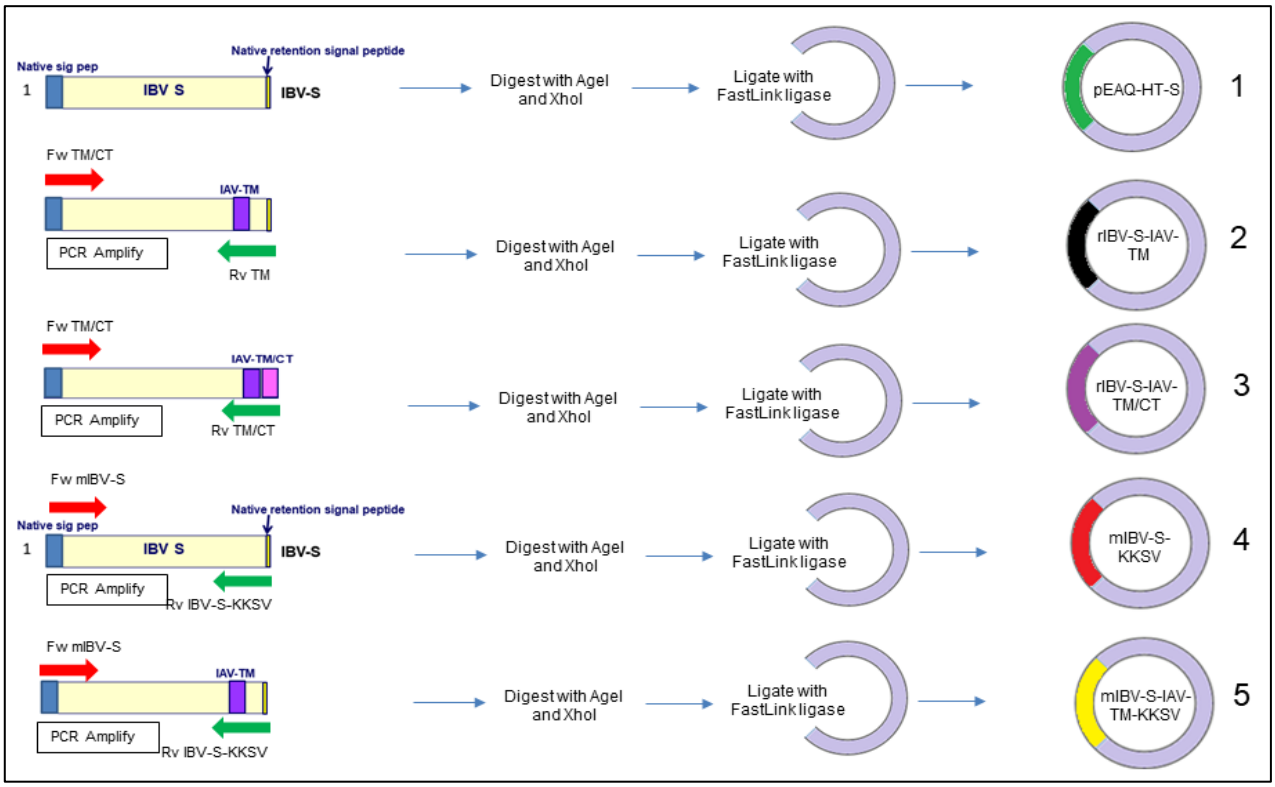

Figure 8: Diagram illustrating the design of pEAQ-HT-S, pEAQ-HT-rIBV-S-IAV-TM, pEAQ-HT-rIBV-S-IAV-TM/CT, pEAQ-HT-mIBV-S-KKSV, and pEAQ-HT-mIBV-S-IAV-TM-KKSV.

3.5.5. Transformation

The constructs were transformed into electrocompetent DH10B cells and then into *A. tumefaciens* using the same protocol described previously (see sections 3.1 and 3.2).

For each construct, PCR validation was performed using Phusion Flash. The PCR products were separated on a 1% agarose gel. Molecular weight marker (Gene Ruler ladder mix, SM0331) was used and pEAQ-HT containing a known insert served as a positive control. Insert-containing colonies (for each construct) were propagated, and the plasmids were extracted. The sequence-validated inserts encoding the individual structural proteins were verified and stored as described above (see section 3.1).

The *Agrobacterium* were cultured and the inoculum for each construct prepared using the protocol described above (see section 3.2).

3.5.6. Infiltration, extraction and analysis

Various combinations of the *Agrobacterium* suspensions were prepared (Fig. 9):

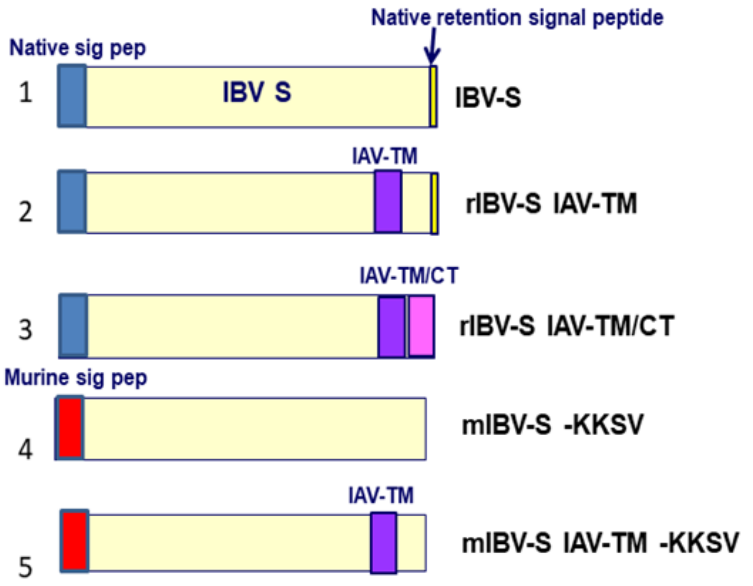

#	Combinations	Target
1	S + M + E 2:1:1 S + M + E 2:1:2	ER
2	S+M+E 2:1:1	ER
3	S + IAV M2 2:1	Secreted
4	S+M+E 2:1:1	Secreted
5	S+M+E 2:1:1	Secreted

Figure 9: Combinations of *Agrobacterium* suspensions for infiltration.

The different combinations were diluted to a final OD_{600} of 1-2 and left at room temperature for 0.5 - 3 hours prior to infiltration.

N. benthamiana ΔXT/FT leaves were infiltrated and harvested as described above (see section 3.3), with the rIBV-S-TM/CT construct being co-infiltrated with the IAV M2 ion channel protein gene (an integral membrane protein of IAV) instead of with the IBV E and M genes.

This was followed by the same extraction and analysis protocol described above (see sections 3.3 and 3.4).

3.5.7. *Agrobacterium* infiltration (addition of N protein to all combinations)

Various combinations of the *Agrobacterium* suspensions were prepared (Fig. 10):

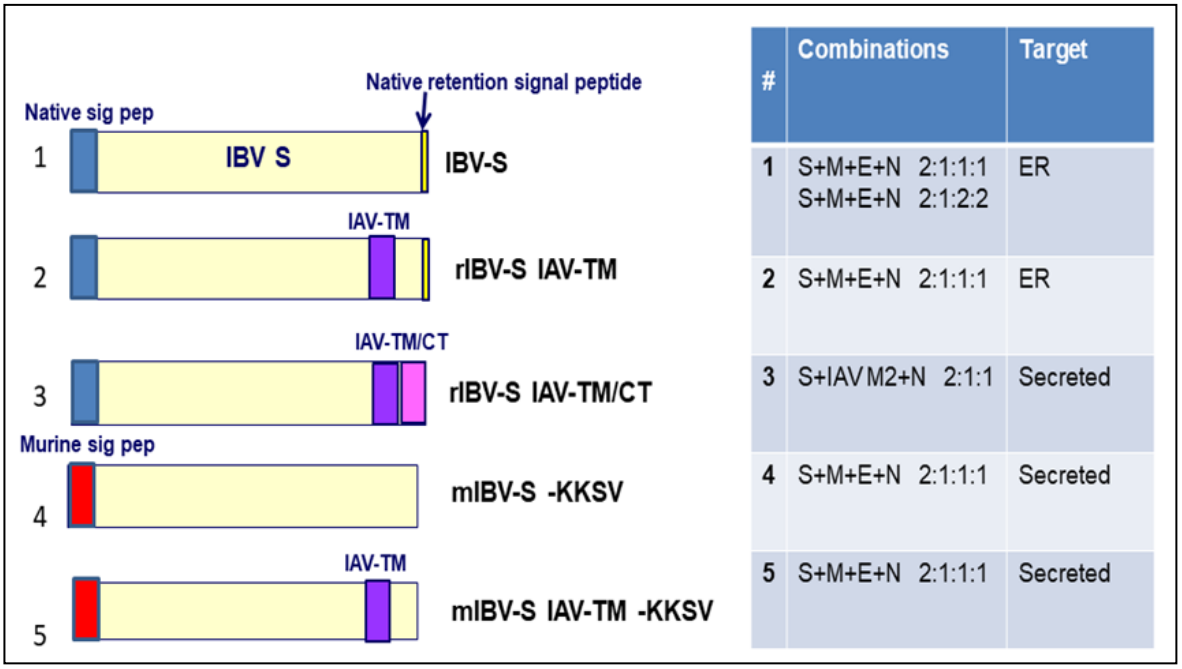

#	Combinations	Target
1	S+M+E+N 2:1:1:1 S+M+E+N 2:1:2:2	ER
2	S+M+E+N 2:1:1:1	ER
3	S+IAV M2+N 2:1:1	Secreted
4	S+M+E+N 2:1:1:1	Secreted
5	S+M+E+N 2:1:1:1	Secreted

Figure 10: Combinations of *Agrobacterium* suspensions for infiltration (with addition of N protein to all combinations).

The different combinations were diluted to a final OD_{600} of 1-2 and left at room temperature for 0.5 - 3 hours prior to infiltration.

N. benthamiana ΔXT/FT leaves were infiltrated and harvested as described above (see section 3.3), with the N protein added to all of the combinations. This was followed by the same extraction and analysis protocol described above (see sections 3.3 and 3.4). The iodixanol fractions were also stained with phosphotungstic acid as an alternative to uranyl acetate staining.

3.5.8. Analysis of leaf sections and Immunogold labelling

Small 1x1 mm size pieces of infiltrated leaves were cut out prior to harvesting and stored in 200 µl of fixative (2.5% Glutaraldehyde, [Wirsam Scientific and Precision Equipment (Pty) Ltd; Merck (Pty) Ltd]) or Immunogold fixative (4% Formaldehyde, [Merck (Pty) Ltd])

fixative. Both fixatives were made up by Ms Antoinette Lensink (Electron microscopy unit, University of Pretoria) in the following manner:

a. Fixative for leaf sections:

2.5% Glutaraldehyde (Wirsam Scientific and Precision Equipment (Pty) Ltd. Item Code = TAA/G003, Item Description = Glutaraldehyde 25% EM 250 ml) in 0.075M phosphate buffer (Merck (Pty) Ltd. Product Code = 1.06346.0500, Product description = Sodium Dihydrogen phosphate monohydrate for analysis EMSURE ACS. REAG. PH EUR; Merck (Pty) Ltd. Product Code = 1.06580.9050, Product description = di-Sodium hydrogen phosphate dihydrate for analysis EMSURE).

The secondary fixative is 1% Osmium tetroxide (Protea Laboratory solutions (Pty) Ltd. Product Code = S-02601-AB, Product description = SPI-Chem Osmium Tetroxide, 1g, Sealed Glass Ampoules).

b. Immunogold fixative:

Phosphate buffered 4% Formaldehyde (Merck (Pty) Ltd. Product Code = 8.18715.1000, Product description = Paraformaldehyde for synthesis, UN: 2213, Haz: 4.1III) with 50 mM lysine (Merck (Pty) Ltd. Product Code = 1.06346.0500, Product description = Sodium Dihydrogen phosphate monohydrate for analysis EMSURE ACS. REAG. PH EUR; Merck (Pty) Ltd. Product Code = 1.06580.9050, Product description = di-Sodium hydrogen phosphate dihydrate for analysis EMSURE; Merck (Pty) Ltd. Product Code = 1.12233.0100, Product description = Lysine Monohydrate for biochemistry)

These were provided to Ms Antoinette Lensink at the UP Faculty of Veterinary Science EM Unit for embedding, analysis and imaging according to in-house methods.

Immunogold labelling was performed by Prof Celia Abolnik, according to the protocol below and processed for imaging by Ms Antoinette Lensink as before.

The following reagents and equipment were used:

- Air dried resin-embedded stained sections on nickel grids (and a positive control)
- Tris-buffered saline Tween-20 (TBS-T) (8.8 g/L NaCl, 0.2 g/L KCl, 3 g/L Tris base, 500 µl/L Tween-20; up to 1 L distilled H_2O; pH 7.4, autoclaved)
- Primary antibody (chicken IBV positive field antiserum) diluted 1:10 in TBS-T
- 25 nm gold-labelled secondary antibody (goat anti-chicken antibody, Abcam, Biocom Africa (Pty) Ltd, Pretoria) at room temperature
- Blocking reagent: negative goat serum (same species as secondary antibody) diluted 1:10 in TBS-T
- Parafilm^{TM} or sterile petri dishes
- Forceps or platinum wire loop

Protocol:

The grids were rinsed twice in 50 µl of TBS-T for five minutes each. They were then incubated in 25 µl of blocking reagent for 30 minutes at room temperature. Thereafter, they were incubated in 50 µl of the primary antibody (1:10 dilution in TBS-T) at room temperature for 2 hours. The negative control was incubated in TBS-T for 2 hours at room temperature. After incubation, the grids were washed 5 times in 50 µl of TBS-T for 5 minutes each. The grids were then incubated in 50 µl of the secondary gold antibody (1:50 dilution in TBS-T) at room temperature for 1 hour. After incubation, the grids were washed 5 times in 50 µl of TBS-T for 5 minutes each. Thereafter, the grids were stained as before (optional).

CHAPTER 4

Results

A series of experiments were performed in order to identify the parameters required for optimal infectious bronchitis virus (IBV) membrane-associated protein expression as well as VLP assembly. Different buffers, *Agrobacterium* strains, construct combinations and ratios were tested. The results of each experiment will be discussed below.

4.1. Experiment 1

In the first experiment, IBV genes encoding the spike (S), membrane (M), and envelope (E) proteins were individually cloned into pEAQ-HT, transformed into DH10B, then into *Agrobacterium tumefaciens*. These were then agroinfiltrated into *Nicotiana benthamiana* ΔXT/FT in various combinations to co-express the membrane-associated proteins optimally. Leaf tissue was harvested at 6 and 8 dpi. Plant proteins were extracted using Bicine and PBS buffers and compared.

The goals of this experiment were:

- to co-express IBV membrane-associated proteins optimally
- to determine the optimal day of harvest
- to determine the ideal extraction buffer
- to determine which *Agrobacterium* strain would be most appropriate for IBV target protein co-expression

4.1.1. Cloning IBV genes into pEAQ-HT vector

In order to achieve these goals, each chicken codon-optimised gene (S, M, and E) was digested with *Age*I and *Xho*I enzymes to excise the target gene insert from the pUC57 vector backbone. The pEAQ-HT vector was also digested with the same enzymes to linearize it and create compatible ends for cloning. Each gene was ligated into pEAQ-HT and transformed into

electrocompetent DH10B cells and designated pEAQ-HT-M and pEAQ-HT-E. These were verified by colony PCR (Taq DNA polymerase) (Fig. 11).

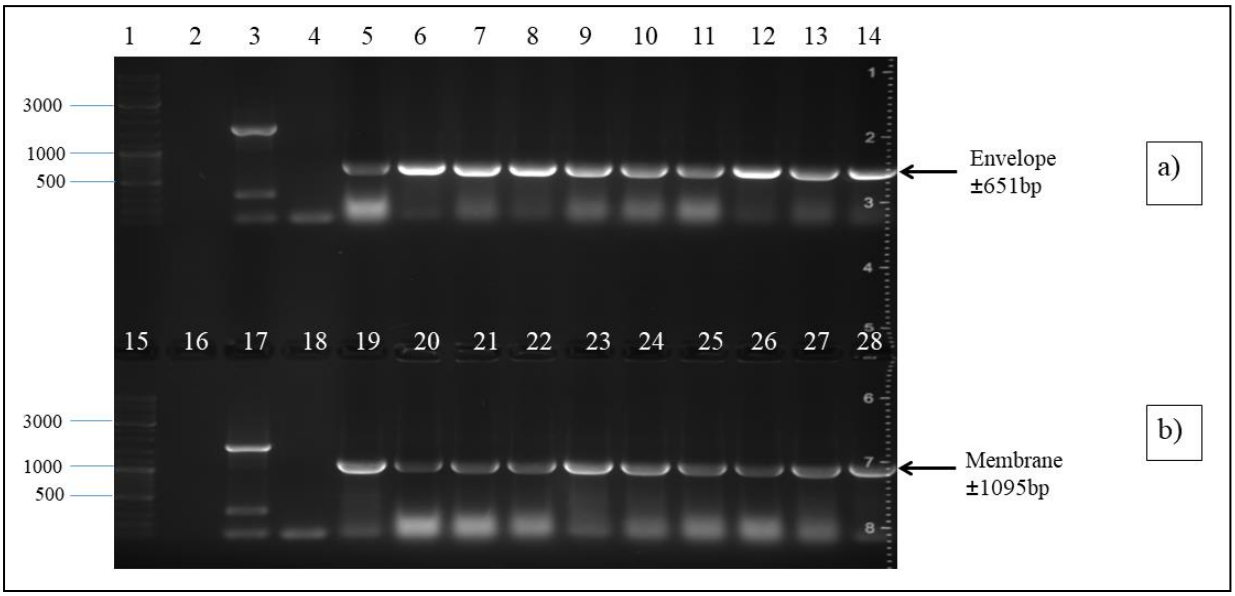

Figure 11: Colony PCR of DH10B cells transformed with a) pEAQ-HT-E. Lane 1: GeneRuler ladder mix SM0331, Lane 3: Positive control pEAQ-HT with a known insert (±1 200 bp), Lane 4: Negative control (no template DNA), Lanes 5-14: pEAQ-HT-E ligation, and b) pEAQ-HT-M. Lane 15: GeneRuler ladder mix SM0331, Lane 17: Positive control pEAQ-HT with a known insert (±1 200 bp), Lane 18: Negative control (no template DNA), Lanes 19-28: pEAQ-HT-M ligation. PCR was performed using pEAQ-HT forward and reverse primers, Table 1. The PCR products were separated on a 1.2% Agarose gel.

A PCR product that correlated with the gene encoding the E protein (351 bp plus 300 bp pEAQ-HT backbone (±651 bp)) (Fig. 11 a) was present in all of the colonies selected for screening (lanes 5-14), and Fig. 11 b) showed a PCR product that correlated with the gene encoding the M protein (795 bp plus 300 bp pEAQ-HT backbone (±1095 bp)) which was also present in all of the colonies selected for screening (lanes 19-28). This is a first indication that the M and E genes were cloned into pEAQ-HT but still needed sequence validation to confirm the successful cloning of these target genes. pEAQ-HT primers were used to amplify the E and M genes. The pEAQ-HT forward primer hybridizes 170bp upstream of the *Age*I site and the pEAQ-HT reverse primer hybridizes 120bp downstream of the *Xho*I site. This results in PCR products approximately 300bp larger than expected, explaining why the bands were noticeably

higher than what was expected for both genes. The expected sizes were 351 bp and 795bp for E and M respectively.

Due to its large size (3 456bp), instead of colony PCR, pEAQ-HT-S was plasmid DNA miniprepped and verified using Phusion Flash II DNA polymerase (Fig. 12).

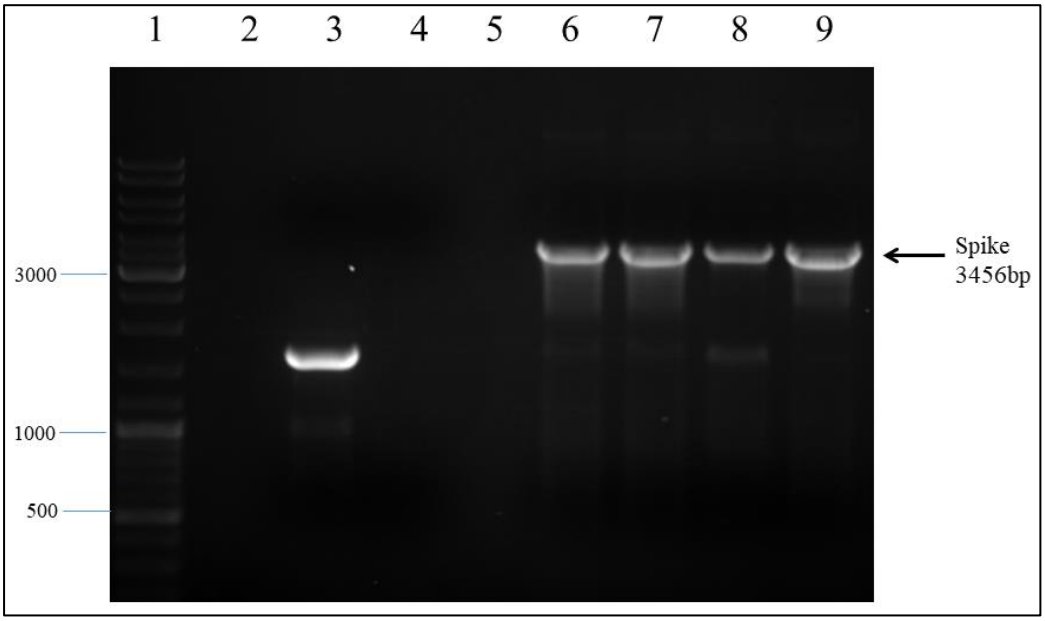

Figure 12: PCR products of plasmid DNA miniprepped DH10B cells harbouring pEAQ-HT-S. Lane 1: GeneRuler ladder mix SM0331, Lane 3: Positive control pEAQ-HT with a known insert (±1 200 bp), Lane 4: Negative control (no template DNA), Lanes 6-9: pEAQ-HT-S DH10B col 1-4 plasmid DNA minipreps. PCR was performed using pEAQ-HT forward and reverse primers, Table 1. The PCR products were separated on a 1% Agarose gel.

A PCR product that correlated with the size of the S gene (3 456 bp) (Fig. 12) was present in the four selected colonies (lanes 6-9). This is indicative that the S gene was successfully cloned into pEAQ-HT but still required sequence validation to confirm the successful cloning of the target gene.

Therefore, according to the results presented, the S, M, and E genes were potentially successfully cloned into the pEAQ-HT expression vector producing three constructs designated pEAQ-HT-IBV-S, pEAQ-HT-IBV-M and pEAQ-HT-IBV-E (Figs 13a-c).

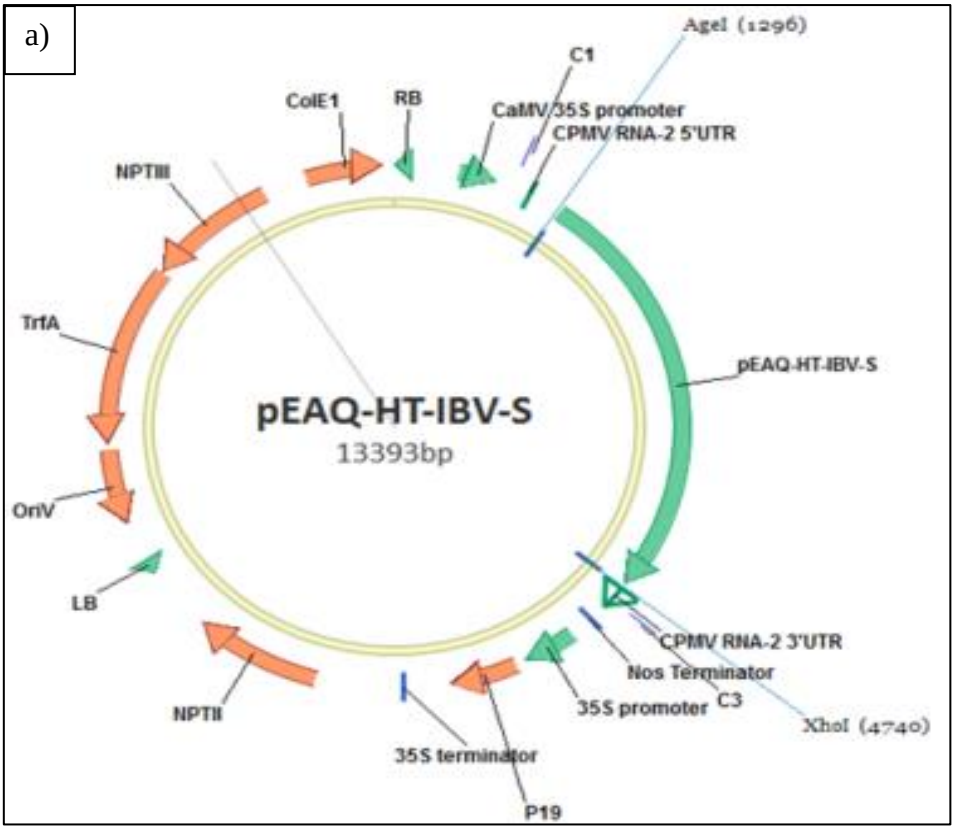

Figure 13a: pEAQ-HT harbouring the gene encoding the Spike protein (S).

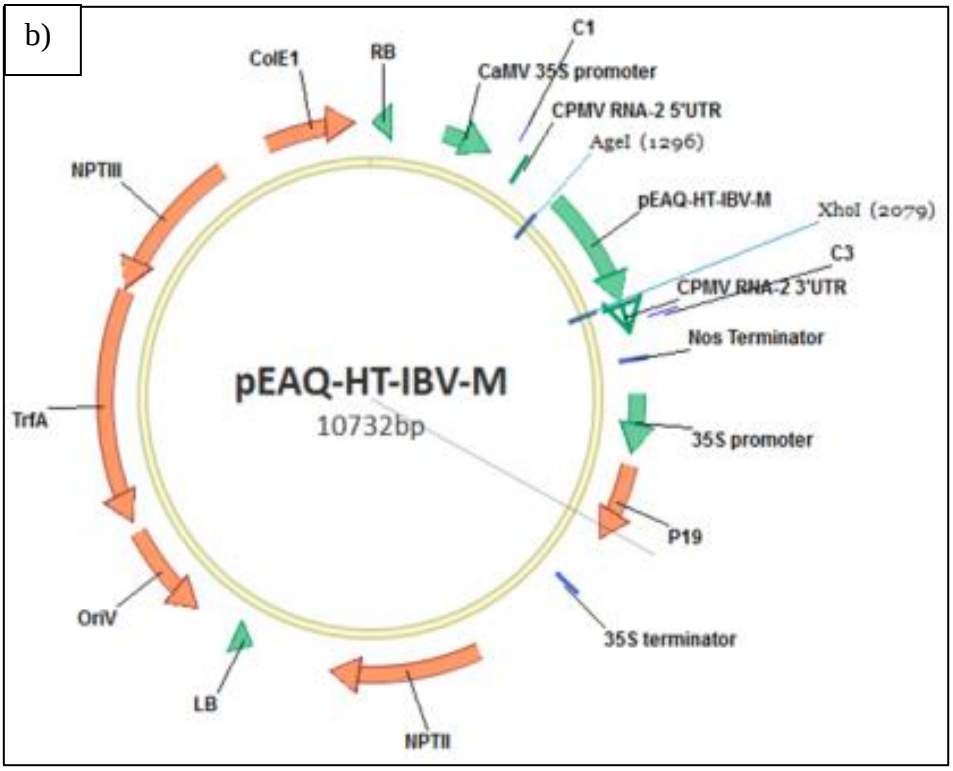

Figure 13b: pEAQ-HT harbouring the gene encoding the Membrane protein (M).

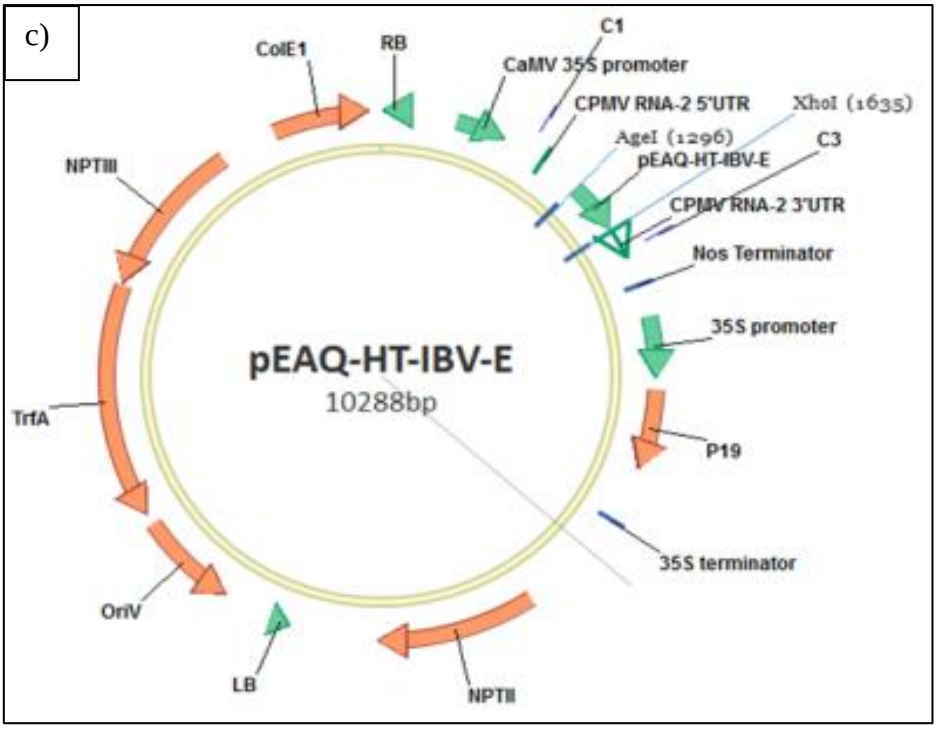

Figure 13c: pEAQ-HT harbouring the gene encoding the Envelope protein (E).

One of the positive clones for each gene insert was propagated and sent to Inqaba Biotechnical Industries (Pty) Ltd for sequence validation, and sequence validated clones were electroporated independently into three different *Agrobacterium* strains (AGL-1, GV3101::pMP90, and LBA4404). Colonies were once more PCR validated before *Agrobacterium* glycerol stocks were prepared. Once more, an aliquot of the pEAQ-HT constructs with the IBV gene inserts of choice were streaked out and the overnight growth was scraped from the plate to prepare liquid cultures for *N. benthamiana* ΔXT/FT plants for agroinfiltration. Various combinations of each were infiltrated.

The following combinations were infiltrated:

Combo 1 -	S:M:E	1:1:1	(in GV3101::pMP90)
Combo 2 -	S:M:E	1:1:1	(in LBA4404)
Combo 3 -	S:E	1:1	(in LBA4404)

4.1.2. Analysis of crude plant proteins

The plant leaf tissue was harvested at 6 and 8 dpi to determine which day the target proteins were optimally expressed to assemble IB VLPs. The plant proteins were extracted using two different buffers (PBS and bicine) and purified by Iodixanol density gradient ultracentrifugation. Fractions (Fr) 7-12 (20-40% Iodixanol) were analysed by Sodium dodecyl sulphate-polyacrylamide gel electrophoresis (SDS-PAGE) and immunoblotting to determine where the proteins (and therefore the VLPs) would be most abundant (Fig. 14).

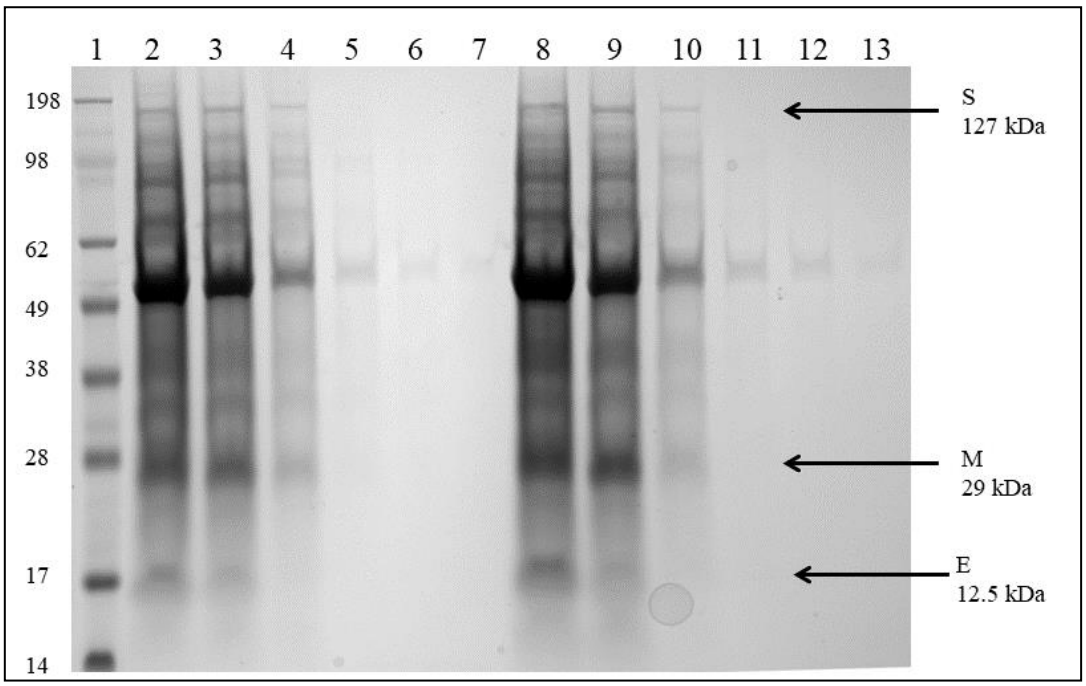

Figure 14: Bolt 4-12% SDS-PAGE analysis of pEAQ-HT IBV S, M, and E proteins co-expressed in *N. benthamiana* ΔXT/FT 6 dpi. Lane 1: SeeBlue Plus MW marker, Lanes 2-7: *Agrobacterium*-mediated (LBA4404) co-expression of all three target proteins (Fr. 12-7), Lanes 8-13: *Agrobacterium*-mediated (GV3101::pMP90) co-expression of all three target proteins (Fr. 12-7).

Agrobacterium strains LBA444 and GV3103::pMP90 were used to co-express all three target proteins (S, M, and E) (Fig. 14). There were higher quantities of the IBV target proteins in fractions 10-12 (20-30% Iodixanol) compared to fractions 7-9 (30-40% Iodixanol), where only very faint bands could be visualised. This indicates that the VLPs (if present) were potentially more abundant in the 30% Iodixanol fractions.

An immunoblot was performed using IBV-specific antiserum to detect the IBV proteins present in the fractions (Fig. 15). *Agrobacterium* strain GV3101::pMP90 was used to mediate protein expression.

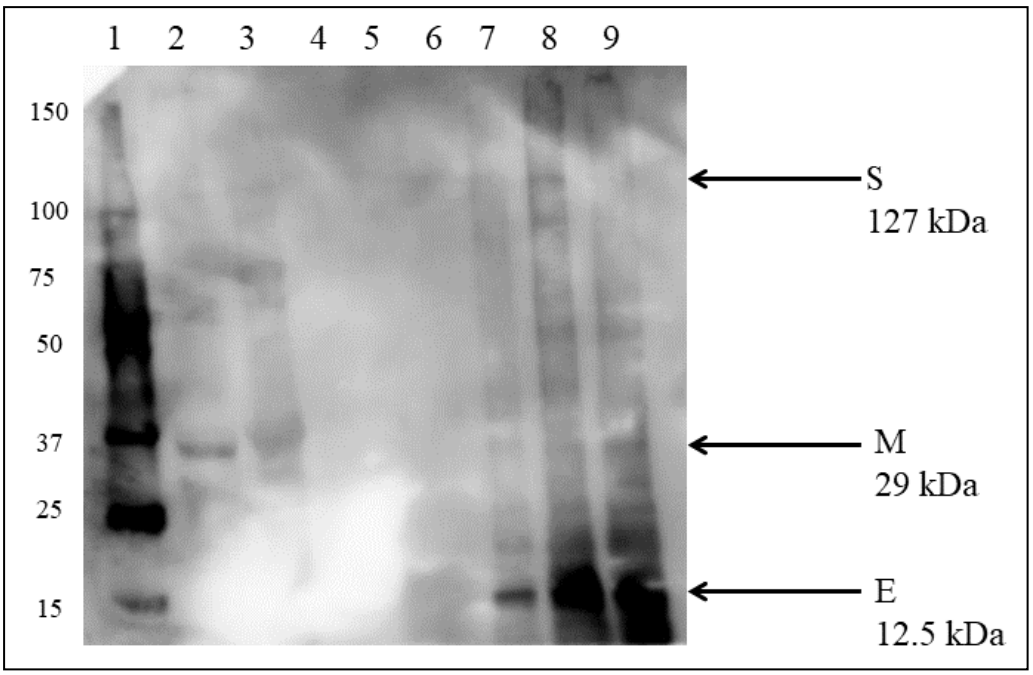

Figure 15: Immunoblot using IBV-specific antiserum to detect pEAQ-HT co-expressed IBV S, M, and E proteins in *N. benthamiana* ΔXT/FT 6 dpi. Lane 1: Western C MW Marker, Lane 2: Positive control IBV QX-like inactivated, Lane 3: negative control pEAQ-HT empty, Lanes 4-9: *Agrobacterium*-mediated (GV3101::pMP90) co-expression of proteins S, M, and E (Fr. 7-12).

The expected band sizes were visualised in fractions 10-12 (20-30% Iodixanol) (Fig. 15), which indicated that the proteins were expressed: S (127 kDa) and M (29 kDa) bands were very faint, whereas E (12.5 kDa) was more distinct. There was a band at ±29kDa in lane 3 (negative control). This may have been due to contamination during sample loading, or it may be a protein present in the pEAQ-HT vector of the same size. In the case of the latter, it may suggest that the bands visualised at 29kDa (lanes 4-9) were not indicative of the M protein.

An immunoblot was performed using the same IBV antiserum, comparing *Agrobacterium* strains LBA4404 and GV3101::pMP90 mediating the expression of the target proteins, and also comparing PBS buffer to bicine buffer for optimal expression and extraction of IBV target proteins, respectively (Fig. 16).

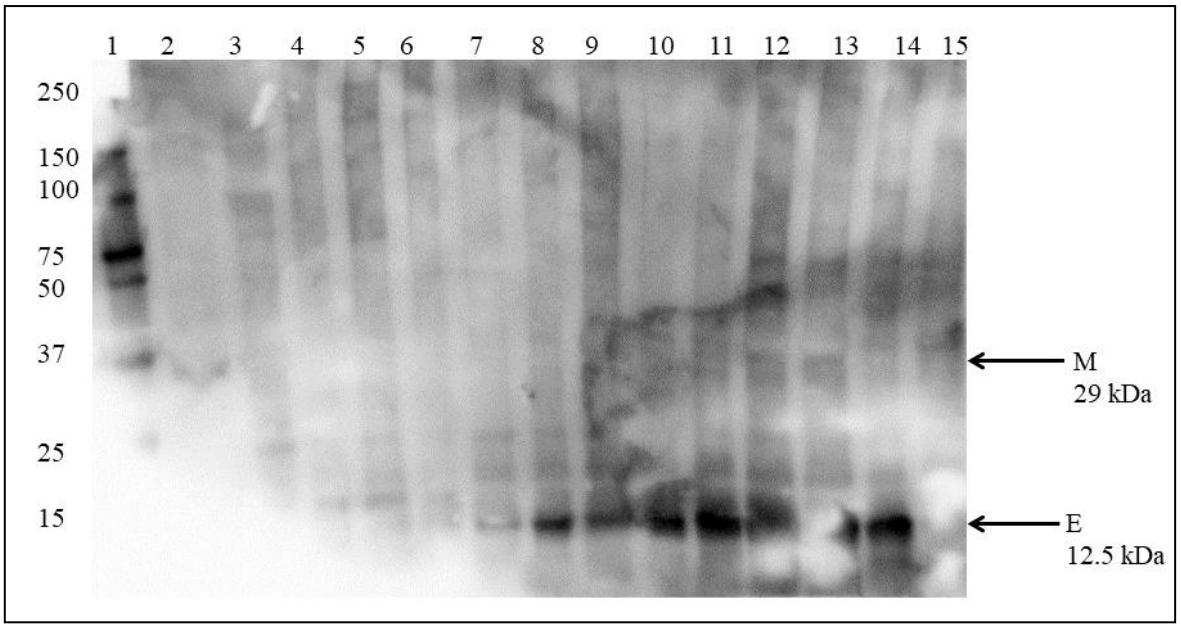

Figure 16: Immunoblot using IBV-specific antiserum to detect pEAQ-HT IBV S, M, and E proteins co-expressed in *N. benthamiana* ΔXT/FT 6 and 8 dpi. Lane 1: Western C MW Marker, Lane 2: Positive control IBV QX-like inactivated, Lane 3: Negative control pEAQ-HT empty, Lane 4-7: *Agrobacterium*-mediated (LBA4404) co-expression of proteins S, M, and E (Lane 4-5, Fr. 10 and 11, 6 dpi, PBS; Lanes 6-7, Fr. 10 and 11, 8 dpi, PBS), Lane 8-13: *Agrobacterium*-mediated (GV3101::pMP90) co-expression of proteins S, M, and E (Lanes 8-9, Fr. 10 and 11, 6 dpi, PBS; Lanes 10-11, Fr. 10 and 11, 8 dpi, PBS; Lanes 12-13, Fr. 10-11, 8 dpi, bicine), Lane 14-15: *Agrobacterium*-mediated (LBA4404) co-expression of proteins S and E (Fr. 10 and 11, 8 dpi, PBS).

Intense bands correlating with the size of protein E (12.5 kDa) were visualised indicating the presence of the target protein (Fig. 16, lanes 8-14). Faint bands correlating with the size of the M protein (29 kDa) were visible (Fig. 16, lanes 10-13). No bands correlating with the S protein (127 kDa) were observed. There was no difference between the leaves extracted with PBS and those extracted with bicine buffer. PBS was therefore used in future experiments as it is more cost-effective to use than bicine. There was also very little difference between the results obtained harnessing LBA4404 or GV3101::pMP90 to mediate the co-expression of target proteins and potential assembly of IB VLPs. The leaves harvested at 8 dpi were yellowed and dried out by the time of harvest. Therefore, leaves were harvested at 6 dpi in all future experiments.

4.1.3. LC-MS/MS based peptide sequencing

Bands correlating to the sizes of each of the three proteins (S, M, and E) were cut out from the SDS-PAGE gel (Fig. 14) and submitted for LC-MS/MS based peptide sequencing (Fig. 17). The gel bands were trypsin digested following the protocol described in materials and methods.

IBV S protein sample 1 (~127 kDa)
(11.6% coverage with 95% confidence; 11 peptides)

MLVKSLFLVTILCALCSANLFDSDNNYVYYYQSAFRPPNGWHLQGGAYAVVNSTNHTSNAGSAQGCTVGVIKDVY
NQSVASIAMTAPLQGMAWFCTAYCNFSDTTVFVTHCYHIRISAMKNGSLFYNLTVSVSKYPNFKSFQCVNNFTSV
YLNGDLVFTSNK**TTDVTSAGVYFKAGGPVNYSIMK**EFKVLAYFVNGTAQDVILCDNSPKGLLACQYNTGNFSDGF
YPFTNSTLVR**EKFIVYR**ESSFNTTLALTNFTFTNVSNAQPNSGGVNTFHLYQTQTAQSGYYNFNLSFLSQFVYKA
SDFMYGSYHPSCSFRPETINSGLWFNSLSVSLTYGPLQGGCKQSVFSGKATCCYAYSYKGPMACK**GVYSGELR**TN
FECGLLVYVTKSDGSRIQTRTEPLVLTQYNYNNITLDKCVAYNIYGRVGQGFITNVTDSAANFSYLADGGLAILD
TSGAIDVFVVQGIYGLNYYKVNPCEDVNQQFVVSGGNIVGILTSRNETGSEQVENQFYVKLTNSSHRRRRSIGQN
VTSCPYVSYGRFCIEPDGSLK**MIVPEELK**QFVAPLLNITESVLIPNSFNLTVTDEYIQTRMDKVQINCLQYVCGN
SLECRKLFQQYGPVCDNILSVVNSVSQK**EDMELLSFYSSTKPK**GYDTPVLSNVSTGEFNISLLLKTPISSSGRSF
IEDLLFTSVETVGLPTDAEYKKCTAGPLGTLKDLICAREYNGLLVLPPIITADMQTMYTASLVGAMAFGGITSAA
AIPFATQIQAR**INHLGITQSLLMK**NQEKIAASFNKAIGHMQEGFR**STSLALQQIQDVVNKQSAILTETMNSLNK**N
FGAITSVIQDIYAQLDAIQADAQVDRLITGR**LSSLSVLASAK**QSEYIRVSQQRELATKKINECVKSQSNRYGFCG
SGRHVLSIPQNAPNGIVFIHFTYTPESFVNVTAIVGFCVNPANASQYAIVPANGRGVFIQVNGSYYITARDMYMP
RDITAGDIVTLTSCQANYVNVNKTVINTFVEDDDFNFNDELSKWWNDTKHELPDFDEFNYTVPVLNISNEIDRIQ
EVIQGLNDSLIDLETLSILKTYIKWPWYVWLAIFFAIIIFILILGWVFFMTGCCGCCCGCFGIIPLMSKCGKK**SS**
YYTTFDNDVVTEQYRPKKSV

IBV S protein sample 2 (~110 kDa)
(2.1% coverage with 95% confidence; 2 peptides)

MLVKSLFLVTILCALCSANLFDSDNNYVYYYQSAFRPPNGWHLQGGAYAVVNSTNHTSNAGSAQGCTVGVIKDVY
NQSVASIAMTAPLQGMAWFCTAYCNFSDTTVFVTHCYHIRISAMKNGSLFYNLTVSVSKYPNFKSFQCVNNFTSV
YLNGDLVFTSNKTTDVTSAGVYFKAGGPVNYSIMKEFKVLAYFVNGTAQDVILCDNSPKGLLACQYNTGNFSDGF
YPFTNSTLVREKFIVYRESSFNTTLALTNFTFTNVSNAQPNSGGVNTFHLYQTQTAQSGYYNFNLSFLSQFVYKA
SDFMYGSYHPSCSFRPETINSGLWFNSLSVSLTYGPLQGGCKQSVFSGKATCCYAYSYKGPMACKGVYSGELRTN
FECGLLVYVTKSDGSRIQTRTEPLVLTQYNYNNITLDKCVAYNIYGRVGQGFITNVTDSAANFSYLADGGLAILD
TSGAIDVFVVQGIYGLNYYKVNPCEDVNQQFVVSGGNIVGILTSRNETGSEQVENQFYVKLTNSSHRRRRSIGQN
VTSCPYVSYGRFCIEPDGSLKMIVPEELKQFVAPLLNITESVLIPNSFNLTVTDEYIQTRMDKVQINCLQYVCGN
SLECRKLFQQYGPVCDNILSVVNSVSQKEDMELLSFYSSTKPKGYDTPVLSNVSTGEFNISLLLKTPISSSGRSF
IEDLLFTSVETVGLPTDAEYKKCTAGPLGTLKDLICAREYNGLLVLPPIITADMQTMYTASLVGAMAFGGITSAA
AIPFATQIQAR**INHLGITQSLLMK**NQEKIAASFNKAIGHMQEGFRSTSLALQQIQDVVNKQSAILTETMNSLNKN
FGAITSVIQDIYAQLDAIQADAQVDRLITGR**LSSLSVLASAK**QSEYIRVSQQRELATKKINECVKSQSNRYGFCG
SGRHVLSIPQNAPNGIVFIHFTYTPESFVNVTAIVGFCVNPANASQYAIVPANGRGVFIQVNGSYYITARDMYMP
RDITAGDIVTLTSCQANYVNVNKTVINTFVEDDDFNFNDELSKWWNDTKHELPDFDEFNYTVPVLNISNEIDRIQ
EVIQGLNDSLIDLETLSILKTYIKWPWYVWLAIFFAIIIFILILGWVFFMTGCCGCCCGCFGIIPLMSKCGKKSS
YYTTFDNDVVTEQYRPKKSV

IBV M protein (~29.4 kDa)
(16.7% coverage with 95% confidence; 5 peptides)

MVENLTIRNWNRLSLTSSQRTVGIIKTLQFFKMSNGTENCTLNTEQAVQLFKEYNLFITAFLLFLTILLQYGYAT
RSRFIYILKMVVLWCFWPLNIAVGVISCIYPPNTGGLVAAIILTVFACLSFIGYWIQSIRLFKRCRSWWSFNPES
NAVGSILLTNGQQCNFAIESVPMVLSPIIKNGALYCEGQWLAKCEPDHLPKDIFVCTPDRRNIYRMVQKYTGDQS
GNKKRFATFVYAKQSVDTGELESVTTAGSNLYT

*No detection of IBV **E** protein (~12.5 kDa)*

Figure 17: Protein confirmation using LC-MS/MS-based peptide sequencing of IBV structural proteins (S, M, and E). LC-MS/MS-based peptide sequence analysis for excised bands resulted in the percentage sequence coverage as indicated below with a number of unique peptides identified with >95% confidence. Peptides with >95% confidence are highlighted in green, those 50-95% confidence in yellow and <50% confidence in red. No peptides were identified for the non-highlighted regions of the sequence (grey).

Both the S (sample 1) and M proteins were confirmed by LC-MS/MS based peptide sequencing (Fig. 17), indicating that these two proteins were expressed in the plant leaf tissue. S (sample 2) was faintly detected in the band cut out at 110kDa. The band at 12.5 kDa was not confirmed to be the E protein.

4.2. Experiment 2

In the second experiment, the cloned IBV genes (S, M and E) were once again agroinfiltrated into *N. benthamiana* ΔXT/FT in various combinations in an attempt to assemble VLPs. Leaf tissue was harvested at 6 dpi. Plant proteins were extracted in PBS buffer.

The goals of this experiment were:

- to identify which protein combinations were needed to assemble IB VLPs
- to determine which *Agrobacterium* strain would be most appropriate for IBV target protein co-expression and IB VLP assembly

4.2.1. Analysis of crude plant proteins

The plant leaf tissue was harvested at 6 dpi. The plant proteins were extracted using PBS buffer and purified by Iodixanol density gradient ultracentrifugation. Fractions 9-12 (20-30% Iodixanol) were analysed by SDS-PAGE and immunoblotting to determine where the target proteins (and potentially, the VLPs) would be most abundant (Fig. 18).

The following combinations were infiltrated (in AGL-1):

Combo 1 - S:M:E 1:1:1

Combo 2 - S:M 1:1

Combo 3 - S:E 1:1

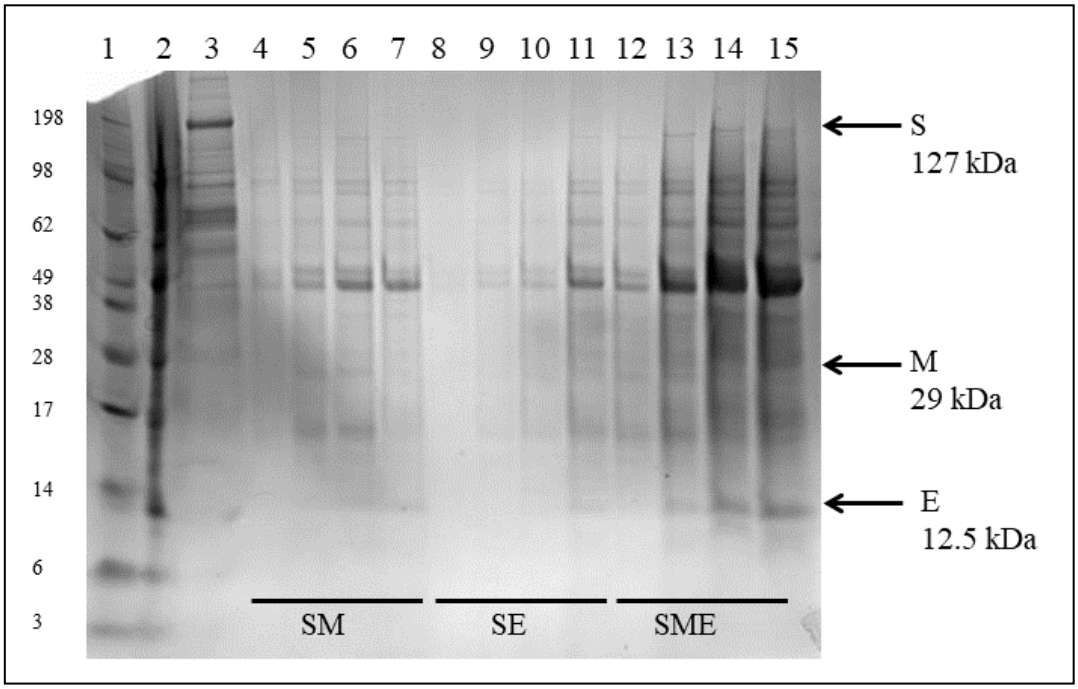

Figure 18: Bolt 4-12% SDS PAGE analysis of pEAQ-HT IBV S, M, and E proteins co-expressed in *N. benthamiana* ΔXT/FT 6 dpi. Lane 1: SeeBlue Plus MW marker, Lane 2: Negative control pEAQ-HT empty, Lane 3: Positive control IBV QX-like inactivated, Lane 4-7: *Agrobacterium*-mediated (AGL-1) co-expression of S and M proteins (Fr. 9-12), Lane 8-11: *Agrobacterium*-mediated (AGL-1) co-expression of S and E proteins (Fr. 9-12), Lane 12-15: *Agrobacterium*-mediated (AGL-1) co-expression of S, M, and E proteins (Fr. 9-12).

Expression and assembly of the IBV structural proteins (S, M, and E) were mediated by *Agrobacterium* strain AGL-1 resulting in S, M and E detected with SDS PAGE (Fig. 18). There was more of the IBV structural proteins visible in fractions 10-12 (20–30% Iodixanol) compared to fraction 9 (30% Iodixanol), where only very faint bands were visible. This further suggests that the VLPs could have been present in fractions 10-12 (20–30% Iodixanol). Protein E was not visible in the SM combination, whilst M was not visible in the SE combination of Coomassie stained SDS PAGE. All three target proteins were visible in the SME combination. A band correlating with the size of S (127 kDa) was visualised very faintly in all the combinations.

An immunoblot was performed using the same IBV antiserum, comparing the different combinations agroinfiltrated with AGL-1 harbouring the constructs of interest (Fig. 19).

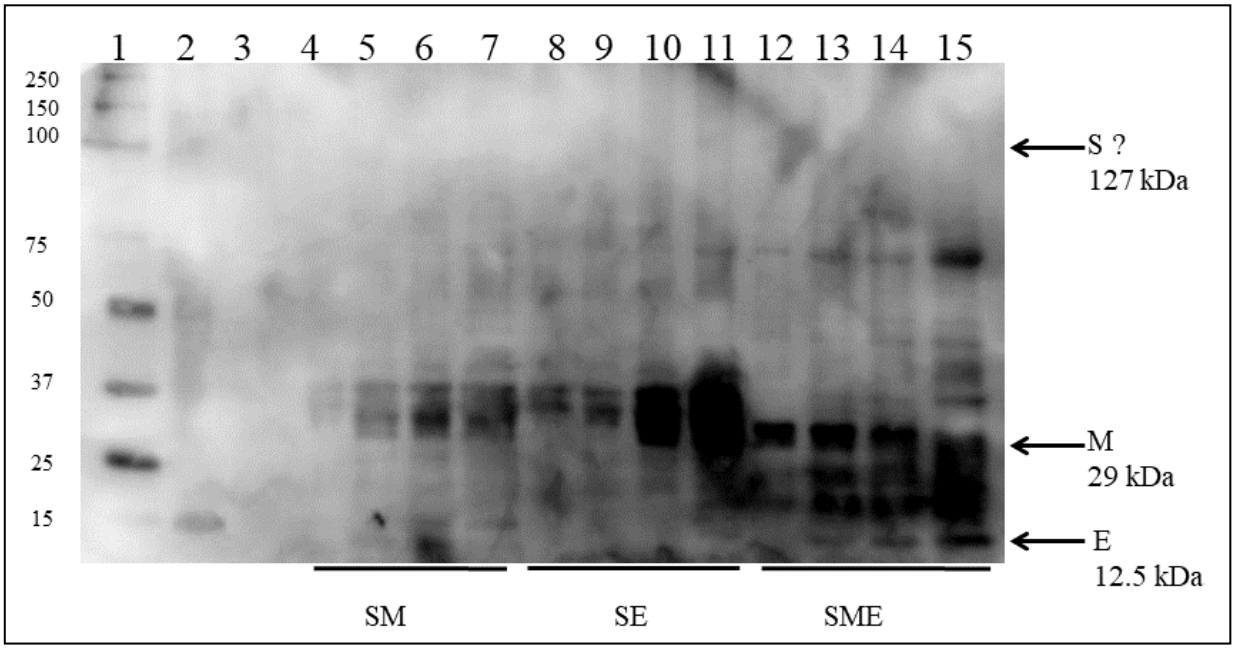

Figure 19: Immunoblot using IBV-specific antiserum to detect pEAQ-HT IBV S, M, and E proteins co-expressed in *N. benthamiana* ΔXT/FT 6 dpi. Lane 1: Western C MW Marker, Lane 2: Negative control pEAQ-HT empty, Lane 3: Positive control IBV QX-like inactivated, Lane 4-7: *Agrobacterium*-mediated (AGL-1) co-expression of S and M proteins (Fr. 9-12), Lane 8-11: *Agrobacterium*-mediated (AGL-1) co-expression of S and E proteins (Fr. 9-12), Lane 12-15: *Agrobacterium*-mediated (AGL-1) co-expression of S, M, and E proteins (Fr. 9-12).

Intense signals that correlated with the size of protein E (12.5 kDa) were visualised (Fig. 19, lanes 13-15). Intense bands correlating with the size of the M protein (29 kDa) were visible (Fig. 19, lanes 4-15) although they should have only been present in lanes 4-7, and 12-15. Thus, the antiserum might detect a plant protein other than protein M. An unknown protein of 75 kDa was also detected (Fig. 19, lanes 11-15). No signal was detected correlating with the S protein (127 kDa) size.

4.2.2. TEM visualisation of VLPs

No IB VLP's were detected using TEM, in any of the iodixanol fractions, with any of the extraction buffers used, for any of the construct combinations and *Agrobacterium* strains used thus far. This was possibly because the VLP yield was too low or the negative staining with uranyl acetate may have resulted in the disassembling of VLPs.

4.3. Experiment 3

In the third experiment, various sequence modifications were made to the native S protein sequence to investigate whether these would enhance the co-expression of IB structural proteins and assembly of VLPs. Two genetically modified versions of the S protein were designed with the aim of improving protein expression in plants and assembly of VLPs. These were designated rIBV-S-IAV-TM and rIBV-S-IAV-TM/CT. The modifications are described in detail in chapter 3.

The cloned IBV genes (S (and the modified versions thereof), M and E) were once again agroinfiltrated into *N. benthamiana* ΔXT/FT in various combinations in an attempt to assemble VLPs. Leaf tissue was harvested at 6 dpi. Plant proteins were extracted PBS buffer.

The goals of this experiment were:

- ❖ to improve protein expression and assemble IB VLPs
- ❖ to identify which protein combinations were needed to assemble IB VLPs
- ❖ to identify which construct ratios would improve IBV target protein co-expression and IB VLP assembly

4.3.1. Cloning recombinant IBV S genes into pEAQ-HT vector

The original S gene was PCR amplified using ultramer primers that would insert *Age*I/*Xho*I sites, and modify the C- or N-terminal sequences as required. The resultant PCR products were RE digested (*Age*I/*Xho*I) before they were individually cloned into a pEAQ-HT construct and transformed into DH10B electrocompetent cells. The presence of each insert was verified using PCR (Phusion Flash II DNA polymerase) (Fig. 20).

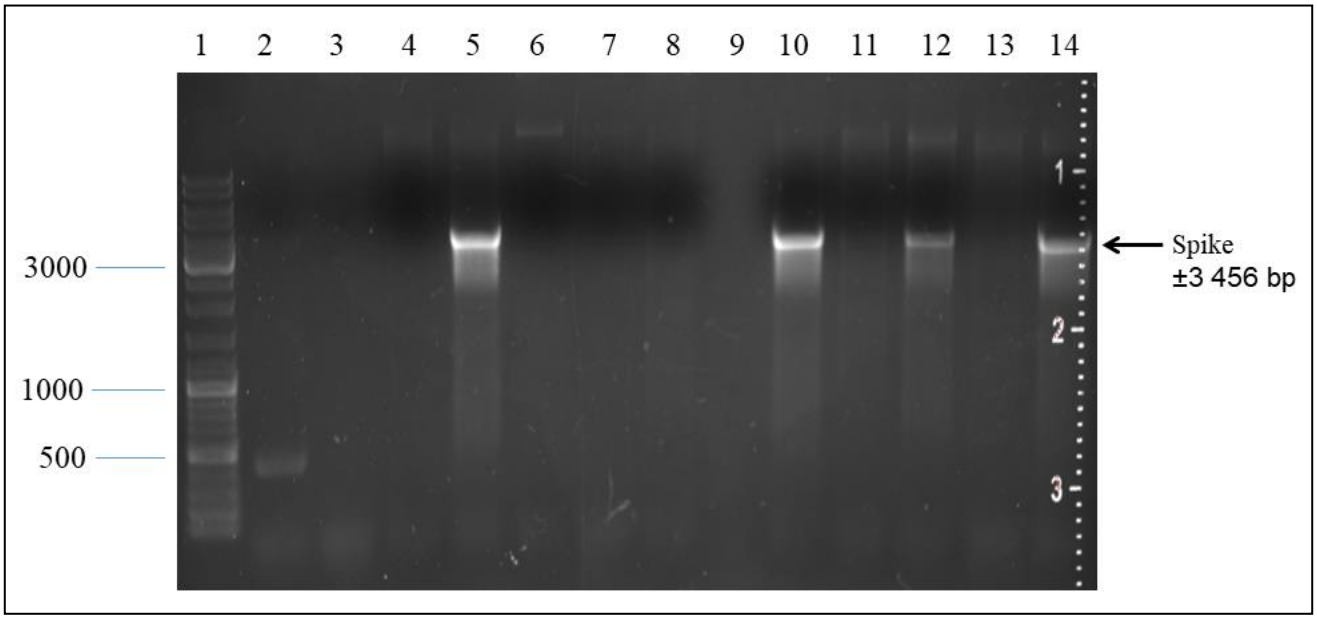

Figure 20: PCR of plasmid DNA from DH10B cells transformed with pEAQ-HT-rIBV-S-TM and pEAQ-HT-rIBV-S-TM/CT. Lane 1: GeneRuler ladder mix SM0331, Lane 3: Positive control pEAQ-HT with a known insert, Lane 4: Negative control (no template DNA), Lane 5-8: pEAQ-HT-rIBV-S-TM DH10B colonies 1-4 plasmid DNA minipreps, Lane 10-14: pEAQ-HT-rIBV-S-TM/CT DH10B colonies 1-4. PCR using pEAQ-HT forward and reverse primers, Table 1. The PCR products were separated on a 1% Agarose gel.

Both rIBV-S-TM and rIBV-S-TM/CT were successfully amplified (Fig. 20) using their respective primers (Table 2) as indicated by the appropriate PCR product size (Fig. 20). A band that correlated with the expected size of the recombinant S gene was present in lane 5 for rIBV-S-TM; and in lanes, 10, 12, and 14 for rIBV-S-TM/CT. This shows that the PCR products (rIBV-S-TM and rIBV-S-TM/CT) were successfully cloned into pEAQ-HT but still required sequence validation to confirm their successful amplification. Lane 2 should have been empty as no template DNA was loaded, therefore it is possible that there was contamination during sample loading. Lane 3 should have contained a band at ±1 200bp, (known insert size in pEAQ-HT). There may not have been enough of the sample loaded to visualise on the gel.

Therefore, according to the results presented, rIBV-S-IAV-TM and rIBV-S-IAV-TM/CT genes were potentially successfully cloned into the pEAQ-HT expression vector producing two constructs (Fig. 21a and b).

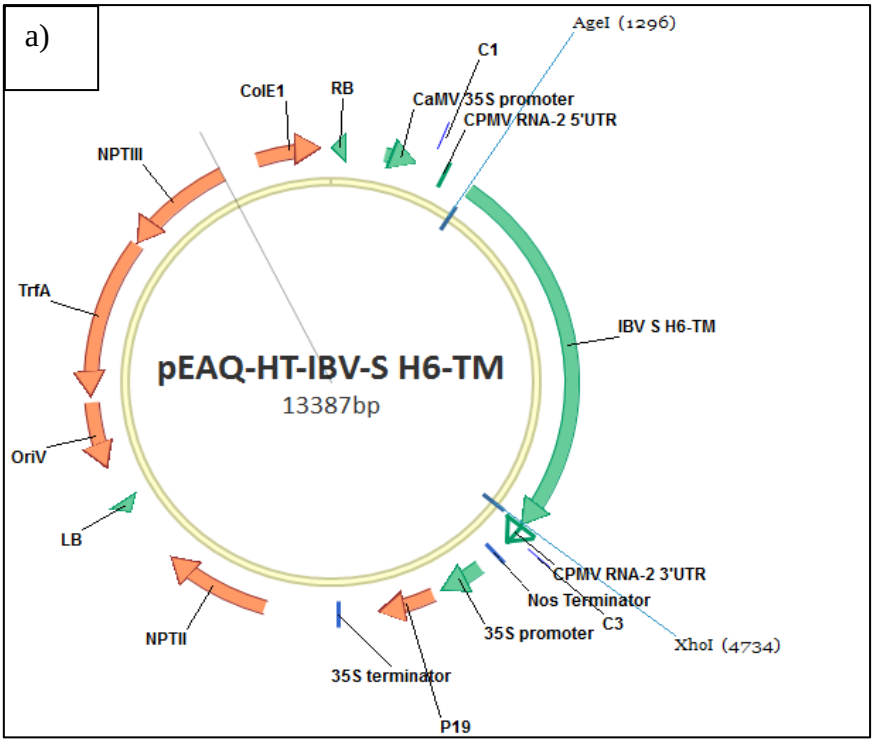

Figure 21a: pEAQ-HT harbouring the gene encoding the recombinant S protein IBV-S H6-TM.

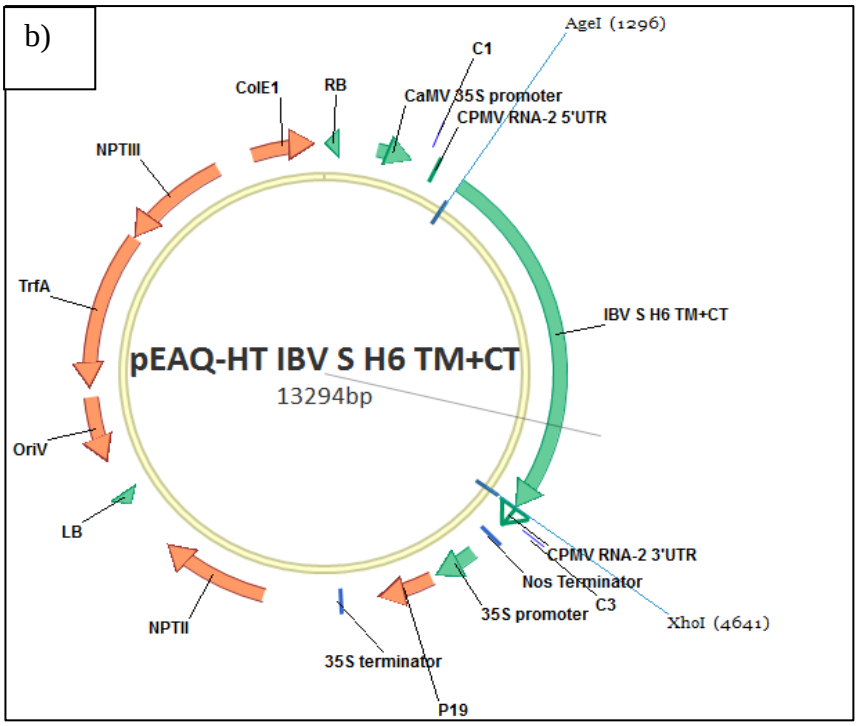

Figure 21b: pEAQ-HT harbouring the gene encoding the recombinant S protein IBV-S H6-TM/CT.

One of the positive clones for each gene insert were propagated and sent to Inqaba Biotechnical Industries (Pty) Ltd for sequence validation, and sequence validated clones were electroporated independently into three independent *Agrobacterium* strains (AGL-1, GV3101::pMP90, and LBA4404). Colonies were PCR validated before *Agrobacterium* glycerol stocks were prepared. An aliquot of the pEAQ-HT constructs with the IBV gene inserts of choice (as well as the IAV M2 gene insert) were streaked out and the overnight growth was scraped from the plate to prepare liquid cultures for *N. benthamiana* ΔXT/FT plants for agroinfiltration. Various combinations of each were infiltrated. M2 is an integral membrane protein of IAV that has been shown to play a role in the assembly and budding of the virus particle (Rossman and Lamb, 2011)). The M2 protein along with the HA and NA (neuraminidase) spike proteins of IAV form tetramers on the surface of the infected cell. It forms ion channels which help with maintaining a constant pH to prevent the sensitive viral HA protein from being exposed to a low intracellular pH (Lal and Chow, 2007). During replication, it assists in the uncoating of the viral nucleoprotein (Lal and Chow, 2007).

The following combinations and ratios were infiltrated (in AGL-1):

Combo 1 -	S:M:E	1:1:1
Combo 2 -	S:M:E	2:1:1
Combo 3 -	S:M:E	2:1:2
Combo 4 -	rIBV-S-TM:M:E	1:1:1
Combo 5 -	rIBV-S-TM/CT	1
Combo 6 -	rIBV-S-TM/CT:M2	1:1

4.3.2. Analysis of crude plant proteins

Agroinfiltrated plant leaves were harvested at 6 dpi. The plant proteins were extracted using PBS buffer and clear lysate was purified by Iodixanol density gradient ultracentrifugation. Fractions 10 and 11 (20-30% Iodixanol) were analysed by SDS-PAGE (Fig. 22) and immunoblotting. *Agrobacterium*-mediated (AGL-1) infiltration of S, rIBV-S-TM and rIBV-S-TM/CT constructs in combination with the E and M genes were conducted. The rIBV-S-TM/CT was co-infiltrated with the IAV M2 ion channel protein gene (to assist with VLP formation) instead of with the IBV E and M genes. Different ratios of the constructs were infiltrated in an attempt to improve S protein expression and formation of VLPs.

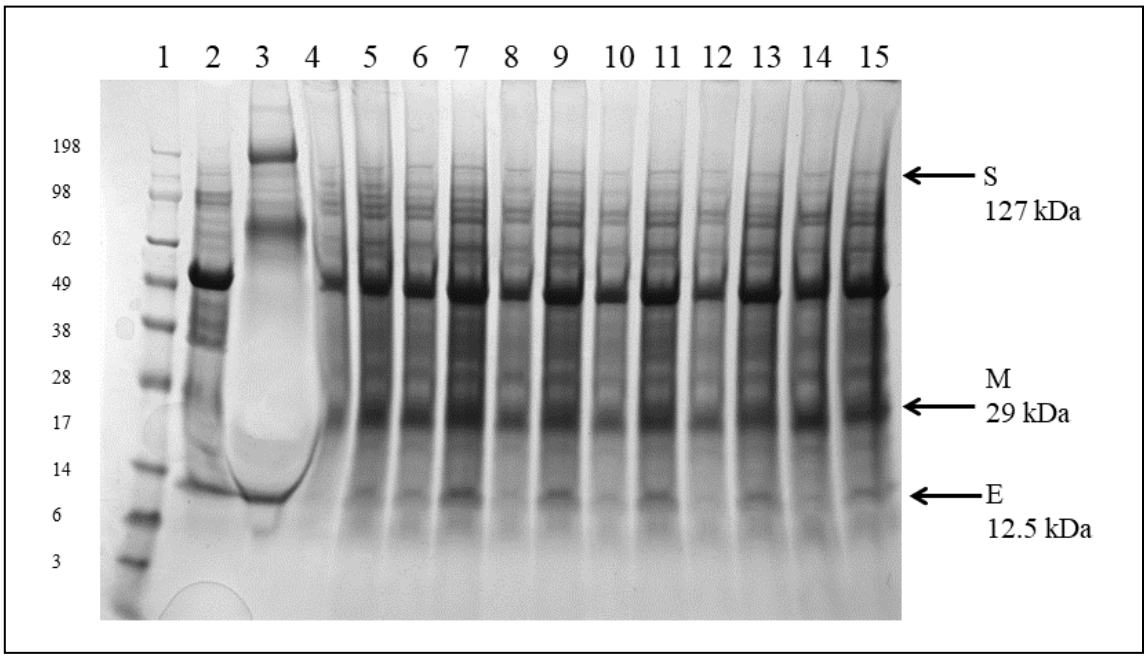

Figure 22: Bolt 4-12% SDS PAGE analysis of pEAQ-HT IBV S (or rIBV-S-TM or rIBV-S-TM/CT), M, E, and IAV M2 ion channel proteins co-expressed in *N. benthamiana* ΔXT/FT 6 dpi. Lane 1: SeeBlue Plus MW marker, Lane 2: Negative control pEAQ-HT empty, Lane 3: Positive control IBV QX-like inactivated, Lane 4-5: S:M:E 1:1:1 (Frs 10-11), Lane 6-7: S:M:E 2:1:1 (Frs 10-11), Lane 8-9: S:M:E 2:1:2 (Frs 10-11), Lane 10-11: rIBV-S-TM:M:E 1:1:1 (Frs 10-11), Lane 12-13: rIBV-S-TM/CT (Frs 10-11), Lane 14-15: rIBV-S-TM/CT:M2 1:1 (Frs 10-11).

Agrobacterium strain AGL-1 was used to co-express the genes encoding all three structural proteins and this was detected using SDS-PAGE (Fig. 22). The bands correlating to the M (29 kDa) and E (12.5 kDa) proteins were present in all the lanes including lanes 12-15 (Fig. 22) which were leaves that were infiltrated without the M and E constructs. The absence of those IBV proteins was anticipated in these plant extracts. Bands of similar size to both the M and E proteins were present in lane 2, the negative control lane, suggesting that the sizes of the M and E proteins corresponded with non-specific protein bands that were present in the plant leaves. This would make it difficult to identify distinct bands correlating to the proteins. Lane 3 (positive control) was warped, making it difficult to identify what bands were or were not present.

An immunoblot was performed using the IBV-specific antiserum to detect the IBV proteins present in the fractions (Fig. 23). *Agrobacterium* strain AGL-1 was used to mediate protein expression.

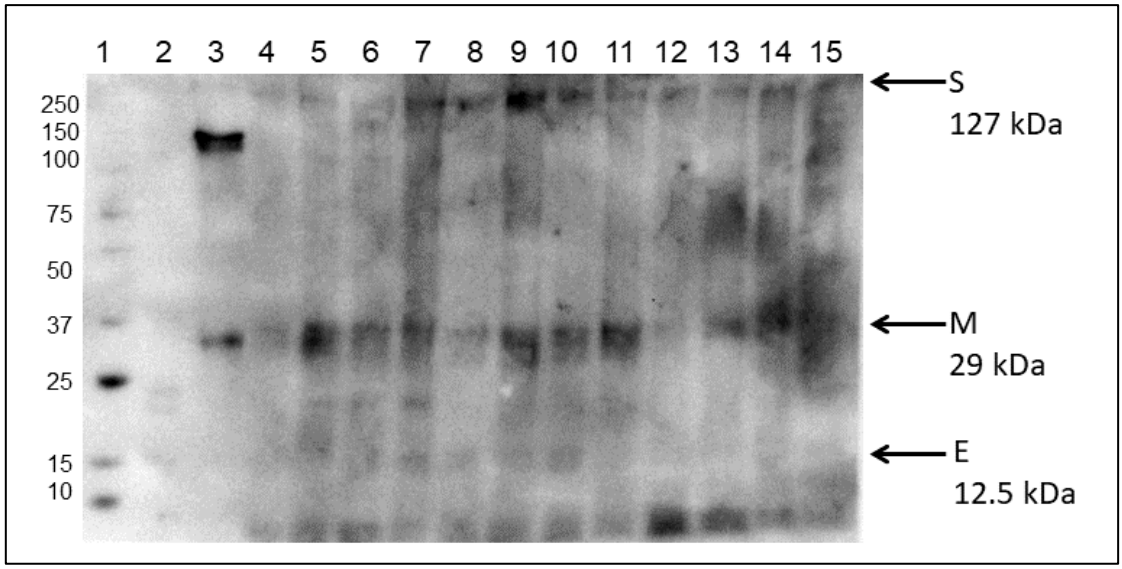

Figure 23: Immunoblot using IBV-specific antiserum to detect pEAQ-HT IBV S (or rIBV-S-TM or rIBV-S-TM/CT), M, and E proteins co-expressed (*Agrobacterium*-mediated (AGL-1) expression) in *N. benthamiana* ΔXT/FT 6 dpi. Lane 1: Western C MW marker, Lane 2: Negative control pEAQ-HT empty, Lane 3: Positive control IBV QX-like inactivated, Lane 4-5: S:M:E 1:1:1 (Frs 10-11), Lane 6-7: S:M:E 2:1:1 (Frs 10-11), Lane 8-9: S:M:E 2:1:2 (Frs 10-11), Lane 10-11: rIBV-S-TM:M:E 1:1:1 (Frs 10-11), Lane 12-13: rIBV-S-TM/CT (Frs 10-11), Lane 14-15: rIBV-S-TM/CT:M2 1:1 (Frs 10-11).

Faint signals correlating with the size of the E protein (12.5 kDa) were detected in lanes 4-10, but not in lanes 12-15 (Fig. 23), which was expected as the plants were infiltrated without the construct encoding the E protein. Bands correlating with the size of the M protein (29 kDa) was visible in lanes 4-11, and far less so in lanes 12-15, which was also expected as the gene encoding the M protein was omitted from the combination infiltrated. Bands correlating with the S protein (127 kDa) size could be visualised in all lanes, more so in lanes 8 and 9, where the S:M:E ratio of infiltration was 2:1:1.

4.3.3. LC-MS/MS based peptide sequencing

Bands correlating to the sizes of each of the proteins (S, rIBV-S-TM, rIBV-S-TM/CT, M, and E) were cut out from the SDS-PAGE gel (Fig. 22) and submitted for LC-MS/MS based peptide sequencing (Fig. 24). The gel bands were trypsin digested following the protocol described in materials and methods.

IBV S protein, Combo 2, fr. 11, 11 peptides, 8.3% coverage (95% confidence)

MLVKSLFLVTILCALCSANLFDSDNNYVYYYQSAFRPPNGWHLQGGAYAVVNSTNHTSNAGSAQGCTVGVIKDVY
NQSVASIAMTAPLQGMAWFCTAYCNFSDTTVFVTHCYHIRISAMKNGSLFYNLTVSVSKYPNFKSFQCVNNFTSV
YLNGDLVFTSNK**TTDVTSAGVYFKAGGPVNYSIMK**EFKVLAYFVNGTAQDVILCDNSPKGLLACQYNTGNFSDGF
YPFTNSTLVREKFIVYRESSFNTTLALTNFTFTNVSNAQPNSGGVNTFHLYQTQTAQSGYYNFNLSFLSQFVYKA
SDFMYGSYHPSCSFRPETINSGLWFNSLSVSLTYGPLQGGCKQSVFSGKATCCYAYSYKGPMACK**GVYSGELR**TN
FECGLLVYVTKSDGSRIQTRTEPLVLTQYNYNNITLDKCVAYNIYGRVGQGFITNVTDSAANFSYLADGGLAILD
TSGAIDVFVVQGIYGLNYYKVNPCEDVNQQFVVSGGNIVGILTSRNETGSEQVENQFYVKLTNSSHRRRRSIGQN
VTSCPYVSYGRFCIEPDGSLK**MIVPEELK**QFVAPLLNITESVLIPNSFNLTVTDEYIQTRMDKVQINCLQYVCGN
SLECRKLFQQYGPVCDNILSVVNSVSQKEDMELLSFYSSTKPKGYDTPVLSNVSTGEFNISLLLKTPISSSGRSF
IEDLLFTSVETVGLPTDAEYKKCTAGPLGTLKDLICAREYNGLLVLPPIITADMQTMYTASLVGAMAFGGITSAA
AIPFATQIQAR**INHLGITQSLLMK**NQEKIAASFNKAIGHMQEGFR**STSLALQQIQDVVNKQSAILTETMNSLNK**N
FGAITSVIQDIYAQLDAIQADAQVDRLITGR**LSSLSVLASAK**QSEYIRVSQQRELATKKINECVKSQSNRYGFCG
SGRHVLSIPQNAPNGIVFIHFTYTPESFVNVTAIVGFCVNPANASQYAIVPANGRGVFIQVNGSYYITARDMYMP
RDITAGDIVTLTSCQANYVNVNKTVINTFVEDDDFNFNDELSKWWNDTKHELPDFDEFNYTVPVLNISNEIDRIQ
EVIQGLNDSLIDLETLSILKTYIKWPLAIYSTVSSSLVLVGLIIAMGLWMCSNGSMQCRVCI

IBV S protein, Combo 3, fr.11, 7 peptides, 7% coverage (95% confidence)

MLVKSLFLVTILCALCSANLFDSDNNYVYYYQSAFRPPNGWHLQGGAYAVVNSTNHTSNAGSAQGCTVGVIKDVY
NQSVASIAMTAPLQGMAWFCTAYCNFSDTTVFVTHCYHIRISAMKNGSLFYNLTVSVSKYPNFKSFQCVNNFTSV
YLNGDLVFTSNK**TTDVTSAGVYFKAGGPVNYSIMK**EFKVLAYFVNGTAQDVILCDNSPKGLLACQYNTGNFSDGF
YPFTNSTLVREKFIVYRESSFNTTLALTNFTFTNVSNAQPNSGGVNTFHLYQTQTAQSGYYNFNLSFLSQFVYKA
SDFMYGSYHPSCSFRPETINSGLWFNSLSVSLTYGPLQGGCKQSVFSGKATCCYAYSYKGPMACK**GVYSGELR**TN
FECGLLVYVTKSDGSRIQTRTEPLVLTQYNYNNITLDKCVAYNIYGRVGQGFITNVTDSAANFSYLADGGLAILD
TSGAIDVFVVQGIYGLNYYKVNPCEDVNQQFVVSGGNIVGILTSRNETGSEQVENQFYVKLTNSSHRRRSIGQN
VTSCPYVSYGRFCIEPDGSLK**MIVPEELK**QFVAPLLNITESVLIPNSFNLTVTDEYIQTRMDKVQINCLQYVCGN
SLECRKLFQQYGPVCDNILSVVNSVSQKEDMELLSFYSSTKPKGYDTPVLSNVSTGEFNISLLLKTPISSSGRSF
IEDLLFTSVETVGLPTDAEYKKCTAGPLGTLKDLICAREYNGLLVLPPIITADMQTMYTASLVGAMAFGGITSAA
AIPFATQIQAR**INHLGITQSLLMK**NQEKIAASFNKAIGHMQEGFR**STSLALQQIQDVVNK**QSAILTETMNSLNKN
FGAITSVIQDIYAQLDAIQADAQVDRLITGR**LSSLSVLASAK**QSEYIRVSQQRELATKKINECVKSQSNRYGFCG
SGRHVLSIPQNAPNGIVFIHFTYTPESFVNVTAIVGFCVNPANASQYAIVPANGRGVFIQVNGSYYITARDMYMP
RDITAGDIVTLTSCQANYVNVNKTVINTFVEDDDFNFNDELSKWWNDTKHELPDFDEFNYTVPVLNISNEIDRIQ
EVIQGLNDSLIDLETLSILKTYIKWPLAIYSTVSSSLVLVGLIIAMGLWMCSNGSMQCRVCI

IBV rIBV-S-TM protein – No detection

IBV rIBV-S-TM/CT protein, Combo 5, fr. 11, 15 peptides, 11.3% coverage (95% confidence)

MLVKSLFLVTILCALCSANLFDSDNNYVYYYQSAFRPPNGWHLQGGAYAVVNSTNHTSNAGSAQGCTVGVIKDVY
NQSVASIAMTAPLQGMAWFCTAYCNFSDTTVFVTHCYHIRISAMKNGSLFYNLTVSVSKYPNFKSFQCVNNFTSV
YLNGDLVFTSNK**TTDVTSAGVYFKAGGPVNYSIMK**EFKVLAYFVNGTAQDVILCDNSPKGLLACQYNTGNFSDGF
YPFTNSTLVREKFIVYRESSFNTTLALTNFTFTNVSNAQPNSGGVNTFHLYQTQTAQSGYYNFNLSFLSQFVYKA
SDFMYGSYHPSCSFRPETINSGLWFNSLSVSLTYGPLQGGCKQSVFSGKATCCYAYSYKGPMACK**GVYSGELR**TN
FECGLLVYVTKSDGSRIQTRTEPLVLTQYNYNNITLDKCVAYNIYGRVGQGFITNVTDSAANFSYLADGGLAILD
TSGAIDVFVVQGIYGLNYYKVNPCEDVNQQFVVSGGNIVGILTSRNETGSEQVENQFYVK**LTNSSHR**RRRSIGQN
VTSCPYVSYGR**FCIEPDGSLKMIVPEELK**QFVAPLLNITESVLIPNSFNLTVTDEYIQTRMDKVQINCLQYVCGN
SLECRKLFQQYGPVCDNILSVVNSVSQKEDMELLSFYSSTKPKGYDTPVLSNVSTGEFNISLLLKTPISSSGRSF
IEDLLFTSVETVGLPTDAEYKKCTAGPLGTLKDLICAREYNGLLVLPPIITADMQTMYTASLVGAMAFGGITSAA
AIPFATQIQAR**INHLGITQSLLMK**NQEKIAASFNK**AIGHMQEGFRSTSLALQQIQDVVNKQSAILTETMNSLNK**N
FGAITSVIQDIYAQLDAIQADAQVDRLITGR**LSSLSVLASAK**QSEYIRVSQQRELATKKINECVKSQSNR**YGFCG**
SGRHVLSIPQNAPNGIVFIHFTYTPESFVNVTAIVGFCVNPANASQYAIVPANGRGVFIQVNGSYYITAR**DMYMP**
RDITAGDIVTLTSCQANYVNVNKTVINTFVEDDDFNFNDELSKWWNDTKHELPDFDEFNYTVPVLNISNEIDRIQ
EVIQGLNDSLIDLETLSILKTYIKWPLAIYSTVSSSLVLVGLIIAMGLWMCSNGSMQCRVCI

IBV rIBV-S-TM/CT protein, Combo 5, fr. 11, 18 peptides, 13.4% coverage (95% confidence)

MLVKSLFLVTILCALCSANLFDSDNNYVYYYQSAFRPPNGWHLQGGAYAVVNSTNHTSNAGSAQGCTVGVIKDVY
NQSVASIAMTAPLQGMAWFCTAYCNFSDTTVFVTHCYHIRISAMKNGSLFYNLTVSVSKYPNFKSFQCVNNFTSV
YLNGDLVFTSNK**TTDVTSAGVYFKAGGPVNYSIMK**EFKVLAYFVNGTAQDVILCDNSPKGLLACQYNTGNFSDGF
YPFTNSTLVR**EK**FIVYRESSFNTTLALTNFTFTNVSNAQPNSGGVNTFHLYQTQTAQSGYYNFNLSFLSQFVYKA
SDFMYGSYHPSCSFRPETINSGLWFNSLSVSLTYGPLQGGCKQSVFSGKATCCYAYSYKGPMACK**GVYSGELR**TN
FECGLLVYVTKSDGSRIQTRTEPLVLTQYNYNNITLDKCVAYNIYGRVGQGFITNVTDSAANFSYLADGGLAILD
TSGAIDVFVVQGIYGLNYYKVNPCEDVNQQFVVSGGNIVGILTSRNETGSEQVENQFYVK**LTNSSHR**RRRSIGQN
VTSCPYVSYGR**FCIEPDGSLKMIVPEELK**QFVAPLLNITESVLIPNSFNLTVTDEYIQTRMDKVQINCLQYVCGN
SLECRKLFQQYGPVCDNILSVVNSVSQK**EDMELLSFYSSTKPK**GYDTPVLSNVSTGEFNISLLLK**TPISSSGR**SF
IEDLLFTSVETVGLPTDAEYKK**CTAGPLGTLK**DLICAREYNGLLVLPPIITADMQTMYTASLVGAMAFGGITSAA
AIPFATQIQAR**INHLGITQSLLMK**NQEKIAASFNK**AIGHMQEGFRSTSLALQQIQDVVNKQSAILTETMNSLNK**N
FGAITSVIQDIYAQLDAIQADAQVDRLITGR**LSSLSVLASAK**QSEYIRVSQQRELATKKINECVKSQSNR**YGFCG**
SGRHVLSIPQNAPNGIVFIHFTYTPESFVNVTAIVGFCVNPANASQYAIVPANGRGVFIQVNGSYYITAR**DMYMP**
RDITAGDIVTLTSCQANYVNVNKTVINTFVEDDDFNFNDELSKWWNDTKHELPDFDEFNYTVPVLNISNEIDRIQ
EVIQGLNDSLIDLETLSILKTYIKWPLAIYSTVSSSLVLVGLIIAMGLWMCSNGSMQCRVCI

IBV E protein, 4 peptides, 30.9% coverage (95% confidence)

MMSLLNKSLEENGSFLTALYIFVACVALYLLGRALQAFVQAADACCLFWYTWVLVPGAKGTAFVYKHTYGR**KLNN**
PELEQVIFNEFPKNGWNNKNPAIFQDVERHGKLHS

IBV M protein – No detection

Figure 24: Protein confirmation using LC-MS/MS-based peptide sequencing of IBV structural proteins (native S, rIBV-S-TM, rIBV-S-TM/CT, M, and E). LC-MS/MS-based peptide sequence analysis for excised bands resulted in the percentage sequence coverage as indicated below with a number of unique peptides identified with >95% confidence. Peptides with >95% confidence are highlighted in green, those 50-95% confidence in yellow and <50% confidence in red. No peptides were identified for the non-highlighted regions of the sequence (grey).

The presence of the S protein at the appropriate size of 127 kDa (IBV S, Combo 2, lane 6; and IBV S, Combo 3, lane 8) was confirmed using LC MS/MS based peptide sequencing. rIBV-S-TM protein could not be detected (Combo 4, lane 10). rIBV-S-TM/CT (Combo 5, lane 12; and Combo 6, lane 14) was detected. IBV M protein (Combo 3, lane 9) at 29 kDa could not be

detected by mass spectrometry. IBV E protein (Combo 3, lane 9) at 12.5 kDa was detected. (See appendix for cut out bands).

4.3.4. TEM visualisation of recombinant S protein VLPs

None of the recombinant S proteins in combination with the selected IBV structural proteins resulted in the assembly of VLPs.

4.4. Experiment 4

In the fourth experiment, two additional genetically modified versions of the S protein were designed with the aim of improving protein expression in plants and assembly of VLPs. These were designated mIBV-S-KKSV and mIBV-S-TM-KKSV. The modifications were described in detail in chapter 3.

The cloned IBV genes (S (and the modified versions thereof), M and E) were once again agroinfiltrated into *N. benthamiana* ΔXT/FT in various combinations to assemble VLPs. Leaf tissue was harvested at 6 dpi. Plant proteins were extracted in PBS buffer.

The goals of this experiment were:

- to improve protein expression and assemble IB VLPs
- to identify which protein combinations were needed to assemble IB VLPs
- to identify which construct ratios would improve IBV target protein co-expression and IB VLP assembly

4.4.1. Cloning recombinant IBV S genes into pEAQ-HT vector

The recombinant S genes modified in experiment 3 were PCR amplified using ultramer primers that would insert *AgeI/Xho*I sites, and modify the C- or N-terminal sequences as required. The resultant PCR products were RE digested (*AgeI/Xho*I) before they were individually cloned into a pEAQ-HT construct and transformed into DH10B electrocompetent cells. The presence of each insert was verified using PCR (Phusion Flash II DNA polymerase) (Fig. 25 and 26).

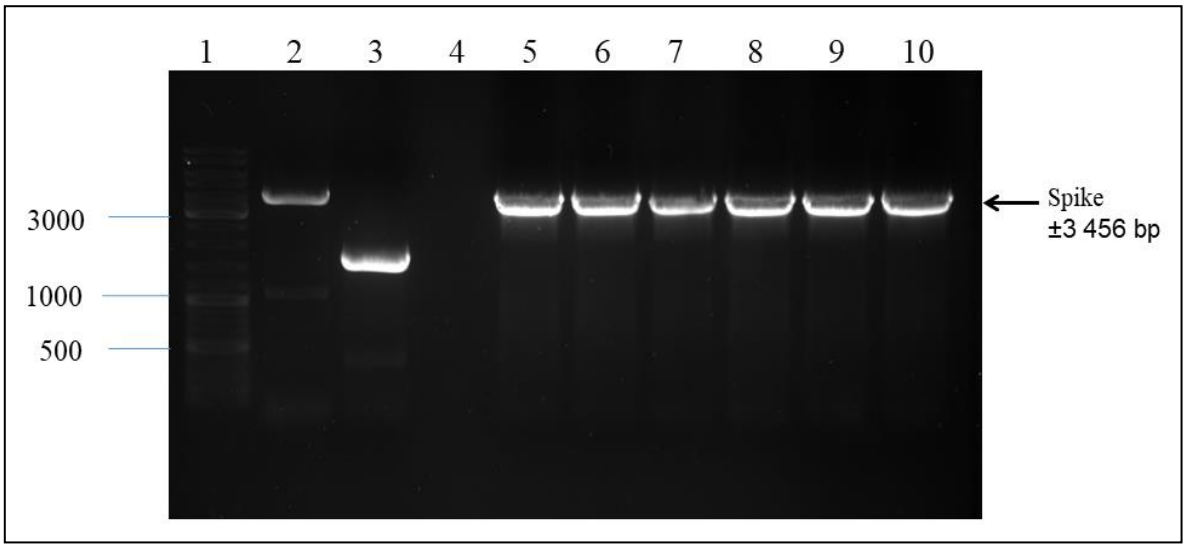

Figure 25: PCR of plasmid DNA from DH10B cells transformed with pEAQ-HT-mIBV-S-KKSV. Lane 1: GeneRuler ladder mix SM0331, Lane 2: negative control (no template DNA), Lane 3: positive control pEAQ-HT with a known insert (±1 200 bp), Lane 5-10: pEAQ-HT-mIBV-S-KKSV DH10B colonies 1-6. PCR using pEAQ-HT forward and reverse primers, Table 1. The PCR products were separated on a 1% Agarose gel.

A band that correlated with the expected size of the recombinant S gene was present in all of the picked colonies (lanes 5 – 10) (Fig. 25). This shows that the PCR product (mIBV-S-KKSV) was successfully cloned into pEAQ-HT but still required sequence validation to confirm their successful amplification. The large fragment (lane 2) correlated to the size of S, therefore it may have been contamination during the preparation of the PCR mixes as no template DNA should have been present.

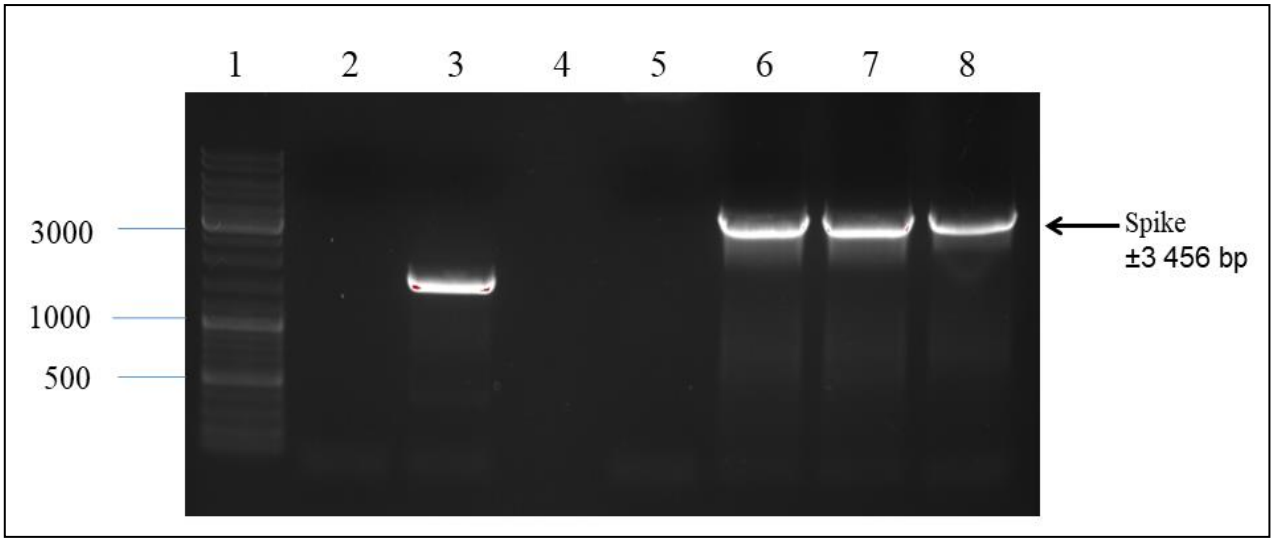

Figure 26: PCR of plasmid DNA from DH10B cells transformed with pEAQ-HT-mIBV-S-TM-KKSV. Lane 1: GeneRuler ladder mix SM0331, Lane 2: Negative control (no template DNA), Lane 3: Positive control pEAQ-HT with a known insert (±1 200 bp), Lane 5-8: pEAQ-HT-mIBV-S-TM-KKSV DH10B colonies 1-4. PCR using pEAQ-HT forward and reverse primers, Table 1. The PCR products were separated on a 1% Agarose gel.

A band that correlated with the expected size of the recombinant S gene was present in 3 of the selected colonies (Fig. 26, lanes 6 – 8). This shows that the PCR product (mIBV-S-TM-KKSV) was successfully cloned into pEAQ-HT but still required sequence validation to confirm their successful amplification.

Therefore, according to the results presented, mIBV-S-KKSV, and mIBV-S-IAV-TM-KKSV genes were potentially successfully cloned into the pEAQ-HT expression vector producing two new constructs (Fig. 27a and b).

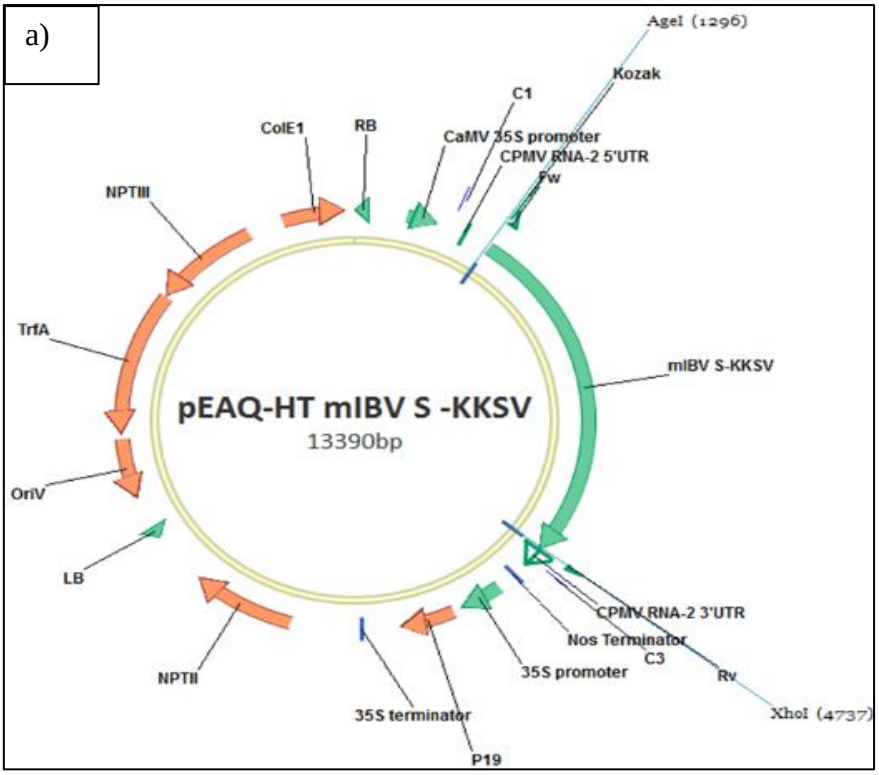

Figure 27a: pEAQ-HT harbouring the gene encoding the recombinant S protein mIBV-S–KKSV.

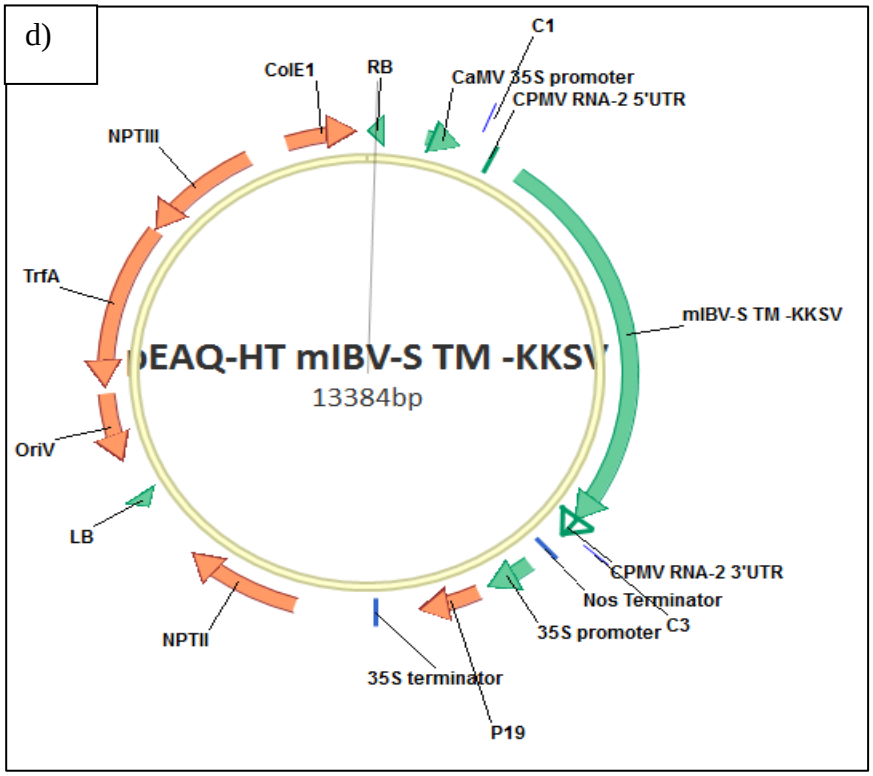

Figure 27b: pEAQ-HT harbouring the gene encoding the recombinant S protein mIBV-S-TM-KKSV.

One of the positive clones for each gene insert were propagated and sent to Inqaba Biotechnical Industries (Pty) Ltd for sequence validation, and sequence validated clones were electroporated independently into three independent *Agrobacterium* strains (AGL-1, GV3101::pMP90, and LBA4404). Colonies were PCR validated before *Agrobacterium* glycerol stocks were prepared. An aliquot of the pEAQ-HT constructs with the IBV gene inserts of choice (as well as the IAV M2 gene insert) were streaked out and the overnight growth was scraped from the plate to prepare liquid cultures for *N. benthamiana* ΔXT/FT plants for agroinfiltration. Various combinations of each were infiltrated.

The following combinations and ratios were infiltrated (in AGL-1 and LBA4404):

Combo 1 -	S:M:E	2:1:1
Combo 2 -	S:M:E	2:1:2
Combo 3 -	rIBV-S-TM:M:E	2:1:1
Combo 4 -	rIBV-S-TM/CT:M2	2:1
Combo 5 -	mIBV-S-KKSV:M:E	2:1:1
Combo 6 -	mIBV-S-TM-KKSV:M:E	2:1:1

4.4.2. Analysis of crude plant proteins

Agroinfiltrated plant leaves were harvested at 6 dpi. The plant proteins were extracted using PBS buffer and clear lysate was purified by Iodixanol density gradient ultracentrifugation. Fractions 10 and 11 (20-30% Iodixanol) were analysed by SDS-PAGE (Fig. 28 and 29) and immunoblotting. *Agrobacterium*-mediated (AGL-1 and LBA4404) infiltration of S, rIBV-S-TM, rIBV-S-TM/CT, mIBV-S-KKSV, and mIBV-S-TM-KKSV constructs in combination with the E and M genes was conducted. The rIBV-S-TM/CT was co-infiltrated with the IAV M2 ion channel protein gene (to assist with VLP formation) instead of with the IBV E and M genes. Different ratios of the constructs were infiltrated in an attempt to improve S protein expression and formation of VLPs.

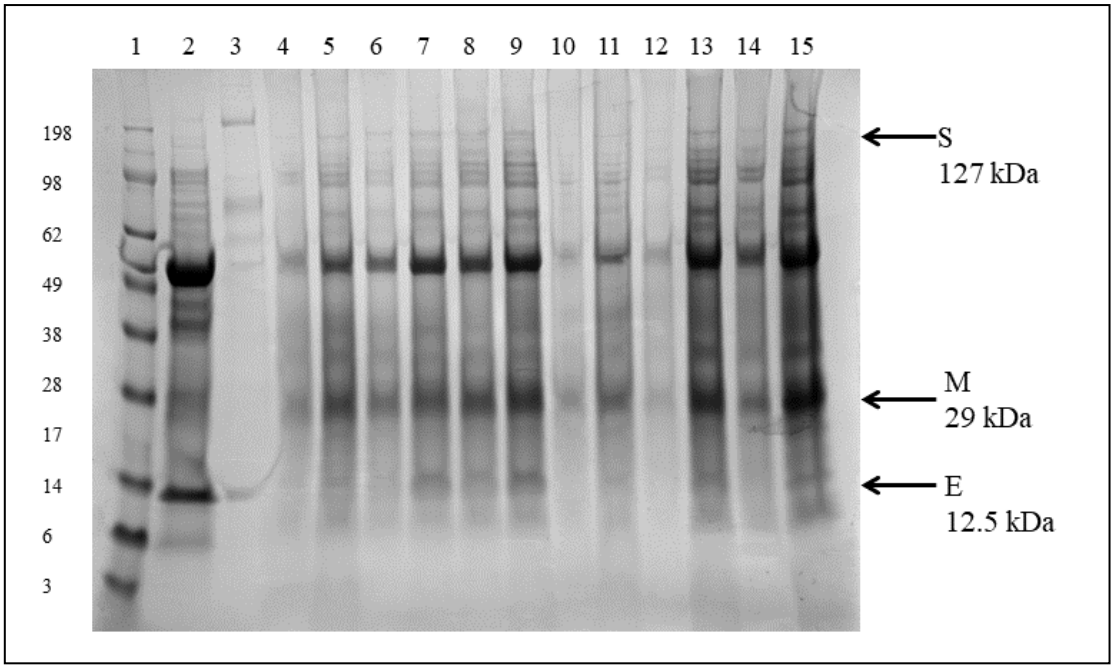

Figure 28: Bolt 4-12% SDS PAGE analysis of pEAQ-HT IBV S (or rIBV-S-TM or rIBV-S-TM/CT or mIBV-S-KKSV or mIBV-S-TM-KKSV), M, E and IAV M2 ion channel proteins co-expressed in *N. benthamiana* ΔXT/FT 6 dpi. *Agrobacterium*-mediated (AGL-1) expression. Lane 1: SeeBlue Plus MW marker, Lane 2: Negative control pEAQ-HT empty, Lane 3: Positive control IBV QX-like inactivated, Lane 4-5: S:M:E 2:1:1 (Frs 10-11), Lane 6-7: S:M:E 2:1:2 (Frs 10-11), Lane 8-9: rIBV-S-TM:M:E 2:1:1 (Frs 10-11), Lane 10-11: rIBV-S-TM/CT:M2 2:1 (Frs 10-11), Lane 12-13: mIBV-S-KKSV:M:E 2:1:1 (Frs 10-11), Lane 14-15: mIBV-S-TM-KKSV:M:E 2:1:1 (Frs 10-11).

Proteins which correlate to the three structural protein sizes were detected by SDS PAGE analysis (Fig. 28). The bands correlating to the M (29 kDa) and E (12.5 kDa) proteins were present in all the lanes including lanes 12-15, but were very faint in lanes 10-12, which were the plants that were infiltrated without those two constructs (Fig. 28). Lanes 10-12 were generally very faint, however, so the proteins may have still been present. There is a band of similar size to both the M and E proteins present in lane 2, the negative control lane, suggesting that the sizes of the M and E proteins corresponded with non-specific protein bands that were present in the plant leaves which would make it difficult to identify distinct bands correlating to them. The band correlating with the size of the S (127 kDa) was very faint in all the lanes (4-15) indicating low S protein expression in spite of the modifications. Lane 3 (positive control) was warped, making it difficult to identify what bands were or were not present.

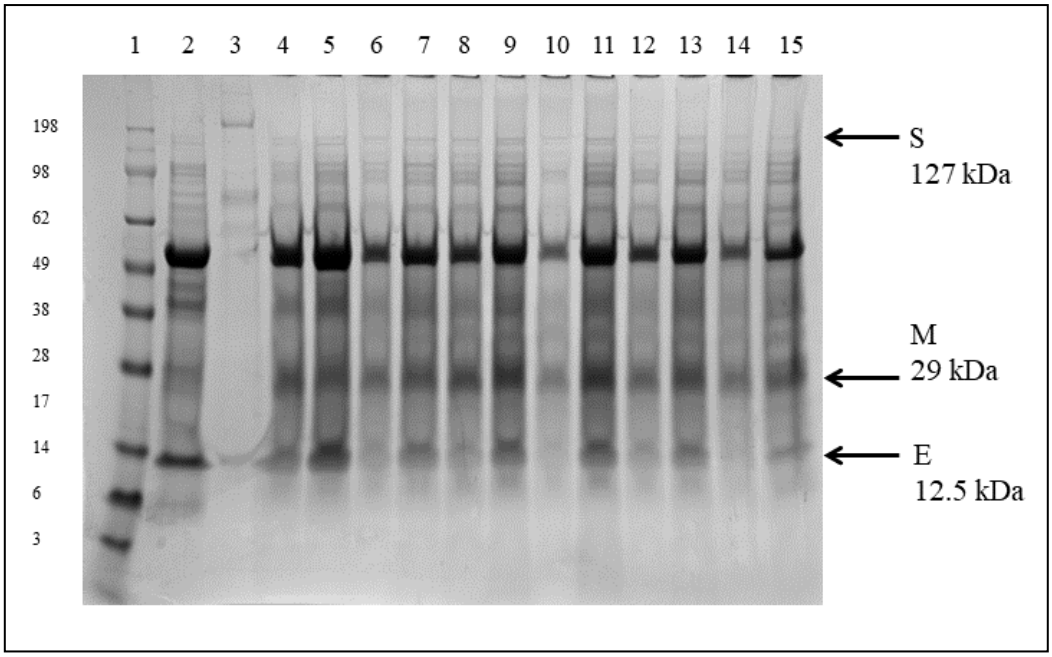

Figure 29: Bolt 4-12% SDS PAGE analysis of pEAQ-HT IBV S (or rIBV-S-TM or rIBV-S-TM/CT or mIBV-S-KKSV or mIBV-S-TM-KKSV), M, E and IAV M2 ion channel proteins co-expressed in *N. benthamiana* ΔXT/FT 6 dpi. *Agrobacterium*-mediated (LBA4404) expression. Lane 1: SeeBlue Plus MW marker, Lane 2: Negative control pEAQ-HT empty, Lane 3: Positive control IBV QX-like inactivated, Lane 4-5: S:M:E 2:1:1 (Frs 10-11), Lane 6-7: S:M:E 2:1:2 (Frs 10-11), Lane 8-9: rIBV-S-TM:M:E 2:1:1 (Frs 10-11), Lane 10-11: rIBV-S-TM/CT:M2 2:1 (Frs 10-11), Lane 12-13: mIBV-S-KKSV:M:E 2:1:1 (Frs 10-11), Lane 14-15: mIBV-S-TM-KKSV:M:E 2:1:1 (Frs 10-11).

Proteins which correlate to the three structural protein sizes were detected by SDS PAGE analysis (Fig. 29). The bands correlating to the M (29 kDa) and E (12.5 kDa) proteins were present in all the lanes including lanes 12-15, but were very faint in lane 10, which was a plant that was infiltrated without those two constructs. Lane 10 was generally very faint, however, so the proteins may have still been present. There is a band of similar size to both the M and E proteins present in lane 2, the negative control lane, suggesting that the sizes of the M and E proteins corresponded with non-specific protein bands that were present in the plant leaves which would make it difficult to identify distinct bands correlating to the proteins. The band correlating with the size of the S (127 kDa) was very faint in all the lanes (4-15) indicating low S protein expression. Lane 3 (positive control) was warped, making it difficult to identify what bands were or were not present.

4.4.3. TEM visualisation of recombinant S protein VLPs

No VLPs were detected using TEM in any of the iodixanol fractions, from any of the construct combinations harnessing AGL-1 or LBA4404 *Agrobacterium*-mediated plant leaf infiltrations. The samples were also stained with phosphotungstic acid (pH 7.4) as an alternative to the acidic uranyl acetate staining, but this also resulted in no detection of VLPs.

In an effort to detect VLPs in freshly harvested leaf material, leaf pieces (1mm x 1mm) were cut out and submerged in fixative prior to extraction and the cross-sections were analysed for VLPs in the intact cell compartments (Figs 30a - d).

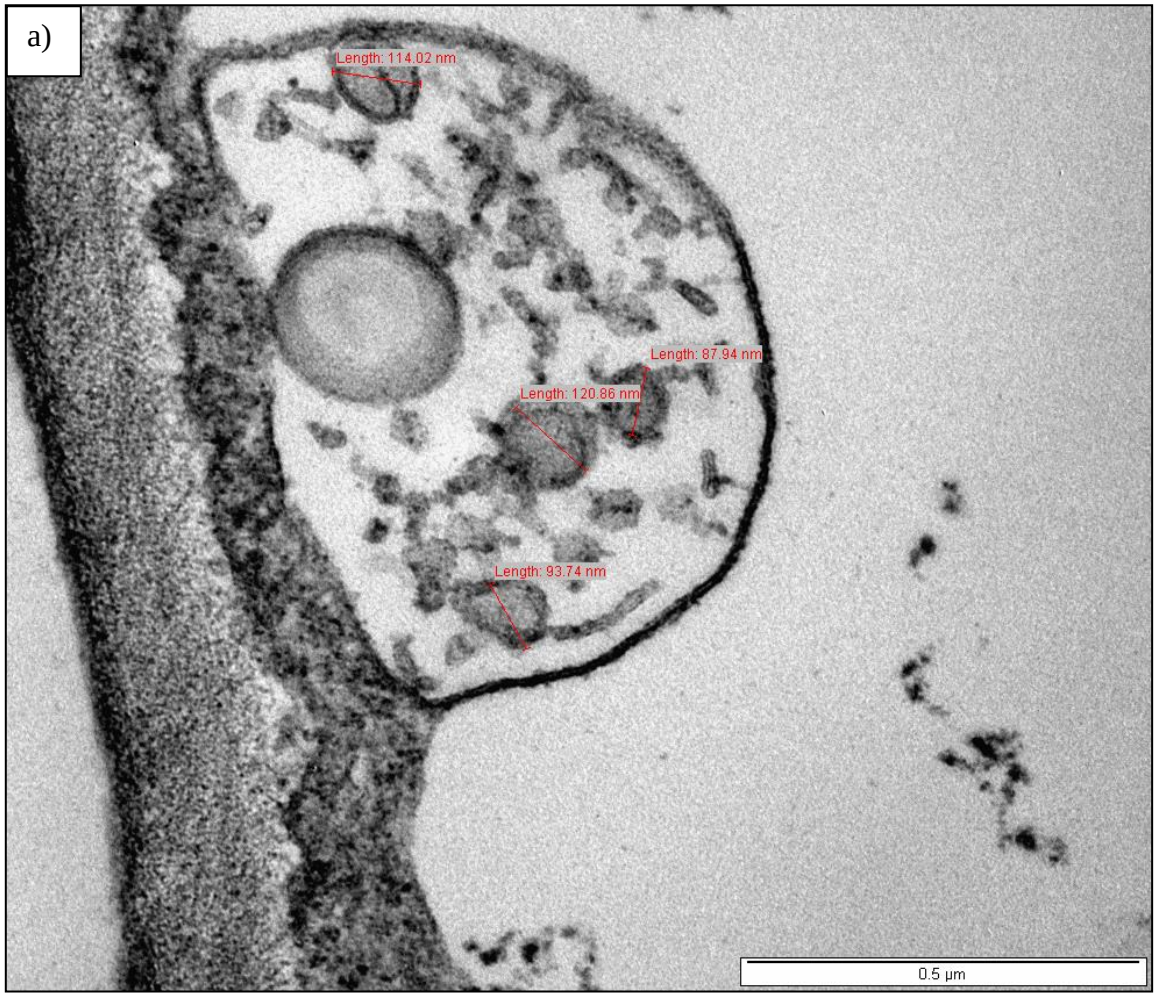

b)

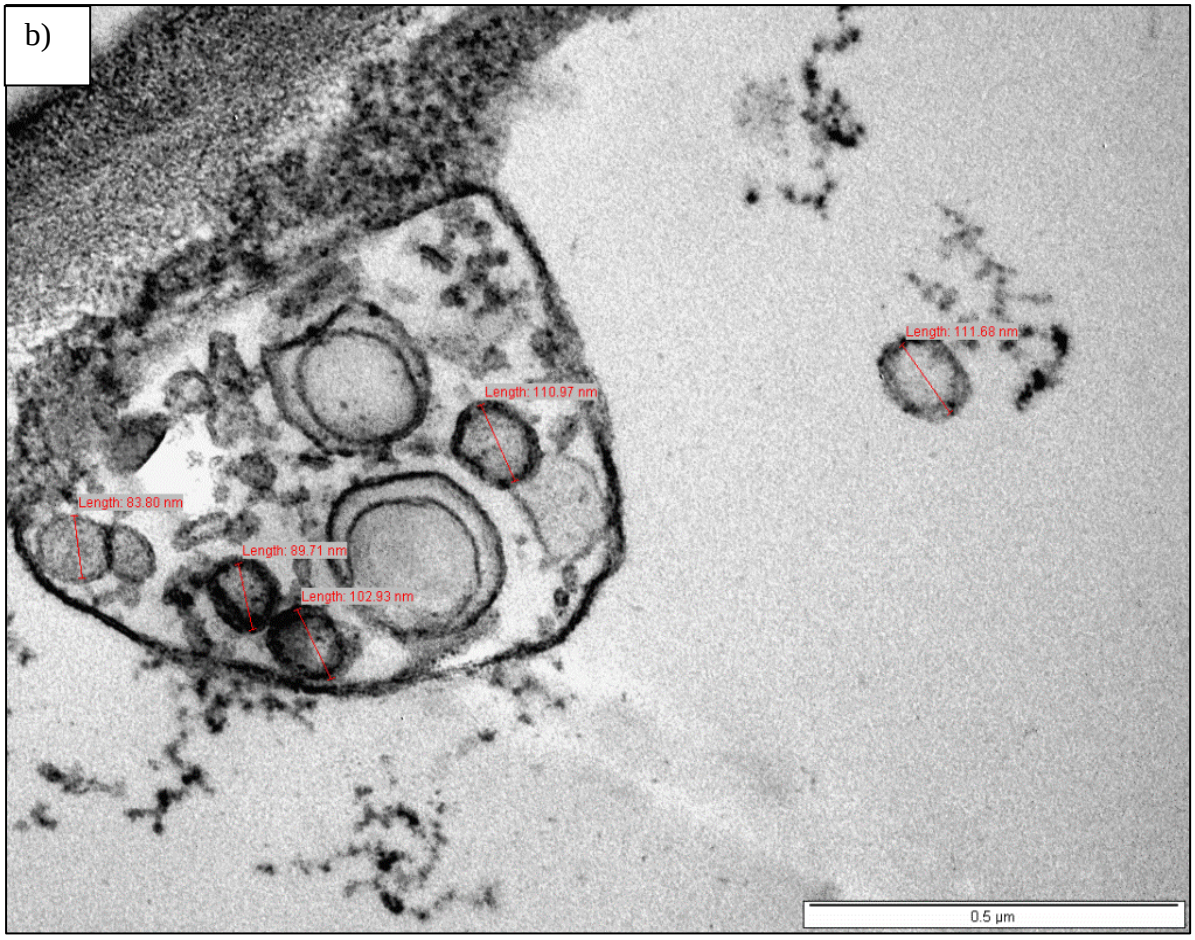

c)

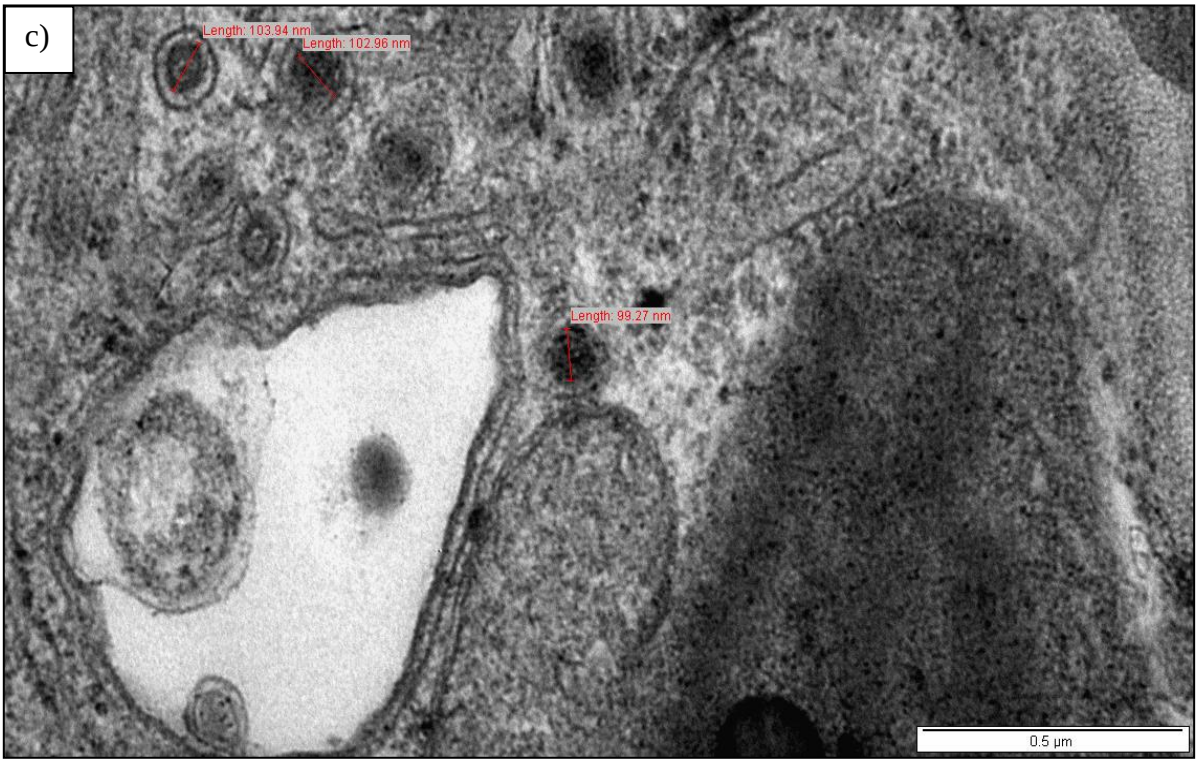

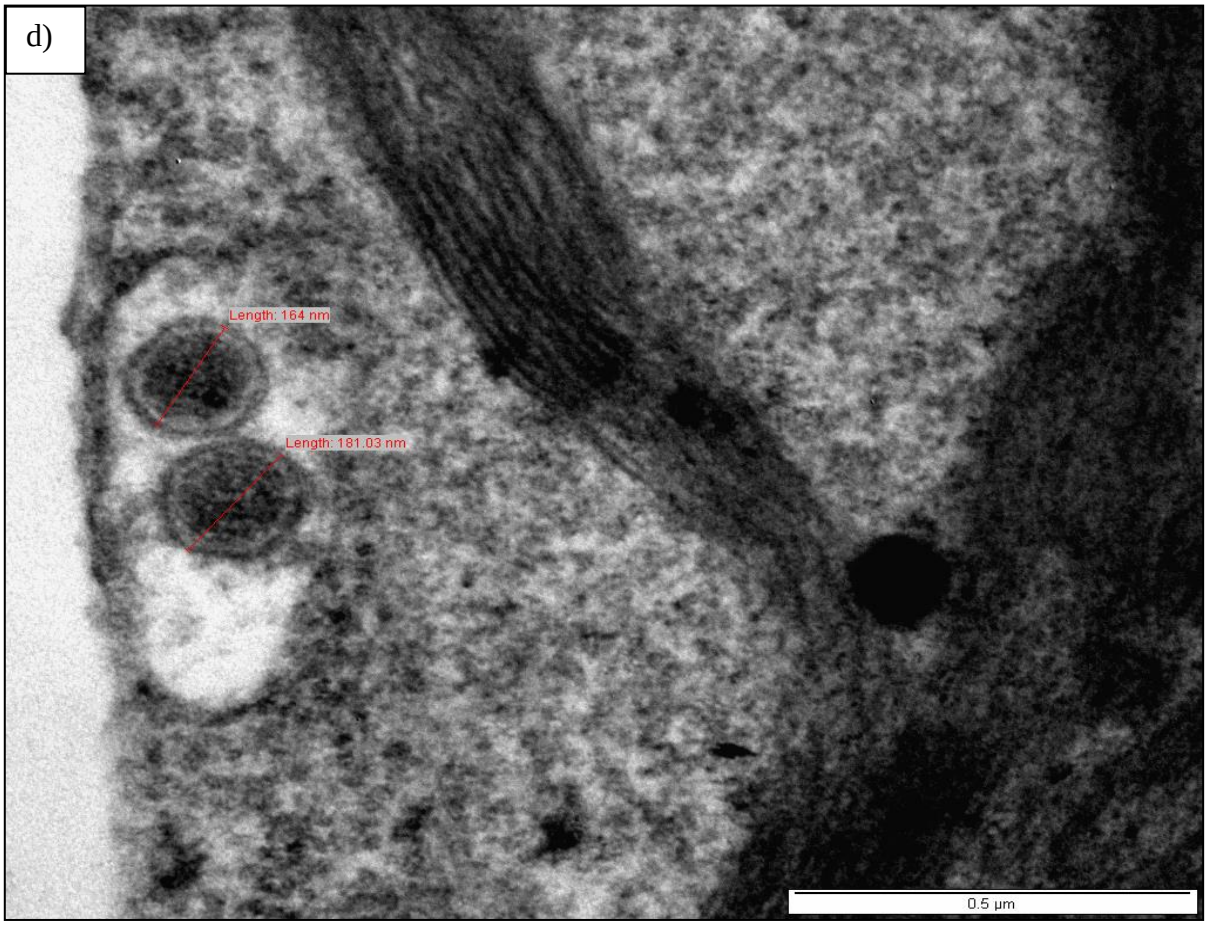

Figure 30: TEM images of potential plant-produced homogenous IB VLPs. Three to four week old *N. benthamiana* ΔXT/FT were co-infiltrated with the S, E and M proteins of IBV. Leaves were harvested 6 dpi. The leaf cross-sections were imaged by TEM revealing the presence of spherical particles matching the expected size of IBV particles. Expression and assembly of the structural proteins were mediated by *Agrobacterium* strain AGL-1. Scale bars, 500 nm.

Spherical structures that resemble IB VLPs of the appropriate sizes (80-120 nm) were detected in the cytoplasm (Figs 30a - d). However, without the spikes surrounding them, it cannot be concluded that they are IB VLPs. They could however, be assembly intermediates expressing the structural proteins but without incorporating the S protein. Ujike and Taguchi, (2015) showed that co-expressing the M proteins with the E protein resulted in the release of sedimentable particles (VLPs) into culture supernatants. When expressed alone in vTF7-3-infected cells, the E protein was also shown to be released into the cultured supernatant in similar particles (Corse and Machamer, 2000).

4.5. Experiment 5

In the fifth experiment, a gene encoding the nucleocapsid (N) protein was cloned into pEAQ-HT, transformed into DH10B, then into *A. tumefaciens* in another attempt to assemble IB VLPs in plants. Ujike and Taguchi (2015) indicated that the N protein is likely to assist with VLP formation. The cloned IBV genes (S (and the modified versions thereof), M, E, and N) were once again agroinfiltrated into *N. benthamiana* ΔXT/FT in various combinations to assemble VLPs. Leaf tissue was harvested at 6 dpi. Plant proteins were extracted in PBS buffer.

The goals of this experiment were:

- to improve protein expression and assemble IB VLPs
- to identify which protein combinations were needed to assemble IB VLPs
- to identify which construct ratios would improve IBV target protein co-expression and IB VLP assembly

4.5.1. Cloning IBV genes into pEAQ-HT vector

In order to achieve these goals, a chicken codon-optimised gene (N) was digested with *Age*I and *Xho*I enzymes to excise the target gene insert from the pUC57 vector backbone. The pEAQ-HT vector was also digested with the same enzymes to linearize it and create compatible ends for cloning. The gene was ligated into pEAQ-HT and transformed into electrocompetent DH10B cells. pEAQ-HT-N was verified by colony PCR (Taq DNA polymerase) (Fig. 31).

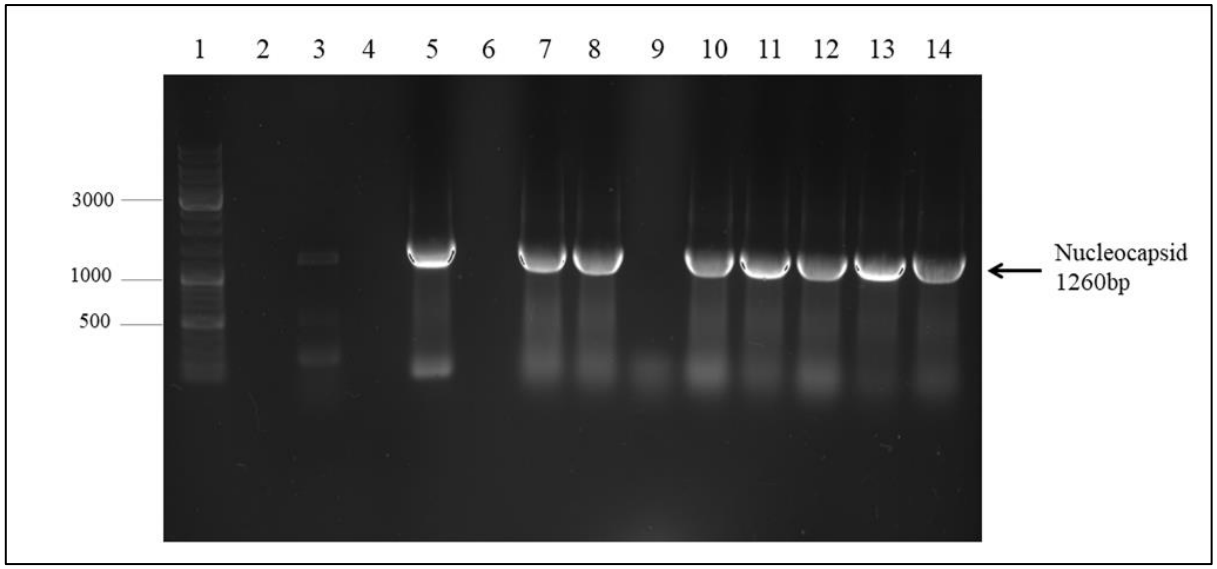

Figure 31: Colony PCR of DH10B cells transformed with pEAQ-HT-N. Lane 1: GeneRuler ladder mix SM0331, Lane 3: Negative control (no template DNA), Lane 5: Positive control pEAQ-HT with a known insert (±1 200 bp), Lanes 7-14: pEAQ-HT-N colonies 1-8. PCR was done using FSC5 forward and reverse primers, Table 1. The PCR products were separated on a 1% Agarose gel.

A PCR product that correlated with the size of the N gene (1260 bp) (Fig. 12) was present in 7 of the 8 colonies selected for screening (lanes 7-14). FSC5 primers were used for screening. The FSC5 forward primer hybridizes only 38 bp upstream of the *Age*I site, while the FSC5 reverse primer hybridizes 60 bp downstream of the *Xho*I site. This results in a PCR product that is approximately 100bp larger than expected. This, however, would not be as noticeable on the gel as the 300bp increase caused by the pEAQ-HT primers was. This is a first indication that the N gene was cloned into pEAQ-HT but still required sequence validation to confirm the successful cloning of the target gene. Lane 3 should have been empty as no template DNA was loaded, therefore it is possible that there was contamination during sample loading.

Therefore, according to the results presented, the N gene was potentially successfully cloned into the pEAQ-HT expression vector producing a new construct (Fig. 32).

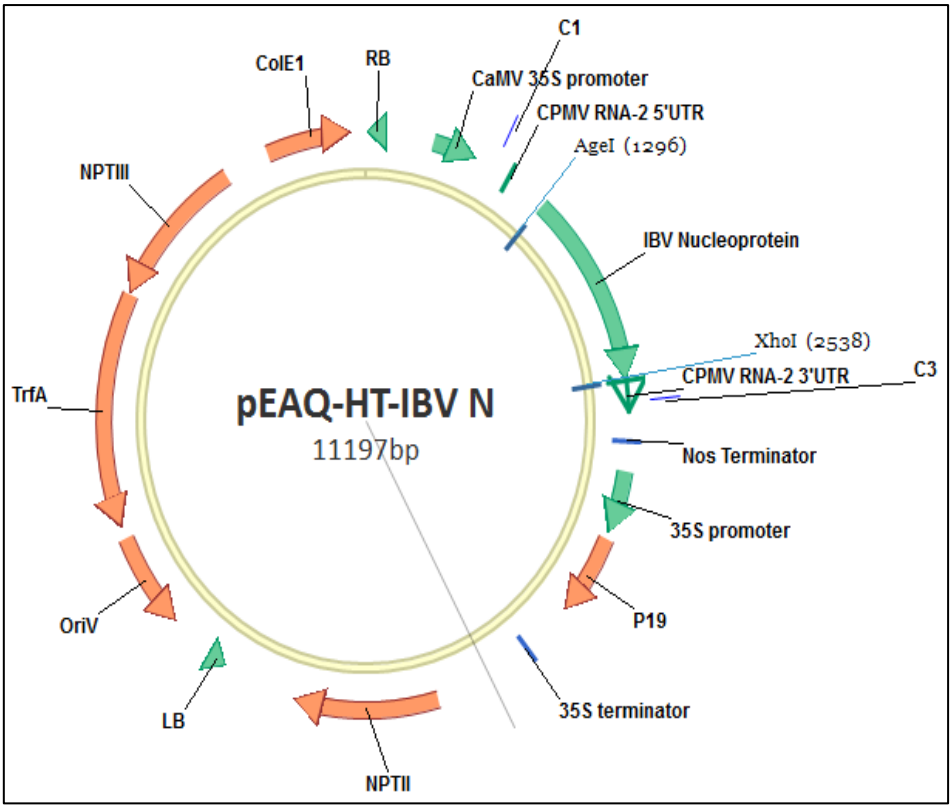

Figure 32: pEAQ-HT harbouring the gene encoding the Nucleocapsid protein (N).

One of the positive clones for the N gene insert were propagated and sent to Inqaba Biotechnical Industries (Pty) Ltd for sequence validation, and the sequence validated clone was electroporated independently into three different *Agrobacterium* strains (AGL-1, GV3101::pMP90, and LBA4404). Colonies were once more PCR validated before *Agrobacterium* glycerol stocks were prepared. Once more, an aliquot of the pEAQ-HT constructs with the IBV gene inserts of choice were streaked out and the overnight growth was scraped from the plate to prepare liquid cultures for *N. benthamiana* ΔXT/FT plants for agroinfiltration. Various combinations of each were infiltrated.

The following combinations and ratios were infiltrated (in AGL-1):

Combo 1 -	S:M:E:N	2:1:1:1
Combo 2 -	S:M:E:N	2:1:2:2
Combo 3 -	rIBV-S-TM:M:E:N	2:1:1:1
Combo 4 -	rIBV-S-TM/CT:M2:N	2:1:1
Combo 5 -	mIBV-S-KKSV:M:E:N	2:1:1:1
Combo 6 -	mIBV-S-TM-KKSV:M:E:N	2:1:1:1

4.5.2. Analysis of crude plant proteins after the addition of the N protein

Agroinfiltrated plant leaves were harvested at 6 dpi. The plant proteins were extracted using PBS buffer and clear lysate was purified by Iodixanol density gradient ultracentrifugation. Fractions 10 and 11 (20-30% Iodixanol) were analysed by SDS-PAGE (Fig. 33) and immunoblotting. *Agrobacterium*-mediated (AGL-1) infiltration of S, rIBV-S-TM, rIBV-S-TM/CT, mIBV-S-KKSV, and mIBV-S-TM-KKSV constructs in combination with the E, M, and N genes was conducted. The rIBV-S-TM/CT was co-infiltrated with the IAV M2 ion channel protein gene (to assist with VLP formation) instead of with the IBV E and M genes. Different ratios of the constructs were infiltrated in an attempt to improve S protein expression and formation of VLPs.

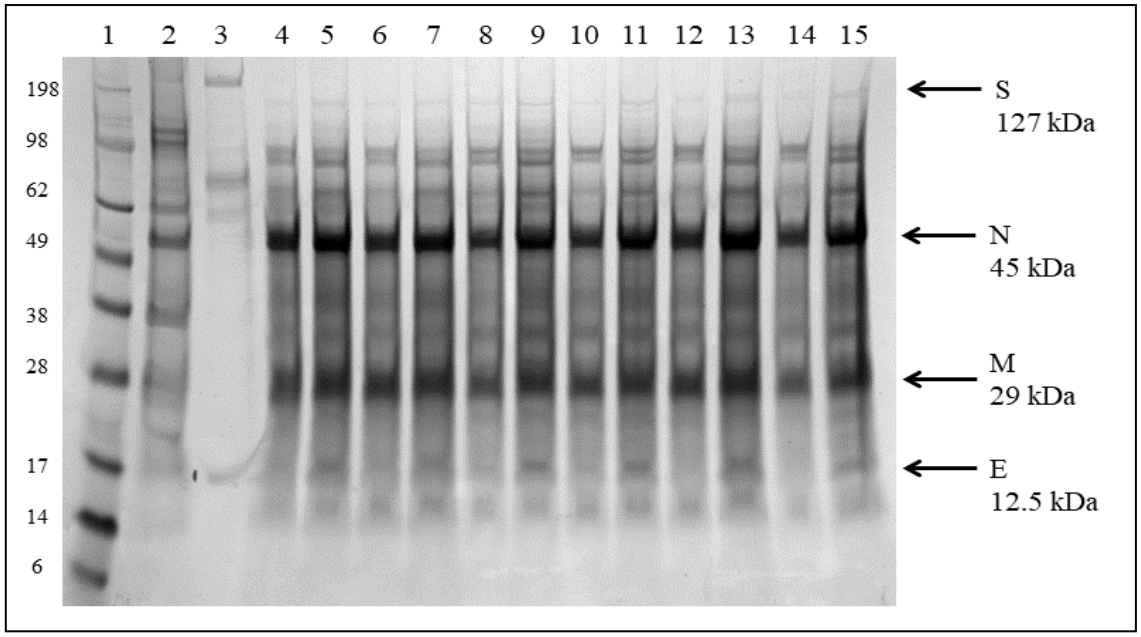

Figure 33: Bolt 4-12% SDS PAGE analysis of pEAQ-HT IBV S (or rIBV-S-TM or rIBV-S-TM/CT or mIBV-S-KKSV or mIBV-S-TM-KKSV), M, E, N, and IAV M2 ion channel proteins co-expressed in *N. benthamiana* ΔXT/FT 6 dpi. *Agrobacterium*-mediated (AGL-1) expression. Lane 1: SeeBlue Plus MW marker, Lane 2: Negative control pEAQ-HT empty, Lane 3: Positive control IBV QX-like inactivated, Lane 4-5: S:M:E:N 2:1:1:1 (Frs 10-11), Lane 6-7: S:M:E:N 2:1:2:2 (Frs 10-11), Lane 8-9: rIBV-S-TM:M:E:N 2:1:1:1 (Frs 10-11), Lane 10-11: rIBV-S-TM/CT:M2:N 2:1:1 (Frs 10-11), Lane 12-13: mIBV-S-KKSV:M:E:N 2:1:1:1 (Frs 10-11), Lane 14-15: mIBV-S-TM-KKSV:M:E:N 2:1:1:1 (Frs 10-11).

Protein bands which correlate to the sizes of the four structural protein sizes were detected when subjected to SDS PAGE analysis (Fig. 33). The bands correlating to the M (29 kDa) and E (12.5 kDa) proteins were present in all the protein extracts represented in all the lanes, including lanes 10-12, where M and E were omitted. Thus, there appears to be unknown plant proteins of similar size to both the M and E proteins in the negative control (pEAQ-empty) (represented in lane 2). This would make it difficult to identify distinct bands correlating to the proteins of interest. The band correlating with the size of the S (127 kDa) was very faint in all the lanes (4-15), again indicating low S protein expression. The N (45kDa) is close to the size of Rubisco (50kDa), the most abundant protein in plants. Therefore, it was difficult to identify a distinct band correlating to the N protein, if it was present.

Subsequently, an immunoblot was performed using IBV-specific antiserum in an attempt to detect the IBV proteins present in the fractions (Fig. 34). *Agrobacterium* strain AGL-1 was used to mediate protein expression.

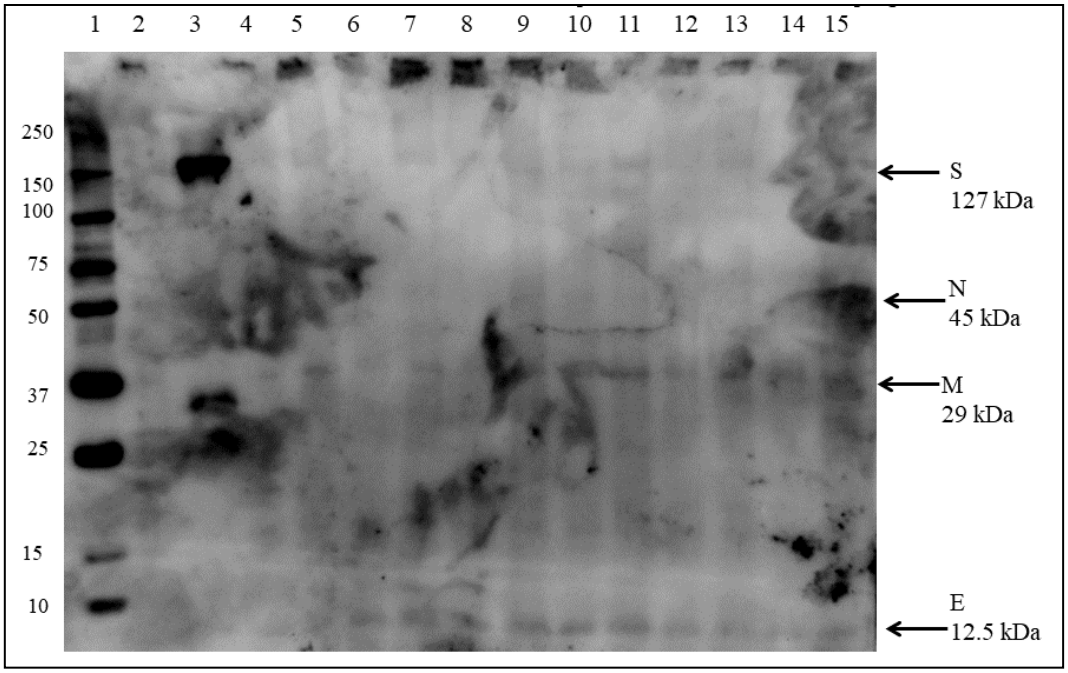

Figure 34: Immunoblot using IBV-specific antiserum to detect pEAQ-HT IBV S (or rIBV-S-TM or rIBV-S-TM/CT or mIBV-S-KKSV or mIBV-S-TM-KKSV), N, M, and E proteins co-expressed in *N. benthamiana* ΔXT/FT 6 dpi. Lane 1: Western C MW marker, Lane 2: Negative control pEAQ-HT empty, Lane 3: Positive control IBV QX-like inactivated, Lane 4-5: S:M:E:N 2:1:1:1 (Frs 10-11), Lane 6-7: S:M:E:N 2:1:2:2 (Frs 10-11), Lane 8-9: rIBV-S-TM:M:E:N 2:1:1:1 (Frs 10-11), Lane 10-11: rIBV-S-TM/CT:M2:N 2:1:1 (Frs 10-11), Lane 12-13: mIBV-S-KKSV:M:E:N 2:1:1:1 (Frs 10-11), Lane 14-15: mIBV-S-TM-KKSV:M:E:N 2:1:1:1 (Frs 10-11).

Protein bands which correlate to the sizes of the target structural protein sizes were detected with immunoblot analysis (Fig. 34). Faint bands correlating with the size of the E protein (12.5 kDa) could be visualised in all lanes 4-10, although they were not expected in lanes 12-15, which were plants that were infiltrated without the gene construct encoding protein E. Bands correlating with the size of the M protein (29 kDa) could be seen in lanes 4-9, and in lanes 12-15. The background made it difficult to identify bands in lanes 10 and 11 which should not be present as the plants were infiltrated without them. Faint bands correlating with the S protein (127 kDa) size could be visualised in all lanes. Bands correlating to the N protein (45 kDa)

were not distinct enough to be visualised with certainty, but were expected to be present in all the lanes if it was co-expressed and formed part of the assembled VLP.

4.5.3. LC-MS/MS based peptide sequencing

Bands correlating to the sizes of each of the four structural proteins (S, rIBV-S-TM, rIBV-S-TM/CT, mIBV-S-KKSV, mIBV-S-TM-KKSV, M, N, and E) were cut out from the SDS-PAGE gel (Fig. 33) and subjected to LC-MS/MS based peptide sequencing (Fig. 35). The gel bands were trypsin digested as described before.

IBV S protein, Combo 1, fr. 11, 15 % (95% confidence), 21 peptides

MLVKSLFLVTILCALCSANLFDSDNNYVYYYQSAFRPPNGWHLQGGAYAVVNSTNHTSNAGSAQGCTVGVIKDVY
NQSVASIAMTAPLQGMAWFCTAYCNFSDTTVFVTHCYHIRISAMKNGSLFYNLTVSVSKYPNFKSFQCVNNFTSV
YLNGDLVFTSNKTTDVTSAGVYFKAGGPVNYSIMKEFKVLAYFVNGTAQDVILCDNSPKGLLACQYNTGNFSDGF
YPFTNSTLVREKFIVYRESSFNTTLALTNFTFTNVSNAQPNSGGVNTFHLYQTQTAQSGYYNFNLSFLSQFVYKA
SDFMYGSYHPSCSFRPETINSGLWFNSLSVSLTYGPLQGGCKQSVFSGKATCCYAYSYKGPMACKGVYSGELRTN
FECGLLVYVTKSDGSRIQTRTEPLVLTQYNYNNITLDKCVAYNIYGRVGQGFITNVTDSAANFSYLADGGLAILD
TSGAIDVFVVQGIYGLNYYKVNPCEDVNQQFVVSGGNIVGILTSRNETGSEQVENQFYVKLTNSSHRRRRSIGQN
VTSCPYVSYGRFCIEPDGSLKMIVPEELKQFVAPLLNITESVLIPNSFNLTVTDEYIQTRMDKVQINCLQYVCGN
SLECRKLFQQYGPVCDNILSVVNSVSQKEDMELLSFYSSTKPKGYDTPVLSNVSTGEFNISLLLKTPISSSGRSF
IEDLLFTSVETVGLPTDAEYKKCTAGPLGTLKDLICAREYNGLLVLPPIITADMQTMYTASLVGAMAFGGITSAA
AIPFATQIQARINHLGITQSLLMKNQEKIAASFNKAIGHMQEGFRSTSLALQQIQDVVNKQSAILTETMNSLNKN
FGAITSVIQDIYAQLDAIQADAQVDRTGRLSSLSVLASAKQSEYIRVSQQRELATKKINECVKSQSNRYGFCGSG
RHVLSIPQNAPNGIVFIHFTYTPESFVNVTAIVGFCVNPANASQYAIVPANGRGVFIQVNGSYYITARDMYMPR
ITAGDIVTLTSCQANYVNVNKTVINTFVEDDDFNFNDELSKWWNDTKHELPDFDEFNYTVPVLNISNEIDRIQEV
IQGLNDSLIDLETLSILKTYIKWPLAIYSTVSSSLVLVGLIIAMGLWMTGCCGCCCGCFGIIPLMSKCGKKSSYY
TTFDNDVVTEQYRPKKSV

IBV S protein, Combo 2, fr. 11, 14.4 % (95% confidence), 15 peptides

MLVKSLFLVTILCALCSANLFDSDNNYVYYYQSAFRPPNGWHLQGGAYAVVNSTNHTSNAGSAQGCTVGVIKDVY
NQSVASIAMTAPLQGMAWFCTAYCNFSDTTVFVTHCYHIRISAMKNGSLFYNLTVSVSKYPNFKSFQCVNNFTSV
YLNGDLVFTSNKTTDVTSAGVYFKAGGPVNYSIMKEFKVLAYFVNGTAQDVILCDNSPKGLLACQYNTGNFSDGF
YPFTNSTLVREKFIVYRESSFNTTLALTNFTFTNVSNAQPNSGGVNTFHLYQTQTAQSGYYNFNLSFLSQFVYKA
SDFMYGSYHPSCSFRPETINSGLWFNSLSVSLTYGPLQGGCKQSVFSGKATCCYAYSYKGPMACKGVYSGELRTN
FECGLLVYVTKSDGSRIQTRTEPLVLTQYNYNNITLDKCVAYNIYGRVGQGFITNVTDSAANFSYLADGGLAILD
TSGAIDVFVVQGIYGLNYYKVNPCEDVNQQFVVSGGNIVGILTSRNETGSEQVENQFYVKLTNSSHRRRRSIGQN
VTSCPYVSYGRFCIEPDGSLKMIVPEELKQFVAPLLNITESVLIPNSFNLTVTDEYIQTRMDKVQINCLQYVCGN
SLECRKLFQQYGPVCDNILSVVNSVSQKEDMELLSFYSSTKPKGYDTPVLSNVSTGEFNISLLLKTPISSSGRSF
IEDLLFTSVETVGLPTDAEYKKCTAGPLGTLKDLICAREYNGLLVLPPIITADMQTMYTASLVGAMAFGGITSAA
AIPFATQIQARINHLGITQSLLMKNQEKIAASFNKAIGHMQEGFRSTSLALQQIQDVVNKQSAILTETMNSLNKN
FGAITSVIQDIYAQLDAIQADAQVDRTGRLSSLSVLASAKQSEYIRVSQQRELATKKINECVKSQSNRYGFCGSG
RHVLSIPQNAPNGIVFIHFTYTPESFVNVTAIVGFCVNPANASQYAIVPANGRGVFIQVNGSYYITARDMYMPRD
ITAGDIVTLTSCQANYVNVNKTVINTFVEDDDFNFNDELSKWWNDTKHELPDFDEFNYTVPVLNISNEIDRIQEV
IQGLNDSLIDLETLSILKTYIKWPLAIYSTVSSSLVLVGLIIAMGLWMTGCCGCCCGCFGIIPLMSKCGKKSSYY
TTFDNDVVTEQYRPKKSV

IBV rIBV-S-TM protein, Combo 3, fr. 11, 2.7 % (95% confidence), 5 peptides

MLVKSLFLVTILCALCSANLFDSDNNYVYYYQSAFRPPNGWHLQGGAYAVVNSTNHTSNAGSAQGCTVGVIKDVY
NQSVASIAMTAPLQGMAWFCTAYCNFSDTTVFVTHCYHIRISAMKNGSLFYNLTVSVSKYPNFKSFQCVNNFTSV
YLNGDLVFTSNKTTDVTSAGVYFKAGGPVNYSIMKEFKVLAYFVNGTAQDVILCDNSPKGLLACQYNTGNFSDGF
YPFTNSTLVREKFIVYRESSFNTTLALTNFTFTNVSNAQPNSGGVNTFHLYQTQTAQSGYYNFNLSFLSQFVYKA
SDFMYGSYHPSCSFRPETINSGLWFNSLSVSLTYGPLQGGCKQSVFSGKATCCYAYSYKGPMACKGVYSGELRTN
FECGLLVYVTKSDGSRIQTRTEPLVLTQYNYNNITLDKCVAYNIYGRVGQGFITNVTDSAANFSYLADGGLAILD
TSGAIDVFVVQGIYGLNYYKVNPCEDVNQQFVVSGGNIVGILTSRNETGSEQVENQFYVKLTNSSHRRRRSIGQN
VTSCPYVSYGRFCIEPDGSLKMIVPEELKQFVAPLLNITESVLIPNSFNLTVTDEYIQTRMDKVQINCLQYVCGN
SLECRKLFQQYGPVCDNILSVVNSVSQKEDMELLSFYSSTKPKGYDTPVLSNVSTGEFNISLLLKTPISSSGRSF
IEDLLFTSVETVGLPTDAEYKKCTAGPLGTLKDLICAREYNGLLVLPPIITADMQTMYTASLVGAMAFGGITSAA
AIPFATQIQARINHLGITQSLLMKNQEKIAASFNKAIGHMQEGFRSTSLALQQIQDVVNKQSAILTETMNSLNKN
FGAITSVIQDIYAQLDAIQADAQVDRTGRLSSLSVLASAKQSEYIRVSQQRELATKKINECVKSQSNRYGFCGSG
RHVLSIPQNAPNGIVFIHFTYTPESFVNVTAIVGFCVNPANASQYAIVPANGRGVFIQVNGSYYITARDMYMPRD
ITAGDIVTLTSCQANYVNVNKTVINTFVEDDDFNFNDELSKWWNDTKHELPDFDEFNYTVPVLNISNEIDRIQEV
IQGLNDSLIDLETLSILKTYIKWPLAIYSTVSSSLVLVGLIIAMGLWMTGCCGCCCGCFGIIPLMSKCGKKSSYY
TTFDNDVVTEQYRPKKSV

IBV rIBV-S-TM/CT protein, Combo 4, fr. 11, 19.3 % (95% confidence), 24 peptides

MLVKSLFLVTILCALCSANLFDSDNNYVYYYQSAFRPPNGWHLQGGAYAVVNSTNHTSNAGSAQGCTVGVIKDVY
NQSVASIAMTAPLQGMAWFCTAYCNFSDTTVFVTHCYHIRISAMKNGSLFYNLTVSVSKYPNFKSFQCVNNFTSV
YLNGDLVFTSNKTTDVTSAGVYFKAGGPVNYSIMKEFKVLAYFVNGTAQDVILCDNSPKGLLACQYNTGNFSDGF
YPFTNSTLVREKFIVYRESSFNTTLALTNFTFTNVSNAQPNSGGVNTFHLYQTQTAQSGYYNFNLSFLSQFVYKA
SDFMYGSYHPSCSFRPETINSGLWFNSLSVSLTYGPLQGGCKQSVFSGKATCCYAYSYKGPMACKGVYSGELRTN
FECGLLVYVTKSDGSRIQTRTEPLVLTQYNYNNITLDKCVAYNIYGRVGQGFITNVTDSAANFSYLADGGLAILD
TSGAIDVFVVQGIYGLNYYKVNPCEDVNQQFVVSGGNIVGILTSRNETGSEQVENQFYVKLTNSSHRRRRSIGQN
VTSCPYVSYGRFCIEPDGSLKMIVPEELKQFVAPLLNITESVLIPNSFNLTVTDEYIQTRMDKVQINCLQYVCGN
SLECRKLFQQYGPVCDNILSVVNSVSQKEDMELLSFYSSTKPKGYDTPVLSNVSTGEFNISLLLKTPISSSGRSF
IEDLLFTSVETVGLPTDAEYKKCTAGPLGTLKDLICAREYNGLLVLPPIITADMQTMYTASLVGAMAFGGITSAA
AIPFATQIQARINHLGITQSLLMKNQEKIAASFNKAIGHMQEGFRSTSLALQQIQDVVNKQSAILTETMNSLNKN
FGAITSVIQDIYAQLDAIQADAQVDRTGRLSSLSVLASAKQSEYIRVSQQRELATKKINECVKSQSNRYGFCGSG
RHVLSIPQNAPNGIVFIHFTYTPESFVNVTAIVGFCVNPANASQYAIVPANGRGVFIQVNGSYYITARDMYMPRD
ITAGDIVTLTSCQANYVNVNKTVINTFVEDDDFNFNDELSKWWNDTKHELPDFDEFNYTVPVLNISNEIDRIQEV
IQGLNDSLIDLETLSILKTYIKWPLAIYSTVSSSLVLVGLIIAMGLWMTGCCGCCCGCFGIIPLMSKCGKKSSYY
TTFDNDVVTEQYRPKKSV

IBV mIBV-S-KKSV protein, Combo 5, fr. 11, 19 % (95% confidence), 17 peptides

MGWSWIFLFLLSGAAGVHCNLFDSDNNYVYYYQSAFRPPNGWHLQGGAYAVVNSTNHTSNAGSAQGCTVGVIKDV
YNQSVASIAMTAPLQGMAWFCTAYCNFSDTTVFVTHCYHIRISAMKNGSLFYNLTVSVSKYPNFKSFQCVNNFTS
VYLNGDLVFTSNKTTDVTSAGVYFKAGGPVNYSIMKEFKVLAYFVNGTAQDVILCDNSPKGLLACQYNTGNFSDG
FYPFTNSTLVREKFIVYRESSFNTTLALTNFTFTNVSNAQPNSGGVNTFHLYQTQTAQSGYYNFNLSFLSQFVYK
ASDFMYGSYHPSCSFRPETINSGLWFNSLSVSLTYGPLQGGCKQSVFSGKATCCYAYSYKGPMACKGVYSGELRT
NFECGLLVYVTKSDGSRIQTRTEPLVLTQYNYNNITLDKCVAYNIYGRVGQGFITNVTDSAANFSYLADGGLAIL
DTSGAIDVFVVQGIYGLNYYKVNPCEDVNQQFVVSGGNIVGILTSRNETGSEQVENQFYVKLTNSSHRRRRSIGQ
NVTSCPYVSYGRFCIEPDGSLKMIVPEELKQFVAPLLNITESVLIPNSFNLTVTDEYIQTRMDKVQINCLQYVCG
NSLECRKLFQQYGPVCDNILSVVNSVSQKEDMELLSFYSSTKPKGYDTPVLSNVSTGEFNISLLLKTPISSSGRS
FIEDLLFTSVETVGLPTDAEYKKCTAGPLGTLKDLICAREYNGLLVLPPIITADMQTMYTASLVGAMAFGGITSA
AAIPFATQIQARINHLGITQSLLMKNQEKIAASFNKAIGHMQEGFRSTSLALQQIQDVVNKQSAILTETMNSLNK
NFGAITSVIQDIYAQLDAIQADAQVDRLITGRLSSLSVLASAKQSEYIRVSQQRELATKKINECVKSQSNRYGFC
GSGRHVLSIPQNAPNGIVFIHFTYTPESFVNVTAIVGFCVNPANASQYAIVPANGRGVFIQVNGSYYITARDMYM
PRDITAGDIVTLTSCQANYVNVNKTVINTFVEDDDFNFNDELSKWWNDTKHELPDFDEFNYTVPVLNISNEIDRI
QEVIQGLNDSLIDLETLSILKTYIKWPWYVWLAIFFAIIIFILILGWVFFMTGCCGCCCGCFGIIPLMSKCGKKS
SYYTTFDNDVVTEQYRP

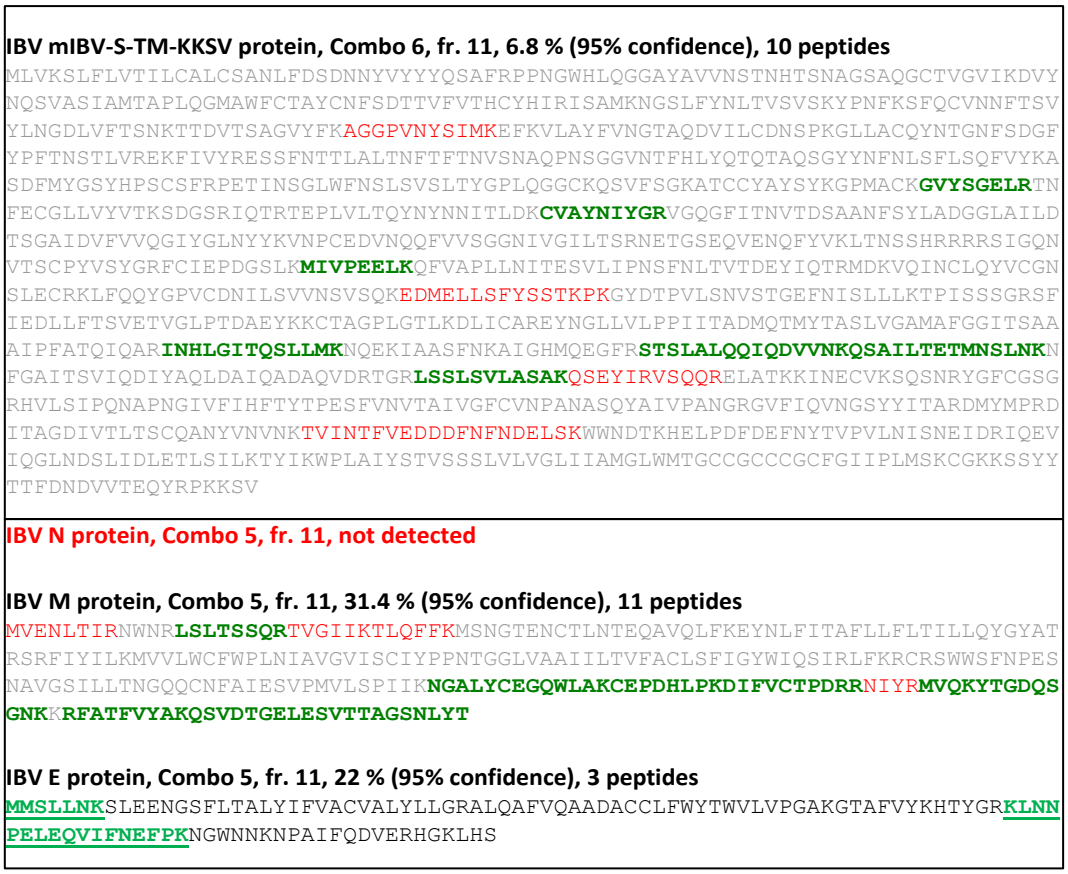

Figure 35: Protein confirmation using LC-MS/MS-based peptide sequencing of IBV structural proteins (S, rIBV-S-TM, rIBV-S-TM/CT, mIBV-S-KKSV, mIBV-S-TM-KKSV, M, N, and E). LC-MS/MS-based peptide sequence analysis for excised bands resulted in the percentage sequence coverage as indicated below with a number of unique peptides identified with >95% confidence. Peptides with >95% confidence are highlighted in green, those 50-95% confidence in yellow and <50% confidence in red. No peptides were identified for the non-highlighted regions of the sequence (grey).

The presence of the S protein at the appropriate size of 127 kDa was confirmed using LC MS/MS based peptide sequencing (IBV S, Combo 1, lane 5; and Combo 2, lane 7), the rIBV-S-TM S protein (Combo 3, lane 9), the rIBV-S-TM/CT S protein (Combo 4, lane 11), the mIBV-S-KKSV S protein (Combo 5, lane 13) and the mIBV-S-TM-KKSV S protein (Combo 6, lane 15). The presence of the M protein at the appropriate size of 29 kDa was confirmed (Combo 5, lane 13), as was the presence of the E protein at 12.5 kDa (Combo 5, lane 13). The N protein at 45 kDa (Combo 5, lane 13) could not be detected by mass spectrometry. (See appendix for cut out bands).

4.5.4. TEM visualisation of recombinant S protein VLPs

Once more, no VLPs were detected in the uranyl acetate stained samples or leaf sections using TEM analysis. In an attempt to detect potential VLPs, Immunogold labelling was used to detect structures resembling intermediates and VLPs.

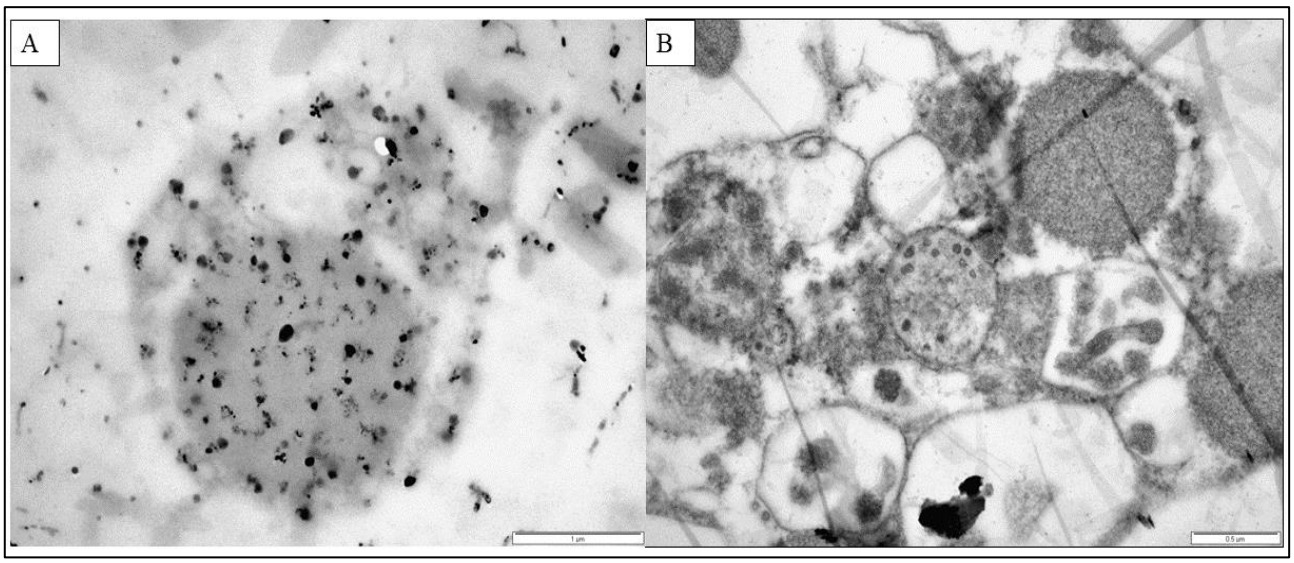

Figure 36a: A) Unstained TEM image of negative control not stained with primary antibody. Scale bar 1000 nm. B) Stained TEM image of negative control labelled with gold-labelled secondary goat anti-chicken antibodies (no evidence of immune-stained VLPs in image B). Scale bar 500 nm.

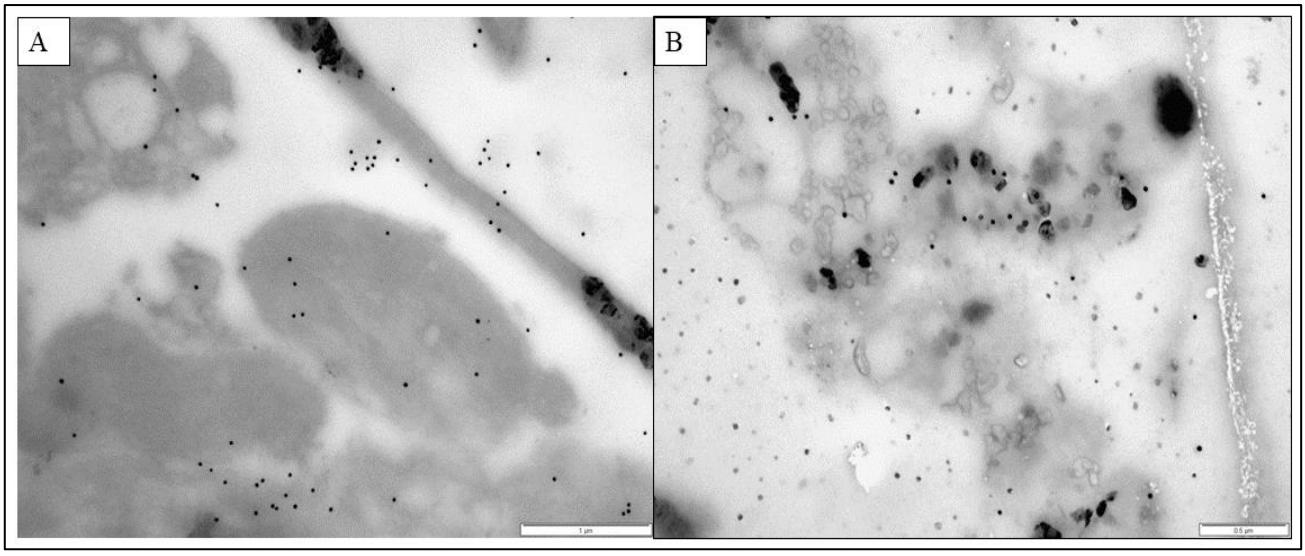

Figure 36b: A) Unstained TEM image of combination 1 (S:M:E:N 2:1:1:1, Fr. 11). Scale bar 1000 nm. B) Stained TEM image of combination 1 (S:M:E:N 2:1:1:1, Fr. 11) labelled with gold-labelled secondary goat anti-chicken antibodies (no evidence of immune-stained VLPs in image B). Scale bar 500 nm.

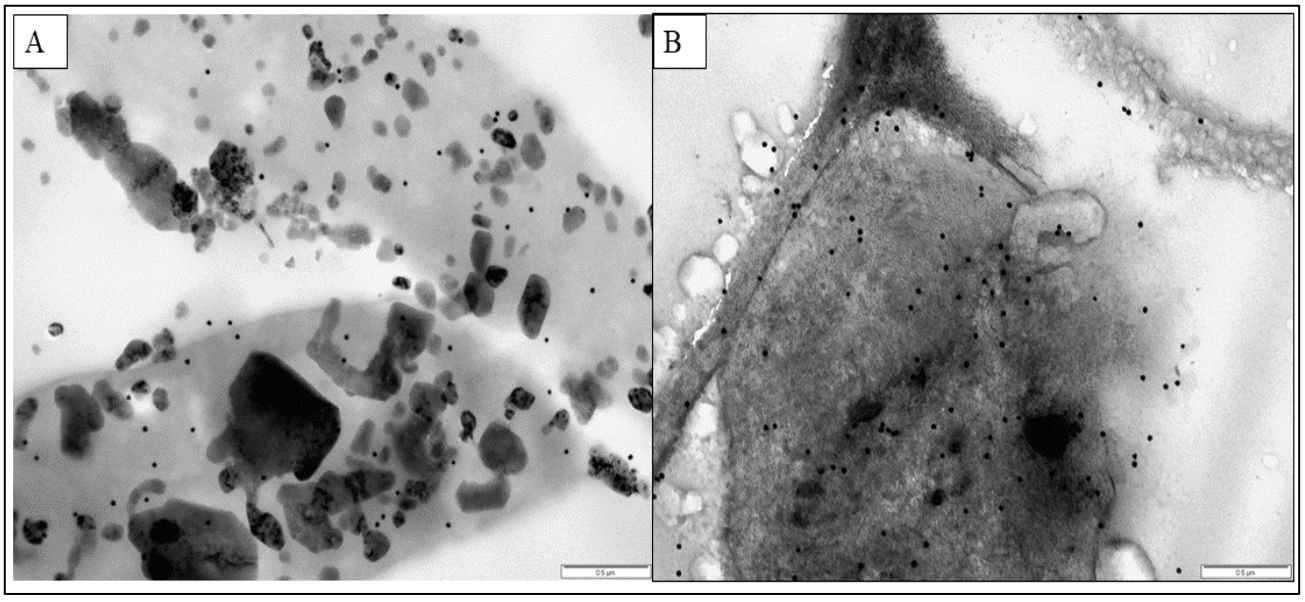

Figure 36c: A) Unstained TEM image of combination 2 (S:M:E:N 2:1:2:2, Fr. 11). Scale bar 500 nm. B) Stained TEM image of combination 2 (S:M:E:N 2:1:2:2, Fr. 11) labelled with gold-labelled secondary goat anti-chicken antibodies (no evidence of immune-stained VLPs in image B). Scale bar 500 nm.

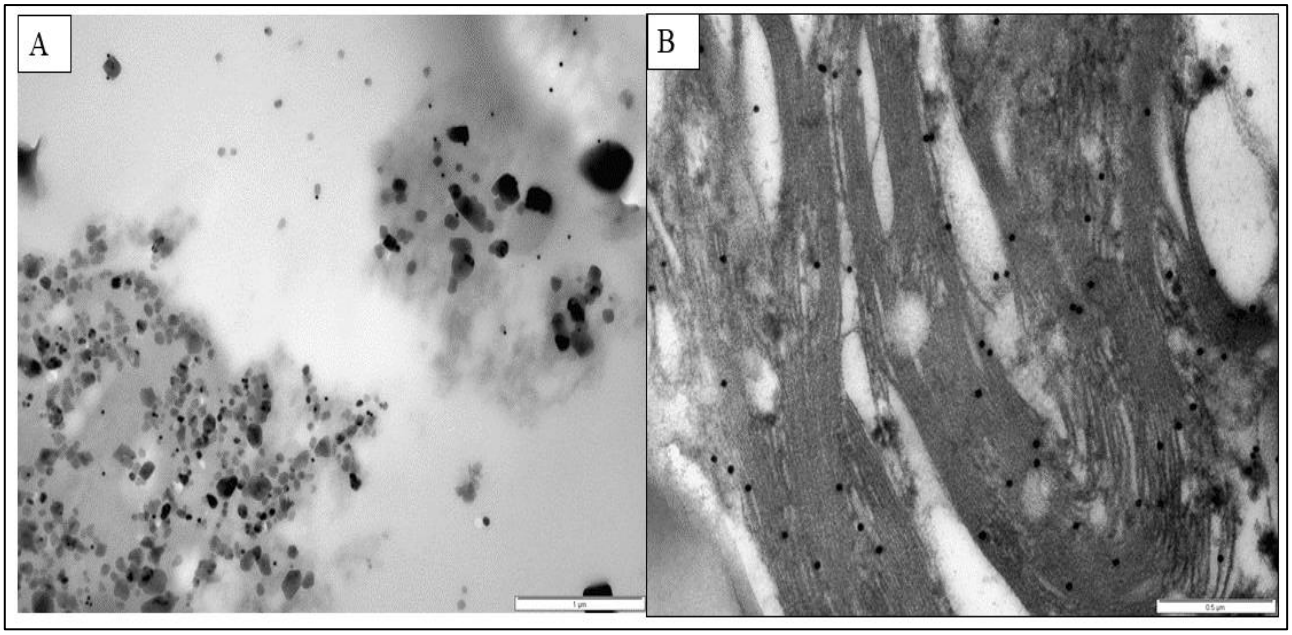

Figure 36d: A) Unstained TEM image of combination 3 (rIBV-S-TM:M:E:N 2:1:1:1, Fr. 11). Scale bar 1000 nm. B) Stained TEM image of combination 3 (rIBV-S-TM:M:E:N 2:1:1:1, Fr. 11) labelled with gold-labelled secondary goat anti-chicken antibodies (no evidence of immune-stained VLPs in image B). Scale bar 500 nm.

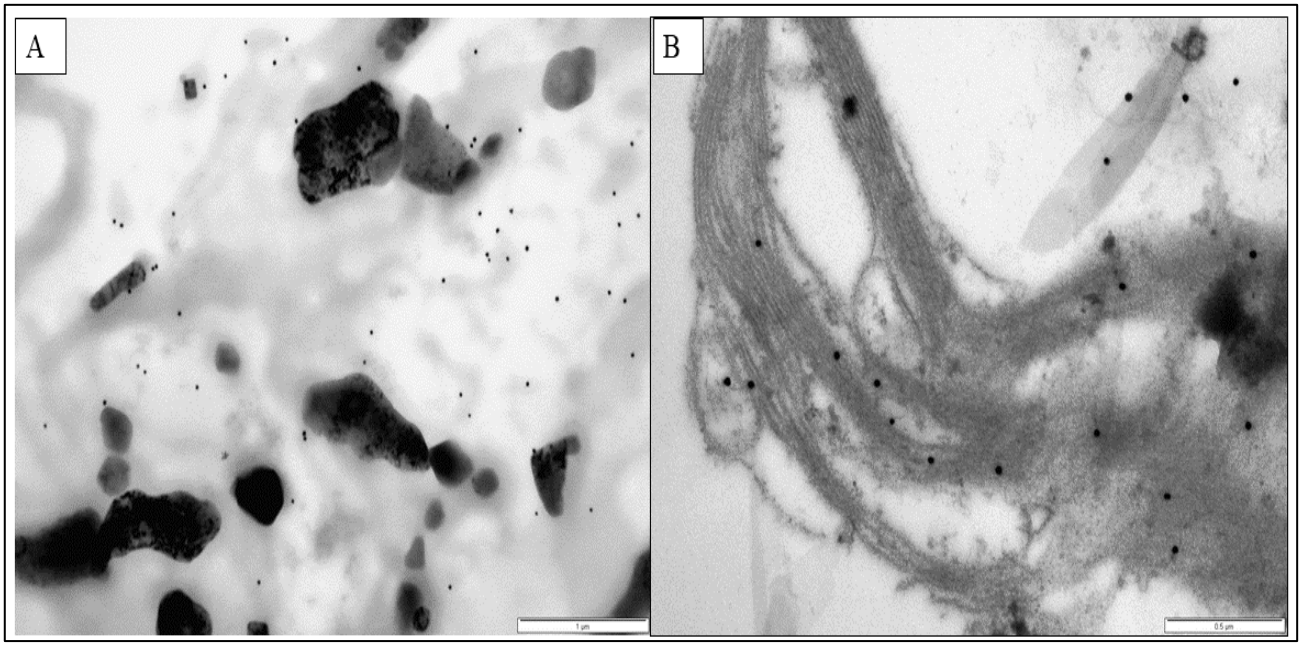

Figure 36e: A) Unstained TEM image of combination 4 (rIBV-S-TM/CT:M2:N 2:1:1, Fr. 11). Scale bar 1000 nm. B) Stained TEM image of combination 4 (rIBV-S-TM/CT:M2:N 2:1:1, Fr. 11) labelled with gold-labelled secondary goat anti-chicken antibodies (no evidence of immune-stained VLPs in image B). Scale bar 500 nm.

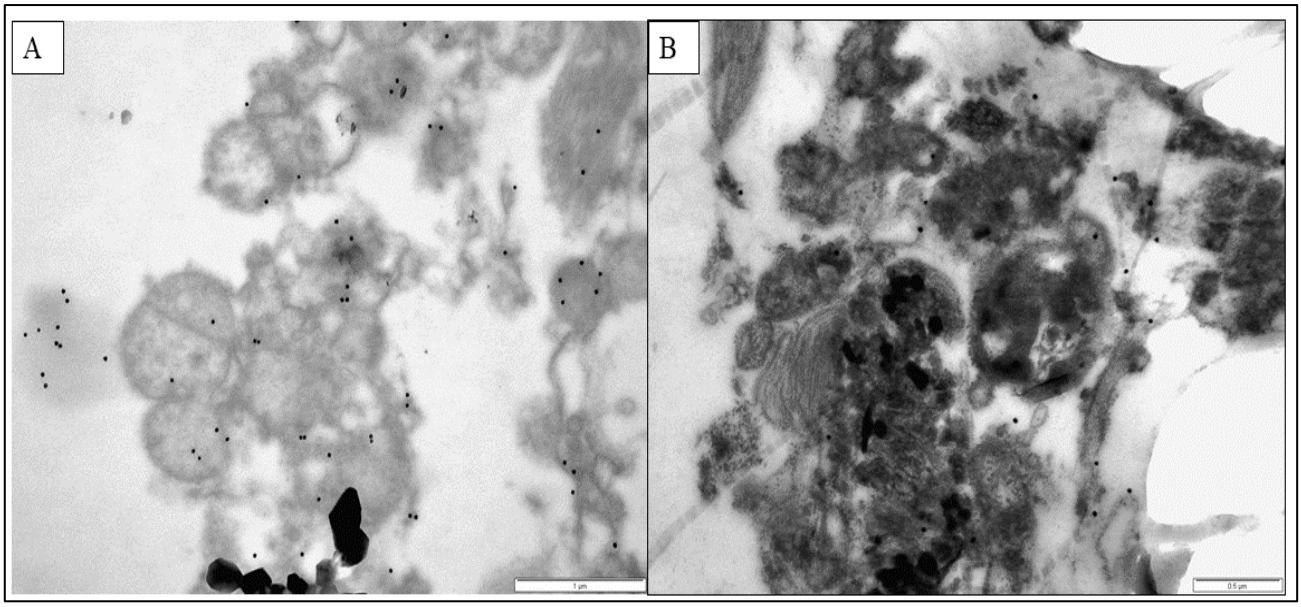

Figure 36f: A) Unstained TEM image of combination 5 (mIBV-S-KKSV:M:E:N 2:1:1:1, Fr. 11). Scale bar 1000 nm. B) Stained TEM image of combination 5 (mIBV-S-KKSV:M:E:N 2:1:1:1, Fr. 11) labelled with gold-labelled secondary goat anti-chicken antibodies (no evidence of immune-stained VLPs in image B). Scale bar 500 nm.

No IBV-like particles were detected using immunogold labelling, although there was partial labelling of plant material visible. There were also no immunogold-labelled particles that matched the expected size and morphology of the IBV particle. This indicates that there were no detectable VLPs assembled in the plants.

CHAPTER 5

Discussion

The aim of this project was to produce infectious bronchitis virus-like particles (VLPs) in *Nicotiana benthamiana* plants by transiently expressing and assembling the major surface antigen, Spike (S) protein with membrane-associated structural proteins of IBV. The full-length S protein was targeted, as this was previously described for VLPs expressed in insect cells (Liu *et al*., 2013b). In addition, various S protein hybrids were produced in an attempt to elevate expression of the S protein and assembly of VLPs.

The S, E, and M proteins of IBV are involved in virus particle assembly, while the N protein is thought to assist in the assembly of the virus particle by interacting with the M and E proteins (Cavanagh, 2007; Jayaram *et al*., 2006). Because VLPs for IBV have not yet been produced in plants, the minimum requirements are not yet established, therefore, different combinations of all four proteins were investigated. For this reason, genes encoding all four structural proteins were chicken codon-optimised, and synthesised chemically. It was previously shown that chicken codon-optimisation of the target genes resulted in elevated expression and assembly of influenza VLPs compared to plant codon-optimisation (Smith *et al*., 2019). This was the reason for chicken codon-optimisation of the target genes.

In this study, the sequence-validated constructs (pEAQ-HT-S, pEAQ-HT-M, and pEAQ-HT-E) were transformed into electrocompetent *A. tumefaciens* (AGL-1, GV3101::pMP90, or LBA4404 strains) in order to determine the most appropriate *Agrobacterium* strain for expression and assembly of VLPs in *N. benthamiana* plants. The plants were then infiltrated with the S, E and M constructs using the three different *Agrobacterium* strains and incubated for 6 and 8 dpi. The plants' growth was monitored throughout this time, and the leaves were still healthy after 6 dpi. By 8 dpi, some of the leaves were beginning to turn yellow and necrotic, dried out or wilted. The conclusion was that the peak expression and therefore, optimal harvest time was 6 dpi.

In order to optimise extraction of the VLPs, two different buffers were used for extraction and the clear lysate was subjected to iodixanol density gradient ultracentrifugation to purify the VLPs. The iodixanol fractions 7-12 (20-40%) were analysed for IBV structural protein content. There was no difference in the results between the leaves extracted with PBS and the leaves

extracted with bicine buffer, therefore PBS was used in all future experiments as it is the standard buffer for vaccine candidates to be tested in target animals. AGL-1 *Agrobacterium*-mediated expression and potential assembly of IB VLPs resulted in clearer protein bands when analysed with sodium dodecyl sulphate-polyacrylamide gel electrophoresis (SDS-PAGE) than with LBA4404 or GV3101::pMP90. The reason for this is unclear, however, AGL-1 *Agrobacterium*-mediated expression of IBV structural proteins was used in a direct comparison with LBA4404 in a number of the experiments.

The presence of protein bands in SDS-PAGE correlating to all three structural proteins show that IB VLPs may be present in the 20-30% Iodixanol fractions. This means that the assembled IB VLPs, if present, were likely to only penetrate as deep as 20-30% Iodixanol. This indicates that the IBV structural proteins may have assembled and formed structures of a high molecular weight (Theunemann *et al*., 2013). Bands correlating to the size of the S protein (127 kDa) were observed in the SDS-PAGE gels, albeit very faintly compared to the other proteins on the gels. This was regardless of the *Agrobacterium* strain used to infiltrate, the ratios used, and the combinations infiltrated. This implies that the S protein may have had a low level of expression in the plants. The later SDS-PAGE results using the recombinant S genes also displayed very faint bands, meaning that expression was still very low even after substituting the TM and CT domains of the S protein with those of the IAV HA protein.

Although in many of the results (immunoblotting) there were bands correlating to the sizes of the target proteins, those bands also appeared in the negative controls. This suggested that the some of the proteins (namely IBV-E and IBV-M) correlated with non-specific protein bands that were present in the plant leaves. This would make it difficult to identify distinct bands correlating to the proteins. This does not necessarily mean that the IBV-E and IBV-M proteins were not present. They may have been present as well as the plant proteins that were present in the negative controls. This is shown by the fact that LC-MS/MS analysis detected several peptides that matched the IBV-E and IBV-M proteins.

Many viral glycoproteins demonstrate low expression levels in plants. The reason for this is unclear, but it has been speculated that this could be due to a lack of essential chaperone proteins to drive protein folding, or as a result of the glycoproteins being incompatible with the endogenous plant chaperones present (Margolin *et al*., 2018). In other heterologous protein expression systems, the lack of sufficient amounts of viral molecular chaperone proteins has proven to be a limiting factor in the expression of viral glycoproteins (Rudolph and Lilie, 1996;

Hsu and Betenbaugh, 1997). Should this be the case in plant expression systems as well, it would introduce the challenge of which chaperone proteins to use for improving glycoprotein expression (Margolin *et al*., 2018). These low glycoprotein expression levels are often linked to severe tissue necrosis (such as the yellowed, dried out leaves also observed in this study) (Howell, 2013). This tissue necrosis may point to stress response in the plant which is a result of misfolded proteins accumulating at the ER (Howell, 2013). It may also have been caused by overexpression of the proteins exceeding the plant system's folding capacity (Liu and Howell, 2010).

The initial immunoblotting results showed bands that were very faint. Bands correlating to the size of the S protein were not visible in the initial immunoblotting results, or were too faint to see if present at all. This again implies almost undetectable low expression of the S protein.

In contrast, the expression of HA alone has been shown to be sufficient for the development of IAV VLPs (D'Aoust *et al*., 2008). Not only that, but many influenza HA glycoproteins have been shown to have unusually high expression levels *in planta* (D'Aoust *et al*., 2008; Shoji *et al*., 2011). In this study, extremely low native S protein expression levels were detected in *N. benthamiana* plants. Key differences between the IAV HA and the IBV S glycoproteins are indicated (Appendix, Table 3). These differences may provide insight as to why the S protein expression was low. We hypothesised that modifying the IBV S protein by substituting the TM and/or CT domains of the S protein with those of the IAV HA protein could potentially improve the expression of the S protein and thus result in the formation of more IBV VLPs.

For the recombinant S protein experiments, the leaves infiltrated with rIBV-S-IAV-TM/CT alone or IBV-S-IAV-TM/CT with the IAV M2 ion channel gene were beginning to dry out and turn yellow after 3 dpi. This could have been because the plants were over-expressing the protein, or that the protein being expressed was toxic to the plant.

After modifying the S protein, the bands correlating to the size of the S protein in the SDS-PAGE gels (Figs 22, 28 and 29) were still faint, indicating that the glycoprotein expression was still very low. However, bands correlating to the size of the S protein had a stronger signal when subjected to immunoblotting (Fig. 23). This implies that although protein expression was still very low, modifying the S protein with the TM and CT domains of IAV HA did slightly improve expression.

Although the N protein is thought to aid in virus-particle formation, the co-infiltration with the N protein made no difference to the S protein bands visualised in the SDS-PAGE or immunoblotting results. The N protein was also not detected with LC-MS/MS.

For LC-MS/MS results to be conclusive, it is preferable that more than one distinctive peptide sequence matches the protein being evaluated (Cottrell, 2011). If enough peptide sequences match with a known protein, it can be used to identify that protein with a degree of confidence (Schaffeld and Markl, 2004). If several MS/MS spectra were to match peptide sequences from a single protein, it would increase the likelihood of that protein being present (Cottrell, 2011). Usually, a protein that only has one peptide sequence that matches it is considered a suspect, and unless that peptide sequence is exclusive to that specific protein, it leaves uncertainty regarding the protein from which it originates (Cottrell, 2011). Mann and Wilm (1994) found that a short stretch of an amino acid sequence could offer sufficient specificity to unambiguously identify a protein, depending on the enzyme specificity, as well as if the peptide mass and enclosing fragment ion mass values were known. With this information in mind, LC-MS/MS results that had three or more peptide sequences that matched the target protein increased the confidence with which the protein could be confirmed.

In experiment 1, IBV S protein sample 1 had 11 peptides that matched that of the IBV S protein. IBV M protein sample had 5 peptides that matched that of the IBV M protein. No peptides were detected for the IBV E protein sample.

In experiment 3, IBV S protein samples from combination 2 and 3 had 11 and 7 peptides, respectively, that matched that of the IBV S protein. No peptides were detected for the rIBV-S-TM protein sample. For rIBV-S-TM/CT, 15 and 18 peptides were detected from the samples taken. No peptides for the IBV-M sample were detected in this case, while 4 peptides were detected for the IBV E protein sample.

In experiment 5, IBV S protein samples from combination 1 and 2 had 21 and 15 peptides, respectively, that matched that of the IBV S protein. The rIBV-S-TM protein sample had 5 peptides matching that of the IBV-S protein, while the rIBV-S-TM/CT protein sample had 24 peptides matching that of the IBV-S protein. The mIBV-S-KKSV protein sample had 17 peptides matching that of the IBV-S protein, while the mIBV-S-TM-KKSV protein sample had 10 peptides matching that of the IBV-S protein. The IBV-M protein sample had 11 peptides matching that of the IBV-M protein and the IBV E protein sample had 3 peptides matching that of the IBV-E protein. There were no matching peptides detected for the IBV-N protein sample.

The number of peptides detected for IBV S increased from experiment 1 to 5. This suggested that the optimisations done to improve expression may have been successful. The number of peptides detected for the rIBV-S-TM, rIBV-S-TM/CT, mIBV-S-KKSV, and the mIBV-S-TM-KKSV protein samples that matched the IBV S protein sequence were higher than for the original protein sequence. This suggested that modifying the IBV S protein sequence may have improved expression.

The number of peptides detected for the IBV-M, IBV-E, and IBV-N protein samples were fairly low or non-existent. This may provide insight as to why VLP formation was not successful.

In this study, no IBV VLPs fitting the expected IBV description could be visualised harnessing negative staining transmission electron microscopy (TEM). Some particles matching the expected size could be seen, but they lacked the characteristic crown formed by the S glycoprotein of coronaviruses. Therefore, it could not be concluded that they were IB VLPs. This means that the S protein may not have been incorporated into the virions, or that the acidic uranyl acetate staining may have broken apart any VLPs that may have been present. The fractions 10-11 (20-30% Iodixanol), which were the fractions with the most distinct protein bands, were also stained with phosphotungstic acid (pH 7.4) to test the latter theory, however, there were still no VLPs detected using TEM.

It has been hypothesised that M proteins of coronaviruses form a dense lattice-like matrix. This matrix is formed by lateral M-M interactions inside the viral envelope (De Haan *et al*., 2000). These interactions have been observed to a degree in morphological studies (Neuman *et al*., 2011). It is suggested that this lattice-like matrix is involved in the assembly of virions. S proteins are thought to be incorporated into the lattice vacancies by interacting with the M proteins (De Haan *et al*., 2000). The incorporation of S proteins into VLPs or virus particles is determined solely by the CT domain. Interactions between the CT domain of the M protein and the TM and CT domains of the S protein are important for S protein incorporation (Bosch *et* al., 2005; de Haan *et al*., 1999). The charge-rich region of the CT domain as well as the palmitoylation of the cysteine-rich motif (CRM) have been shown to be important for this incorporation (Bosch *et al*., 2005; Thorp *et al*., 2006; Ujike and Taguchi, 2015). A lack of M-S interactions caused by an under-palmitoylation of S proteins results in a reduced amount of S proteins being incorporated (Thorp *et al*., 2006). This suggests that substituting this domain may have had a negative effect on the M-S interactions required for S protein incorporation. It

is possible that the recombinant S proteins were counterproductive to the production of fully assembled VLPs.

In addition to the negative staining TEM, leaf cross-sections were also imaged by TEM revealing the presence of spherical particles matching the expected size of IBV particles. However, without the characteristic spikes surrounding IB VLPs, the results were inconclusive. Immunogold labelling was used to determine whether they were indeed IBV VLPs or assembly intermediates. There were no particles labelled that had the size and morphology of an IBV particle. Thus, the IBV structural proteins may be expressed, but fail to assemble into VLPs. It could also be that the integrity of the particles was disrupted by the staining processes or that the S protein was not being incorporated into any formed particles.

Theunemann *et al*., (2013) found that co-expressing all four structural proteins of Bluetongue virus (BTV 8) resulted in the formation of a combination of different particle types. Some of these particles resembled core-like particles (CLPs), while others were notably larger particles that were less structured than the CLPs in appearance. Others seemed to be assembly intermediates that were between CLPs and VLPs (Theunemann *et al*., 2013). When all four BTV-8 structural proteins were expressed together from separate pEAQ-HT constructs, VP3 was over-represented which led to the formation of assembly intermediates and subcore-like particles. In order to deal with this, the pEAQexpress vector was used to express two of the proteins on the same T-DNA, therefore down-regulating the formation of CLPs in favour of VLP formation (Theunemann *et al*., 2013). This may be a good approach to preventing the formation of assembly intermediates and producing VLPs.

Conclusion and Future Perspectives

IBV structural proteins were potentially expressed in *N. benthamiana* ΔXT/FT plant leaf material, but in low quantities as confirmed by SDS-PAGE, transmission electron microscopy and immunological detection. The immunogold labelling did not reveal the presence of any particles with the characteristic morphology and size of IBV. However, the presence of the protein bands in SDS-PAGE confirmed to be IBV structural proteins by liquid chromatography-mass spectrometry (LC-MS/MS) based peptide sequencing, indicates that the structural proteins did assemble into high molecular weight structures. The number of peptides detected for IBV S increased from experiment 1 to 5. This suggested that the optimisations done to improve expression may have been successful. The number of peptides detected for

the rIBV-S-TM, rIBV-S-TM/CT, mIBV-S-KKSV, and the mIBV-S-TM-KKSV protein samples that matched the IBV S protein sequence were higher than for the original protein sequence. This suggested that modifying the IBV S protein sequence may have improved expression. The number of peptides detected for the IBV-M, IBV-E, and IBV-N protein samples were fairly low or non-existent. This may provide insight as to why VLP formation may not have been successful. The immunoblotting results were not conclusive enough to make significant conclusions regarding the formation of VLPs. The presence of the IBV bands in the negative control made it difficult to confirm the identity of the proteins. However, combined with the SDS-PAGE results, and the LC-MS/MS results, there is still a possibility that high molecular weight structures did form. The expression may have been too low to visualise under the TEM or the acidic uranyl acetate staining may have broken apart the few assembled structures. It could also be that the S protein was not incorporated into the virus particles. This could be due to a number of reasons. Firstly, as with many other viral glycoproteins, the S protein may demonstrate low expression levels in plants. Modifying the S protein with the TM and CT domain of the IAV HA protein did not improve expression sufficiently enough to result in fully assembled IB VLPs under the TEM. This could have been because the CT domain of the S protein is essential for the protein's incorporation into virus or virus-like particles. Substituting this domain may have had a negative effect on the M-S interactions required for S protein incorporation. Another reason could be that there was a lack of molecular chaperone proteins required for glycoprotein expression.

In future, alternative designs of the S protein and the addition of molecular chaperone genes will potentially improve S protein expression and elevate the numbers of VLPs produced, resulting in a commercially viable vaccine product. It may also be important to modulate the expression of the IBV structural proteins in order to decrease the formation of assembly intermediates and potentially assist in the formation of VLPs. Further optimisation is required to improve protein expression and form VLP.

Another future approach may be to experiment with linking the S1 subunit of the S protein to the TM and CT domain of influenza HA (with a linker). Previously, researchers Lv *et al*., (2014) and Wu *et al*., (2019) found that this approach resulted in the formation of VLPs that resembled either influenza particles or IBV particles respectively. This was a surprising result, as the S2 subunit was absent and it is the S2 subunit that is responsible for anchoring the S1 subunit to the membrane (Lai and Cavanagh, 1997).

References

Abolnik, C., 2015. Genomic and single nucleotide polymorphism analysis of infectious bronchitis coronavirus. Infection, genetics and evolution 32. 416-424.

Ahmed, H. N., 1954. Incidence and treatment of some infectious viral respiratory diseases of poultry in Egypt. [PhD thesis]. Egypt: Faculty of Veterinary Medicine, Cairo University.

Ahmed, A. A. S., 1964. Infektiose Bronchitis des huhmes in Agypten. Berl Munchen Tieraerzl Wschr 77. 481-484.

Bande, F., Arshad, S. S., Bejo, M. H., Kadkhodaei, S., Omar, A. R., 2016. Prediction and In Silico Identification of Novel B-Cells and T-Cells Epitopes in the S1-Spike Glycoprotein of M41 and CR88 (793/B) Infectious Bronchitis Virus Serotypes for Application in Peptide Vaccines. Advances in Bioinformatics 2016. 1-5.

Bellier, B., Klatzmann, D., 2013. Virus-like particle-based vaccines against hepatitis C virus infection. Expert Review of Vaccines 2. 143-154.

Bentley, K., Armesto, M., Britton, P., 2013. Infectious bronchitis virus as a vector for the expression of heterologous genes. PLoS One 8. e67875.

Bijlenga, G., Cook, J. K., Gelb Jr, J., de Wit, J. J., 2004. Development and use of the H strain of avian infectious bronchitis virus from the Netherlands as a vaccine: a review. Avian Pathology 33. 55 - 557.

Binns, M. M., Boursnell, M. E., Cavanagh, D., Pappin, D. J., Brown, T. D., 1985. Cloning and sequencing of the gene encoding the spike protein of the coronavirus IBV. Journal of General Virology 66 (pt 4). 719-726.

Blokhina, E. A., Kupriyanov, V. V., Ravin, N. V., Skryabin, K. G., 2013. The Method of Noncovalent in vitro Binding of Target Proteins to Virus-Like Nanoparticles Formed by Core Antigen of Hepatitis B. Virus. Dokl Akad Nauk 448. 719–721.

Bochkov, Y. A., Batchenko, G. V., Shcherbakova, L. O., Borisov, A. V., Drygin, V. V., 2006. Molecular epizootiology of avian infectious bronchitis in Russia. Avian Pathology 35. 379 - 393.

Boonstra, S. Blijleven, J. S., Roos, W. H., Onck, P. R., van der Giessen, E., van Oijen, A. M., 2018. Hemagglutinin-Mediated Membrane Fusion: A Biophysical Perspective. Annual review of biophysics 47. 153-173.

Bosch, B. J., de Haan, C. A., Smits, S. L., Rottier, P. J., 2005. Spike protein assembly into the coronavirion: Exploring the limits of sequence requirements. Virology 334. 306-318.

Boursnell, M. E. G., Brown, T. D. K., Foulds, I. J., Green, P. F., Tomley, F. M., Binns, M. M., 1987. Completion of the sequence of the genome of the coronavirus avian infectious bronchitis virus. Journal of General Virology 68. 57-77.

Box, P. G., Beresford, A. V., Roberts, B., 1980. Protection of laying hens against infectious bronchitis with inactivated emulsion vaccines. Vet Rec 106. 264-268.

Box, P. G., Ellis, K. R., 1985. Infectious bronchitis in laying hens: interference with response to emulsion vaccine by attenuated live vaccine. Avian Pathol 14. 9-22.

Bright, R. A., Carter, D. M., Daniluk, S., Toapanta, F. R., Ahmad, A., 2007. Influenza virus-like particles elicit broader immune responses than whole virion inactivated influenza virus or recombinant hemagglutinin. Vaccine 25. 3871–3878.

Broadfoot, D. I., Pomeroy, B. S., Smith Jr, W. M., 1954. Effect of infectious bronchitis on egg production. J Am Vet Med Assoc 124. 128-130.

Butcher, G. D., Winterfield, R. W., Shapiro, D. P., 1990. Pathogenesis of H13 nephropathogenic infectious bronchitis virus. Avian Dis 34. 916-921.

Callison, S. A., Hilt, D. A., Boynton, T. O., Sample, B. F., Robison, R., Swayne, D. E., Jackwood, M. W., 2006. Development and evaluation of a real-time Taqman RT-PCR assay for the detection of infectious bronchitis virus from infected chickens. Journal of Virol Methods 138. 60-65.

Carrat, F., Flahault, A., 2007. Influenza vaccine: The challenge of antigenic drift. Vaccine 25. 6852–6862.

Casais, R., Thiel, V., Siddell, S. G., Cavanagh, D., Britton, P., 2001. Reverse genetics system for the avian coronavirus infectious bronchitis virus. J. Virol 75. 12359-12369.

Casais, R., Dove, B., Cavanagh, D., Britton, P., 2003. Recombinant avian infectious bronchitis virus expressing a heterologous spike gene demonstrates that the spike protein is a determinant of cell tropism. Journal of Virology 77. 9084-9089.

Castilho, A., Strasser, R., Stadlmann, J., Grass, J., Jez, J., Gattinger, P., Kunert, R., Quendler, H., Pabst, M., Leonard, R., Altmann, F., Steinkellner, H., 2010. In planta protein sialylation through overexpression of the respective mammalian pathway. J. Biol. Chem. 285. 15923-15930.

Castilho, A., Steinkellner, H., 2012. Glyco-engineering in plants to produce human-like N-glycan structures. Biotechnology Journal 7. 1088-1098.

Caton, A. J., Brownlee, G. G., Yewdell, J. W., Gerhard, W., 1982. The antigenic structure of the influenza virus A/PR/8/34 hemagglutinin (H1 subtype). Cell 31. 417-427.

Cavanagh, D., Davis, P. J., Darbyshire, J. H., Peters, R. W., 1986. Coronavirus IBV: virus retaining spike glycopolypeptide S2 but not S1 is unable to induce virus-neutralizing or haemagglutination-inhibiting antibody, or induce chicken tracheal protection. Journal of General Virology 67 (pt 7). 1435-1442.

Cavanagh, D., Davis, P. J., Mockett, A. P., 1988. Amino acids within hypervariable region 1 of avian coronavirus IBV (Massachusetts serotype) spike glycoprotein are associated with neutralisation epitopes. Virus Res 11. 141-150.

Cavanagh, D., Davis, P. J., Cook, J. K., Li, D., Kant, A., Koch, G., 1992. Location of the amino acid diffeences in the S1 spike glycoprotein subunit of closely related serotypes of infectious bronchitis virus. Avian Pathology 21. 33-43.

Cavanagh, D., Elus, M. M., Cook, J. K., 1997. Relationship between sequence variation in the S1 spike protein of infectious bronchitis virus and the extent of cross-protection *in vivo*. Avian Pathology 26. 63-74.

Cavanagh, D., Naqi, S. A., 1997. Infectious Bronchitis. In B.W. Calnek (ed). Diseases of Poultry, 10th edition. Vol 18. 511 - 527.

Cavanagh, D., 2001. A nomenclature for avian coronavirus isolates and the question of species status. Avian Pathology 30. 109-115.

Cavanagh, D., 2007. Coronavirus avian infectious bronchitis virus. Veterinary Research 38. 281 - 297.

Cavanagh, D., Gelb Jr, J., 2008. Infectious Bronchitis. In Saif, Y. M., Fadly, A. M., Glisson, J. R., McDougald, L. R., Nolan, L. K., Swayne, D. E. (Eds). Diseases of Poultry. Wiley-Blackwell, Ames, IA, USA, 117 - 135.

Chen, Q., Dent, M., Hurtado, J., Stahnke, J., McNulty, A., Leuzinger, K., Lai, H., Transient protein expression by agroinfiltration in lettuce. Methods Mol Biol 1385. 55-67.

Chong, K. T., Apostolov, K., 1982. The pathogenesis of nephritis in chickens induced by infectious bronchitis virus. J Comp Pathol 92. 199-211.

Chroboczek, J., Szurgot, I., Szolajska, E., 2014. Virus-like particles as vaccine. Acta Biochimica Polonica 61. 531-539.

Collisson, E. W., Pei, J., Dzielawa, J., Seo, S. H., 2000. Cytotoxic T lymphocytes are critical in the control of infectious bronchitis virus in poultry. Dev. Comp. Immunol 24. 187-200.

Cook, J. K., 1984. The classification of new serotypes of infectious bronchitis virus isolated from poultry flocks in Britain between 1981 and 1983. Avian Pathology. 13. 733 – 741.

Cook, J. K., Smith, H. W., Huggins, M. B., 1986. Infectious bronchitis immunity: its study in chickens experimentally infected with mixtures of infectious bronchitis virus and *Escherichia coli*. Journal of General Virology 67. 1427-1434.

Cook, J. K., Orbell, S. J., Woods, M. A., Huggins, M. B., 1999. Breadth of protection of the respiratory tract provided by different live-attenuated infectious bronchitis vaccines against challenge with infectious bronchitis viruses of heterologous serotypes. Avian Pathology 28. 477-485.

Cook, J, K., Jackwood, M., Jones, R, C., 2012. The long view: 40 years of infectious bronchitis research. Avian Pathology 41. 239-250.

Copeland, C. S., Doms, R. W., Bolzau, E. M., Webster, R. G. and Helenius, A., 1986. Assembly of influenza hemagglutinin trimers and its role in intracellular transport. Journal of Cellular Biology 103. 1179 – 1191.

Corse, E., Machamer, C. E., 2000. Infectious bronchitis virus E protein is targeted to the golgi complex and directs release of virus-like particles. Journal of virology 74 (9). 4319-4326.

Corse, E., Machamer, C. E., 2003. The cytoplasmic tails of infectious bronchitis virus E and M proteins mediate their interaction. Virology 312. 25-34.

Cottrell, J. S., 2011. Protein identification using MS/MS data. Journal of proteomics 74 (10). 1842-1851.

Cumming, R. B., 1963. Infectious avian nephrosis (uraemia) in Australia. Austral Vet J 39. 145-147.

Cumming, R. B., 1969. The control of avian infectious bronchitis/ nephrosis in Australia. Austral Vet J 45. 200-203.

D'Aoust, M., Lavoie, P., Couture, M. M., Trépanier, S., Guay, J., Dargis, M., Mongrand, S., Landry, N., Ward, B. J., Vézina, L., 2008. Influenza virus-like particles produced by transient expression in *Nicotiana benthamiana* induce a protective immune response against a lethal viral challenge in mice. Plant Biotechnology Journal 6. 930-940.

Darteil, R., Bublot, M., Laplace, E., Bouquet, J. F., Audonnet, J. C., Rivière, M., 1995. Herpesvirus of turkey recombinant viruses expressing infectious bursal disease virus (IBDV) VP2 immunogen induce protection against an IBDV virulent challenge in chickens. Virology 211. 481-490.

de Groot, R. J., Baker, S. C., Baric, R., Enjuanes, L., Gorbalenya, A. E., Holmes, K. V., Perlman, S., Poon, L., Rottier, P. J. M., Talbot, P. J., Woo, P. C. Y., Ziebuhr, J., 2011. Coronaviridae, in: King, A.M.Q., Adams, M.J., Carstens, E.B., Lefkowitz, E.J. (Eds.), Virus Taxonomy: Ninth Report of the International Committee on Taxonomy of Viruses. Elsevier Academic Press, San Diego, pp. 774-796.

de Groot, R. J., Baker, S. C., Baric, R., Enjuanes, L., Gorbalenya, A. E., Holmes, K. V., Perlman, S., Poon, L., Rottier, P. J. M., Talbot, P. J., Woo, P. C. Y., Ziebuhr, J., 2012. Family Coronaviridae. Academic Press: San Diego, CA, USA.

de Haan, C. A., Smeets, M., Vernooij, F., Vennema, H., Rottier, P. J., 1999. Mapping of the coronavirus membrane protein domains involved in interaction with the spike protein. J Virol 73. 7441–7452.

de Haan, C. A., Vennema, H., Rottier, P. J., 2000. Assembly of the coronavirus envelope: Homotypic interactions between the M proteins. Journal of Virology 74. 4967-4978.

de Wit, J. J., 2000. Detection of infectious bronchitis. Avian Pathology 29. 71-93.

de Wit, J. J., Cook, J. K., van der Heijden, H. M., 2011. Infectious bronchitis virus variants: a review of the history, current situation and control measures. Avian Pathology 40. 223-235.

Dertzbaugh, M. T., 1998. “Genetically engineered vaccines: an overview,” Plasmid 39 (2), 100–113.

Dhinaker, R. G., Jones, R. C., 1997. Infectious bronchitis virus: Immunopathogenesis of infection in the chicken. Avian Pathology 26. 677-706.

Eid, A. M., 1998. Infectious bronchitis virus infection in Egypt. In: Kaleta EF, Heffels-Redmann U, editors. Proceedings of the International Symposium on Infectious Bronchitis and Pneumovirus Infections in Poultry; Rauischholzhausen, (Germany). P. 145-156.

Eissa, Y. M., Zaher, A., Nafai, E., 1963. Studies on respiratory diseases. Isolation of infectious bronchitis virus. J Arab Vet Med Ass 23. 381.

Ekiert, D. C., Bhabha, G., Elsliger, M. A., Friesen, R. H., Jongeneelen, M., Throsby, M., Goudsmit, J., Wilson, I. A., 2009. Antibody recognition of a highly conserved influenza virus epitope. Science 324. 246-251.

El-Houadfi, M., Jones, R. C., 1985. Isolation of avian infectious bronchitis viruses in Morocco including an enterotropic variant. Vet Rec 116. 445.

El-Houadfi, M., Jones, R. C., Cook, J. K., Ambali, A, G., 1986. The isolation and characterization of six avian infectious bronchitis viruses isolated in Morocco. Avian Pathology 15. 93-105.

Eterradossi, N., Britton, P., 2013. Avian infectious bronchitis. In: Biological Standards Commission, editor. Manual of diagnostic tests and vaccines for terrestrial animals. Paris World Organization for Animal Health.

Faulkner, O. B., Estevez, C., Yu, Q., Suarez, D. L., 2013. “Passive antibody transfer in chickens to model maternal antibody after avian influenza vaccination,” Veterinary Immunology and Immunopathology 152 (3-4). 341–347.

Faye, L., Boulaflous, A., Benchabane, M., Gomord, V., Michaud, D., 2005. Protein modifications in the plant secretory pathway: current status and practical implications in molecular pharming. Vaccine 23. 1770-1778.

Floss, D. M., Falkenburg, D., Conrad, U., 2007. Production of vaccines and therapeutic antibodies for veterinary applications in transgenic plants: an overview. Transgenic Res 16. 315-332.

Fouchier, R. A., V. Munster, A. Wallensten, T. M. Bestebroer, S. Herfst, D. Smith, G. F. Rimmelzwaan, B. Olsen, and A. D. Osterhaus. 2005. Characterization of a novel influenza A virus hemagglutinin subtype (H16) obtained from black-headed gulls. Journal of Virology. 79. Pp. 2814–2822.

Gelb, J. J., Perkins, B. E., Rosenberger, J. K., Allen, P. H., 1981. Serologic and cross-protection studies with several infectious bronchitis virus isolates from Delmarva-reared broiler chickens. Avian Diseases 25. 655– 666.

Gelb, J. J., Jackwood, M. W., 2008. Infectious Bronchitis. In: A laboratory manual for the isolation, identification and characterization of avian pathogens. 5th ed. L. Dufour-Zavala, D. E. Swayne, J. R. Glisson, J. E. Pearson. W. M. Reed, M. W. Jackwood, and P. Woolcock, eds. American Association of Avian Pathologists, Kennett Square, PA. 146 - 149.

Gelvin, S. B., 2003. *Agrobacterium*-mediated plant transformation: the biology behind the "gene-Jockeying" tool. Microbiol. Mol. Biol. R. 67. 16-37.

Gething, M. J., McCammon, K., Sambrook, J., 1986. Expression of wild-type and mutant forms of influenza hemagglutinin: the role of folding in intracellular transport. Cell 46. 939–950.

Giritch, A., Marillonnet, S., Engler, C., van Eldik, G., Botterman, J., Klimyuk, V., Gleba, Y., 2006. Rapid high-yield expression of full-size IgG antibodies in plants coinfected with noncompeting viral vectors. Proc Natl Acad Sci 103 (40). 14701-14706.

Godeke, G. J., de Haan, C. A., Rossen, J. W., Vennema, H., Rottier, P. J., 2000. Assembly of spikes into coronavirus particles is mediated by the carboxy-terminal domain of the spike protein. Journal of Virolology 74. 1566–1571.

Grgacic, E. V. L., Andersen, D. A., 2006. Virus-like particles: Passport to immune recognition. Methods 40. 60-65.

Guo, Z., Wang, H., Yang, T., Wang, X., Lu, D., Li, Y., Zhang, Y., 2010. Priming with a DNA vaccine and boosting with an inactivated vaccine enhance the immune response against infectious bronchitis virus. J. Virol. Methods 167 (1). 84-89.

Hagemeijer, M. C., Verheije, M. H., Ulasli, M., Shaltiel, I. A., de Vries, L. A., Reggiori, F., Rottier, P. J., de Haan, C. A., 2010. Dynamics of coronavirus replication-transcription complexes. Journal of Virology 84. 2134-2149.

Hanada K., Suzuki, Y., Gojobori, T., 2004. A large variation in the rates of synonymous substitution for RNA viruses and its relationship to a diversity of viral infection and transmission modes. Molecular Biology and Evolution 21. 1074 – 1080.

He, R., Dobie, F., Ballantine, M., Leeson, A., Li, Y., Bastien, N., Cutts, T., Andonov, A., Cao, J., Booth, T. F., Plummer, F. A., Tyler, S., Baker, L., Li, X., 2004. Analysis of multimerization of the SARS coronavirus nucleocapsid protein. Biochem. Biophys. Res. Commun 316. 476-483.

Hefferon, K., 2013. Plant-derived pharmaceuticals for the developing world. Biotechnol. J. 8. 1193-1202.

Ho, Y., Lin, P. H., Liu, C. Y., Lee, S. P., Chao, Y. C., 2004. Assembly of human severe acute respiratory syndrome coronavirus-like particles. Biochem Biophys Res Commun 318. 833–838.

Hodgson, T., Casais, R., Dove, B., Britton, P., Cavanagh, D., 2004. Recombinant infectious bronchitis coronavirus Beaudette with the spike protein gene of the pathogenic M41 strains remains attenuated but induces protective immunity. J. Virol 78. 13804-13811.

Hopkins, S. R., Yoder, H. W., 1986. Reversion to virulence of chicken-passaged infectious bronchitis vaccine virus. Avian Dis 30. 221-223.

Horimoto, T., Nakayama, K., Smeekens, S. P., Kawaoka, Y., 1994. Proprotein-processing endoproteases PC6 and furin both activate hemagglutinin of virulent avian influenza viruses. J. Virol. 6. 6074–6078.

Howell, S. H., 2013. Endoplasmic reticulum stress responses in plants. Annu. Rev. Plant. Biol 64. 477-499.

Hsu, T. A., Betenbaugh, M. J., 1997. Coexpression of molecular chaperone BiP improves immunoglobulin solubility and IgG secretion from Trichoplusia in insect cells. Biotechnol. Prog 13. 96-104.

Ignjatovic, E. J., Ashton, F., 1996. Detection and differentiation of avian infectious bronchitis viruses using a monoclonal antibody-based ELISA. Avian Pathology 25. 721-736.

Isin, B., Doruker, P., Bahar, I., 2002. Functional motions of influenza virus hemagglutinin: a structure-based analytical approach. Biophys. J. 82. 569–581.

Jackwood, M. W., Hilt, D. A., Sellers, H. S., Williams, S. M., Lasher, H. N., 2010. Rapid heat-treatment attenuation of infectious bronchitis virus. Avian Pathology 39. 227-233.

Jackwood, M. W., 2012. Review of infectious bronchitis virus around the world. Avian Diseases Digest 56. 634 - 641.

Jackwood, M. W., Hall, D., Handel, A., 2012. Molecular evolution and emergence of avian gammacoronaviruses. Infect. Genet. Evol 12. 1305-1311.

Jackwood, M. W., de Wit, S., 2013. Infectious Bronchitis. *Diseases of Poultry*. Chapter 4. Pp. 139 - 153.

Jackwood, M. W., Jordan, B. J., Roh, H. J., Hilt, D. A., Williams, S. M., 2015. Evaluating protection against infectious bronchitis virus by clinical signs, ciliostasis, challenge virus detection, and histopathology. Avian Dis 59. 368-374.

Jansen, T., Hofmans, M. P., Theelen, M. J., Manders, F., Schijns, V. E., 2006. Structure- and oil type-based efficacy of emulsion adjuvants. Vaccine 24. 5400-5405.

Jayaram, H., Fan, H., Bowman, B. R., Ooi, A., Jayaram, J., Collisson, E. W., Lescar, J., Prasad, B. V., 2006. X-ray structures of the N- and C- terminal domains of a coronavirus nucleocapsid protein: implications for nucleocapsid formation. Journal of Virology 80. Pp. 6612-6620.

Jennings, G. T., Bachmann, M. F., 2008. The coming of age of virus-like particle vaccines. Biol Chem 389. 521-536.

Johnson, M. A., Pooley, C., Ignjatovic, J., Tyack, S. G., 2003. A recombinant fowl adenovirus expressing the S1 gene of infectious bronchitis virus protects against challenge with infectious bronchitis virus. Vaccine 21. 2730-2736.

Jones, R. C., Savage, C. E., Naylor, C. J., Cook, J. K., El-Houadfi, M. A., 2004. Possible North African progenitor of the major European infectious bronchitis variant (793B, 4/91, CR88). In: Kaleta EF, Heffels-Redmann U, editors. Proceedings of the IV International Symposium on Avian Corona- and Pneumovirus Infections; Rauischholzhausen, (Germany). P. 105-111.

Jordan, B. J., 2016. Spray application of infectious bronchitis virus vaccines in the hatchery: How efficient are we? XXIV Congreso de Avicultura Centramericano y del Caribe. http://www.anaviguatemala.og/xxiv-congreso-de-avicultura-centroamericano-y-del-caribe/.

Jordan, B., 2017. Vaccination against infectious bronchitis virus: a continuous challenge. Veterinary Microbiology. 1 - 7.

Jungherr, E. I., Chomiak, T. W., Luginbuhl, R. E., 1956. Immunologic differences in strains of infectious bronchitis virus. Proc. 60th annual meeting U.S. Livestock Sanitary Association. 203 - 209.

Kant, A., Koch, G., van Roozelaar, D. J., Kusters, J. G., Poelwijk, F. A., van der Zeijst, B. A., 1992. Location of antigenic sites defined by neutralizing monoclonal antibodieson the S1 avian infectious bronchitis virus glycopolypeptide. Journal of General Virology 73 (Pt 3). 591-596.

Kelly, P. J., Chitauro, D., Rohde, C., Rukwava, J., Majok, A., Davelaar, F., Mason, P. R., 1994. Diseases and management of backyard chicken flocks in Chitungwiza, Zimbabwe. Avian Dis 38. 626-629.

Khataby, K., Fellahi, S., Loutfi, C., Mustapha, E. M., 2016. Avian infectious bronchitis virus in Africa: a review. Veterinary Quarterly 36, 2. 71-75.

Kido, H. Yokogoshi, Y., Sakai, K., Tashiro, M., Kishino, Y., Fukutomi, A., Katunuma, N., 1992. Isolation and characterization of a novel trypsin-like protease found in rat bronchiolar epithelial Clara cells. J. Biol. Chem. 267, 13573–13579.

Knoetze, A. D., Moodley, N., Abolnik, C., 2014. Two genotypes of infectious bronchitis virus are responsible for serological variation in KwaZulu-Natal poultry flocks prior to 2012. Onderstepoort Journal of Veterinary Research 81. 1-10.

Koch, G., Hartog, L., Kant, A., van Roozelaar, D. J., 1990. Antigenic domains on the peplomer protein of avian infectious bronchitis virus: correlation with biological functions. Journal of General Virology 71 (pt 9). 1929-1935.

Kusters, J. G., Niesters, H. G., Lenstra, J. A., Horzinek, M. C., van der Zeijst, B. A., 1989. Phylogeny of antigenic variants of avian coronavirus IBV. Virology 169. 217-221.

Kusters J. G., Jager, E. J., Niesters, H. G. M., van der Zeijst, B. A. M., 1990. Sequence evidence for RNA recombination in field isolates of avian coronavirus infectious bronchitis virus. Vaccine 8. 605 - 608.

Kwon, H. M., Jackwood, M. W., Gelb, J., 1993. Differentiation of infectious-bronchitis virus serotypes using polymerase chain-reaction and restriction-fragment-length-polymorphism analysis. Avian Dis 37. 194-202.

Ladman, B. S., Pope, C. R., Ziegler, A. F., Swieczkowski, T., Callahan, C. J., Davison, S., Gelb Jr, J., 2002. Protection of chickens after live and inactivated virus vaccination against challenge with nephropathogenic infectious bronchitis virus PA/ Wolgemuth/ 98. Avian Dis 46. 938-944.

Ladman, B. S., Loupos, A. B., Gelb Jr, J., 2006. Infectious bronchitis virus S1 gene sequence comparison is a better predictor of challenge of immunity in chickens than serotyping by virus neutralization. Avian Pathology 35. 127-133.

Lai, M. M., Cavanagh, D., 1997. The molecular biology of coronaviruses. Adv Virus Res 48. 1-100.

Lal, S. K., Chow, V. T. K., 2007. Avian Influenza H5N1 Virus: An Emerging Global Pandemic. Lal SK (ed): Emerging Viral Diseases of Southeast Asia. Issues Infect Dis. Basel, Karger, vol 4, 59–77.

Lewicki, D. N., Gallagher, T. M., 2002. Quaternary structure of coronavirus spikes in complex with carcinoembryonic antigen-related cell adhesion molecule cellular receptors. J. Biol. Chem 277. 19727-19734.

Li, H., Wang, Y., Han, Z., Wang, Y., Liang, S., Jiang, L., Hu, Y., Kong, X., Liu, S., 2016. Recombinant duck enteritis viruses expressing major structural proteins of the infectious bronchitis virus provide protection against infectious bronchitis in chickens. Antiviral Research 130. 19 - 26.

Lim, K. P., Liu, D. X., 2001. The missing link in coronavirus assembly. Retention of the avian coronavirus infectious bronchitis virus envelope protein in the pre-golgi compartments and physical interaction between the envelope and membrane proteins. J. Biol. Chem 276. 17515-17523.

Liu, F., Wu, X., Li, L., Ge, S., Liu, Z., Wang, Z., 2013a. Virus-like particles: Promising platforms with characteristics of DIVA for veterinary vaccine design. Comparative Immunology, Microbiology and Infectious Diseases 36. 343–352.

Liu, G., Lv, L., Yin, L., Li, X., Luo, D., Liu, K., Xue, C., Cao, Y. 2013b. Assembly and immunogenicity of coronavirus-like particles carrying infectious bronchitis virus M and S proteins. Vaccine 31. Pp. 5524-5530.

Liu, H. J., Lee, L. H., Shih, W. L., Lin, M. Y., Liao, M. H., 2003. Detection of infectious bronchitis virus by multiplex polymerase chain reaction and sequence analysis. Journal of Virological Methods 109. 31 - 37.

Liu, J. X., Howell, S. H., 2010. Endoplasmic reticulum protein quality control and its relationship to environmental stress responses in plants. Plant Cell 22. 2930-2942.

Liu, S., Xu, Q., Han, Z., Liu, X., Li, H., Guo, H., 2014. Origin and characteristics of the recombinant novel avian infectious bronchitis coronavirus isolate ck/CH/LJL/111054. Infect Genet Evol 23. 189-195.

Lv, L., Li, X., Liu, G., Li, R., Liu, Q., Shen, H., Wang, W., Xue, C., Cao, Y., 2014. Production and immunogenicity of chimeric virus-like particles containing the spike glycoprotein of infectious bronchitis virus. J. Vet. Sci 15 (2). 209-216.

Ma, J. K., Christou, P., Chikwamba, R., Haydon, H., Paul, M., Ferrer, M. P., Ramalingam, S., Rech, E., Rybicki, E., Wigdorovitz, A., Yang, D. C., Thangaraj, H., 2013. Realising the value of plant molecular pharming to benefit the poor in developing countries and emerging economies. Plant Biotechnology Journal 11. 1029-1033.

Magadán, J. G., Khurana, S., Das, S. R., Frank, G. M., Stevens, J., Golding, H., Bennink, J. R., Yewdell, J. W., 2013. Influenza A Virus Hemagglutinin Trimerization Completes Monomer Folding and Antigenicity. Journal of Virology 87 (17). 9742-9753.

Mann, M., Wilm, M., 1994. Error-tolerant identification of peptides in sequence databases by peptide sequence tags. Analytical Chemistry 66 (22). 4390-4399.

Margine, I., Hai, R., Albrecht, R. A., Obermoser, G., Harrod, A. C., Banchereau, J., Palucka, K., García-Sastre, A., Palese, P., Treanor, J. J., Krammer, F., 2013. H3N2 influenza virus infection induces broadly reactive hemagglutinin stalk antibodies in humans and mice. Journal of Virology 87. 4728-4737.

Margolin, E., Chapman, R., Williamson, A., Rybicki, E. P., Meyers, A. E., 2018. Production of complex viral glycoproteins in plants as vaccine immunogens. Plant Biotechnology Journal 16. 1531-1545.

Marquardt, W. W., Snyder, D. B., Schlotthober, B. A., 1981. Detection and quantification of antibodies to infectious bronchitis virus by enzyme-linked immunosorbent assay. Avian Dis 25. 713-722.

Masters, P., Perlman, S., 2013. Coronaviridae. In: Howley, P., Knipe, D. M., (Eds). Fields Virology. Kluwer, Wolters. Chapter 28. Pp. 825–858.

Matthijs, M. G., Bouma, A., Velkers, F. C., van Eck, J. H., Stegeman, J. A., 2008. Transmissibility of infectious bronchitis virus H120 vaccine strain among broilers under experimental conditions. Avian Dis 52. 461-466.

McGinnes, L. W., Morrison, T. G., 2014. Newcastle disease virus-like particles: Preparation, Purification, Quantification, and Incorporation of Foreign Glycoproteins. Curr Protoc Microbiol 30. 1-28.

Mockett, A. P., Darbyshire, J. H., 1981. Comparative studies with an enzyme-linked immunsorbent assay (ELISA) for antibodies to avian infectious bronchitis virus. Avian Pathology 10. 1-10.

Morgan, R. W., Gelb Jr, J., Schreurs, C. S., Lutticken, D., Rosenberger, J. K., Sondermeijer, P. J., 1992. Protection of chickens from Newcastle and Marek's diseases with a recombinant herpesvirus of turkeys vaccine expressing the Newcastle disease virus fusion protein. Avian Dis 36. 858-870.

Morley, A. J., Thomson, D. K., 1984. Swollen-head syndrome in broiler chickens. Avian Dis 28. 238-243.

Moustafa, K., Makhzoum, A., Tremouillaux-Giller, J., 2016. Molecular faming on rescue of pharma industry for next generations. Crit. Rev. Biotechnol 36. 840-850.

Mushi, E. Z., Binta, M. G., Chabo, R. G., Itebeng, K., 2006. Diseases of indigenous chickens in Bokaa village, Kgatleng district, Botswana. J S Afr Vet Assoc 77. 131-133.

Nakauchi, M., Kariwa, H., Kon, Y., Yoshii, K., Maeda, A., Takashima, I., 2008. Analysis of severe acute respiratory syndrome coronavirus structural proteins in virus-like particle assembly. Microbiol Immunol 52. 625–630.

Nayak, B., Kumar, S., DiNapoli, J. M., Paldurai, A., Perez, D. R., Collins, P. L., Samal, S. K., 2010. Contributions of the Avian Influenza Virus HA, NA, and M2 Surface Proteins to the Induction of Neutralizing Antibodies and Protective Immunity. Journal of Virology Vol 84. No 5. Pp. 2408 – 2420.

Neu, K. E., Henry Dunand, C. J., Wilson, P. C., 2016. Heads, stalks and everything else: how can antibodies eradicate influenza as a human disease? Curr Opin Immunol 42. 48-55.

Neuman, B. W., Kiss, G., Kundig, A. H., Bhella, D., Baksh, M. F., Connelly, S., Droese, B., Klaus, J. P., Makino, S., Sawicki, S. G., Siddell, S. G., Stamou, D. G., Wilson, I. A., Kuhn, P., Buchmeier, M. J., 2011. A structural analysis of M protein in coronavirus assembly and morphology. J. Struct. Biol 174. 11-22.

Ning, J. F., Zhu, W., Xu, J. P., Zheng, C. Y., Meng, X. L., 2009. Oral delivery of DNA vaccine encoding VP28 against white spot syndrome virus in crayfish by attenuated *Salmonella typhimurium*. Vaccine 27. 1127–1135.

Noad, R., Roy, P., 2003. Virus-like particles as immunogens. Trends in Microbiol 11. 438-444.

Ong, H. K., Tan, W. S., Ho, K. L., 2017. Virus like particles as a platform for cancer vaccine development. Peer J. 1-31.

Oshop, G. L., Elankumaran, S., Heckert, R. A., 2002. DNA vaccination in the avian. Vet. Immunol. Immunopathol 89. 1–12.

Pan, Z., Zhang, X., Geng, S., Cheng, N., Sun, L., Liu, B., Huang, J., Jiao, X., Priming with a DNA vaccine delivered by attenuated Salmonella typhimurium and boosting with a killed vaccine confers protection of chickens against infection with the H9 subtype of avian influenza virus. Vaccine 27 (7). 1018-1023.

Perlman, S., Gallagher, T., Snijder, E. J., 2008. *Nidoviruses*. ASM Press, Washington, DC.

Pillet, S., Aubin, E., Trepanier, S., Bussiere, D., Dargis, M., Poulin, J. F., Yassine-Diab, B., Ward, B. J., Landry, N., 2016. A plant-derived quadrivalent virus like particle influenza vaccine induces cross-reactive antibody and T cell response in healthy adults. Clinical Immunlogy 168. 72-87.

Pogue, G. P., Vojdani, F., Palmer, K. E., Hiatt, E., Hume, S., Phelps, J., Long, L., Bohorova, N., Kim, D., Pauly, M., Velasco, J., Whaley, K., Zeitlin, L., Garger, S. J., White, E., Bai, Y., Haydon, H., Bratcher, B., 2010. Production of pharmaceutical-grade recombinant aprotinin and a monoclonal antibody product using plant-based transient expression systems. Plant Biotechnology Journal 8. 638-654.

Promkuntod, N., van Eijndhoven, R. E., de Vrieze, G., Grone, A., Verheije, M. H., 2014. Mapping of the receptor-binding domain and amino acids critical for attachment in the spike protein of avian coronavirus infectious bronchitis virus. Virology 448. 26-32.

Raymond, F. L., Caton, A. J., Cox, N. J., Kendal, A. P., Brownlee, G. G., 1986. The antigenicity and evolution of influenza H1 haemagglutinin, from 1950–1957 and 1977–1983: two pathways from one gene. Virology 148. 275–287.

Rosenthal, P., Zhang, X., Formanowski, F., 1988. Structure of the haemagglutininesterase-fusion glycoprotein of influenza C virus, Nature 396.

Rossman, J. S., Lamb, R. A., 2011. Influenza virus assembly and budding. Virology 411. 229–236.

Ruano, M., El-Attrache, J., Villegas, P., 2000. A rapid-plate hemagluttination assay for the detection of infectious bronchitis virus. Avian diseases 44. 99 - 104.

Ruch, T. R., Machamer, C. E., 2011. The hydrophobic domain of infectious bronchitis virus E protein alters the host secretory pathway and is important for release of infectious virus. Journal of Virology 85. Pp. 675-685.

Rudolph, R., Lilie, H., 1996. In vitro folding of inclusion body proteins. FASEB J 10. 49-56.

Rybicki, E. P., 2009. Plant-produced vaccines: promise and reality. Drug Discov. Today 14. 16-24.

Rybicki, E. P., 2010. Plant-made vaccines for humans and animals. Plant Biotechnology Journal 8. 620-637.

Rybicki, E. P., Hitzeroth, I. I., Meyers, A., Dus Santos, M. J., Wigdorovitz, A., 2013. Developing country applications of molecular farming: case studies in South Africa and Argentina. Curr. Pham. Des. 19. 5612-5621.

Sainsbury, F., and Lomonossoff, G. P., 2008. Extremely high level and rapid transient protein production in plants without the use of viral replication. *Plant Physiology*. 148. 1212 - 1218.

Sainsbury, F., Thuenemann, E. C., and Lomonossoff, G. P., 2009. pEAQ: Versatile expression vectors for easy and quick transient expression of heterologous proteins in plants. *Plant Biotechnology Journal*. 7. 682 - 693.

Sainsbury, F., Cañizares, M. C., and Lomonossoff, G. P., 2010. Cowpea mosaic virus: The plant virus-based biotechnology workhorse. *Annual Review of Phytopathology*, 48. 437 - 455.

Sainsbury, F., Saxena, P., Geisler, K, Osbourn, A., Lomonossoff, G. P., 2012. Using a virus-derived system to manipulate plant natural product biosynthetic pathways. Methods in Enzymology. Volume 517. Chapter 9. 185 - 202.

Sainsbury, F., Saxena, P., Geisler, K., Osbourn, A., Lomonossoff, G. P., 2013. Using a virus-derived system to manipulate plant natural product biosynthetic pathways. Methods in Enzymology 517. 185-187.

Saléry, M., 2017. Autogenous vaccines in Europe: national approaches to authorisation. Regulatory rapporteur, Topra, 14 (6). 27-32.

Saunders, K., Sainsbury, F., Lomonossoff, G. P., 2009. Efficient generation of Cowpea mosaic virus empty virus-like particles by the proteolytic processing of precursors in insect cells and plants. Virology. 393. 329 - 337. Schalk, A. F., Hawn, M. C., 1931. An apparently new respiratory disease in baby chicks. Journal of the American Veterinary Medical Association 78. 413 - 422.

Schaffeld, M., Markl, J., 2004. Fish keratins. Methods in cell biology 78. 627-671.

Şereflioğlu, Ş., Yapıcı, E., Tekarslan Şahin, Ş. H., Özsoy, Y., Üstündağ, C. B., 2017. Targeted drug delivery and vaccinology approaches using virus-like particles for cancer. Istanbul J Pharm 47 (3). 112-119.

Sheludko, Y. V., Sindarovska, Y. R., Gerasymenko, I. M., Bannikova, M. A., Kuchuk, N. V., 2007. Comparison of several *Nicotiana* species as hosts for high scale *Agrobacterium* mediated transient expression. Biotechnol Bioeng 96. 608–614.

Shevchenko, A., Tomas, H., Havlis, J., Olsen, J. V., Mann, M., 2007. In-gel digestion for mass spectrometric characterization of proteins and proteomes. Nature Protocols 1 (6). 2856 - 2860.

Shoji, Y., Chichester, J. A., Jones, M., Manceva, S. D., Damon, E., Mett, V., Musiychuk, K., Bi, H., Farrance, C., Shamloul, M., Kushnir, N., Sharma, S., Yusibov, V., 2011. Plant-based rapid production of recombinant subunit hemagglutinin vaccines targeting H1N1 and H5N1 influenza. Hum. Vaccin. 7 (Suppl). 41-50.

Siegrist, C. A., 2001. Neonatal and early life vaccinology. Vaccine 19. 3331–3346.

Siu, Y. L., Teoh, K. T., Lo, J., Chan, C. M., Kien, F., Escriou, N., Tsao, S. W., Nicholls, J. M., Altmeyer, R., Peiris, J. S., Bruzzone, R., Nal, B., 2008. The M, E, and N structural proteins of the severe acute respiratory syndrome coronavirus are required for efficient assembly, trafficking, and release of virus-like particles. J Virol 82. 11318–11330.

Skehel, J. J., Wiley, D. C., 2000. Receptor binding and membrane fusion in virus entry: The influenza hemagglutinin. Annu. Rev. Biochem. 69. 531–569.

Smith, T., O'Kennedy, M. M., Wandrag, D. B. R., Adeyemi, M., Abolnik, C., 2019. Efficacy of a plant-produced virus-like particle vaccine in chickens challenged with Influenza A H6N2 virus. Plant Biotechnology Journal. 1-11.

Soltanialvar, M., Bagherpour, A., Akbarnejad, F., 2016. Roll of hemagglutinin gene in the biology of avian influenza virus. Asian Pacific Journal of Tropical Disease 6 (6). 443-446.

Song, C. S., Lee, Y. J., Lee, C. W., Sung, H. W., Kim, J. H., Mo, I. P., Izumiya, Y., Jang, H. K., Mikami, T., 1998. Induction of protective immunity in chickens vaccinated with infectious bronchitis virus S1 glycoprotein expressed by a recombinant baculovirus. Journal of General Virology 79 (Pt. 4). 719–723.

Sriwilaijaroen, N., and Suzuki, Y., 2012. Molecular basis of the structure and function of H1 hemagglutinin of influenza virus. Proc. Jpn. Acad, Ser B Vol 88. Pp 226 – 249.

Stieneke-Grober, A., Vey, M., Angliker, H., Shaw, E., Thomas, G., Roberts, C., Klenk, H. D., Garten, W., 1992. Influenza virus hemagglutinin with multibasic cleavage site is activated by furin, a subtilisin-like endoprotease. EMBO J. 11. 2407–2414.

Stoger, E., Fischer, R., Moloney, M., Ma, J. K., 2014. Plant molecular pharming for the treatment of chronic and infectious diseases. Annu. Rev. Plant Biol. 65. 743-768.

Strasser, R., Stadlmann, J., Schähs, M., Stiegler, G., Quendler, H., Mach, L., Glössl, J., Weterings, K., Pabst, M., Steinkellner, H., 2008. Generation of glyco-engineered *Nicotiana benthamiana* for the production of monoclonal antibodies with a homogeneous human-like N-glycan structure. Plant Biotechnology Journal 6. 392-402.

Terregino, C., Toffan, A., Beato, M. S., De Nardi, R., Vascellari, M., Meini, A., Ortali, G., Mancin, M., Capua, I., 2008. Pathogeniity of a QX strain of infectious bronchitis virus in specific pathogen free and commercial broiler chickens, and evaluation of protection induced

by a vaccination programme based on the Ma4 and 4/91 serotypes. Avian Pathology 37. 487 - 493.

Thekisoe, M. M. O., Mbati, P. A., Bisschop, S. P. R., 2003. Diseases of free-ranging chickens in the Qwa-Qwa district of the Northeastern Free State province of South Africa. J S Afr Vet Assoc 74. 14-16.

Theunemann, E. C., Meyers, A. E., Verwey, J., Rybicki, E. P., Lomonossoff, G. P., 2013. A method for rapid production of heteromultimeric protein complexes in plants: assembly of protective bluetongue virus-like particles. Plant Biotechnology Journal. 1-8.

Thorp, E. B., Boscarino, J. A., Logan, H. L., Goletz, J. T., Gallagher, T. M., 2006. Palmitoylations on murine coronavirus spike proteins are essential for virion assembly and infectivity. Journal of Virology 80. 1280-1289.

Toffan A., Monne, I., Terregino, C., Cattoli, G., Hodobo, C. T., Gadaga, B., Makaya, P. V., Mdlongwa, E., Swiswa, S., 2011. QX-like infectious bronchitis virus in Africa. Vet Rec 169. 589.

Tong, S., Zhu, X., Li, Y., Shi, M., Zhang, J., Bourgeois, M., Yang, H., Chen, X., Recuenco, S., Gomez, J., 2013. New world bats harbor diverse influenza A viruses. PLoS Path 9. 1078–1084.

Toro, H., Zhang, J. F., Gallardo, R. A., van Santen, V. L., van Ginkel, F. W., Joiner, K. S., Breedlove, C., 2014a. S1 of distinct IBV population expressed from recombinant adenovirus confers protection against challenge. Avian Dis 58. 211-215.

Toro, H., Zhao, W., Breedlove, C., Zhang, Z., van Santen, V. L., Yu, Q., 2014b. Infectious bronchitis virus S2 expressed from recombinant virus confers broad protection against challenge. Avian Dis 58. 83-89.

Tschofen, M., Knopp, D., Hood, E., Stoger, E., 2016. Plant molecular farming: Much more than medicines. Annu. Rev. Anal. Chem (Palo Alto Calif) 9. 271-294.

Ujike, M., Taguchi, F., 2015. Incorporation of Spike and Membrane glycoproteins into coronavirus virions. Viruses 7. 1700-1725.

Ukrami, A., Sakurai, A., Ishikawa, M., Yap, M. L., Flores-Garcia, Y., Haseda, Y., Aoshi, T., Zavala, F. P., Rossman, M. G., Kuno, S., Ueno, R., Akahata, W., 2017. Development of a novel

virus-like particle vaccine platform that mimics the immature form of alphavirus. Clinical and Vaccine Immunology Vol 24. Issue 7. Pp 1-14.

Umar, A., Shah, M. A. A., Munir, M. T., Ahsan, U., 2016. Infectious Bronchitis Virus: evolution and vaccination. World's Poultry Science Journal, Vol. 27. Issue 1. 49 – 60.

Vagnozzi, A., Zavala, G., Riblet, S. M., Mundt, A., Garcia, M., 2012. Protection induced by commercially available live-attenuated and recombinant viral vector vaccines against infectious laryngotracheitis virus in broiler chickens. Avian Pathol 41. 21-31.

van Eck, J. H., 1983. Effects of experimental infection of fowl with EDS'76 virus, infectious bronchitis virus and/ or fowl adenovirus on laying performance. Vet Q 5. 11-25.

van Roeckel, H., Bullis, K. L., Flint, O. S., Clarke, M. K., 1942. Poultry disease control service. Massachusetts Agricultural Experiment Station. MA Annual Report. Bulletin 388. 99 - 103.

Vardakou, M., Sainsbury, F., Rigby, N., Mulholland, F., and Lomonossoff, G. P., 2012. Expression of active recombinant human gastric lipase in *Nicotiana benthamiana* using the CPMV-HT transient expression systems. Protein expression and Purification. 81. 69 - 74.

Weber, J., Cheinsong-Popov, R., Callow, D., Adams, S., Patou, G., Hodgkin, K., Martin, S., Gotch, F., Kingsman, A., 1995. Immunogenicity of the yeast recombinant p17/p24:Ty virus-like particles (p24-VLP) in healthy volunteers. Vaccine 13. 831-834.

Webster, R. G., Bean, W. J., Gorman, O. T., Chambers, T. M., Kawaoka. Y., 1992. Evolution and ecology of influenza A viruses. Microbiol. Rev. 56. Pp. 152–179.

Wickramasinghe, I. N., de Vries, R. P., Grone, A., de Haan, C. A., Verheije, M. H., 2011. Binding of avian coronavirus spike proteins to host factors reflects virus tropism and pathogenicity. Journal of Virology 85. 8903-8912.

Wickramasinghe, I. N. A., van Beurden, S. J., Weerts, E. A. W. S., Verheije, M. H., 2014. The avian coronavirus spike protein. Virus Research 194, 37 - 48.

Wiley, D. C., Skehel, J. J., 1987. The structure and function of the hemagglutinin membrane glycoprotein of influenza virus. Annu. Rev. Biochem. 56. 365–394.

Wilson, I., Skehel, J. J., 1981. Structure of the haemagglutinin membrane glycoprotein of influenza virus at 3 A resolution. Nature 289. 366–373.

Wu, X., Zhai, X., Lai, Y., Zuo, L., Zhang, Y., Mei, X., Xiang, R., Kang, Z., Zhou, L., Wang, H., 2019. Construction and immunogenicity of novel chimeric virus-like particles bearing antigens of infectious bronchitis virus and Newcastle disease virus. Viruses 11 (254). 1-13.

Xu, P., Wu, X., Wang, H., Ma, B., Ding, M., Yang, X., 2016. Assembly and immunogenicity of baculovirus-derived infectious bronchitis virus-like particles carrying membrane, envelope and the recombinant spike proteins. Biotechnol Lett 38. 299-304

Yang, T., Wang, H. N., Wang, X., Tang, J. N., Lu, D., Zhang, Y. F., Guo, Z. C., Li, Y. L., Gao, R., Kang, R. M., 2009. The protective immune response against infectious bronchitis virus induced by multi-epitope based peptide vaccines. Bioscience, Biotechnology, and Biochemistry 73. 1500 - 1504.

Yang, X., Zhou, Y., Li, J., Fu, L., Ji, G., Zeng, F., Zhou, L., Gao, W., Wang, H., 2016. Recombinant infectious bronchitis virus (IBV) H120 vaccine strain expressing the hemagglutinin-neuraminidase (HN) protein of Newcastle disease virus (NDV) protects against IBV and NDV challenge. Archives of Virology 161. 1209 - 1216.

Yao, J., Weng, Y., Dickey, A., Wang, K. Y., 2015. Plants as Factories for Human Pharmaceuticals: Applications and Challenges. International Journal of Molecular Sciences 16. 28549-28565.

Yu, L., Liu, W., Schnitzlein, W. M., Tripathy, D. N., Kwang, J., 2001. Study of protection by recombinant fowl poxvirus expressing C-terminal nucleocapsid protein of infectious bronchitis virus against challenge. Avian Dis. 45. 340–348.

Zdanowicz, M., Chroboczek, J., 2016. Virus-like particles as drug vectors. Acta biochimica Polonica Vol 63. No 3. 469–473.

Zhang, Y., Wang, H. N., Wang, T., Fan, W. Q., Zhang, A. Y., Wei, K., Tian, G. B., Yang, X., 2010. Complete genome sequence and recombination analysis of infectious bronchitis virus attenuated vaccine strain H120. Virus Genes 41. Pp. 377 - 388.

Zhou, J., Cheng, L., Zheng, X., Wu, J., Shang, S.., Wang, J., Chen, J., 2004. Generation of the transgenic potato expressing full-length spike protein of infectious bronchitis virus. Journal of Biotechnology 111. 121-130.

Ziebuhr, J., Snijder, E. J., Gorbalenya, A. E., 2000. Virus-encoded proteinases and proteolytic processing in the nidovirales. Journal of General Virology 81. 853 - 879.

Appendix

UNIVERSITEIT VAN PRETORIA
UNIVERSITY OF PRETORIA
YUNIBESITHI YA PRETORIA

Research Ethics Committee

PROJECT TITLE	**Development of plant produced virus-like particles displaying the spike glycoprotein of infectious bronchitis virus as potential vaccines.**
PROJECT NUMBER	**REC031-18**
RESEARCHER/PRINCIPAL INVESTIGATOR	**Kamogelo Sepotokele**

STUDENT NUMBER (where applicable)	
DISSERTATION/THESIS SUBMITTED FOR	**MSc**

SUPERVISOR	**Prof Celia Abolnik**

APPROVED	Date **15 June 2018**
CHAIRMAN: UP Research Ethics Committee	Signature M.M. Duncan.

BioBasic IBV Nucleotide sequences:

Chicken codon optimised Spike gene with *Age*I and *Xho*I sites in italics (N- and C-terminal, respectively):

CGC*ACCGGT***ATG**CTGGTGAAGAGCCTGTTCCTGGTGACAATTCTGTGCGCTCTGTGCTCCGCTAACCTGTTTGA
TAGCGATAATAACTACGTGTACTACTACCAGTCCGCTTTTAGACCACCAAACGGCTGGCACCTGCAGGGCGGC
GCCTACGCAGTGGTGAATAGCACAAACCACACCTCCAACGCTGGCAGCGCACAGGGATGTACAGTGGGCGTG
ATCAAGGATGTGTATAATCAGAGCGTGGCAAGCATTGCAATGACAGCCCCTCTGCAGGGCATGGCATGGTTCT
GCACAGCCTATTGCAACTTCTCTGACACCACCGTGTTTGTGACACACTGCTACCACATCAGAATCAGCGCCAT
GAAGAACGGATCTCTGTTCTACAACCTGACCGTGAGCGTGAGTAAATACCCCAACTTTAAGAGCTTCCAGTGC
GTGAACAACTTCACCTCTGTGTATCTGAATGGAGACCTGGTGTTCACCAGCAACAAGACTACCGATGTGACTA
GCGCCGGCGTGTACTTTAAGGCCGGAGGACCAGTGAACTACAGCATTATGAAAGAGTTTAAGGTGCTGGCCTA
CTTTGTGAACGGCACAGCACAGGACGTGATTCTGTGCGATAACTCTCCCAAGGGACTGCTGGCTTGTCAGTAC
AACACAGGCAACTTTTCTGACGGATTTTACCCCTTCACTAATAGCACACTGGTGAGAGAGAAGTTTATTGTGT
ACAGAGAGAGCAGCTTCAACACAACCCTGGCCCTGACTAACTTCACCTTCACAAACGTGAGCAACGCTCAGCC
TAACTCCGGAGGGGTGAATACATTCCACCTGTACCAGACCCAGACAGCTCAGAGCGGCTACTACAACTTCAAT
CTGAGCTTCCTGAGCCAGTTCGTGTACAAGGCAAGCGATTTCATGTACGGAAGCTATCACCCATCATGCTCCTT
TAGACCTGAGACAATCAATTCTGGGCTGTGGTTTAATTCCCTCTCAGTTAGCCTGACATATGGTCCACTCCAGG
GAGGCTGCAAGCAGAGCGTTTTCAGCGGGAAAGCCACCTGCTGCTACGCCTACAGCTACAAGGGACCAATGG
CCTGTAAGGGCGTGTACAGTGGAGAGCTGAGGACTAATTTCGAGTGCGGACTGCTGGTGTACGTGACAAAGTC
CGATGGCAGCAGGATTCAAACCAGAACAGAGCCTCTGGTGCTCACACAGTACAACTACAATAATATTACTCTG
GATAAATGTGTTGCATACAACATCTATGGAAGAGTGGGCCAGGGCTTCATTACCAACGTGACCGACTCAGCTG
CTAACTTTAGCTACCTGGCCGACGGCGGCCTGGCTATCCTGGATACCAGCGGGGCCATCGACGTGTTTGTGGT
GCAGGGAATCTATGGCCTGAACTACTATAAAGTGAATCCCTGCGAGGACGTGAACCAGCAGTTCGTGGTGAG
CGGAGGGAACATCGTTGGAATTCTGACCTCCAGGAACGAGACCGGATCTGAGCAGGTGGAAAACCAGTTCTA
CGTGAAACTGACTAATAGTTCTCACAGAAGAAGACGATCTATTGGCCAGAACGTGACCTCCTGCCCCTACGTG
AGCTATGGCCGCTTCTGCATCGAGCCTGACGGCAGCCTTAAAATGATCGTGCCTGAGGAGCTGAAGCAGTTCG
TGGCTCCGCTGCTGAACATTACCGAGAGCGTGCTGATCCCCAACTCTTTTAACCTGACAGTGACAGATGAGTA
CATTCAGACCAGGATGGACAAGGTGCAGATCAACTGCCTGCAGTACGTGTGCGGCAACAGCCTGGAGTGCAG
GAAACTGTTCCAGCAGTACGGACCTGTGTGTGATAATATCCTGAGCGTCGTGAATTCTGTGTCCCAGAAGGAA
GATATGGAACTGCTGAGCTTCTATAGCTCTACCAAGCCAAAAGGATACGACACCCCCGTGCTGTCTAACGTGA
GCACCGGAGAGTTCAACATCAGCCTGCTGCTGAAAACCCCTATCAGCAGCAGCGGAAGAAGCTTTATCGAGG
ACCTGCTGTTTACTAGCGTGGAGACTGTGGGCCTGCCCACCGACGCTGAGTACAAGAAGTGCACAGCCGGGCC
TCTGGGCACCCTGAAGGACCTCATCTGCGCAAGAGAATACAATGGACTGCTGGTGCTGCCCCCCATCATCACA
GCTGACATGCAGACCATGTATACAGCATCTCTGGTGGGCGCTATGGCATTCGGCGGGATCACCTCCGCTGCCG
CTATCCCCTTCGCCACACAGATCCAGGCCAGGATTAACCACCTGGGAATCACCCAGTCTCTGCTGATGAAGAA
CCAGGAGAAGATCGCTGCAAGCTTTAACAAGGCCATCGGGCACATGCAGGAGGGGTTCAGGAGCACATCCCT
GGCTCTGCAGCAGATCCAGGATGTGGTGAACAAGCAGTCAGCTATTCTGACAGAGACAATGAACAGCCTGAA
CAAGAATTTCGGGGCAATCACATCCGTGATCCAGGATATCTACGCACAGCTGGACGCAATCCAGGCTGATGCA
CAGGTGGACAGGTTGATCACAGGCCGCCTGAGCTCTCTGAGCGTGCTGGCATCCGCAAAACAGAGCGAGTAC
ATCAGGGTGTCTCAGCAGAGAGAGCTGGCTACTAAGAAGATCAACGAATGCGTGAAGAGCCAGAGCAATAGA
TACGGATTCTGCGGCTCCGGAAGGCACGTGCTGAGCATCCCCCAGAACGCCCCCAACGGCATTGTGTTCATTC

ACTTTACATACACTCCCGAGAGCTTCGTGAACGTGACCGCTATTGTGGGATTCTGTGTGAACCCCGCTAACGCC
TCTCAGTACGCAATTGTGCCTGCTAACGGGAGAGGCGTGTTCATTCAGGTGAACGGAAGCTATTACATTACCG
CCAGAGATATGTACATGCCTCGCGACATCACTGCTGGCGATATCGTGACACTGACCTCTTGCCAGGCTAATTA
CGTGAACGTGAACAAAACTGTGATTAACACCTTCGTGGAGGATGATGATTTTAACTTCAACGATGAGCTGAGC
AAATGGTGGAATGACACCAAGCATGAACTCCCAGACTTTGATGAGTTCAACTACACAGTGCCCGTGCTGAACA
TCAGTAACGAGATTGACAGAATCCAGGAAGTGATCCAGGGCCTGAACGACAGCCTGATCGATCTGGAGACCC
TGAGCATTCTGAAGACCTACATCAAGTGGCCCTGGTACGTGTGGCTGGCTATCTTCTTTGCTATCATCATCTTC
ATCCTGATTCTGGGGTGGGTGTTCTTTATGACCGGGTGCTGCGGATGCTGCTGCGGCTGCTTTGGAATCATCCC
ACTGATGAGTAAGTGCGGCAAGAAGAGCAGCTACTACACCACATTTGATAATGATGTGGTGACTGAGCAGTA
TAGACCAAAGAAGAGCGTG**TGA***CTCGAG*CGG

Spike amino acid sequence (Protein ID AKC34133.1):

MLVKSLFLVTILCALCSANLFDSDNNYVYYYQSAFRPPNGWHLQGGAYAVVNSTNHTSNAGSAQGCTVGVIKDV
YNQSVASIAMTAPLQGMAWFCTAYCNFSDTTVFVTHCYHIRISAMKNGSLFYNLTVSVSKYPNFKSFQCVNNFTSV
YLNGDLVFTSNKTTDVTSAGVYFKAGGPVNYSIMKEFKVLAYFVNGTAQDVILCDNSPKGLLACQYNTGNFSDGF
YPFTNSTLVREKFIVYRESSFNTTLALTNFTFTNVSNAQPNSGGVNTFHLYQTQTAQSGYYNFNLSFLSQFVYKASD
FMYGSYHPSCSFRPETINSGLWFNSLSVSLTYGPLQGGCKQSVFSGKATCCYAYSYKGPMACKGVYSGELRTNFEC
GLLVYVTKSDGSRIQTRTEPLVLTQYNYNNITLDKCVAYNIYGRVGQGFITNVTDSAANFSYLADGGLAILDTSGAI
DVFVVQGIYGLNYYKVNPCEDVNQQFVVSGGNIVGILTSRNETGSEQVENQFYVKLTNSSHRRRRSIGQNVTSCPY
VSYGRFCIEPDGSLKMIVPEELKQFVAPLLNITESVLIPNSFNLTVTDEYIQTRMDKVQINCLQYVCGNSLECRKLFQ
QYGPVCDNILSVVNSVSQKEDMELLSFYSSTKPKGYDTPVLSNVSTGEFNISLLLKTPISSSGRSFIEDLLFTSVETVG
LPTDAEYKKCTAGPLGTLKDLICAREYNGLLVLPPIITADMQTMYTASLVGAMAFGGITSAAAIPFATQIQARINHL
GITQSLLMKNQEKIAASFNKAIGHMQEGFRSTSLALQQIQDVVNKQSAILTETMNSLNKNFGAITSVIQDIYAQLDAI
QADAQVDRLITGRLSSLSVLASAKQSEYIRVSQQRELATKKINECVKSQSNRYGFCGSGRHVLSIPQNAPNGIVFIHF
TYTPESFVNVTAIVGFCVNPANASQYAIVPANGRGVFIQVNGSYYITARDMYMPRDITAGDIVTLTSCQANYVNVN
KTVINTFVEDDDFNFNDELSKWWNDTKHELPDFDEFNYTVPVLNISNEIDRIQEVIQGLNDSLIDLETLSILKTYIKW
PWYVWLAIFFAIIIFILILGWVFFMTGCCGCCCGCFGIIPLMSKCGKKSSYYTTFDNDVVTEQYRPKKSV

Chicken codon optimised Nucleocapsid gene with *Age*I and *Xho*I sites in italics (N- and C-terminal, respectively) and the Kozak region underlined:

GGG*ACCGGT*GCCACC**ATG**GCTAGCAGCAAGGCAACAGGCAAAACAGATGCTCCAGCACCTATTATCAAACTG
GGAGGACCTAAACCACCTAAAGTGGGCAGCAGCGGCAACGCATCTTGGTTCCAGCCAATCAAGGCCAAAAAG
CTGAACAGCCCACAGCCAAAGTTCGAAGGAAGCGGGGTGCCAGATAATGAAAACCTGAAACTGAGCCAGCAG
CATGGGTACTGGAGAAGGCAGGCAAGATACAAACCCGGAAAAGGAGGAAGGAAACCAGTTCCAGATGCTTG
GTACTTTTACTATACCGGCACAGGACCCGCTGCAGATCTGAACTGGGGCGAGAATCAGGATGGAATTGTGTGG
GTTGCTGCTAAGGGAGCAGATACAAAAAGTAGAAGCAACCAGGGCACAAGAGATCCTGATAAGTTTGATCAG
TACCCCCTGAGGTTTTCTGATGGAGGCCCCGACGGCAACTTCAGATGGGACTTCATCCCAATTAACAGAGGCA
GATCCGGCCGCAGCACTGCTGCCTCTAGCGCTGCATCTAGCAGAGCCCCATCAAGAGAAGGTTCTAGGGGACG
CAGATCCGGAGCCGAGGATGATCTGATTGCTAGAGCAGCTAAAATCATTCAGGACCAGCAGAAAAAGGGCGC
TAGAATCACAAAAGCTAAGGCTGATGAAATGGCTCATAGGAGGTATTGCAAGAGAACAATTCCACCAGGCTA

TAAGGTGGATCAGGTGTTCGGACCAAGGACCAAAGGTAAAGAGGGAAATTTTGGAGATGATAAAATGAATGA
GGAAGGAATCAGAGATGGAAGAGTTACAGCAATGCTGAACCTGGTGCCAAGCTCACATGCATGCCTGTTCGG
TTCCAGGGTGACACCCAAGTTGCAGCCCGATGGACTGCACCTGAGATTTGAGTTTACAACTGTGGTGCCTAGA
GATGATCCACAGTTTGATAACTACGTGAAAATTTGTGATCAGTGCGTGGATGGAGTGGGAACAAGACCTAAA
GATGATGAACCAAGACCTAAAAGCAGGCCAAATAGTCGCCCTGCCACTAGAGGAAACAGCCCTGCTCCTAAG
CAGCAGAGGCCTAAGAAGGAGAAGAAACCTAAAAAACAGGATGATGAGGTGGATAAGGCTCTGACAAGCGA
TGAGGAAAGGAACAATGCCCAGCTGGAATTCGATGATGAGCCCAAAGTGATCAACTGGGGCGATAGCGCCCT
GGGCGAGAACGAGCTG**TGA***CTCGAG*GGATCCGGG

Nucleocapsid amino acid sequence (Protein ID AKC34140.1):

MASSKATGKTDAPAPIIKLGGPKPPKVGSSGNASWFQPIKAKKLNSPQPKFEGSGVPDNENLKLSQQHGYWRRQAR
YKPGKGGRKPVPDAWYFYYTGTGPAADLNWGENQDGIVWVAAKGADTKSRSNQGTRDPDKFDQYPLRFSDGGP
DGNFRWDFIPINRGRSGRSTAASSAASSRAPSREGSRGRRSGAEDDLIARAAKIIQDQQKKGARITKAKADEMAHRR
YCKRTIPPGYKVDQVFGPRTKGKEGNFGDDKMNEEGIRDGRVTAMLNLVPSSHACLFGSRVTPKLQPDGLHLRFEF
TTVVPRDDPQFDNYVKICDQCVDGVGTRPKDDEPRPKSRPNSRPATRGNSPAPKQQRPKKEKKPKKQDDEVDKAL
TSDEERNNAQLEFDDEPKVINWGDSALGENEL

Chicken codon optimised Membrane gene with *Age*I and *Xho*I sites in italics (N- and C-terminal, respectively):

CGC*ACCGGT***ATG**GTGGAGAACCTGACCATCAGAAACTGGAACAGACTGAGCCTGACAAGCAGCCAGAGAACA
GTGGGAATCATCAAGACACTGCAGTTCTTTAAAATGAGCAACGGCACAGAGAACTGTACCCTGAACACAGAG
CAGGCTGTGCAGCTGTTTAAAGAATACAACCTGTTTATTACAGCTTTCCTGCTGTTTCTGACAATCCTGCTGCA
GTACGGATACGCCACAAGAAGCAGATTCATCTACATCCTGAAGATGGTGGTGCTGTGGTGCTTCTGGCCACTG
AACATTGCTGTGGGCGTGATTAGCTGCATCTACCCTCCTAATACTGGAGGCCTGGTGGCAGCTATCATCCTGAC
AGTGTTCGCTTGCCTGAGCTTCATCGGCTACTGGATCCAGTCTATTAGACTGTTTAAAAGGTGCAGAAGCTGGT
GGAGCTTTAATCCAGAGAGCAACGCTGTGGGAAGCATCCTGCTGACAAACGGCCAGCAGTGCAACTTCGCAA
TCGAGAGCGTGCCCATGGTGCTGTCACCCATTATCAAGAACGGAGCCCTGTATTGCGAGGGACAGTGGCTGGC
TAAATGCGAACCCGATCACCTGCCTAAAGACATCTTCGTGTGCACACCAGATAGAAGAAACATCTACAGAATG
GTGCAGAAGTACACCGGAGATCAGAGCGGCAACAAGAAGAGATTTGCCACATTTGTGTACGCTAAGCAGAGC
GTGGATACAGGAGAGCTGGAGAGCGTGACAACAGCTGGAAGCAACCTGTACACA**TGA***CTCGAG*CGG

Membrane amino acid sequence (Protein ID AKC34136.1):

MVENLTIRNWNRLSLTSSQRTVGIIKTLQFFKMSNGTENCTLNTEQAVQLFKEYNLFITAFLLFLTILLQYGYATRSR
FIYILKMVVLWCFWPLNIAVGVISCIYPPNTGGLVAAIILTVFACLSFIGYWIQSIRLFKRCRSWWSFNPESNAVGSIL
LTNGQQCNFAIESVPMVLSPIIKNGALYCEGQWLAKCEPDHLPKDIFVCTPDRRNIYRMVQKYTGDQSGNKKRFAT
FVYAKQSVDTGELESVTTAGSNLYT

Chicken codon optimised Envelope gene with *Age*I and *Xho*I sites in italics (N- and C-terminal, respectively):

CGC*ACCGGT***ATG**ATGAGCCTGCTGAACAAGAGCCTGGAGGAGAACGGAAGCTTCCTGACAGCTCTGTACATCT
TCGTGGCTTGCGTGGCTCTGTACCTGCTGGGAAGAGCTCTGCAGGCCTTTGTGCAGGCTGCTGATGCTTGCTGC
CTGTTTTGGTACACATGGGTGCTGGTGCCAGGAGCCAAAGGAACAGCTTTTGTGTACAAACACACATACGGAA
GAAAGCTGAACAACCCAGAGCTGGAGCAAGTGATCTTCAACGAGTTTCCAAAAAACGGATGGAACAACAAAA
ACCCAGCTATTTTTCAGGATGTGGAAAGACACGGAAAACTGCACAGC**TGA***CTCGAG*CGG

Envelope amino acid sequence (Protein ID AKC34135.1):

MMSLLNKSLEENGSFLTALYIFVACVALYLLGRALQAFVQAADACCLFWYTWVLVPGAKGTAFVYKHTYGRKLN
NPELEQVIFNEFPKNGWNNKNPAIFQDVERHGKLHS

Recombinant Spike Gene Sequences:

rIBV-S-IAV-TM gene:

GAC*ACCGGT***ATG**CTGGTGAAGAGCCTGTTTCTGGTGACCATTCTGTGCGCCCTGTGCAGCGCTAATCTGTTTGA
TAGCGATAATAACTACGTGTACTACTACCAGAGCGCCTTCAGGCCTCCCAATGGCTGGCACCTGCAGGGAGGA
GCTTACGCAGTGGTGAACAGCACCAACCACACCTCTAATGCCGGAAGCGCTCAGGGCTGCACCGTGGGAGTG
ATCAAGGACGTGTACAACCAGAGTGTGGCTAGTATCGCTATGACAGCCCCACTGCAGGGAATGGCTTGGTTTT
GCACAGCCTACTGCAACTTTAGCGATACAACAGTCTTTGTGACACACTGCTACCACATTAGAATCTCAGCCAT
GAAAAATGGAAGCCTGTTCTATAACCTGACCGTGAGCGTGAGTAAGTATCCTAATTTTAAATCTTTTCAGTGC
GTGAATAACTTTACCAGCGTGTACCTGAACGGCGATCTGGTGTTTACCTCTAACAAAACCACTGATGTGACAA
GTGCAGGAGTTTATTTTAAGGCCGGGGGCCCCGTGAATTACTCTATCATGAAGGAGTTTAAAGTGCTCGCCTA
CTTTGTGAATGGAACAGCACAGGATGTGATCCTGTGCGACAATAGCCCTAAGGGCCTGCTGGCTTGCCAGTAT
AACACAGGAAACTTTTCCGATGGCTTCTATCCTTTCACGAACAGTACACTGGTGAGGGAAAAGTTTATTGTGT
ACAGAGAGAGCAGCTTTAACACTACCCTGGCACTGACTAACTTCACTTTTACCAACGTGAGTAACGCTCAGCC
CAACAGCGGCGGAGTGAATACATTTCACCTGTACCAGACCCAGACCGCTCAGAGTGGCTACTATAATTTCAAC
CTGAGTTTTCTGTCCCAGTTTGTGTACAAGGCCTCTGATTTCATGTACGGCAGCTACCATCCCTCCTGCTCCTTT
AGGCCCGAAACAATTAATAGTGGACTGTGGTTCAACTCCCTGAGCGTGAGCCTGACCTACGGCCCCCTGCAGG
GCGGCTGCAAGCAGTCTGTGTTTAGCGGCAAGGCCACCTGCTGCTACGCCTACAGCTACAAAGGCCCCATGGC
ATGCAAGGGCGTGTACAGCGGCGAACTGAGGACCAATTTTGAATGCGGGCTGCTGGTGTATGTCACCAAATCT
GATGGCAGCAGAATCCAGACAAGAACCGAGCCTCTGGTGCTGACACAGTATAACTACAATAACATTACACTG
GATAAGTGCGTGGCTTACAATATCTACGGCAGGGTGGGACAGGGCTTCATCACTAACGTGACAGATAGCGCC
GCCAATTTTAGTTACCTGGCCGATGGCGGACTCGCTATCCTGGACACATCCGGAGCCATCGATGTGTTCGTGGT
GCAGGGAATCTACGGACTGAACTACTACAAAGTGAACCCATGCGAGGACGTGAACCAGCAGTTTGTGGTGAG
TGGAGGCAACATCGTGGGTATTCTGACCAGCAGGAATGAGACAGGAAGCGAGCAGGTGGAAAACCAGTTCTA
CGTGAAGCTGACAAACAGCTCCCACAGGAGGAGGAGAAGCATCGGACAGAACGTGACAAGCTGCCCTTACGT
GAGCTATGGCAGATTTTGCATTGAGCCAGATGGCAGCCTGAAGATGATCGTGCCCGAAGAGCTGAAGCAGTTC

GTGGCTCCACTGCTGAACATTACTGAGAGCGTGCTGATCCCCAACAGCTTTAACCTTACCGTGACAGATGAGT
ACATCCAGACAAGGATGGATAAGGTGCAGATTAACTGTCTGCAGTACGTTTGCGGCAATTCACTGGAGTGTCG
AAAGCTGTTTCAGCAGTACGGTCCGGTGTGTGACAACATCCTGTCTGTGGTGAACAGCGTGTCACAGAAAGAA
GACATGGAACTGCTGAGCTTCTATAGCTCAACCAAGCCTAAAGGCTACGACACCCCCGTGCTGAGCAACGTGA
GCACCGGCGAGTTTAACATCTCACTCCTGCTGAAGACCCCAATCAGCTCCTCAGGGAGATCTTTCATCGAGGA
CCTGCTGTTCACTAGCGTGGAGACAGTGGGTCTCCCTACTGACGCCGAATACAAGAAGTGCACCGCTGGCCCA
CTGGGCACCCTGAAGGATCTGATCTGCGCTAGAGAGTACAACGGGCTGCTCGTGCTGCCCCCTATCATTACCG
CTGATATGCAGACAATGTACACCGCTAGCCTGGTGGGGGCCATGGCATTTGGGGGGATTACAAGTGCTGCCGC
CATCCCATTTGCCACACAGATTCAGGCTAGAATTAACCACCTGGGAATTACCCAGTCTCTGCTGATGAAAAAC
CAGGAGAAAATCGCTGCCTCTTTTAACAAAGCAATCGGACACATGCAGGAAGGTTTTAGGAGCACCAGCCTC
GCTCTGCAGCAGATTCAGGACGTGGTGAACAAGCAGAGCGCCATCCTCACAGAGACAATGAATTCCCTGAAC
AAGAACTTCGGCGCTATTACTAGCGTGATCCAGGATATCTATGCTCAGCTCGATGCCATCCAGGCAGATGCAC
AGGTGGATAGGACCGGAAGACTGAGCTCACTGAGCGTGCTGGCTAGCGCTAAGCAGAGCGAGTACATCAGGG
TGAGCCAGCAGAGAGAGCTGGCAACCAAGAAAATTAACGAGTGTGTGAAGAGCCAGAGTAATCGCTACGGGT
TCTGCGGGTCCGGAAGACATGTGCTGAGCATTCCCCAGAACGCACCCAATGGCATTGTGTTCATTCACTTCAC
CTACACTCCCGAGAGCTTTGTGAACGTGACAGCAATCGTGGGATTTTGCGTGAATCCCGCCAATGCATCCCAG
TATGCCATTGTGCCCGCTAACGGGAGAGGAGTGTTCATCCAGGTGAACGGCTCCTACTACATCACCGCTAGAG
ATATGTACATGCCCAGAGATATCACCGCCGGGGATATCGTCACTCTGACTAGCTGTCAGGCTAACTACGTGAA
CGTGAACAAGACTGTGATTAACACATTCGTGGAAGACGATGATTTTAACTTCAACGACGAGCTTAGTAAGTGG
TGGAACGATACTAAGCACGAGCTGCCTGATTTTGATGAATTCAACTACACTGTGCCCGTGCTGAACATTAGCA
ATGAGATCGATAGAATCCAAGAGGTCATCCAGGGGCTGAACGATAGCCTGATCGATCTTGAGACACTGAGCA
TACTGAAGACATACATCAAGTGGCCCCTGGCTATCTATAGTACCGTGAGTAGCTCACTGGTGCTGGTGGGCCT
GATTATCGCAATGGGACTGTGGATGACAGGCTGCTGCGGATGCTGCTGCGGGTGCTTCGGCATCATCCCCCTG
ATGAGCAAGTGCGGAAAGAAGAGCAGCTACTACACAACATTCGATAACGATGTGGTGACCGAGCAGTACAGA
CCTAAGAAAAGCGTG**TGA***CTCGAG*CAA

rIBV-S-IAV-**TM** amino acid sequence:

MLVKSLFLVTILCALCSANLFDSDNNYVYYYQSAFRPPNGWHLQGGAYAVVNSTNHTSNAGSAQGCTVGVIKDV
YNQSVASIAMTAPLQGMAWFCTAYCNFSDTTVFVTHCYHIRISAMKNGSLFYNLTVSVSKYPNFKSFQCVNNFTSV
YLNGDLVFTSNKTTDVTSAGVYFKAGGPVNYSIMKEFKVLAYFVNGTAQDVILCDNSPKGLLACQYNTGNFSDGF
YPFTNSTLVREKFIVYRESSFNTTLALTNFTFTNVSNAQPNSGGVNTFHLYQTQTAQSGYYNFNLSFLSQFVYKASD
FMYGSYHPSCSFRPETINSGLWFNSLSVSLTYGPLQGGCKQSVFSGKATCCYAYSYKGPMACKGVYSGELRTNFEC
GLLVYVTKSDGSRIQTRTEPLVLTQYNYNNITLDKCVAYNIYGRVGQGFITNVTDSAANFSYLADGGLAILDTSGAI
DVFVVQGIYGLNYYKVNPCEDVNQQFVVSGGNIVGILTSRNETGSEQVENQFYVKLTNSSHRRRRSIGQNVTSCPY
VSYGRFCIEPDGSLKMIVPEELKQFVAPLLNITESVLIPNSFNLTVTDEYIQTRMDKVQINCLQYVCGNSLECRKLFQ
QYGPVCDNILSVVNSVSQKEDMELLSFYSSTKPKGYDTPVLSNVSTGEFNISLLLKTPISSSGRSFIEDLLFTSVETVG
LPTDAEYKKCTAGPLGTLKDLICAREYNGLLVLPPIITADMQTMYTASLVGAMAFGGITSAAAIPFATQIQARINHL
GITQSLLMKNQEKIAASFNKAIGHMQEGFRSTSLALQQIQDVVNKQSAILTETMNSLNKNFGAITSVIQDIYAQLDAI
QADAQVDRTGRLSSLSVLASAKQSEYIRVSQQRELATKKINECVKSQSNRYGFCGSGRHVLSIPQNAPNGIVFIHFT
YTPESFVNVTAIVGFCVNPANASQYAIVPANGRGVFIQVNGSYYITARDMYMPRDITAGDIVTLTSCQANYVNVNK
TVINTFVEDDDFNFNDELSKWWNDTKHELPDFDEFNYTVPVLNISNEIDRIQEVIQGLNDSLIDLETLSILKTYIKWP
LAIYSTVSSSLVLVGLIIAMGLWMTGCCGCCCGCFGIIPLMSKCGKKSSYYTTFDNDVVTEQYRPKKSV

rIBV-S-IAV-TM/CT gene:

GAC*ACCGGT***ATG**CTGGTGAAGAGCCTGTTCCTGGTGACTATCCTGTGCGCCCTGTGCAGCGCTAACCTGTTCGA
TTCTGATAACAATTACGTGTATTACTACCAGTCTGCCTTTAGACCACCTAACGGCTGGCACCTGCAGGGAGGA
GCCTACGCCGTGGTGAACAGCACAAACCACACCAGCAACGCCGGATCTGCTCAGGGCTGCACAGTGGGAGTG
ATTAAGGATGTGTACAACCAGTCAGTGGCTTCCATCGCCATGACCGCCCCTCTGCAGGGCATGGCTTGGTTTTG
CACCGCCTACTGCAACTTTAGCGATACCACTGTGTTCGTGACACACTGCTACCACATTCGCATTAGCGCCATGA
AGAACGGGAGCCTGTTTTATAACCTGACAGTGTCAGTGTCTAAATACCCTAACTTTAAGTCCTTCCAGTGCGTG
AACAATTTTACTAGCGTGTACCTGAACGGAGACCTGGTGTTCACTTCAAATAAGACTACTGATGTGACTAGCG
CAGGAGTTTACTTTAAAGCAGGAGGCCCTGTGAATTACTCAATAATGAAGGAGTTTAAAGTCCTGGCCTACTT
CGTGAATGGAACAGCCCAGGACGTGATCCTGTGCGATAACTCCCCCAAGGGCCTGCTGGCCTGTCAGTACAAC
ACCGGAAACTTTAGCGATGGCTTCTACCCCTTTACCAACTCAACCCTTGTGAGGGAGAAGTTTATCGTGTACA
GGGAATCTAGCTTCAACACCACTCTGGCTCTGACCAACTTCACCTTTACAAACGTGAGCAACGCCCAGCCAAA
CTCCGGAGGAGTGAACACTTTCCACCTGTATCAGACACAGACCGCCCAGAGCGGATACTACAACTTCAACCTG
TCCTTCCTGAGCCAATTTGTGTACAAAGCCTCCGATTTCATGTACGGATCATATCATCCCTCTTGCAGCTTTAG
ACCTGAGACCATCAACAGCGGACTGTGGTTCAATTCTCTGTCAGTCTCTCTGACCTACGGACCCCTCCAGGGC
GGGTGCAAGCAGTCCGTGTTTAGCGGCAAGGCAACATGCTGCTACGCCTACAGCTACAAGGGACCCATGGCCT
GCAAAGGCGTGTATTCCGGAGAGCTGAGAACCAACTTCGAATGTGGACTGCTGGTTTACGTGACCAAGAGCG
ATGGCAGCAGAATCCAGACCAGAACCGAGCCTCTCGTGCTGACACAGTACAATTACAACAACATTACACTGG
ATAAATGCGTGGCCTACAACATCTACGGGAGGGTCGGCCAGGGCTTCATCACAAACGTGACTGATAGCGCTGC
AAACTTTAGCTACCTGGCCGATGGCGGCCTGGCCATCCTGGATACCAGCGGAGCCATTGACGTGTTTGTGGTG
CAGGGAATCTACGGGCTGAACTACTACAAAGTGAACCCCTGCGAGGATGTGAACCAGCAGTTCGTTGTGAGC
GGGGGAAACATCGTGGGGATTCTGACATCCCGCAATGAGACTGGCAGCGAACAGGTTGAGAATCAGTTCTAC
GTCAAGCTCACAAATTCCAGCCACAGACGGAGGCGCTCCATTGGCCAGAATGTGACAAGCTGTCCCTACGTGA
GCTACGGCAGGTTTTGCATTGAGCCAGATGGCAGCCTGAAAATGATTGTGCCTGAGGAACTGAAACAGTTCGT
GGCTCCTCTGCTGAACATCACAGAGTCCGTGCTGATTCCAAATTCCTTTAACCTGACTGTTACTGACGAGTACA
TCCAGACCAGAATGGATAAGGTGCAGATCAACTGCCTGCAGTACGTGTGCGGTAACTCCCTGGAGTGCAGGA
AGCTGTTCCAGCAGTACGGCCCCGTGTGTGATAACATTCTGTCAGTGGTGAACTCAGTGAGTCAGAAAGAGGA
CATGGAGCTGCTCAGCTTTTACTCTTCCACCAAGCCAAAGGGGTACGATACTCCCGTGCTGTCTAATGTGAGC
ACAGGCGAGTTCAACATTTCCCTGCTGCTGAAGACTCCAATTTCTAGCAGCGGCCGGAGCTTTATTGAGGATC
TGCTGTTTACTAGTGTGGAGACTGTGGGACTGCCCACAGACGCCGAGTACAAGAAGTGCACCGCCGGGCCACT
GGGGACCCTGAAAGACTTGATTTGCGCAAGAGAGTACAACGGCCTGCTGGTGCTGCCACCCATCATTACAGCC
GACATGCAGACAATGTACACAGCATCTCTGGTGGGGGCAATGGCCTTTGGAGGCATCACCTCCGCTGCCGCTA
TTCCATTTGCAACACAGATCCAGGCAAGGATAAACCACCTGGGCATTACCCAGAGTCTGCTGATGAAGAACCA
GGAGAAAATCGCCGCTAGCTTTAACAAGGCTATTGGACACATGCAGGAGGGCTTTAGGAGCACTTCTCTGGCC
CTGCAGCAGATACAGGACGTGGTTAACAAGCAGAGCGCCATCCTGACTGAGACCATGAATAGCCTGAACAAA
AACTTTGGAGCCATTACTTCTGTGATCCAGGACATCTACGCACAGCTGGACGCCATCCAGGCCGATGCACAGG
TGGATCGGCTGATCACAGGCAGACTGAGCTCCCTGAGCGTGCTGGCCAGCGCTAAGCAGAGCGAATACATCA
GGGTGAGCCAGCAGAGGGAGCTGGCTACTAAGAAGATTAACGAATGCGTGAAAAGCCAGTCAAATAGATACG
GCTTTTGCGGCTCAGGCAGACACGTGCTGAGCATCCCACAGAATGCACCTAACGGCATCGTGTTCATTCACTTT
ACCTACACCCCAGAGTCTTTCGTGAACGTGACCGCTATTGTGGGGTTCTGCGTGAACCCAGCCAACGCCAGCC
AGTACGCCATCGTGCCCGCAAACGGAAGAGGAGTGTTTATCCAGGTGAACGGCAGCTACTACATCACCGCAA
GAGATATGTATATGCCACGGGACATCACAGCTGGCGACATCGTGACACTGACCAGCTGCCAGGCTAACTACGT
GAATGTGAACAAGACTGTGATTAACACCTTTGTGGAAGATGATGATTTCAACTTCAATGACGAGCTGAGCAAG
TGGTGGAACGATACTAAGCATGAACTGCCCGACTTTGATGAGTTTAACTACACAGTGCCCGTGCTGAACATTA

GCAACGAGATTGATAGGATCCAGGAAGTGATCCAGGGCCTGAATGATTCACTGATCGATCTGGAGACCCTGA
GCATCCTGAAGACATACATTAAGTGGCCCCTGGCCATCTACAGCACCGTGAGCAGCAGCCTGGTGCTGGTGGG
ACTGATCATCGCTATGGGACTGTGGATGTGCTCTAACGGTAGCATGCAGTGTAGAGTGTGCATC**TGA***CTCGAG*
CTA

rIBV-S-IAV-**TM**/*CT* amino acid sequence:

MLVKSLFLVTILCALCSANLFDSDNNYVYYYQSAFRPPNGWHLQGGAYAVVNSTNHTSNAGSAQGCTVGVIKDV
YNQSVASIAMTAPLQGMAWFCTAYCNFSDTTVFVTHCYHIRISAMKNGSLFYNLTVSVSKYPNFKSFQCVNNFTSV
YLNGDLVFTSNKTTDVTSAGVYFKAGGPVNYSIMKEFKVLAYFVNGTAQDVILCDNSPKGLLACQYNTGNFSDGF
YPFTNSTLVREKFIVYRESSFNTTLALTNFTFTNVSNAQPNSGGVNTFHLYQTQTAQSGYYNFNLSFLSQFVYKASD
FMYGSYHPSCSFRPETINSGLWFNSLSVSLTYGPLQGGCKQSVFSGKATCCYAYSYKGPMACKGVYSGELRTNFEC
GLLVYVTKSDGSRIQTRTEPLVLTQYNYNNITLDKCVAYNIYGRVGQGFITNVTDSAANFSYLADGGLAILDTSGAI
DVFVVQGIYGLNYYKVNPCEDVNQQFVVSGGNIVGILTSRNETGSEQVENQFYVKLTNSSHRRRRSIGQNVTSCPY
VSYGRFCIEPDGSLKMIVPEELKQFVAPLLNITESVLIPNSFNLTVTDEYIQTRMDKVQINCLQYVCGNSLECRKLFQ
QYGPVCDNILSVVNSVSQKEDMELLSFYSSTKPKGYDTPVLSNVSTGEFNISLLLKTPISSSGRSFIEDLLFTSVETVG
LPTDAEYKKCTAGPLGTLKDLICAREYNGLLVLPPIITADMQTMYTASLVGAMAFGGITSAAAIPFATQIQARINHL
GITQSLLMKNQEKIAASFNKAIGHMQEGFRSTSLALQQIQDVVNKQSAILTETMNSLNKNFGAITSVIQDIYAQLDAI
QADAQVDRLITGRLSSLSVLASAKQSEYIRVSQQRELATKKINECVKSQSNRYGFCGSGRHVLSIPQNAPNGIVFIHF
TYTPESFVNVTAIVGFCVNPANASQYAIVPANGRGVFIQVNGSYYITARDMYMPRDITAGDIVTLTSCQANYVNVN
KTVINTFVEDDDFNFNDELSKWWNDTKHELPDFDEFNYTVPVLNISNEIDRIQEVIQGLNDSLIDLETLSILKTYIKW
P**LAIYSTVSSSLVLVGLIIAMGLW***MCSNGSMQCRVCI*

mIBV-S-KKSV gene:

ATGGGCTGGAGCTGGATTTTTCTGTTTCTGCTGAGCGGCGCGGCGGGCGTGCATTGCAACCTGTTTGATAGCG
ATAACAACTATGTGTATTATTATCAGAGCGCGTTTCGCCCGCCGAACGGCTGGCATCTGCAGGGCGGCGCGTA
TGCGGTGGTGAACAGCACCAACCATACCAGCAACGCGGGCAGCGCGCAGGGCTGCACCGTGGGCGTGATTAA
AGATGTGTATAACCAGAGCGTGGCGAGCATTGCGATGACCGCGCCGCTGCAGGGCATGGCGTGGTTTTGCACC
GCGTATTGCAACTTTAGCGATACCACCGTGTTTGTGACCCATTGCTATCATATTCGCATTAGCGCGATGAAAAA
CGGCAGCCTGTTTTATAACCTGACCGTGAGCGTGAGCAAATATCCGAACTTTAAAAGCTTTCAGTGCGTGAAC
AACTTTACCAGCGTGTATCTGAACGGCGATCTGGTGTTTACCAGCAACAAAACCACCGATGTGACCAGCGCGG
GCGTGTATTTTAAAGCGGGCGGCCCGGTGAACTATAGCATTATGAAAGAATTTAAAGTGCTGGCGTATTTTGT
GAACGGCACCGCGCAGGATGTGATTCTGTGCGATAACAGCCCGAAAGGCCTGCTGGCGTGCCAGTATAACAC
CGGCAACTTTAGCGATGGCTTTTATCCGTTTACCAACAGCACCCTGGTGCGCGAAAAATTTATTGTGTATCGCG
AAAGCAGCTTTAACACCACCCTGGCGCTGACCAACTTTACCTTTACCAACGTGAGCAACGCGCAGCCGAACAG
CGGCGGCGTGAACACCTTTCATCTGTATCAGACCCAGACCGCGCAGAGCGGCTATTATAACTTTAACCTGAGC
TTTCTGAGCCAGTTTGTGTATAAAGCGAGCGATTTTATGTATGGCAGCTATCATCCGAGCTGCAGCTTTCGCCC
GGAAACCATTAACAGCGGCCTGTGGTTTAACAGCCTGAGCGTGAGCCTGACCTATGGCCCGCTGCAGGGCGGC
TGCAAACAGAGCGTGTTTAGCGGCAAAGCGACCTGCTGCTATGCGTATAGCTATAAAGGCCCGATGGCGTGCA
AAGGCGTGTATAGCGGCGAACTGCGCACCAACTTTGAATGCGGCCTGCTGGTGTATGTGACCAAAAGCGATG
GCAGCCGCATTCAGACCCGCACCGAACCGCTGGTGCTGACCCAGTATAACTATAACAACATTACCCTGGATAA
ATGCGTGGCGTATAACATTTATGGCCGCGTGGGCCAGGGCTTTATTACCAACGTGACCGATAGCGCGGCGAAC

TTTAGCTATCTGGCGGATGGCGGCCTGGCGATTCTGGATACCAGCGGCGCGATTGATGTGTTTGTGGTGCAGG
GCATTTATGGCCTGAACTATTATAAAGTGAACCCGTGCGAAGATGTGAACCAGCAGTTTGTGGTGAGCGGCGG
CAACATTGTGGGCATTCTGACCAGCCGCAACGAAACCGGCAGCGAACAGGTGGAAAACCAGTTTTATGTGAA
ACTGACCAACAGCAGCCATCGCCGCCGCCGCAGCATTGGCCAGAACGTGACCAGCTGCCCGTATGTGAGCTAT
GGCCGCTTTTGCATTGAACCGGATGGCAGCCTGAAAATGATTGTGCCGGAAGAACTGAAACAGTTTGTGGCGC
CGCTGCTGAACATTACCGAAAGCGTGCTGATTCCGAACAGCTTTAACCTGACCGTGACCGATGAATATATTCA
GACCCGCATGGATAAAGTGCAGATTAACTGCCTGCAGTATGTGTGCGGCAACAGCCTGGAATGCCGCAAACT
GTTTCAGCAGTATGGCCCGGTGTGCGATAACATTCTGAGCGTGGTGAACAGCGTGAGCCAGAAAGAAGATAT
GGAACTGCTGAGCTTTTATAGCAGCACCAAACCGAAAGGCTATGATACCCCGGTGCTGAGCAACGTGAGCAC
CGGCGAATTTAACATTAGCCTGCTGCTGAAAACCCCGATTAGCAGCAGCGGCCGCAGCTTTATTGAAGATCTG
CTGTTTACCAGCGTGGAAACCGTGGGCCTGCCGACCGATGCGGAATATAAAAAATGCACCGCGGGCCCGCTG
GGCACCCTGAAAGATCTGATTTGCGCGCGCGAATATAACGGCCTGCTGGTGCTGCCGCCGATTATTACCGCGG
ATATGCAGACCATGTATACCGCGAGCCTGGTGGGCGCGATGGCGTTTGGCGGCATTACCAGCGCGGCGGCGAT
TCCGTTTGCGACCCAGATTCAGGCGCGCATTAACCATCTGGGCATTACCCAGAGCCTGCTGATGAAAAACCAG
GAAAAAATTGCGGCGAGCTTTAACAAAGCGATTGGCCATATGCAGGAAGGCTTTCGCAGCACCAGCCTGGCG
CTGCAGCAGATTCAGGATGTGGTGAACAAACAGAGCGCGATTCTGACCGAAACCATGAACAGCCTGAACAAA
AACTTTGGCGCGATTACCAGCGTGATTCAGGATATTTATGCGCAGCTGGATGCGATTCAGGCGGATGCGCAGG
TGGATCGCCTGATTACCGGCCGCCTGAGCAGCCTGAGCGTGCTGGCGAGCGCGAAACAGAGCGAATATATTC
GCGTGAGCCAGCAGCGCGAACTGGCGACCAAAAAAATTAACGAATGCGTGAAAAGCCAGAGCAACCGCTATG
GCTTTTGCGGCAGCGGCCGCCATGTGCTGAGCATTCCGCAGAACGCGCCGAACGGCATTGTGTTTATTCATTTT
ACCTATACCCCGGAAAGCTTTGTGAACGTGACCGCGATTGTGGGCTTTTGCGTGAACCCGGCGAACGCGAGCC
AGTATGCGATTGTGCCGGCGAACGGCCGCGGCGTGTTTATTCAGGTGAACGGCAGCTATTATATTACCGCGCG
CGATATGTATATGCCGCGCGATATTACCGCGGGCGATATTGTGACCCTGACCAGCTGCCAGGCGAACTATGTG
AACGTGAACAAAACCGTGATTAACACCTTTGTGGAAGATGATGATTTTAACTTTAACGATGAACTGAGCAAAT
GGTGGAACGATACCAAACATGAACTGCCGGATTTTGATGAATTTAACTATACCGTGCCGGTGCTGAACATTAG
CAACGAAATTGATCGCATTCAGGAAGTGATTCAGGGCCTGAACGATAGCCTGATTGATCTGGAAACCCTGAGC
ATTCTGAAAACCTATATTAAATGGCCGTGGTATGTGTGGCTGGCGATTTTTTTTGCGATTATTATTTTTATTCTG
ATTCTGGGCTGGGTGTTTTTTATGACCGGCTGCTGCGGCTGCTGCTGCGGCTGCTTTGGCATTATTCCGCTGAT
GAGCAAATGCGGC

mIBV-S-KKSV amino acid sequence:

MGWSWIFLFLLSGAAGVHCNLFDSDNNYVYYYQSAFRPPNGWHLQGGAYAVVNSTNHTSNAGSAQGCTVGVIK
DVYNQSVASIAMTAPLQGMAWFCTAYCNFSDTTVFVTHCYHIRISAMKNGSLFYNLTVSVSKYPNFKSFQCVNNF
TSVYLNGDLVFTSNKTTDVTSAGVYFKAGGPVNYSIMKEFKVLAYFVNGTAQDVILCDNSPKGLLACQYNTGNFS
DGFYPFTNSTLVREKFIVYRESSFNTTLALTNFTFTNVSNAQPNSGGVNTFHLYQTQTAQSGYYNFNLSFLSQFVYK
ASDFMYGSYHPSCSFRPETINSGLWFNSLSVSLTYGPLQGGCKQSVFSGKATCCYAYSYKGPMACKGVYSGELRTN
FECGLLVYVTKSDGSRIQTRTEPLVLTQYNYNNITLDKCVAYNIYGRVGQGFITNVTDSAANFSYLADGGLAILDTS
GAIDVFVVQGIYGLNYYKVNPCEDVNQQFVVSGGNIVGILTSRNETGSEQVENQFYVKLTNSSHRRRRSIGQNVTS
CPYVSYGRFCIEPDGSLKMIVPEELKQFVAPLLNITESVLIPNSFNLTVTDEYIQTRMDKVQINCLQYVCGNSLECRK
LFQQYGPVCDNILSVVNSVSQKEDMELLSFYSSTKPKGYDTPVLSNVSTGEFNISLLLKTPISSSGRSFIEDLLFTSVET
VGLPTDAEYKKCTAGPLGTLKDLICAREYNGLLVLPPIITADMQTMYTASLVGAMAFGGITSAAAIPFATQIQARIN
HLGITQSLLMKNQEKIAASFNKAIGHMQEGFRSTSLALQQIQDVVNKQSAILTETMNSLNKNFGAITSVIQDIYAQL
DAIQADAQVDRLITGRLSSLSVLASAKQSEYIRVSQQRELATKKINECVKSQSNRYGFCGSGRHVLSIPQNAPNGIVF

IHFTYTPESFVNVTAIVGFCVNPANASQYAIVPANGRGVFIQVNGSYYITARDMYMPRDITAGDIVTLTSCQANYVN
VNKTVINTFVEDDDFNFNDELSKWWNDTKHELPDFDEFNYTVPVLNISNEIDRIQEVIQGLNDSLIDLETLSILKTYI
KWPWYVWLAIFFAIIIFILILGWVFFMTGCCGCCCGCFGIIPLMSKCGKKSSYYTTFDNDVVTEQYRP

mIBV-S-IAV-TM-KKSV gene:

ACCGGTGCCACCATGGGATGGAGCTGGATCTTTCTTTTCCTCCTGTCAGGAGCTGCAGGTGTCCATTGCAATCT
GTTTGATAGCGATAATAACTACGTGTACTACTACCAGAGCGCCTTCAGGCCTCCCAATGGCTGGCACCTGCAG
GGAGGAGCTTACGCAGTGGTGAACAGCACCAACCACACCTCTAATGCCGGAAGCGCTCAGGGCTGCACCGTG
GGAGTGATCAAGGACGTGTACAACCAGAGTGTGGCTAGTATCGCTATGACAGCCCCACTGCAGGGAATGGCT
TGGTTTTGCACAGCCTACTGCAACTTTAGCGATACAACAGTCTTTGTGACACACTGCTACCACATTAGAATCTC
AGCCATGAAAAATGGAAGCCTGTTCTATAACCTGACCGTGAGCGTGAGTAAGTATCCTAATTTTAAATCTTTTC
AGTGCGTGAATAACTTTACCAGCGTGTACCTGAACGGCGATCTGGTGTTTACCTCTAACAAAACCACTGATGT
GACAAGTGCAGGAGTTTATTTTAAGGCCGGGGGCCCCGTGAATTACTCTATCATGAAGGAGTTTAAAGTGCTC
GCCTACTTTGTGAATGGAACAGCACAGGATGTGATCCTGTGCGACAATAGCCCTAAGGGCCTGCTGGCTTGCC
AGTATAACACAGGAAACTTTTCCGATGGCTTCTATCCTTTCACGAACAGTACACTGGTGAGGGAAAAGTTTAT
TGTGTACAGAGAGAGCAGCTTTAACACTACCCTGGCACTGACTAACTTCACTTTTACCAACGTGAGTAACGCT
CAGCCCAACAGCGGCGGAGTGAATACATTTCACCTGTACCAGACCCAGACCGCTCAGAGTGGCTACTATAATT
TCAACCTGAGTTTTCTGTCCCAGTTTGTGTACAAGGCCTCTGATTTCATGTACGGCAGCTACCATCCCTCCTGCT
CCTTTAGGCCCGAAACAATTAATAGTGGACTGTGGTTCAACTCCCTGAGCGTGAGCCTGACCTACGGCCCCCT
GCAGGGCGGCTGCAAGCAGTCTGTGTTTAGCGGCAAGGCCACCTGCTGCTACGCCTACAGCTACAAAGGCCCC
ATGGCATGCAAGGGCGTGTACAGCGGCGAACTGAGGACCAATTTTGAATGCGGGCTGCTGGTGTATGTCACCA
AATCTGATGGCAGCAGAATCCAGACAAGAACCGAGCCTCTGGTGCTGACACAGTATAACTACAATAACATTA
CACTGGATAAGTGCGTGGCTTACAATATCTACGGCAGGGTGGGACAGGGCTTCATCACTAACGTGACAGATAG
CGCCGCCAATTTTAGTTACCTGGCCGATGGCGGACTCGCTATCCTGGACACATCCGGAGCCATCGATGTGTTC
GTGGTGCAGGGAATCTACGGACTGAACTACTACAAAGTGAACCCATGCGAGGACGTGAACCAGCAGTTTGTG
GTGAGTGGAGGCAACATCGTGGGTATTCTGACCAGCAGGAATGAGACAGGAAGCGAGCAGGTGGAAAACCA
GTTCTACGTGAAGCTGACAAACAGCTCCCACAGGAGGAGGAGAAGCATCGGACAGAACGTGACAAGCTGCCC
TTACGTGAGCTATGGCAGATTTTGCATTGAGCCAGATGGCAGCCTGAAGATGATCGTGCCCGAAGAGCTGAAG
CAGTTCGTGGCTCCACTGCTGAACATTACTGAGAGCGTGCTGATCCCCAACAGCTTTAACCTTACCGTGACAG
ATGAGTACATCCAGACAAGGATGGATAAGGTGCAGATTAACTGTCTGCAGTACGTTTGCGGCAATTCACTGGA
GTGTCGAAAGCTGTTTCAGCAGTACGGTCCGGTGTGTGACAACATCCTGTCTGTGGTGAACAGCGTGTCACAG
AAAGAAGACATGGAACTGCTGAGCTTCTATAGCTCAACCAAGCCTAAAGGCTACGACACCCCCGTGCTGAGC
AACGTGAGCACCGGCGAGTTTAACATCTCACTCCTGCTGAAGACCCCAATCAGCTCCTCAGGGAGATCTTTCA
TCGAGGACCTGCTGTTCACTAGCGTGGAGACAGTGGGTCTCCCTACTGACGCCGAATACAAGAAGTGCACCGC
TGGCCCACTGGGCACCCTGAAGGATCTGATCTGCGCTAGAGAGTACAACGGGCTGCTCGTGCTGCCCCCTATC
ATTACCGCTGATATGCAGACAATGTACACCGCTAGCCTGGTGGGGGCCATGGCATTTGGGGGGATTACAAGTG
CTGCCGCCATCCCATTTGCCACACAGATTCAGGCTAGAATTAACCACCTGGGAATTACCCAGTCTCTGCTGATG
AAAAACCAGGAGAAAATCGCTGCCTCTTTTAACAAAGCAATCGGACACATGCAGGAAGGTTTTAGGAGCACC
AGCCTCGCTCTGCAGCAGATTCAGGACGTGGTGAACAAGCAGAGCGCCATCCTCACAGAGACAATGAATTCC
CTGAACAAGAACTTCGGCGCTATTACTAGCGTGATCCAGGATATCTATGCTCAGCTCGATGCCATCCAGGCAG
ATGCACAGGTGGATAGGACCGGAAGACTGAGCTCACTGAGCGTGCTGGCTAGCGCTAAGCAGAGCGAGTACA
TCAGGGTGAGCCAGCAGAGAGAGCTGGCAACCAAGAAAATTAACGAGTGTGTGAAGAGCCAGAGTAATCGCT
ACGGGTTCTGCGGGTCCGGAAGACATGTGCTGAGCATTCCCCAGAACGCACCCAATGGCATTGTGTTCATTCA

CTTCACCTACACTCCCGAGAGCTTTGTGAACGTGACAGCAATCGTGGGATTTTGCGTGAATCCCGCCAATGCA
TCCCAGTATGCCATTGTGCCCGCTAACGGGAGAGGAGTGTTCATCCAGGTGAACGGCTCCTACTACATCACCG
CTAGAGATATGTACATGCCCAGAGATATCACCGCCGGGGATATCGTCACTCTGACTAGCTGTCAGGCTAACTA
CGTGAACGTGAACAAGACTGTGATTAACACATTCGTGGAAGACGATGATTTTAACTTCAACGACGAGCTTAGT
AAGTGGTGGAACGATACTAAGCACGAGCTGCCTGATTTTGATGAATTCAACTACACTGTGCCCGTGCTGAACA
TTAGCAATGAGATCGATAGAATCCAAGAGGTCATCCAGGGGCTGAACGATAGCCTGATCGATCTTGAGACACT
GAGCATACTGAAGACATACATCAAGTGGCCCCTGGCTATCTATAGTACCGTGAGTAGCTCACTGGTGCTGGTG
GGCCTGATTATCGCAATGGGACTGTGGATGACAGGCTGCTGCGGATGCTGCTGCGGGTGCTTCGGCATCATCC
CCCTGATGAGCAAGTGCGGAAAGAAGAGCAGCTACTACACAACATTCGATAACGATGTGGTGACCGAGCAGT
ACAGACCTTGACTCGAG

mIBV-S-IAV-**TM**-KKSV amino acid sequence:

MGWSWIFLFLLSGAAGVHCNLFDSDNNYVYYYQSAFRPPNGWHLQGGAYAVVNSTNHTSNAGSAQGCTVGVIK
DVYNQSVASIAMTAPLQGMAWFCTAYCNFSDTTVFVTHCYHIRISAMKNGSLFYNLTVSVSKYPNFKSFQCVNNF
TSVYLNGDLVFTSNKTTDVTSAGVYFKAGGPVNYSIMKEFKVLAYFVNGTAQDVILCDNSPKGLLACQYNTGNFS
DGFYPFTNSTLVREKFIVYRESSFNTTLALTNFTFTNVSNAQPNSGGVNTFHLYQTQTAQSGYYNFNLSFLSQFVYK
ASDFMYGSYHPSCSFRPETINSGLWFNSLSVSLTYGPLQGGCKQSVFSGKATCCYAYSYKGPMACKGVYSGELRTN
FECGLLVYVTKSDGSRIQTRTEPLVLTQYNYNNITLDKCVAYNIYGRVGQGFITNVTDSAANFSYLADGGLAILDTS
GAIDVFVVQGIYGLNYYKVNPCEDVNQQFVVSGGNIVGILTSRNETGSEQVENQFYVKLTNSSHRRRRSIGQNVTS
CPYVSYGRFCIEPDGSLKMIVPEELKQFVAPLLNITESVLIPNSFNLTVTDEYIQTRMDKVQINCLQYVCGNSLECRK
LFQQYGPVCDNILSVVNSVSQKEDMELLSFYSSTKPKGYDTPVLSNVSTGEFNISLLLKTPISSSGRSFIEDLLFTSVET
VGLPTDAEYKKCTAGPLGTLKDLICAREYNGLLVLPPIITADMQTMYTASLVGAMAFGGITSAAAIPFATQIQARIN
HLGITQSLLMKNQEKIAASFNKAIGHMQEGFRSTSLALQQIQDVVNKQSAILTETMNSLNKNFGAITSVIQDIYAQL
DAIQADAQVDRTGRLSSLSVLASAKQSEYIRVSQQRELATKKINECVKSQSNRYGFCGSGRHVLSIPQNAPNGIVFIH
FTYTPESFVNVTAIVGFCVNPANASQYAIVPANGRGVFIQVNGSYYITARDMYMPRDITAGDIVTLTSCQANYVNV
NKTVINTFVEDDDFNFNDELSKWWNDTKHELPDFDEFNYTVPVLNISNEIDRIQEVIQGLNDSLIDLETLSILKTYIK
WP**LAIYSTVSSSLVLVGLIIAMGLW**MTGCCGCCCGCFGIIPLMSKCGKKSSYYTTFDNDVVTEQYRP

Design of IBV-S-IAV-TM and IBV-S-IAV-TM/CT sequences:

>AKC34133.1 spike protein **[INFECTIOUS BRONCHITIS VIRUS]TM** S2 = TDAE…??

MLVKSLFLVTILCALCSA/NLFDSDNNYVYYYQSAFRPPNGWHLQGGAYAVVNSTNHTSNAGSAQGCTVGVIKDV
YNQSVASIAMTAPLQGMAWFCTAYCNFSDTTVFVTHCYHIRISAMKNGSLFYNLTVSVSKYPNFKSFQCVNNFTSV
YLNGDLVFTSNKTTDVTSAGVYFKAGGPVNYSIMKEFKVLAYFVNGTAQDVILCDNSPKGLLACQYNTGNFSDGF
YPFTNSTLVREKFIVYRESSFNTTLALTNFTFTNVSNAQPNSGGVNTFHLYQTQTAQSGYYNFNLSFLSQFVYKASD
FMYGSYHPSCSFRPETINSGLWFNSLSVSLTYGPLQGGCKQSVFSGKATCCYAYSYKGPMACKGVYSGELRTNFEC
GLLVYVTKSDGSRIQTRTEPLVLTQYNYNNITLDKCVAYNIYGRVGQGFITNVTDSAANFSYLADGGLAILDTSGAI
DVFVVQGIYGLNYYKVNPCEDVNQQFVVSGGNIVGILTSRNETGSEQVENQFYVKLTNSSHRRRR▼SIGQNVTSCP
YVSYGRFCIEPDGSLKMIVPEELKQFVAPLLNITESVLIPNSFNLTVTDEYIQTRMDKVQINCLQYVCGNSLECRKLF
QQYGPVCDNILSVVNSVSQKEDMELLSFYSSTKPKGYDTPVLSNVSTGEFNISLLLKTPISSSGRSFIEDLLFTSVETV
GLP▼**690**TDAEYKKCTAGPLGTLKDLICAREYNGLLVLPPIITADMQTMYTASLVGAMAFGGITSAAAIPFATQIQA

RINHLGITQSLLMKNQEKIAASFNKAIGHMQEGFRSTSLALQQIQDVVNKQSAILTETMNSLNKNFGAITSVIQDIYA
QLDAIQADAQVDRLITGRLSSLSVLASAKQSEYIRVSQQRELATKKINECVKSQSNRYGFCGSGRHVLSIPQNAPNGI
VFIHFTYTPESFVNVTAIVGFCVNPANASQYAIVPANGRGVFIQVNGSYYITARDMYMPRDITAGDIVTLTSCQANY
VNVNKTVINTFVEDDDFNFNDELSKWWNDTKHELPDFDEFNYTVPVLNISNEIDRIQEVIQGLNDSLIDLETLSILKT
YIKWP**WYVWLAIFFAIIIFILILGWVFF**MTGCCGCCCGCFGIIPLMSKCGKKSSYYTTFDNDVVTEQYRPKKSV

>**H6 HA** Sub-lineage I (2016) avian influenza virus **TM** *CT* HA2
MGWSWIFLFLLSGAAGVHCDKICIGYHANNSTTQVDTILEKNITVTHSIELLETQKEERFCRVLNKAPLDLRECTIEG
WMLGNPRCDILLEDQRWSYIVERPSASNGICYPGPLNEIEELRSLIGSGERVERFEMFPKSTWNGVDTENGITRACSS
STGGSSFYRNLLWIIKNKSASYPVIKGTYNNTGNQPIIYFWGVHHPPDADRQNNLYGSGDRYIRMGTESMHFAKGP
EIAARPSVNGQRGRIDYYWSVLNPGETLNIESNGNFIAPRYAYRFFSTNKKGVIFKSNLPIENCDAQCQTTLGVLRTN
KTFQNVSPQWTGECPKYVKSKSLRLATGLRNVPQVETR▼GIFGAIAGFIEGGWTGMIDGWYGYHHENSQGSGYA
ADRDSTQKAIDGITNKVNTIIDKMNTQFEAVGHEFSNLERRIDNLNKRMEDGLLDVWTYNAELLVLLENERTLDLH
DANVKNLYERVKSQLRDNANDLGNGCFEFWHKCDNDCMESVKNGTYDYPKYQDESKLNRQKIESVKLDNLGVY
QI**LAIYSTVSSSLVLVGLIIAMGLW***MCSNGSMQCRVCI*-

rS-H6 **TM** (Chimeric IBV/**H6-TM**)
MLVKSLFLVTILCALCSANLFDSDNNYVYYYQSAFRPPNGWHLQGGAYAVVNSTNHTSNAGSAQGCTVGVIKDV
YNQSVASIAMTAPLQGMAWFCTAYCNFSDTTVFVTHCYHIRISAMKNGSLFYNLTVSVSKYPNFKSFQCVNNFTSV
YLNGDLVFTSNKTTDVTSAGVYFKAGGPVNYSIMKEFKVLAYFVNGTAQDVILCDNSPKGLLACQYNTGNFSDGF
YPFTNSTLVREKFIVYRESSFNTTLALTNFTFTNVSNAQPNSGGVNTFHLYQTQTAQSGYYNFNLSFLSQFVYKASD
FMYGSYHPSCSFRPETINSGLWFNSLSVSLTYGPLQGGCKQSVFSGKATCCYAYSYKGPMACKGVYSGELRTNFEC
GLLVYVTKSDGSRIQTRTEPLVLTQYNYNNITLDKCVAYNIYGRVGQGFITNVTDSAANFSYLADGGLAILDTSGAI
DVFVVQGIYGLNYYKVNPCEDVNQQFVVSGGNIVGILTSRNETGSEQVENQFYVKLTN**SSHRRRR▼S**IGQNVTSCP
YVSYGRFCIEPDGSLKMIVPEELKQFVAPLLNITESVLIPNSFNLTVTDEYIQTRMDKVQINCLQYVCGNSLECRKLF
QQYGPVCDNILSVVNSVSQKEDMELLSFYSSTKPKGYDTPVLSNVSTGEFNISLLLKTPISSSGRSFIEDLLFTSVETV
GLPTDAEYKKCTAGPLGTLKDLICAREYNGLLVLPPIITADMQTMYTASLVGAMAFGGITSAAAIPFATQIQARINH
LGITQSLLMKNQEKIAASFNKAIGHMQEGFRSTSLALQQIQDVVNKQSAILTETMNSLNKNFGAITSVIQDIYAQLD
AIQADAQVDRTGRLSSLSVLASAKQSEYIRVSQQRELATKKINECVKSQSNRYGFCGSGRHVLSIPQNAPNGIVFIHF
TYTPESFVNVTAIVGFCVNPANASQYAIVPANGRGVFIQVNGSYYITARDMYMPRDITAGDIVTLTSCQANYVNVN
KTVINTFVEDDDFNFNDELSKWWNDTKHELPDFDEFNYTVPVLNISNEIDRIQEVIQGLNDSLIDLETLSILKTYIKW
P**LAIYSTVSSSLVLVGLIIAMGLW**MTGCCGCCCGCFGIIPLMSKCGKKSSYYTTFDNDVVTEQYRPKKSV

rS-H6 **TM**/*CT* Chimeric IBV/**H6 TM**&*CT*
MLVKSLFLVTILCALCSANLFDSDNNYVYYYQSAFRPPNGWHLQGGAYAVVNSTNHTSNAGSAQGCTVGVIKDV
YNQSVASIAMTAPLQGMAWFCTAYCNFSDTTVFVTHCYHIRISAMKNGSLFYNLTVSVSKYPNFKSFQCVNNFTSV
YLNGDLVFTSNKTTDVTSAGVYFKAGGPVNYSIMKEFKVLAYFVNGTAQDVILCDNSPKGLLACQYNTGNFSDGF
YPFTNSTLVREKFIVYRESSFNTTLALTNFTFTNVSNAQPNSGGVNTFHLYQTQTAQSGYYNFNLSFLSQFVYKASD
FMYGSYHPSCSFRPETINSGLWFNSLSVSLTYGPLQGGCKQSVFSGKATCCYAYSYKGPMACKGVYSGELRTNFEC
GLLVYVTKSDGSRIQTRTEPLVLTQYNYNNITLDKCVAYNIYGRVGQGFITNVTDSAANFSYLADGGLAILDTSGAI
DVFVVQGIYGLNYYKVNPCEDVNQQFVVSGGNIVGILTSRNETGSEQVENQFYVKLTNSSHRRRRSIGQNVTSCPY
VSYGRFCIEPDGSLKMIVPEELKQFVAPLLNITESVLIPNSFNLTVTDEYIQTRMDKVQINCLQYVCGNSLECRKLFQ

QYGPVCDNILSVVNSVSQKEDMELLSFYSSTKPKGYDTPVLSNVSTGEFNISLLLKTPISSSGRSFIEDLLFTSVETVG
LPTDAEYKKCTAGPLGTLKDLICAREYNGLLVLPPIITADMQTMYTASLVGAMAFGGITSAAAIPFATQIQARINHL
GITQSLLMKNQEKIAASFNKAIGHMQEGFRSTSLALQQIQDVVNKQSAILTETMNSLNKNFGAITSVIQDIYAQLDAI
QADAQVDRLITGRLSSLSVLASAKQSEYIRVSQQRELATKKINECVKSQSNRYGFCGSGRHVLSIPQNAPNGIVFIHF
TYTPESFVNVTAIVGFCVNPANASQYAIVPANGRGVFIQVNGSYYITARDMYMPRDITAGDIVTLTSCQANYVNVN
KTVINTFVEDDDFNFNDELSKWWNDTKHELPDFDEFNYTVPVLNISNEIDRIQEVIQGLNDSLIDLETLSILKTYIKW
P**LAIYSTVSSSLVLVGLIIAMGLW***MCSNGSMQCRVCI-*

Restriction enzyme digests of constructs:

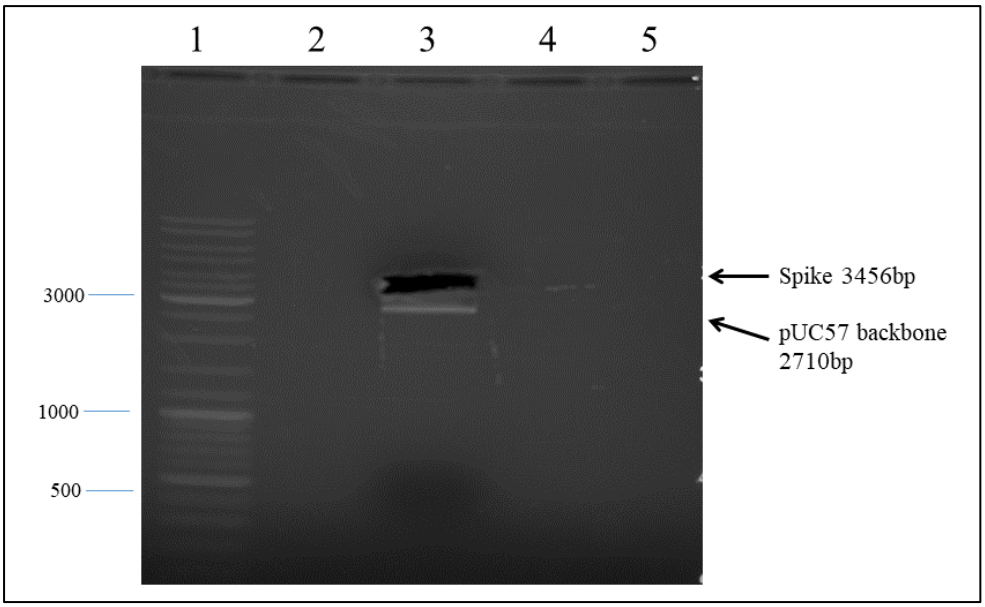

Figure 37: Restriction enzyme digest of pUC57-S plasmid with *Age*I and *Xho*I restriction enzymes. Lane 1: GeneRuler ladder mix SM0331, Lane 3: pUC57-S *Age*I/*Xho*I digest cut out. The PCR products were separated on a 1% Agarose gel.

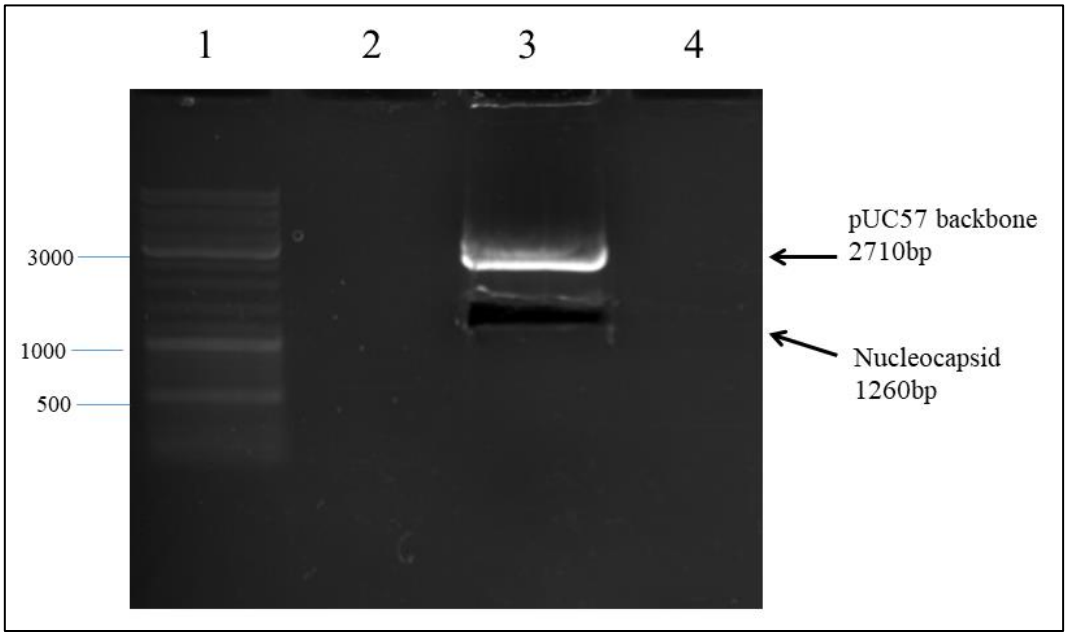

Figure 38: Restriction enzyme digest of pUC57-N plasmid with *Age*I and *Xho*I restriction enzymes. Lane 1: GeneRuler ladder mix SM0331, Lane 3: pUC57-N *Age*I/*Xho*I digest cut out. The PCR products were separated on a 1% Agarose gel.

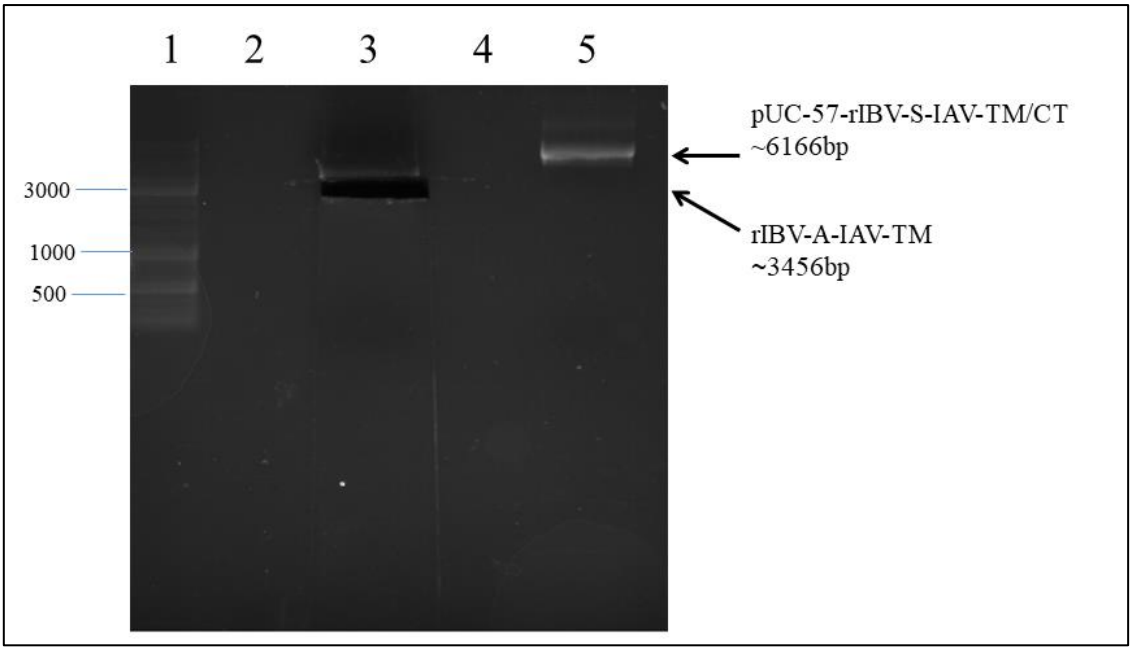

Figure 39: Restriction enzyme digest of rIBV-S-IAV-TM PCR product with *Age*I and *Xho*I restriction enzymes. Lane 1: GeneRuler ladder mix SM0331, Lane 3: rIBV-S-IAV-TM PCR product *Age*I/*Xho*I digest cut out, Lane 5: pUC57-rIBV-S-IAV-TM/CT undiluted. The PCR products were separated on a 1% Agarose gel.

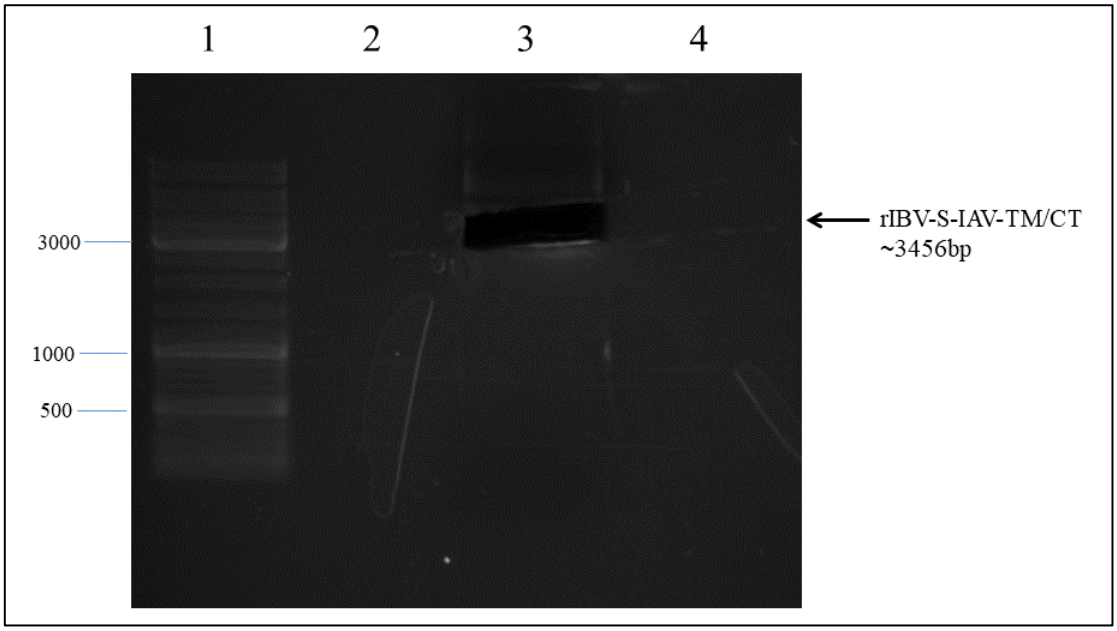

Figure 40: Restriction enzyme digest of rIBV-S-IAV-TM/CT PCR product with *Age*I and *Xho*I restriction enzymes. Lane 1: GeneRuler ladder mix SM0331, Lane 3: rIBV-S-IAV-TM/CT PCR product *Age*I/*Xho*I digest cut out. The PCR products were separated on a 1% Agarose gel.

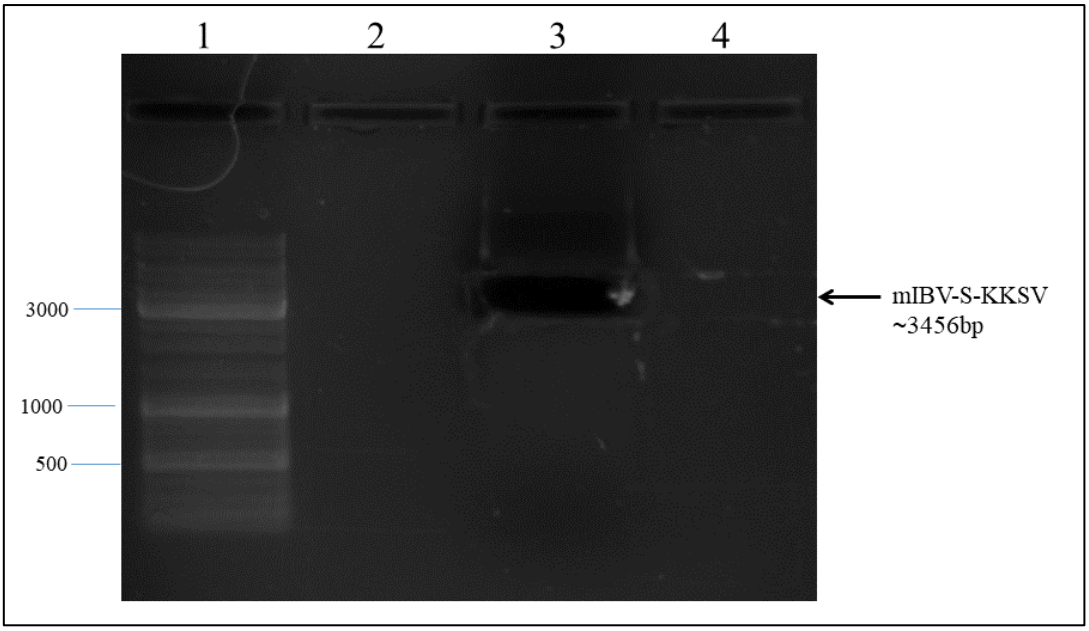

Figure 41: Restriction enzyme digest of mIBV-S-KKSV PCR product with *Age*I and *Xho*I restriction enzymes. Lane 1: GeneRuler ladder mix SM0331, Lane 3: mIBV-S-KKSV PCR product *Age*I/*Xho*I digest cut out. The PCR products were separated on a 1% Agarose gel.

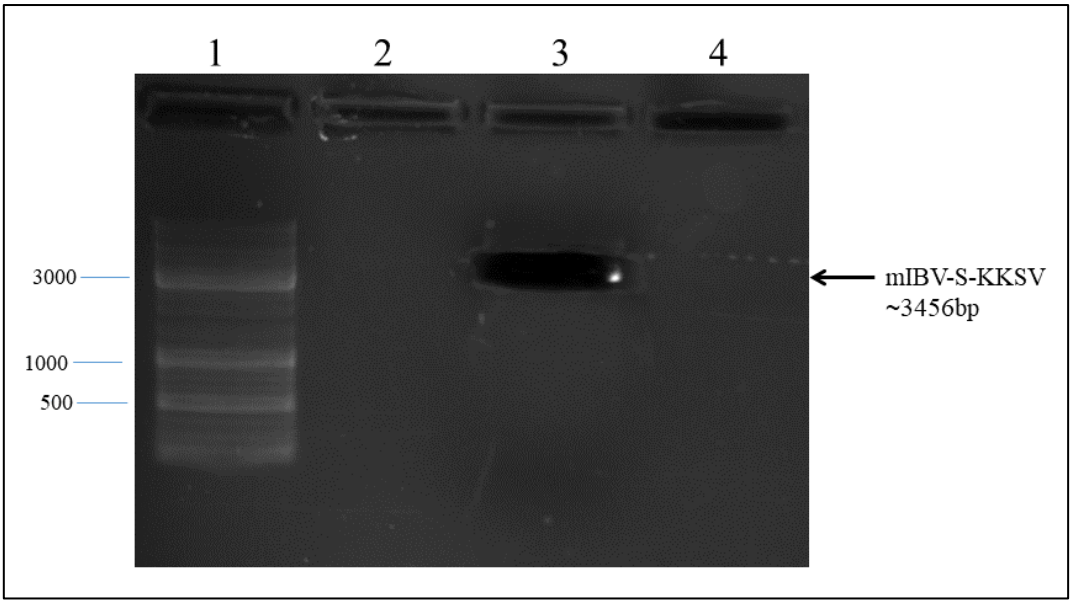

Figure 42: Restriction enzyme digest of mIBV-S-IAV-TM-KKSV PCR product with *Age*I and *Xho*I restriction enzymes. Lane 1: GeneRuler ladder mix SM0331, Lane 3: mIBV-S-IAV-TM-KKSV PCR product *Age*I/*Xho*I digest cut out. The PCR products were separated on a 1% Agarose gel.

KAPA HIFI PCR Amplification of genes:

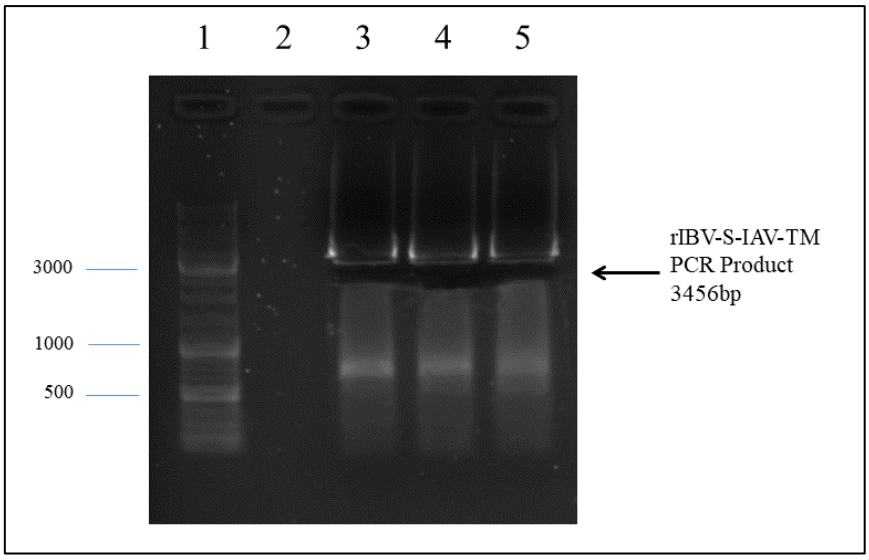

Figure 43: KAPA HIFI PCR product of rIBV-S-IAV-TM using Fw TM-CT and Rv TM primers as described in Materials and methods (Table 2). Lane 1: GeneRuler ladder mix SM0331, Lane 3: rIBV-S-IAV-TM PCR products cut out at annealing temperature of 60.1°C, 61.9°C and 64.9°C, lanes 3-5. PCR products separated on a 1% Agarose gel.

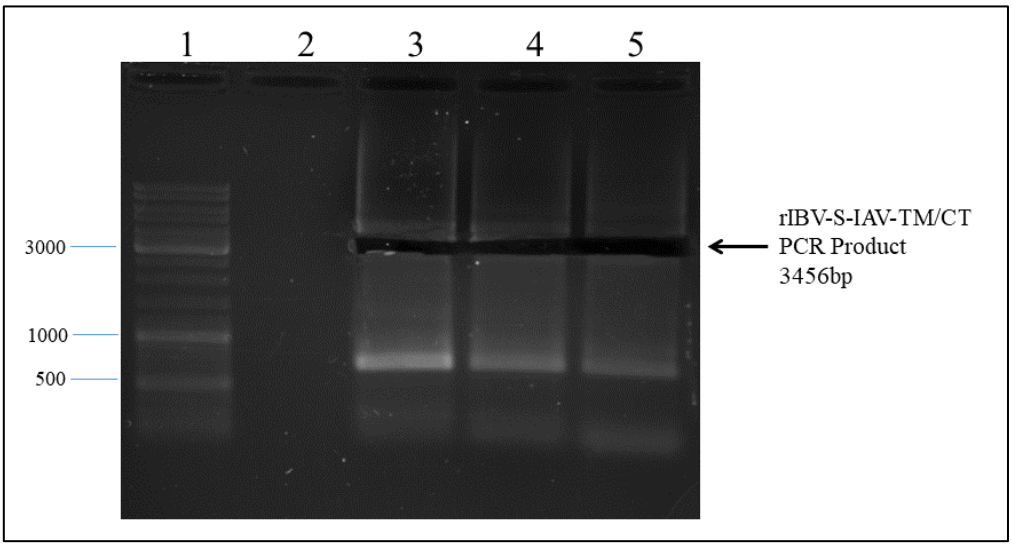

Figure 44: KAPA HIFI PCR product of rIBV-S-IAV-TM/CT using Fw TM-CT and Rv TM-CT primers (Table 2). Lane 1: GeneRuler ladder mix SM0331, Lane 3: rIBV-S-IAV-TM/CT PCR product cut out at an annealing temperature of 55°C, 56.7°C and 60.4°C, lanes 3-5. PCR products separated on a 1% Agarose gel.

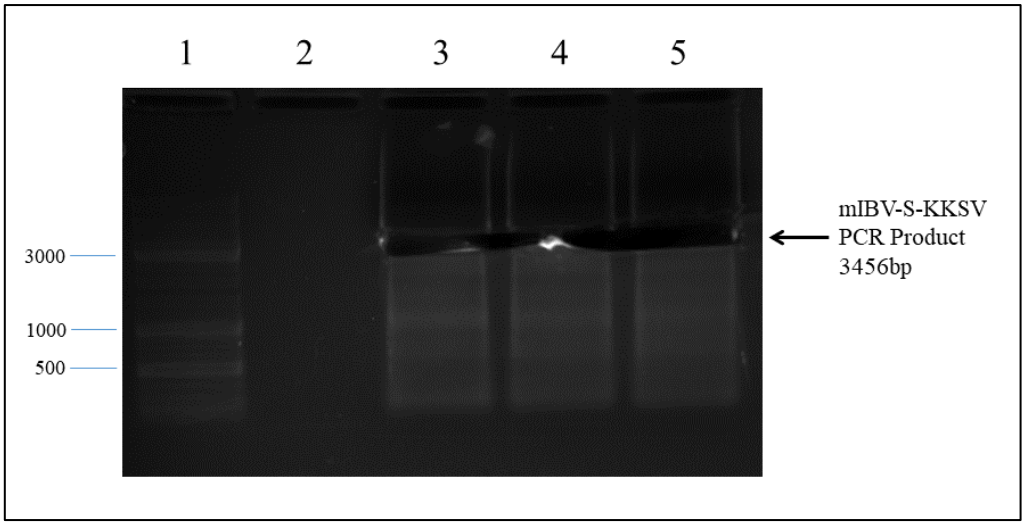

Figure 45: KAPA HIFI PCR product of mIBV-S-KKSV using Fw mIBV-S and Rv IBV-S-KKSV primers (Table 2). Lane 1: GeneRuler ladder mix SM0331, Lane 3: mIBV-S-KKSV PCR product cut out at an annealing temperature of 58°C, 59.9°C and 62.6°C, lanes 3-5. PCR products separated on a 1% Agarose gel.

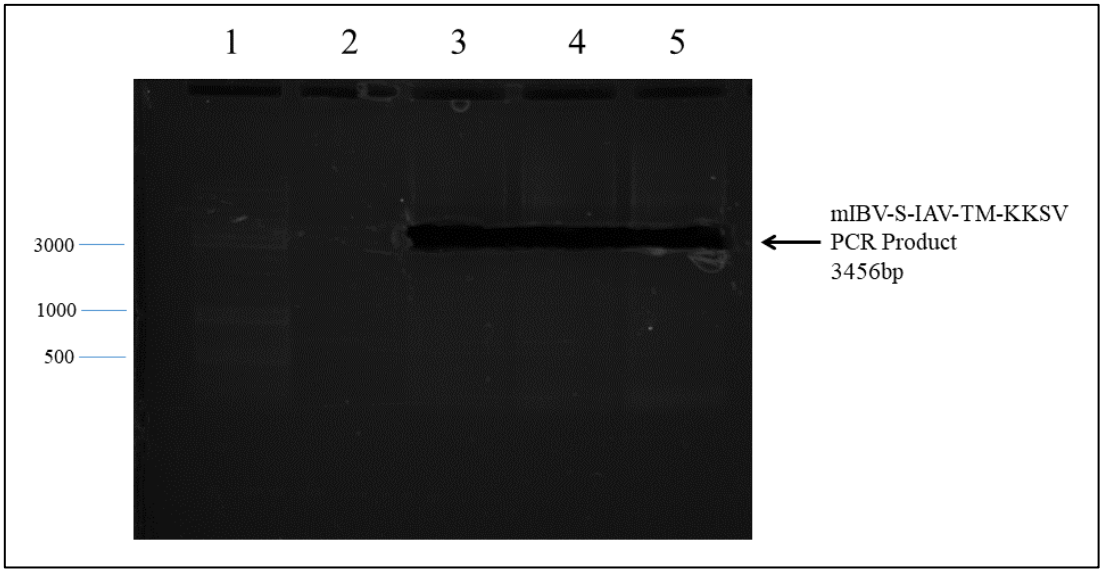

Figure 46: KAPA HIFI PCR product of mIBV-S-IAV-TM-KKSV with Fw mIBV-S and Rv IBV-S-KKSV primers (Table 2). Lane 1: GeneRuler ladder mix SM0331, Lane 3: mIBV-S-IAV-TM-KKSV PCR product cut out at an annealing temperature of 55.1°C, 57°C and 60.4°C, lanes 3-5. PCR products separated on a 1% Agarose gel.

Bolt gel cut outs for LCMS-MS/MS based peptide sequencing:

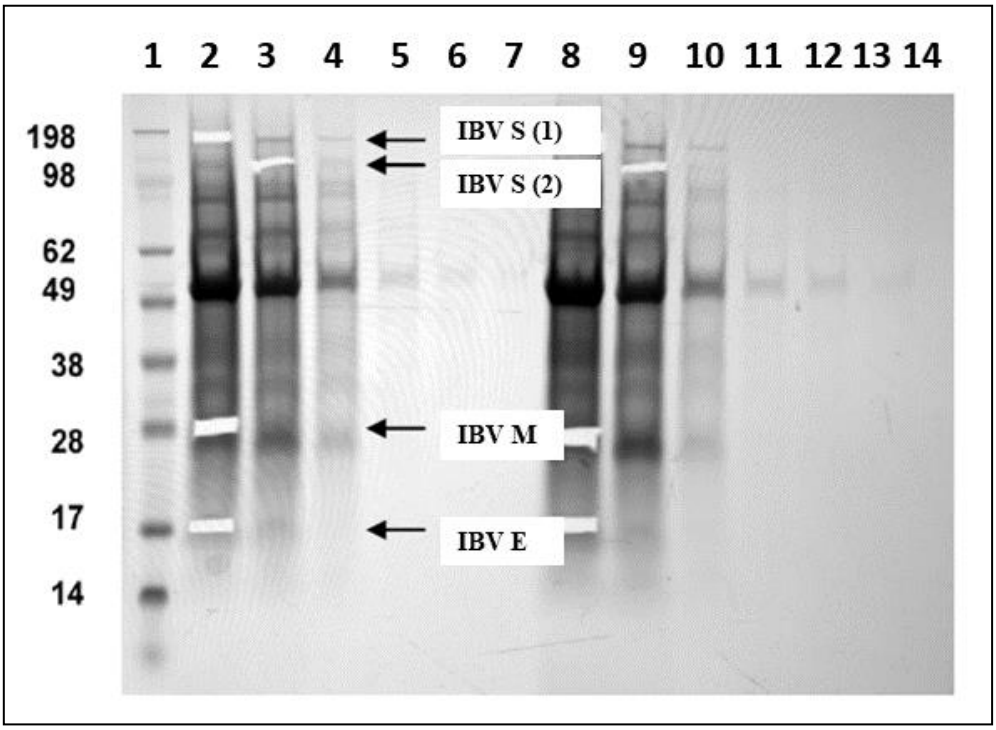

Figure 47: Bolt 4-12% SDS PAGE analysis of pEAQ-HT IBV S, M, and E proteins co-expressed in *N. benthamiana* ΔXT/FT 6 dpi. *Agrobacterium*-mediated (LBA4404 or GV3101::pMP90; lanes 1-5 and 7-12, respectively) pEAQ-HT expressed target genes. Bands were cut out for LCMS-MS/MS based peptide sequencing. IBV S (1) – Spike original Fr. 11 (±127kDa), IBV S (2) – Spike original (2) Fr. 11 (±127kDa), IBV M – Membrane Fr. 11 (±30kDa), IBV E – Envelope Fr. 11 (±13kDa).

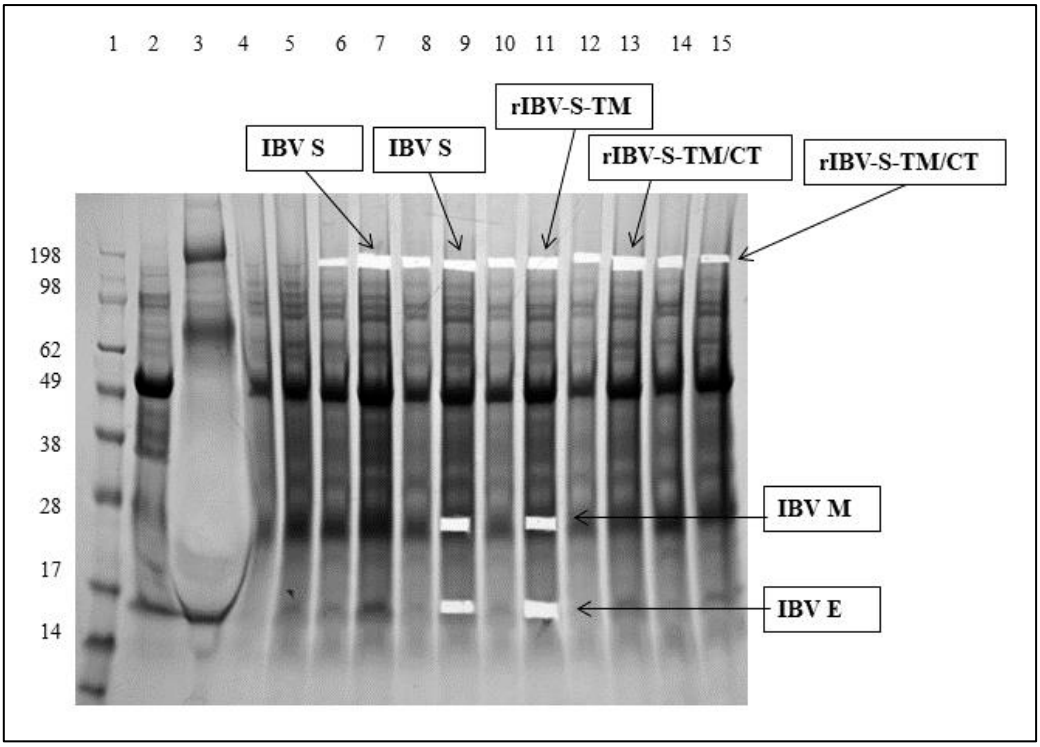

Figure 48: Bolt 4-12% SDS PAGE analysis of pEAQ-HT IBV S (or rIBV-S-TM or rIBV-S-TM/CT), M, and E proteins co-expressed in *N. benthamiana* ΔXT/FT 6 dpi. *Agrobacterium*-mediated (AGL-1) expression. Bands were cut out for LCMS-MS/MS based peptide sequencing. IBV S – Spike original (Combo 2) Fr. 11 (±127kDa), IBV S – Spike original (Combo 3) Fr. 11 (±127kDa), rIBV-S-TM (Combo 4) Fr. 11 (±127kDa), rIBV-S-TM/CT (Combo 5) Fr. 11 (±127kDa), rIBV-S-TM/CT (Combo 6) Fr. 11 (±127kDa), Membrane (Combo 4) Fr. 11 (±30kDa), Envelope (Combo 4) Fr. 11 (±13kDa).

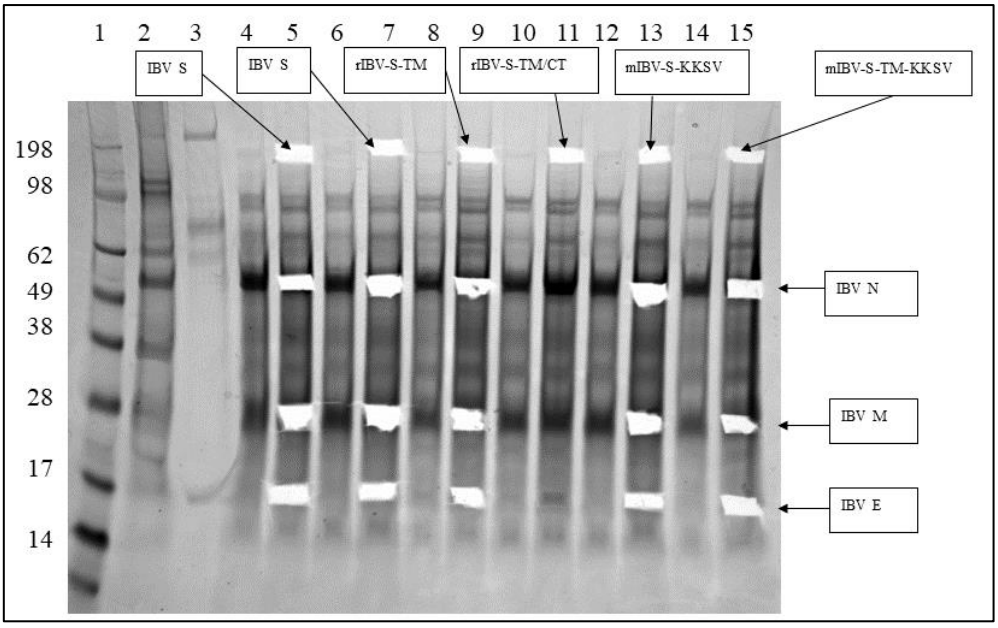

Figure 49: Bolt 4-12% SDS PAGE analysis of pEAQ-HT IBV S (or rIBV-S-TM or rIBV-S-TM/CT or mIBV-S-KKSV or mIBV-S-TM-KKSV), N, M, and E proteins co-expressed in *N. benthamiana* ΔXT/FT 6 dpi. *Agrobacterium*-mediated (AGL-1) expression. Bands were cut out for LCMS-MS/MS based peptide sequencing. IBV S (Fr. 11) - Spike original (±127kDa), IBV S (Fr. 11) - Spike original (±127kDa), rIBV-S-TM (Fr. 11) (±127kDa), rIBV-S-TM/CT (Fr. 11) (±127kDa), mIBV-S-KKSV E: C5 – S (Fr. 11) (±127kDa), mIBV-S-TM-KKSV (Fr. 11) (±127kDa), IBV N (Fr. 11) (±45kDa), IBV M (Fr. 11) (±30kDa), IBV E (Fr. 11) (±13kDa).

Comparison of IBV S and IAV HA:

Table 3: A comparison between the IBV S protein and the IAV HA protein

	Infectious Bronchitis Virus S (Spike) Protein	Avian Influenza Virus HA (Hemagglutinin) Protein
Size	20nm (16 – 21nm) length (Liu *et al*., 2013b; Jackwood and de Wit, 2013). Prior to glycosylation, monomer is 128kDa (Masters and Perlman, 2013), 200kDa after glycosylation (Binns *et al*., 1985; Wickramasinghe *et al*., 2014).	13.5nm length trimer (Boonstra *et al*., 2018). 72kDa in size (D'Aoust *et al*., 2008). Each monomer is 60kDa in size prior to glycosylation, after which its size increases (Sriwilaijaroen and Suzuki, 2012).
Structure and composition	Club-shaped spikes on the IBV surface giving virion crown-like appearance (Liu *et al*., 2013b; Jackwood and de Wit, 2013). The IBV trimer is made up of subunits S1 (520aa) and S2 (625aa) (Jackwood and de Wit, 2013). The S1 subunit at the N-terminal forms the bulb of the oligomeric spike protein and is a part of the large ectodomain, while the S2 subunit at the C-terminal end forms a narrow stalk as well as the short TM and endodomain, and forms the smaller part of the ectodomain (Wickramasinghe *et al.*, 2014). Spike is a type 1 membrane protein that is made up of a receptor binding domain, precoil domain, heptad repeat regions, a cleavage site, interhelical domain, fusion peptide, TM domain, as well as a cytoplasmic tail (Koch *et al*., 1990; Perlman *et al*., 2008).	Spike-shaped projection on the outer surface of AIV (Nayak *et al*., 2010; Isin at al., 2002). HA0 homo-trimer is cleaved into HA1 (327aa) and HA2 (222aa) subunits (Copeland *et al*., 1986). The HA glycoprotein is made up of a globular region of antiparallel β sheets that contain HA1 residues (the receptor binding domain) as well as a stalk region that contains both HA1 and HA2 residues (this is a triple-stranded coiled coil of α-helices) (Wilson and Skehel, 1981, Wiley and Skehel, 1987). On top of the R domain is the receptor binding site and the highly variable antigenic binding loops that surround it. These loops carry carbohydrate side chains (Skehel and Wiley, 2000). The HA_1 subunit is made up of the vestigial esterase and the fusion subdomains (Wilson and Skehel, 1981; Rosenthal *et al*., 1988).
Function	S1 subunit contains the receptor-binding domain that facilitates host cell attachment (Promkuntod *et al*., 2014). It is a viral fusion peptide that is involved in viral attachment to host cell, fusion to host cell membrane, and entry of virus into cell) (Casais *et al*., 2003; Wickramasinghe *et al*., 2011; Masters and Perlman, 2013)	Receptor binding and viral fusion (Nayak *et al*., 2010). Plays a role in host cell attachment and entry (Sriwilaijaroen and Suzuki, 2012). It stimulates neutralisation antibody responses by the host (Sriwilaijaroen and Suzuki, 2012)
Where it is formed	The viral subgenomic messenger RNAs are transcribed in the cytoplasm along with the translation of the viral proteins (Jackwood and de Wit, 2013). Spike (along with envelope and membrane) proteins are inserted into the Golgi membrane (Jackwood and de Wit, 2013). The S protein is directed to the ER by a cleaved N-terminal signal peptide where it gets terminal N-linked glycosylation (Binns *et al*., 1985; Wickramasinghe *et al*., 2014).	HA gets cotranslationally translocated across the membrane of the rough ERforming the homo-trimer, HA0 (Gething *et al*., 1986). The HA_0 precursor gets transported to the plasma membrane via the Golgi network and is cleaved by cellular proteases, resulting in the HA_1 and HA_2 subunits (Copeland *et al*., 1986).
Post-translational processing	The S1 and S2 subunits are generated through post-translational cleavage of the spike protein by a furin-like host cell protease (Liu *et al*., 2013b; Cavanagh *et al*. 1986).	The virus particle only becomes infectious when the HA precursor (HA_0) gets cleaved into its HA_1 and HA_2 subunits (Sriwilaijaroen and Suzuki, 2012). Low pathogenic IAV (LPAI) strains are cleaved by trypsin-like proteases, including tryptases, mini-plasmin, bacterial proteases, and the blood-clotting factor Xa (*in vitro*), while high pathogenic IAV (HPAI) strains are cleaved by a range of more ubiquitous intracellular proteases, including proprotein convertase 6 (PC6) and furin which are found in a range of host cells, causing lethal infections in poultry (Soltanialvar *et al.*, 2016; Horimoto *et al*., 1994; Stieneke- Gröber *et al*., 1992; Kido *et al*., 1992).

Immunity	The S glycoprotein induces neutralizing antibodies in the host (Kant *et al*., 1992; Koch *et al*., 1990). Antibodies for hemagglutination inhibition (HI) as well as virus-neutralisation and serotype-specific antibodies are directed against the first third of the amino part of the spike glycoprotein (Koch *et al*., 1990). In chickens that are infected with the virus, both cellular and humoral immune responses are induced by the spike protein (Cavanagh, 2007).	HA is a major contributor to induction of neutralizing antibodies and protective immunity (Nayak *et al*., 2010).
Epitopes	The epitopes that induce neutralizing antibodies are very closely linked to three hypervariable regions that are located in the S1 part of the spike gene (Cavanagh *et al*., 1988). Five conformation-dependent antigenic sites (epitopes) have been characterised on the S1 subunit, as well as an immunodominant region on the S2 subunit (Koch *et al*., 1990; Kusters *et al.*, 1989). S1 subunit contains epitopes for inducing hemaggluttination inhibition (HI), neutralisation, as well as serotype-specific antibodies (Cavanagh *et al.* 1986). The S2 subunit also contains antigenic epitopes (Toro *et al*., 2014).	There are at least five different overlapping antigenic sites that have been characterised, and these were located in the globular head of the HA protein (Caton *et al*., 1982; Raymond *et al*., 1986). The globular head domain of the HA protein contains the epitopes to which most neutralizing antibodies are directed. This is where the sialic acid binding site is located (Magadán *et al*., 2013). These are the most abundant neutralizing antibodies elicited after infection and vaccination (Neu *et al*., 2016). However protective stalk antibodies have been located in humans (Magine *et al*., 2013; Ekiert *et al*., 2009). The stem-head domain of HA is conserved between strains as well as subtypes (Soltanialvar *et al.*, 2016)
Serotypes	Mutations that occur in the S1 gene of the spike protein lead to an infinite number of new genotypes and serotypes of the virus (Liu *et al*., 2003). The specific circulating antibodies that are developed against the epitopes of the S protein following exposure define the IBV serotype (Jackwood and de Wit, 2013).	There are 16 different serotypes of the HA protein (Fouchier *et al*., 2005; Webster *et al*., 1992). Two more subtypes have been discovered in bats (Tong *et al*., 2013). Mutations in the antigenic sites of IAV (HA) lead to new subtypes of the virus emerging (Carrat and Flahault, 2007).